Role of the chemokines CCL17 and CCL22 in bacterial infection and IL-33-induced immune responses

Manja Wibke Thiem

ORCID ID:
000-0003-4412-3996

from Berlin, Germany

Submitted in total fulfilment of the requirements of the joint degree of
Doctor of Philosophy (PhD)
of
The Medical Faculty
The Rheinische Friedrich-Wilhelms-Universität Bonn
And
The Department of Microbiology and Immunology
The University of Melbourne

Bonn/Melbourne, 2023

Performed and approved by The Medical Faculty of The Rheinische Friedrich-Wilhelms-Universität Bonn and The University of Melbourne.

1. Supervisor:	Prof. Dr. Irmgard Förster
2. Supervisor:	Prof. Dr. Natalio Garbi
Co-Supervisors (shared):	Prof. José Villadangos, PhD Prof. Richard A. Strugnell, PhD Nancy Wang, PhD

Month and year of the original thesis submission: March 2023
Month and year of the oral examination: November 2023

Institute in Bonn: Life & Medical Sciences (LIMES) Institute

Director: Prof. Dr. Waldemar Kolanus

Table of Contents

Abbreviations

A	AP-1	Activator protein 1
	APC	Antigen-presenting cells
	ATR	Acid tolerance response
B	BAT	Brown adipose tissue
	bCCL17/22	Biotinylated CCL17/22
	bCXCL1	Biotinylated CXCL1
	BDL	Bile duct ligation
	BM	Bone marrow
	BMDC	Bone marrow-derived dendritic cells
	BN-PAGE	Blue native-polyacrylamide gel electrophoresis
	BSA	Bovine serum albumin
C	CAR	Acylcarnitines
	CARD	Caspase Recruitment Domain
	CCL	Chemokine ligand
	CCR	Chemokine receptor
	Cer	Ceramides
	CFU	Colony-forming units
	CFU-E	Colony-forming units-erythroid
	CHS	Contact hypersensitivity assay
	COPS	Core O-Polysaccharide
D	DABCO	Triethylenediamine
	DAG	Diacylglycerols
	DAMP	Damage-associated molecular pattern
	DC	Dendritic cells
	DMEM	Dulbecco's Modified Eagle Medium
	DNFB	2,4-dinitro-1-fluorobenzene
E	ECM	Extracellular matrix
	EDTA	Ethylenediaminetetraacetic acid

	eff	Effector
	EGFP	Enhanced green fluorescent protein
	ELISA	Enzyme Linked Immunosorbent Assay
F	FA	Fatty acids
	FACS	Fluorescence-activated cell sorting
	FAE	Follicle-associated epithelium
	FCS	Fetal bovine serum
	FMP	Fluorescence minus one
	FoxP3	Forkhead-box protein P3
G	GALT	Gut-associated lymphoid tissue
	GATA3	GATA binding protein 3
	GI	Gastrointestinal
	GITR	Glucocorticoid-induced TNFR-related protein
	GM-CSF	Granulocyte-macrophage colony-stimulating factor
	GMP	Granulocyte/macrophage progenitors
	GRC	Genetic Resource Center
H	H_2SO_4	Sulfuric acid
	h	Hours
	H&E	Haematoxylin and eosin
	HCl	Hydrochloric acid
	HEK	Human embryonic kidney cell line
	HEK:mCCR4	Murine CCR4-expressing human embryonic kidney cell line
	HEPES	N-2-hydroxyethylpiperazine-N-2-ethane sulfonic acid
	HFD	High fat diet
	HSC	Haematopoietic stem cells
I	i.p.	Intraperitoneal injection
	ICOS	Inducible T-cell costimulatory
	IEC	Intestinal epithelial cells
	IFNγ	Interferon gamma
	IL	Interleukin

	IL-1RAcP	IL-1 receptor accessory protein
	ILC	Innate lymphoid cells
	ILF	Isolated lymphoid follicles
	IMDM	Iscove’s Modified Dulbecco’s Medium (IMDM)
	iNTS	Invasive non-typhoidal Salmonellosis
	iWAT	Inguinal white adipose tissue
K	KLRG1	Killer Cell Lectin Like Receptor G1
	KO	Knock out
L	LB	Luria-Bertani
	LD	Live-Dead
	LPC	Lysophosphatidylcholines
	LPE	Lysophosphatidylethanolamines
	LPS	Lipopolysaccharide
M	M cells	Microfold cells
	MDC	Macrophage-derived chemokine
	MDR	Multidrug resistance
	MEP	Megakaryocyte/erythrocyte progenitors
	MFI	Mean fluorescence intensity
	MHC I	Major histocompatibility complex class I
	MHC II	Major histocompatibility complex class II
	min	Minutes
	MkP	Megakaryocyte progenitors
	mLN	Mesenteric lymph nodes
	MPP	Multipotent progenitors
	MS	Mass spectrometry
	MutuDC	Murine tumor dendritic cells
N	NADPH	Nicotinamide adenine dinucleotide phosphate
	NF-κB	nuclear factor 'kappa-light-chain-enhancer' of activated B-cells
	NHS	N-hydroxysulfosuccinimide

	NK cell	Natural killer cells
	NLR	NOD-like receptor
	NOD	Nucleotide oligomerisation domain
	Nramp1	Natural resistance-associated macrophage protein 1
	Nrp1	Neuropilin-1
	NTS	Non-typhoidal *Salmonella*
P	PAMP	Pathogen-associated molecular patterns
	PBS	Phosphate-buffered saline
	PCR	Polymerase-chain reaction
	PE	Phosphatidylethanolamines
	PI	Phosphatidylinositols
	PI3K	Phosphoinositide 3-kinase
	PP	Peyer's patches
	PreMegE	Promegakaryocytes
	ProEry	Proerythroblasts
	PRR	pattern recognition receptors
	pT_{reg} cell	peripherally-derived regulatory T cell
	PS	Phosphatidylserines
R	RBC	Red blood cells
	RIPA buffer	Radioimmunoprecipitation assay buffer
	RNS	Reactive nitrogen species
	RORγT	Retinoic acid-related orphan receptor gamma T
	ROS	Reactive oxygen species
	RPMI	Rosewell Park Memorial Institute 1640
S	SABV	BV421-coupled streptavidin
	SAPE	PE-coupled streptavidin
	SCV	*Salmonella*-containing vacuole
	SED	Subepithelial dome
	SM	Sphingomyelin
	SNP	Single nucleotide polymorphism

	SPF	Specific pathogen-free
	SPI-1	*Salmonella* Pathogenicity Island 1
	SPI-2	*Salmonella* Pathogenicity Island 2
	ST2	Suppression of tumorgenicity 2
	STM	*Salmonella enterica* serovar Typhimurium
T	T3SS	Type III secretion system
	TAG	Triacylglycerides
	TAGODD	Triacylglycerides with an odd number of carbon atoms
	TARC	Thymus and activation-regulated chemokine
	T-bet	T-box-containing protein expressed in T cells
	TCEP	Tris(2-carboxyethyl)phosphine
	T_{conv}	Conventional T cells
	TCV	Typhoid conjugate vaccines
	TEAB	Triethylammoniumbicarbonat
	TFE	2,2,2-trifluorethanol
	TGF-β	Transforming growth factor-beta
	TIR	Toll-Interleukin-1 receptor
	T_h	T helper cells
	TLR	Toll-like receptor
	TNFα	Tumor-necrose factor α
	T_{reg} cell	Regulatory T cell
	tT_{reg} cell	Thymus-derived regulatory T cell
U	UCP-1	Uncoupled protein 1
V	VAT	Visceral adipose tissue
	Vi-PS	Vi polysaccharide
	Vi-TT	Vi polysaccharide-tetanus toxoid
W	WAT	White adipose tissue
	wt	Wild type

List of tables

List of figures

Abstract

The chemokines CCL17 and CCL22 are primarily expressed by dendritic cells (DC) and macrophages. Both chemokines share the receptor CCR4, which is expressed on DC and macrophages as well as on a variety of different T cell subsets, including T_h1 cells, T_h2 cells, and regulatory T (T_{reg}) cells. As ligands of CCR4, CCL17 and CCL22 recruit T cells, facilitate the T cell-DC interaction, and sensitise DC for migration. However, CCL17 and CCL22 differ in their distinct signaling pathways and functions, a phenomenon that has been termed biased agonism. CCL17 is involved in the induction and enhancement of numerous allergic and inflammatory diseases. In contrast, CCL22 is rather associated with an immunosuppressive environment. Moreover, CCL17 induces migration and activation of T_h1 and T_h2 cells as well as sensitising DC migration towards CCR7-ligands, whereas CCL22 facilitates the recruitment of T_{reg} cells. In addition, CCL22 shows higher receptor-binding affinity and induces desensitisation and internalisation of CCR4 more rapidly than CCL17. Although CCL17 and CCL22 were extensively studied in allergic, inflammatory, and autoimmune diseases as well as in the tumor microenvironment, their involvement in infectious diseases has not been well described. Furthermore, IL-33 stimulates the production of CCL17 and CCL22 by DC. In the context of *Salmonella* infection, IL-33 can be produced by intestinal stroma cells after stimulation with bacterial ligands and IL-33 secretion by pericryptal fibroblasts was shown to be directly protective against the infection. Hence, the aim of this thesis was to elucidate the differential function of CCL17 and CCL22 in the context of *Salmonella* infection and IL-33-mediated immune responses in organs linked to *Salmonella* dissemination and beyond.

Using a vaccination/challenge *Salmonella* mouse model, wt, $CCL17^{E/E}$ $CCL22^{-/-}$, and $CCR4^{-/-}$ mice were investigated for their antigen-specific $CD4^+$ T cell response. Vaccinated $CCL17^{E/E}$ $CCL22^{-/-}$ and $CCR4^{-/-}$ mice were less protected against *Salmonella* challenge, while vaccinated wt mice survived with 100 %, potentially suggesting an impaired recruitment or positioning of $CD4^+$ T cells and a subsequent defect in clearing the infection.

In the context of IL-33-mediated immune responses, CCL22 appeared to play a detrimental role in IL-33-induced adipose tissue fibrosis as adipose tissue morphology

exhibited less signs of inflammation, indicated by fibrosis and immune cell infiltration, in CCL22-deficient mice. Moreover, CCL17 and CCL22 were involved in adipose tissue homeostasis in the inguinal white adipose tissue as well as the brown adipose tissue in the case of CCL22. Absence of CCL17, CCL22, and CCR4 caused eosinophilia in the blood, potentially due to an impaired recruitment of eosinophils from the bloodstream into the tissue. Additionally, while IL-33 impaired bone marrow erythropoiesis independently of the CCL17/CCL22/CCR4-axis and thereby caused extramedullary erythropoiesis in the spleen, CCL22 promoted the expansion of basophilic erythroblasts in the spleen.

Lastly, comparison of $CCL17^{E/E}$ $CCL22^{-/-}$ and $CCR4^{-/-}$ mice revealed certain phenotypic differences, suggesting the existence of a second receptor for CCL17 and CCL22. Using a chemokine-based receptor staining approach, it was confirmed that CCR4-deficient T cells in the thymus and spleen were still able to bind both chemokines. A putative second receptor, however, was not involved in mediating chemotaxis as CCR4-deficiency abrogated migration of primary T cells from the thymus and of the T cell lymphoma cell line BW5147.3.

In conclusion, uncovering both protective and detrimental functions of CCL17 and CCL22 as well as an additional player in the CCL17/CCL22/CCR4-axis opens new aspects to consider in future applications, disease studies and even therapeutically approaches.

Declaration

The work that is presented in this thesis was conducted at the University of Bonn, the laboratory of Professor Dr. Irmgard Förster, and at the University of Melbourne, the laboratory of Professor Jose Villadangos. The research work was funded by grants obtained from the Deutsche Forschungsgemeinschaft. Manja Wibke Thiem was supported by the Melbourne International Fee Remission Scholarship.

This is to certify that,

(i) the thesis comprises only my original work toward the PhD except where indicated in the preface

(ii) due acknowledgement has been made in the text to all other material used, and

(iii) the thesis is less than 100.000 words in length, exclusive of tables, maps, bibliographies and appendices.

Manja Wibke Thiem

Preface

My contribution to the experiments within each section was as follows:

Chapter 3: 95 %
Chapter 4: 100 %
Chapter 5: 100 %
Chapter 6: 95 %

I acknowledge the important contributions of others to experiments presented herein:
Chapter 3

- The STM challenge/vaccination experiment, shown in Figure 3.1C, was performed by Adrian Semeniuk at the LIMES Intsitute in Bonn.

Chapter 6

- The generation of the CCR4-deficient BW5147.3 cell and their validation by PCR and sequencing, shown in Figure 6.1A-C and Figure S3, was performed by Philip Hatzfeld at the LIMES Institute in Bonn.

Acknowledgments

The present thesis would not have been possible without the incredible support I have received from many kind, smart, funny and inspiring individuals throughout. I am grateful to each and every one of you for your support and encouragement during this memorable journey.

First of all, I want to thank my primary supervisor Prof. Irmgard Förster in Bonn for taking me on as a PhD student and providing me with the chance to work and grow as an independent scientist. Her incredible expertise, feedback and support guided me through this PhD journey at not only one but two different institutions and continents.

Secondly, thank you to my Melbourne supervisors Prof. Jose Villadangos and Prof. Richard Strugnell. Their direct and focused yet relaxed and supportive attitude made them fantastic supervisors.

Further, I want to thank everybody from the Förster and Weighardt laboratory, who were more than colleagues to me. Thank you for all the scientific discussions – realistic and fictitious, the small coffee breaks and the many activities outside the lab. You are the best lab I could have wished for! Thank you to Heike, who provided me with good advice on both my project and administrative work. A big thank you goes to Philip, who not only helped in generating the CCR4-deficient cell lines, but also matched my sarcastic, sometimes even dark, humour joke for joke and made me feel quiet at home from the first time I set foot into the lab. I also want to thank Marlene and Fred, two incredible colleagues, who became my friends in a blink of an eye. I loved our inside jokes and deep conversations, reaching from enthusiastic, scientific discussions to movie recommendations. Moreover, I appreciated how we lifted each other up in difficult times and hope we will stay in contact long after we have finished our PhD.

In addition, I want to thank my two labs in Melbourne for making me feel welcomed from the beginning. Thank you for all of our conversations in the office and the friendly atmosphere. Special thanks go to Jo Pooley for her tremendous efforts and skills in organising literally anything, especially the shipment of my samples from Bonn to

Melbourne. I also want to thank Nancy Wang, who has been incredibly encouraging and always provided valuable input for my project.

I would like to acknowledge all collaborators for their expertise and help in setting up and performing specialised aspects of experimental procedures and data analysis. Additionally, I would like to mention my PhD committee members, Prof. Jason Mackenzie and A/Prof. Hayley Newton for their support, advice and encouragement.

Many thanks to the IRTG2168 coordinators, especially for organising the exchange between Bonn and Melbourne and the extraordinary opportunity that provided. I am very grateful for your assistance in navigating the requirements and challenges that studying at two exceptional Universities presented.

Thank you to everybody that made my PhD journey memorable - from drinking Glühwein at the Christmas market in Bonn to dressing up for carnival or learning how to shoot with bow and arrow. Thank you also to all the people in Melbourne that contributed to my exploration of Australia, including a hiking-trip through Tasmania, my first opera at the Sydney opera house, visiting Perth and Adelaide, and seeing koalas, quokkas, and kangaroos in wild-life. Special thanks go out to Rebecca and Leonie, my two travel buddies in Australia. I enjoyed our trips immensely, even if I am still traumatised by all the stairs we had to climb, and hope we experience many more of these awesome trips in the future. I am grateful to Darya; it was always a pleasure and fun with you regardless of whether we were working alongside each other or enjoying our free time together. Thank you to Lea, my friend and desk neighbour, for her support and always open ears. I loved our talks in the morning and am so grateful that we have met.

Most importantly, I would like to thank my family, especially my parents, for their continuous support, understanding and love throughout this adventurous ride.
Mama und Papa, danke für eure Unterstützung und Liebe nicht nur in den letzten vier Jahren, sondern auch weit darüber hinaus. Ihr habt nie aufgehört an mich zu glauben, auch dann nicht, oder vielleicht genau dann nicht, wenn ich es selbst nicht konnte. Ich kann nicht in Worte fassen, wie viel es mir bedeutet immer auf euch zählen zu können. Ohne euch, wäre ich nicht der Mensch, der ich heute bin. Ich habe euch lieb.

List of publications

Cornelis, R., Hahne, S., Taddeo, A., Petkau, G., Malko, D., Durek, P., **Thiem, M**., Heiberger, L., Peter, L., Mohr, E., Klaeden, C., Tokoyoda, K., Siracusa, F., Hoyer, B. F., Hiepe, F., Mashregi, M., Melchers, F., Chang. H., Radbruch, A. (2020) Stromal Cell-Contact Dependent PI3K and APRIL Induced NF-κB Signaling Prevent Mitochondrial- and ER Stress Induced Death of Memory Plasma Cells, *Cell Reports,* 32(5), DOI: 10.1016/j.celrep.2020.107982

Erazo, A. B., Wang, N., Standke, L., Semeniuk, A. D., Fülle, L., Cengiz, S. C., **Thiem, M**., Weighardt, H., Strugnell, R. A., Förster, I. (2021) CCL17-expressing dendritic cells in the intestine are preferentially infected by Salmonella but CCL17 plays a redundant role in systemic dissemination, *Immun. Inflamm. Dis.*, 9(3), DOI: 10.1002/iid3.445

Shin, H., Prasad, V., Lupancu, T., Malik, S., Achuthan, A., Biondo, M., Kingwell, B. A., **Thiem, M.**, Gottschalk, M., Weighardt, H., Förster, I., de Steiger, R., Hamilton, J. A., Lee, K. M.-C. (2023) The GM-CSF/CCL17 pathway in obesity-associated osteoarthritic pain and disease in mice, *Osteoarthritis Cartilage,* S1063-4584(23), DOI: 10.1016/j.joca.2023.05.008

Chapter 1: Introduction

1.1 The immune system

The immune system is a complex system of physical barriers, mediators, and cell populations. Together they mediate defence or inflammatory response mechanisms against a broad spectrum of pathogens, including bacteria, viruses, and parasites, tissue injury, both chemical and mechanical, toxins and even cancer cells. In vertebrates, the immune system is comprised of the innate and adaptive immunity. While innate immune responses provide protection against a broad spectrum of antigens and are rapidly induced, adaptive immune responses are highly specific and acquired over time. However, both responses are strongly interconnected and required to form an effective immune response and long-lasting immunity (Murphy and Weaver, 2017).

Within the innate immune response, physical barriers like the skin and mucosal membranes of the respiratory and gastrointestinal (GI) tract, as well as chemical barriers, including the acidic environment within the stomach and secretion of antimicrobial molecules, are the first line of defence against pathogens. Antimicrobial enzymes, such as lysozyme and pepsin can destroy pathogens through digestion of the bacterial cell wall and proteolysis, respectively. Defensins (antimicrobial peptides) can directly lyse bacterial cell membranes by forming pores. Additionally, a system of plasma proteins, called the complement system, targets and opsonises pathogens for elimination by phagocytosis, which is mediated by immune cells. If pathogens overcome the physical and chemical barriers, innate immune cells are activated and engage in a variety of effector mechanisms to eliminate the pathogen. Activation of innate immune cells is initiated by pathogen-associated molecular patterns (PAMP) or damage-associated molecular patterns (DAMP), which can be recognised by pattern recognition receptors (PRR). Prominent PRR include nucleotide-binding oligomerisation domain (NOD)-, leucine-rich repeat-containing receptors (NLR) and Toll-like receptors (TLR). The innate immune system contains

numerous cell types: innate lymphoid cells (ILC), granulocytes (basophils, eosinophils, and neutrophils), natural killer (NK) cells, mast cells, dendritic cells (DC), and macrophages (Figure 1.1). Neutrophils, DC, and macrophages can eliminate pathogens by phagocytosis. Thereby, pathogens are engulfed and taken up by the phagocytes. Within the cell, pathogens are enclosed in a phagosome that subsequently merges with a lysosome, forming the phagolysosome. Enzymes, formerly contained in the lysosome, break down and kill the pathogen. In some circumstances, however, pathogens can escape the innate immune system due to the development of resistance mechanisms. In this case, the activation of the adaptive immune response is essential to eliminate the pathogen (Murphy and Weaver, 2017).

The adaptive immune response is orchestrated by T cells, B cells, and secreted antibodies (Figure 1.1). T cell activation requires antigen presentation by antigen-presenting cells (APC) such as DC. Therefore, DC are an important link between the innate and adaptive immune system. Once activated DC have taken up and degraded the pathogen intracellularly via phagocytosis, they can present the resulting small pathogen-derived peptide fragments (antigens) in association with their major histocompatibility complex (MHC) molecules on the cell surface. In secondary lymphoid organs, such as the spleen or draining lymph nodes, DC present the antigens to $CD4^+$ or $CD8^+$ T cells via MHC class II and MHC class I (MHC II/MHC I), respectively. Antigens are recognised by T cells through their antigen-specific T cell receptor (TCR) and together with a second co-stimulatory signal this induces T cell priming and activation. Activated naïve T cells proliferate and differentiate into effector T cells. Cytotoxic $CD8^+$ T cells recognise and kill virus-infected cells. In contrast, $CD4^+$ T helper (T_h) cells can further differentiate into functionally distinct subsets (different transcription factors, different cytokines) like T_h1, T_h2, and T_h17 cells. T_h1 cells support the elimination of intracellular viral and bacterial pathogens by enhancing macrophage activation, while T_h2 cells are strongly involved in the immune response against extracellular parasites, allergens, and toxins. Lastly, T_h17 cells promotes the removal of fungi and extracellular

bacteria. Additionally, $CD4^+$ T cells can give rise to regulatory T (T_{reg}) cells, specialised in controlling the immune response to maintain self-tolerance and homeostasis (Murphy and Weaver, 2017).

Activation of B cells requires antigen binding by the respective B cell through the B cell receptor (BCR), which usually detects antigens in their native conformation. Although interaction of B cells with antigen-specific T_h cells is often required, B cell activation can also be T cell-independent, which is dependent on the antigen. Activated B cells can differentiate into plasma cells, continuously supplying the host with pathogen-specific antibodies. Secreted antibodies promote pathogen clearance by neutralisation, complement activation, and labeling of foreign substances for phagocytosis by agglutination or precipitation (Schlageter and Kozel, 1990; Hellwig *et al.*, 2001; Hessell *et al.*, 2007; Forthal, 2008; Murphy and Weaver, 2017).

Natural killer T (NKT) cells and yδ T cells share characteristics of both the innate and adaptive immune response, possibly forming further links between the innate and adaptive immune system (Shin *et al.*, 2005; Kinjo *et al.*, 2005; Peng *et al.*, 2007; Jensen *et al.*, 2008; Pasman and Kasper, 2017).

Although the adaptive immune response needs to be acquired and therefore takes longer to be fully developed, it is highly specific due to the high variability of the TCR and BCR. Moreover, the immunological memory generated secures a rapid response upon re-infection with the same pathogen (Murphy and Weaver, 2017). However, some evidence has also pointed to an immunological memory acquired by the innate immune system, an immunological process called trained immunity (Naik *et al.*, 2017; Christ *et al.*, 2018; Netea *et al.*, 2020; Ochando *et al.*, 2023).

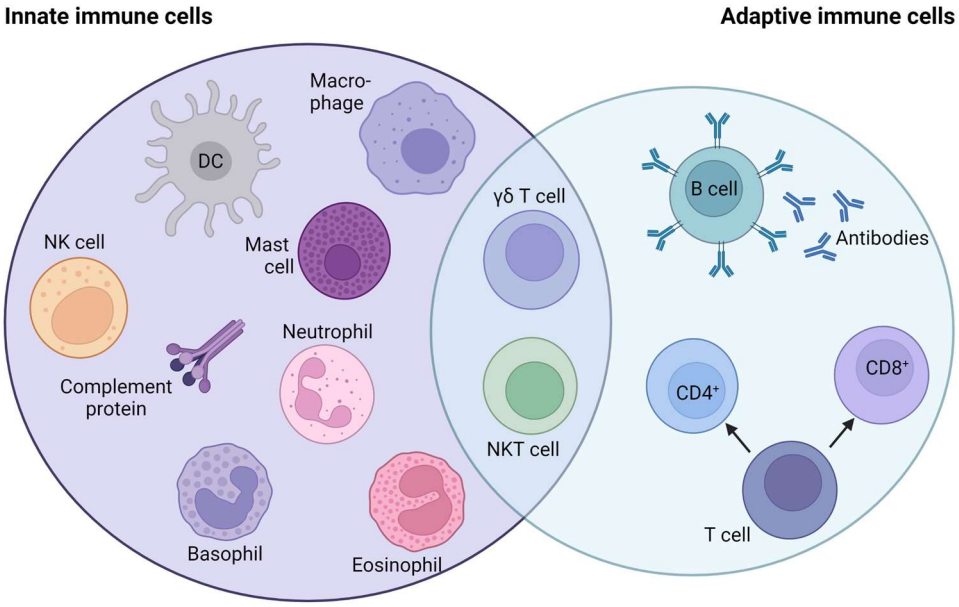

Figure 1.1: Overview of cellular components within the innate and adaptive immune system
Innate immune cells include ILC, granulocytes (basophils, eosinophils, and neutrophils), NK cells, mast cells, dendritic cells (DC), and macrophages. The adaptive immune response is mediated by T cells ($CD4^+$ and $CD8^+$ T cells) and B cells. NKT cells and γδ T cells share characteristics of both the innate and adaptive immune response. The innate immune response is fast acting but limited in specificity, whereas the adaptive immune response takes more time to be activated but is highly specific. (Figure created with BioRender)

1.1.1 The bone marrow – origin of adult haematopoiesis

The bone marrow (BM) is the site of blood cell development, termed haematopoiesis, throughout adult life, ensuring the physiological supply of platelets, red blood cells, and white blood cells (leukocytes). All these cell types arise from pluripotent haematopoietic stem cells (HSC) in a process called haematopoiesis which is depicted in Figure 1.2 (Murphy and Weaver, 2017).

HSC emerge from the yolk sac, the aorta, umbilical arteries, and the placenta early on during the foetal development and colonise the liver at around five weeks of gestation. The liver becomes the main haematopoietic site in the foetus, where the HSC expand, mature, and develop into mature erythroid, lymphoid, and myeloid cells (Medvinsky *et al.*, 1996; Kumaravelu *et al.*, 2002). While extra-embryonic

haematopoiesis, meaning the emergence of HSC from the yolk sac and similar, stops around week 10-12 or E12 in human and mice, respectively, haematopoiesis continues within the liver until 20-24 weeks of gestation or until birth in mice. HSC migrate from the liver to the foetal thymus and spleen. Both sites support the expansion but not the *de novo* synthesis of HSC. During the second trimester in humans or shortly before birth in mice, HSC colonise the BM and give rise to a small pool of HSC, maintaining haematopoiesis throughout adult life (Johnson and Jones, 1973; Johnson and Moore, 1975; Ogawa *et al.*, 1988; Godin and Cumano, 2005; De Kleer *et al.*, 2014). HSC are self-renewing cells which is achieved through asymmetric cell division and results in one daughter cell retaining the HSC characteristics of self-renewal and differentiation potential and one daughter cell differentiating into a specific cell type (Rhyu *et al.*, 1994; Gómez-López *et al.*, 2014). HSC give rise to multipotent progenitors (MPP) (Pronk *et al.*, 2007; Wilson *et al.*, 2008; Pietras *et al.*, 2015). The heterogeneous MPP compartment can be divided into four distinct subsets. MPP1 are similar to HSC (Wilson *et al.*, 2008; Cabezas-Wallscheid *et al.*, 2014) and potentially give rise to functionally distinct and lineage-biased MPP which are characterised as megakaryocyte/erythroid-biased MPP2, granulocyte/macrophage-biased MPP3, and lymphoid-biased MPP4 (Wilson *et al.*, 2008; Cabezas-Wallscheid *et al.*, 2014; Pietras *et al.*, 2015; Bonaud *et al.*, 2021). MPP4 differentiate into common lymphoid progenitors, whereas MPP2 and MMP3 both give rise to common myeloid progenitors with a subsequent bias towards granulocyte/macrophage (GMP) or megakaryocyte/erythrocyte (MEP) progenitors. Additionally, new evidence suggests that MPP2 can also bypass traditional lineage checkpoints and directly differentiate into megakaryocyte progenitors (MkP) (Rodriguez-Fraticelli *et al.*, 2018; Noetzli *et al.*, 2019).

The common lymphoid progenitors are the origin of the lymphoid lineage and can give rise to ILC, NK cells, B cells, and T cells (Murphy and Weaver, 2017). On the other side, common myeloid progenitors can give rise to the myeloid lineage via GMP or MEP. GMP develop into granulocytes (basophils, eosinophils, and neutrophils), monocytes, DC, and macrophages. MEP are the starting point for

development of erythrocytes (erythropoiesis) and megakaryocytes (Murphy and Weaver, 2017). Fate-committed megakaryocyte progenitors (MkP), derived from MEP, develop in distinct stages from megakaryoblasts over promegakaryocytes (PreMegE) to granular megakaryocytes. These megakaryocytes are producers of platelets, which are crucial for thrombosis (Nakorn *et al.*, 2003; Ward *et al.*, 2018). Interestingly, the majority of immature DC arise directly from common myeloid progenitors but can also develop from common lymphoid progenitors (Murphy and Weaver, 2017).

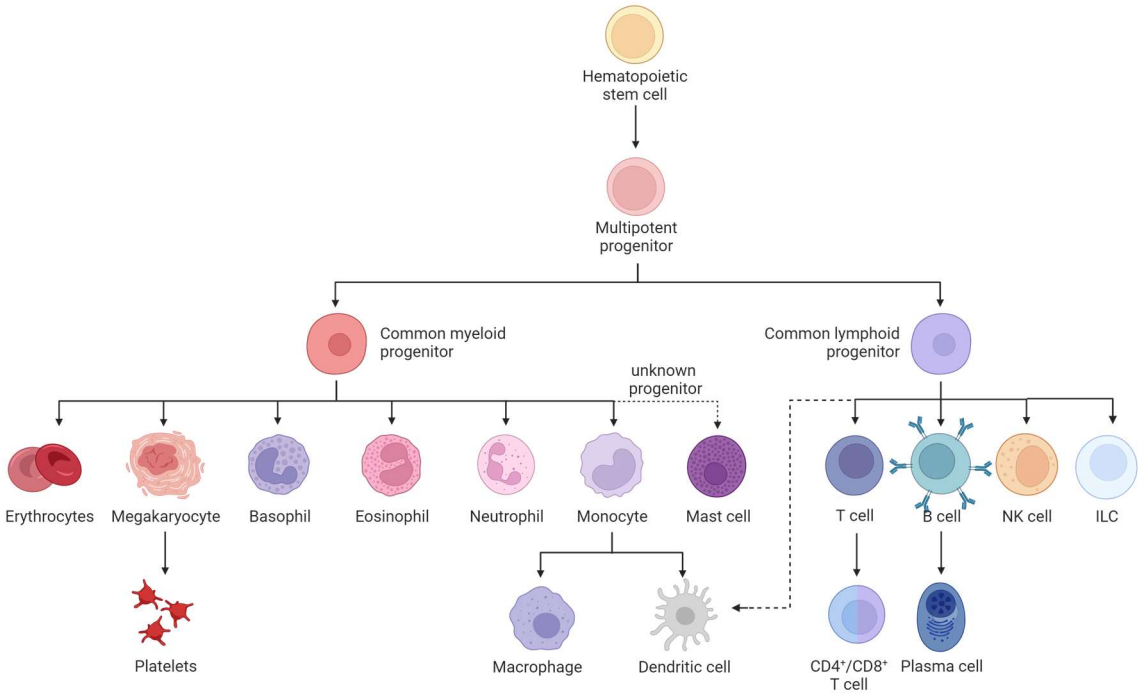

Figure 1.2: Haematopoietic cells derived from haematopoietic stem cells in the BM
HSC give rise to MPP and subsequently two types of common progenitor cells. From a common myeloid progenitor, erythrocytes, megakaryocytes, basophiles, eosinophils, neutrophils, macrophages, DC and mast cells develop. Macrophages and DC differentiate from monocytes in the tissue. Mast cells also differentiate from an unknown progenitor in the tissue. A common lymphoid progenitor gives rise to T cells, B cells, NK cells, and ILC. After antigen encounter, T cells differentiate into $CD4^+$ or $CD8^+$ T cells, while B cells differentiate into antibody-producing plasma cells. (Figure created with BioRender)

The distinct cell fate decisions are determined by environmental cues of the BM. For example, CXCL12, produced by stromal cells in the BM, promotes the differentiation towards the B cell lineage (Beck *et al.*, 2014; Fistonich *et al.*, 2018; Miao *et al.*, 2020). All cell types of the lymphoid and myeloid lineage travel through the blood into tissues or lymphoid organs where they differentiate and mature. Basophils, eosinophils, and neutrophils as well as megakarcyocytes and erythrocytes, however, remain and circulate within the blood (Murphy and Weaver, 2017).

1.1.1.1 Extramedullary haematopoiesis

Although the BM is the primary site for haematopoiesis in adult life, in certain cases generation of blood cells can occur in the periphery, a process called extramedullary haematopoiesis (Bozzini *et al.*, 1970; Kim, 2010). Extramedullary haematopoiesis is caused by microbial infections or diseases with impaired BM function such as leukaemia or myeloproliferative neoplasms (Talmon, 2010; Vassiliou *et al.*, 2012; Bao *et al.*, 2018; Cenariu *et al.*, 2021). In primary myelofibrosis, a disease in which fibrous material gradually replaces BM tissue (BM fibrosis), stem cells and progenitor cells are displaced into the spleen and liver, becoming alternative haematopoietic sites. Simultaneously, alterations of the BM stem cell niche form an environment that is no longer supportive of haematopoiesis (Pereira *et al.*, 1990; Thiele *et al.*, 1992). Main sites of extramedullary haematopoiesis in response to immune responses are spleen and liver. Depending on the disease state, however, induction of haematopoiesis can also occur in the lung, kidneys, and the peritoneal cavity (Holden *et al.*, 2006; Alexander *et al.*, 2015; Singh *et al.*, 2017; Casaccia *et al.*, 2017; Stanchina *et al.*, 2019). Myelopoiesis and high cytokine levels are strong promoter of extramedullary haematopoiesis. In Forkhead-box protein P3 (FoxP3)-deficient scurfy mice levels of granulocyte-macrophage colony-stimulating factor (GM-CSF) and interleukin (IL)-3 are increased due to expansion of $CD11b^+$ myeloid cells and promote the proliferation of haematopoietic progenitor cells (Clark *et al.*, 1999). Lack of $FoxP3^+$ T_{reg} cells drives excessive activation of GM-CSF- and IL-3-producing T cells, thereby promoting excessive extramedullary haematopoiesis. Scurfy mice

could be rescued by introducing functional FoxP3$^+$ T_{reg} cells into newborn pups, which suppressed extramedullary haematopoiesis (Lee *et al.*, 2009). Other factors that can impact haematopoiesis are TLR ligands. As haematopoietic progenitors express TLR, TLR ligands can directly activate those cells. Furthermore, lipopolysaccharide (LPS) injections lead to increased myeloid cell numbers, partially due to the promotion of myeloid cell development from lymphoid progenitors, in the BM and spleen *in vivo* (Nagai *et al.*, 2006). The involvement of TLR and TLR ligands in myelopoiesis suggests a significant impact for infections on haematopoiesis and extramedullary haematopoiesis. Indeed, *Leishmania major* infection caused increased numbers of myeloid progenitors and colony-forming unit cells in the spleens of BALB/c and to a greater extent in C57BL/6 mice (Mirkovich *et al.*, 1986). Defects in extramedullary haematopoiesis are detrimental. While inadequate extramedullary haematopoiesis causes impaired production and maturation of blood cells, excessive extramedullary haematopoiesis results in inflammatory diseases (Kim, 2010; Fernández-García *et al.*, 2020).

1.1.1.2 Erythropoiesis

Erythrocytes are essential for gas exchange and oxygen transport between the lung and the peripheral tissue, assisting in metabolic processes (Ney, 2011). Through ferrous haemoglobin, erythrocytes can bind and transport oxygen to the tissue via the bloodstream. The low pH and the decreased oxygen pressure in the tissue decreases the affinity of haemoglobin to oxygen, thereby releasing and supplying oxygen to the tissue. The erythrocyte takes up carbon dioxide and transports it to the lung where it is exhaled (Browne, 1868; Kuhn *et al.*, 2017).

Mature erythrocytes are generated from BM-derived erythropoietic progenitors in a process called erythropoiesis (Moras *et al.*, 2017; Murphy and Weaver, 2017). It is a continuous process and generates approximately $2.5x10^6$ erythrocytes per second in humans (Palis, 2014; Seu *et al.*, 2017). The production of erythrocytes, however, is counteracted by the elimination of senescent erythrocytes in the spleen and to some part in the liver (Kay, 1975; Stijlemans *et al.*, 2015; Theurl *et al.*, 2016; Klei *et*

al., 2017). This balance ensures optimal oxygen delivery to the tissue while preventing blood viscosity due to high blood cell numbers (Paulson *et al.*, 2020).
During haematopoiesis in the BM, HSC give rise to MPP and subsequently to MEP, which are the starting point for the development of mature erythrocytes (Sun *et al.*, 2014; Busch *et al.*, 2015; Karamitros *et al.*, 2018; Tusi *et al.*, 2018) (Figure 1.3). Within the BM, MEP differentiate into erythroid-restricted progenitors, also called burst forming unit-erythroid, which themselves give rise to colony-forming unit-erythroid (CFU-E) and subsequently proerythroblasts (ProEry). Afterwards, the terminal erythroid differentiation is initiated during which erythroid-committed progenitors maturate into reticulocytes (Dzierzak and Philipsen, 2013; Moras *et al.*, 2017). ProEry accumulate around one central macrophage, forming an erythroblastic island (Bessis, 1958; Manwani and Bieker, 2008; Chasis and Mohandas, 2008). The macrophage provides iron and facilitates both proliferation and differentiation (Bessis and Breton-Gorius, 1957; Bessis and Breton-Gorius, 1962; Rhodes *et al.*, 2008; Moras *et al.*, 2017). Gradually, ProEry undergo chromatin condensation and cell size reduction, initiate haemoglobin production, and show a reduced proliferative activity (Dzierzak and Philipsen, 2013; Moras *et al.*, 2017). They differentiate into basophilic erythroblasts, followed by polychromatic and orthochromatic erythroblasts. Orthochromatic erythroblasts develop into reticulocytes, also called immature erythrocytes. In this process, they expel their nucleus, thereby generating pyrenocytes (Yoshida *et al.*, 2005), and lose all of their organelles, including the endoplasmatic reticulum, the mitochondria, and the Golgi apparatus. Pyrenocytes, which consist of the nucleus surrounded by the plasma membrane, are taken up and eliminated by the central macrophage of the erythroblastic island (Yoshida *et al.*, 2005). The remaining membrane-bound organelles are further eliminated by the reticulocyte through a combinatorial pathway of autophagy and exosomes (Gronowicz *et al.*, 1984; Dubiel and Rapoport, 1989; Blanc *et al.*, 2005; Koury *et al.*, 2005). Additionally, the reticulocyte loses between 20 to 30 % of its cell surface during the maturation process (Waugh *et al.*, 1997; Da Costa *et al.*, 2001). Reticulocytes are released from the erythroblastic island and

enter the bloodstream (Chasis *et al.*, 1989) where they complete their maturation into functional erythrocytes through membrane-cytoskeleton rearrangement leading to the typical and flexible biconcave form of mature erythrocytes (Mel *et al.*, 1977; Waugh *et al.*, 1997; Waugh *et al.*, 2001; Malleret *et al.*, 2013). The reticulocyte population is very heterogeneous, encompassing various stages until they become erythrocytes, differing in morphology, size, metabolic state, and the expression of surface markers like CD71 (Malleret *et al.*, 2013; Ovchynnikova *et al.*, 2017). Maturation of reticulocytes into erythrocytes takes approximately one to two days in the circulation (Chasis *et al.*, 1989).

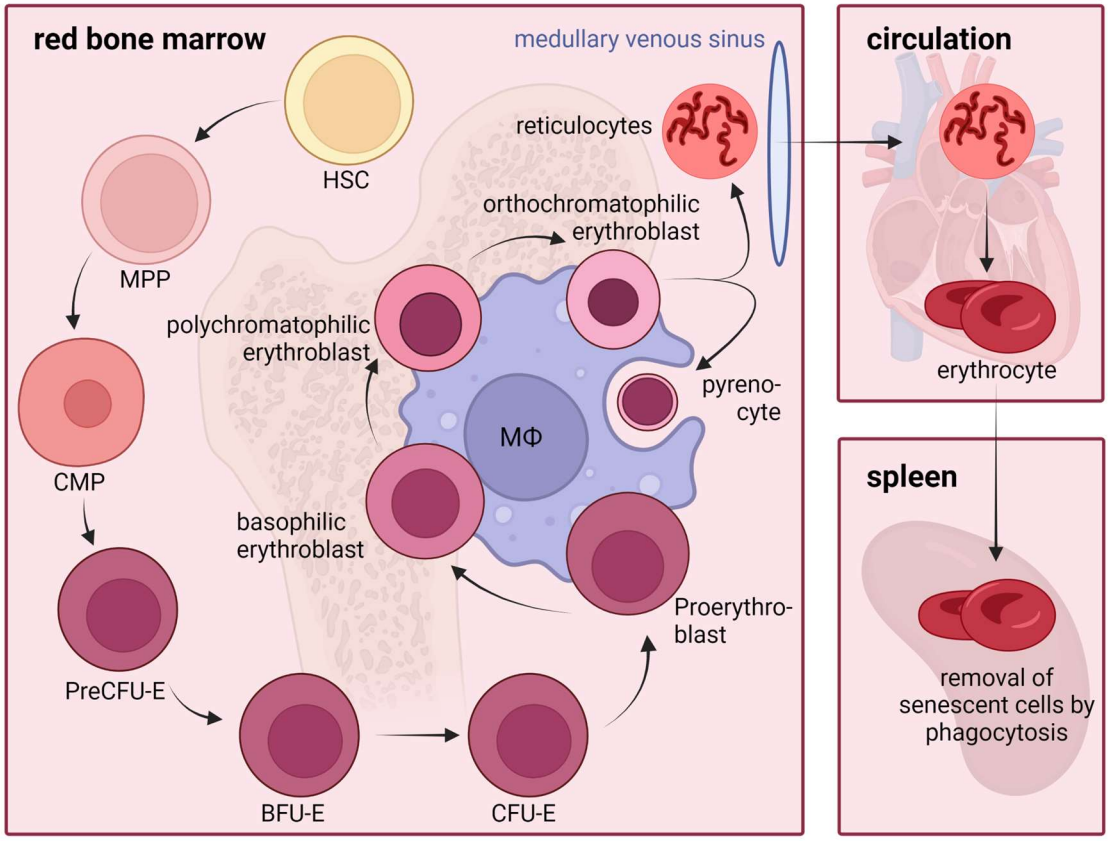

Figure 1.3: Generation of erythrocytes
HSC give rise to MPP, followed by CMP. CMP commit to the erythroid lineage and differentiate subsequently into MEP, BFU-E, CFU-E, and ProEry. ProEry attach to and accumulate around one central macrophage, forming an erythroblastic island. At this erythroblastic island terminal erythroblast differentiation is initiated. Gradually, ProEry undergo chromatin condensation and cell size reduction, developing from basophilic to polychromatic and orthochromatic erythroblasts. Orthochromatic erythroblasts shed their nucleus, thereby generating each a reticulocyte and pyrenocyte. The pyrenocytes are removed through phagocytes by the central macrophage, while reticulocytes leave the BM and enter the circulation. Within the circulation, reticulocytes mature into erythrocytes, losing all of their remaining organelles and undergo membrane-cytoskeleton rearrangement. Mature erythrocytes travel to the bloodstream and exchange oxygen and carbon dioxide between the lung and tissues. Senescent erythrocytes are removed through phagocytes, primarily in the spleen. (Figure created with BioRender).

The main regulator of erythropoiesis is erythropoietin, a hormone that promotes the proliferation and differentiation of erythrocyte progenitors as well as inhibiting erythroblast apoptosis (Ji *et al.*, 2011). Additionally, the central macrophage of the

erythroblastic island is crucial for the terminal erythroid differentiation. Numerous proteins mediate the interaction between the erythrocytes and the macrophage. Most prominent is the erythroblast-macrophage protein expressed on the cell surface of both macrophages and erythroblasts which mediates attachment between the cell types. While mice deficient for the erythroblast-macrophage protein survive until birth, they show impaired erythroblastic island formation, absent interaction between the macrophage and erythroblasts, and defects in terminal erythroid maturation (Soni *et al.*, 2006).

Although the BM is the primary site of erythropoiesis, it can also occur in the spleen when BM erythropoiesis is impaired (Greenwald *et al.*, 2019; Jing *et al.*, 2021). Certain infection-induced inflammations can suppress erythropoiesis in the BM, meanwhile enhancing splenic erythropoiesis (Jackson *et al.*, 2010; Millot *et al.*, 2010; Chou *et al.*, 2012).

1.1.2 Immunology in the gastrointestinal tract

The gastrointestinal (GI) tract is exposed to a broad range of commensal microbes and dietary antigens. It is the site for digestion and uptake of nutrients while simultaneously maintaining immune homeostasis and differentiating between the commensal gut microbiota and invading pathogens. This is achieved by the extraordinary architecture of the GI tract. Numerous levels of infolding generate a large overall surface area. The immense surface area grants maximal nutrient uptake and holds the largest immune cell number throughout the body (Mason *et al.*, 2008).

The mucosal immune defence is comprised of the intestinal epithelial barrier, the gut-associated lymphoid tissue (GALT), and the lamina propria. Functionally, it can be separated into inductive and effector sites. Inductive sites are localised at highly organised aggregations of lymphoid follicles including mesenteric lymph nodes (mLN), isolated lymphoid follicles (ILF), and Peyer's patches (PP) (Mowat and Viney, 1997; Brandtzaeg *et al.*, 2008; Mason *et al.*, 2008). Within these inductive sites, sampled antigens activate B and T cells (Weinstein and Cebra, 1991; Lorenz and

Newberry, 2004; Lécuyer *et al.*, 2014; Ahluwalia *et al.*, 2017). Effector functions, however, are performed at effector sites that are found throughout the epithelium and the lamina propria. Consequently, effector cells are more broadly dispersed within the tissues (Mowat and Viney, 1997; Mowat, 2003; Brandtzaeg *et al.*, 2008; Mason *et al.*, 2008).

The intestinal epithelium is formed by a monolayer of intestinal epithelial cells (IECs) such as endocrine cells, enterocytes, microfold (M) cells, Paneth cells, and Goblet cells (Figure 1.4). IECs and the mucosal layer separate the gut lumen from the underlying lamina propria and form the main biochemical and physical barrier against invading microorganisms (Johansson *et al.*, 2008; Scaldaferri *et al.*, 2012; Shimada *et al.*, 2013; Peterson and Artis, 2014; Choi *et al.*, 2023). The selectivity of the intestinal barrier guarantees an exclusion of foreign substances or antigens while allowing the absorption of nutrients, electrolytes, and water (Groschwitz and Hogan, 2009; Bischoff *et al.*, 2014). Loss of integrity is associated with the pathogenesis of various GI diseases, such as irritable bowel syndrome and inflammatory bowel disease (Scaldaferri *et al.*, 2012; Öhman *et al.*, 2015; Chao *et al.*, 2017; Awad *et al.*, 2023). Additionally, Paneth cells secrete antimicrobial proteins such as defensins and lysozymes that can disrupt the cell surface of pathogens (Wilson *et al.*, 1999; Bevins and Salzman, 2011; Gallo and Hooper, 2012; Schroeder *et al.*, 2015; Bel *et al.*, 2017).

The primary inductive site of the mucosal immune defence are PP, which are mostly localised in the distal ileum (Mason *et al.*, 2008). Their structural organisation resembles that of lymph nodes (Figure 1.4). Large B cell follicles are intercepted with smaller T cell zones and surrounded by a dome-like structure, called the subepithelial dome (SED). The SED is covered by a single layered follicle-associated epithelium (FAE) and thereby separated from the intestinal lumen. The FEA contains M cells, which continuously mediate luminal antigen uptake via endocytosis and phagocytosis and transport the antigens to APC within the underlying SED (Mantis *et al.*, 2002; Hase *et al.*, 2009; Lelouard *et al.*, 2012; Mabbott *et al.*, 2013; Sakhony *et al.*, 2015; Jinnohara *et al.*, 2017). Subsequently, APCs can present the antigens

to T cells in the PP or the mLN. Activated lymphocytes emigrate from the PP and mLN and enter the bloodstream, from where they can selectively re-enter the intestinal effector sites (Murphy and Weaver, 2017).

The lamina propria, one of the two effector sites, is a layer of loosely packed connective tissue beneath the intestinal epithelium and houses the majority of intestinal immune cells, including ILC, DC, macrophages, mast cells, and IgA-secreting plasma cells as well as effector B and T cells (Wershil and Furuta, 2008; Mason *et al.*, 2008). The other effector site, the intestinal epithelium, contains primarily intraepithelial lymphocytes that show both effector and regulatory functions (Denning *et al.*, 2007; Masopust *et al.*, 2010; Mowat and Agace, 2014).

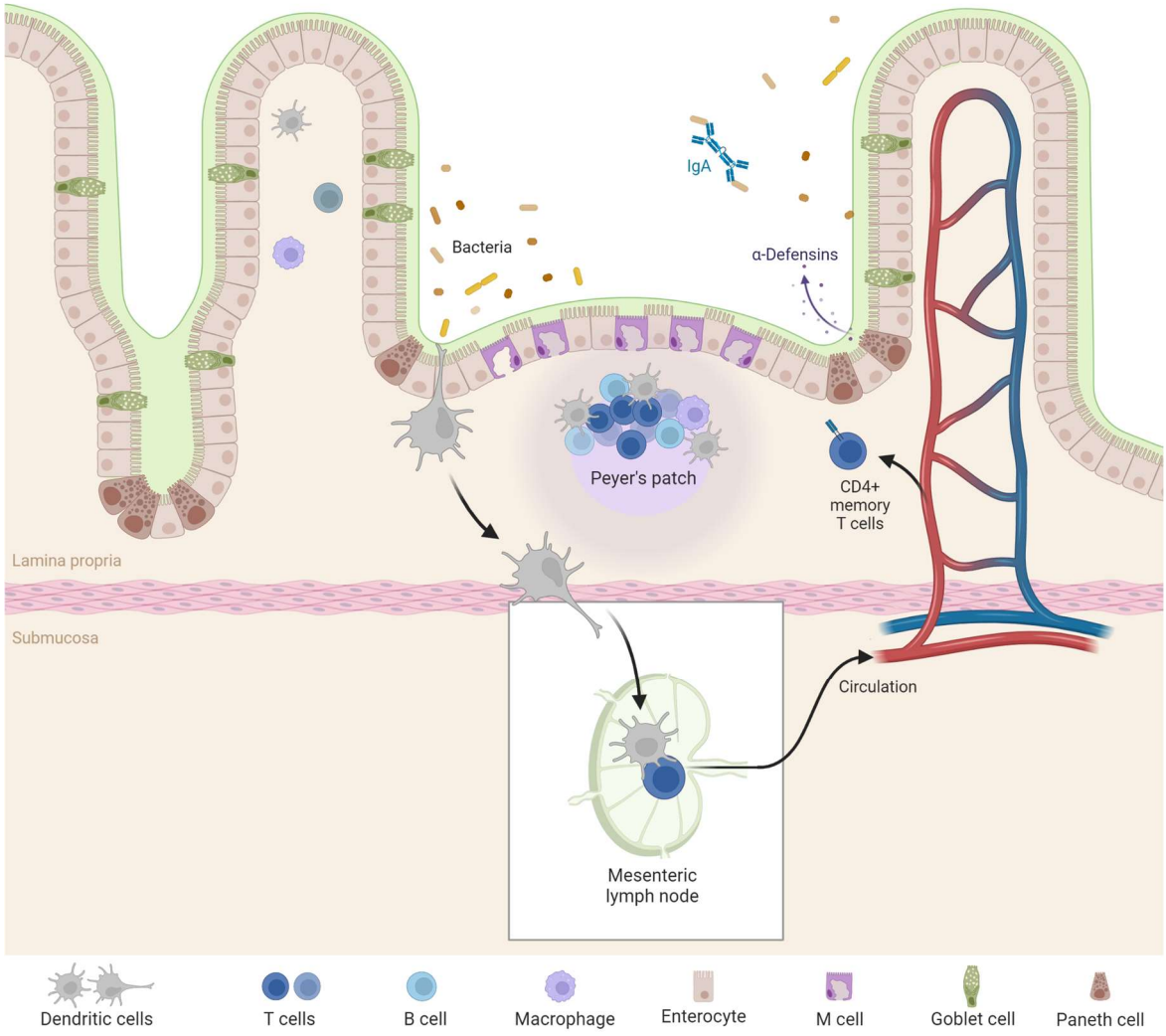

Figure 1.4: Organisation of the mucosal immune defence
The intestinal epithelium is formed by a monolayer of intestinal epithelial cells (IEC) including enterocytes, M cells, Goblet cells, and Paneth cells, and separates the gut lumen from the underlying lamina propria. Paneth cells secrete antimicrobial proteins like defensins, while Goblet cells produce the mucus covering the epithelium. PP contains B cell follicles intercepted with smaller T cell zones and are surrounded by the subepithelial dome (SED). They are separated from the gut lumen by a single layered follicle-associated epithelium (FAE), which is rich in M cells continuously sampling and transporting antigens to underlying DC. DC migrate towards the mLN and present antigens to T cells. Activated T cells enter the circulation and can re-enter the lamina propria or intestinal epithelium to execute effector functions. (Figure created with BioRender)

1.1.3 Regulatory T cells

T_{reg} cells play a central role in maintaining tissue homeostasis and immune tolerance, thereby, preventing the development of autoimmune diseases (Sakaguchi *et al.*, 1995; Wang *et al.*, 2007; Piao *et al.*, 2008). Although the idea of suppressor T cells already arose in the early 1970s (Gershon and Kondo, 1970; Gershon and Kondo, 1971), $CD4^+$ $CD25^+$ T_{reg} cells, suppressing the T cell response, were first discovered in 1995 (Sakaguchi *et al.*, 1995). Several studies have since confirmed the suppressive activity of T_{reg} cells on activation, cytokine production, and proliferation of effector T cells (Thornton and Shevach, 1998a; Takahashi *et al.*, 2000; Oberle *et al.*, 2007; Frimpong-Boateng *et al.*, 2010; Sojka and Fowell, 2011; Faustino *et al.*, 2012; Dowling *et al.*, 2018; Sakurai *et al.*, 2020). Development, maintenance, and function of T_{reg} cells is dependent on the transcription factor FoxP3. Indeed, ectopic expression of FoxP3 provides $CD4^+$ effector T_h cells with a T_{reg} cell phenotype and suppressive functions (Hori *et al.*, 2003; Sakaguchi, 2004; Fontenot *et al.*, 2017). Absence of FoxP3 leads to severe autoimmunity in both humans and mice (Wildin *et al.*, 2001; Brunkow *et al.*, 2001), highlighting the critical role of T_{reg} cells in mediating immune tolerance.

T_{reg} cells arise from two different pathways. Thymus-derived T_{reg} (tT_{reg}) cells develop within the thymus upon strong TCR stimulation via the recognition of a self-antigen and a CD28 co-stimulatory signal (Owen *et al.*, 2019; Santamaria *et al.*, 2021). In contrast to conventional T (T_{conv}) cells, meaning effector T_h cells, the TCR repertoire of tT_{reg} cells is highly self-reactive, defining $CD4^+$ T cell subtype fate (Romagnoli *et al.*, 2002; Hsieh *et al.*, 2004; Pacholczyk *et al.*, 2006; Klein *et al.*, 2019). Peripheral T_{reg} (pT_{reg}) cells, however, can develop from naïve $CD4^+$ T cells in secondary lymphoid tissues. This transformation is induced upon antigen exposure and in the presence of transforming growth factor-beta (TGF-β) under inflammatory and non-inflammatory conditions (Chen *et al.*, 2003; Abbas *et al.*, 2013; Yadav *et al.*, 2013). pT_{reg} cells mainly mediate intestinal immune tolerance towards dietary antigens and the gut microbiota. Kim *et al*. showed that the abnormal T_h1 response to dietary antigens was suppressed by pT_{reg} cells (Kim *et al.*, 2016). Additionally, pT_{reg} cells are

essential in the immune response against intestinal pathogens and either promote or suppress the inflammatory response (Xu *et al.*, 2018; Yordanova *et al.*, 2019; Cosovanu and Neumann, 2020). Conserved non-coding sequence 1 (CNS1) is a regulatory element needed for *Foxp3* gene transcription (Josefowicz *et al.*, 2012). CNS1-deficient mice showed an impairment in pT_{reg} cells, but not tT_{reg} cells, generation, leading to the spontaneous development of inflammation in the lung and gastrointestinal tissue.

To distinguish between tT_{reg} cells and pT_{reg} cells, a variety of markers have been tested. Most broadly used are the transcription factor Helios and surface receptor Neuropilin-1 (Nrp1) (Yadav *et al.*, 2012; Weiss *et al.*, 2012; Koizumi and Ishikawa, 2019). Within the thymus, $FoxP3^+$ T_{reg} cells show high Helios expression, whereas Helios expression is only found on approximately 70 % of T_{reg} cells in the periphery (Thornton *et al.*, 2010). However, *in vitro* generated T_{reg} cells and pT_{reg} cells show upregulation of Helios as the transcription factor is induced during T cell activation (Akimova *et al.*, 2011; Gottschalk *et al.*, 2012). In contrast, Nrp1 appears to be exclusively expressed on tT_{reg} cells (Yadav *et al.*, 2012). Treatment of ovalbumin-specific TCR.Tg BALB/c mice with low doses of antigen generated pT_{reg} cells that failed to express Nrp1 (Yadav *et al.*, 2012). Similarly, mucosa-generated pT_{reg} cells showed low Nrp1 expression levels compared to tT_{reg} cells. Nrp1 is upregulated in T_{reg} cells shortly before emigration from the thymus (Weiss *et al.*, 2012). Although Nrp1 can be used to distinguish tT_{reg} cells and pT_{reg} cells in circulating cells, it has to be noted that this is not the case in inflamed tissues as pT_{reg} cells can upregulate Nrp1 during inflammation (Weiss *et al.*, 2012; Yadav *et al.*, 2013).

T_{reg} cell subsets are heterogeneous and can be further separated based on their activation status. tT_{reg} cells leaving the thymus and circulating within secondary lymphoid organs are classified as naïve-like central T_{reg} cells. Upon antigen encounter, the tT_{reg} cells become activated and differentiate into effector T_{reg} cells, marked by the upregulation of effector molecules, including inducible T cell costimulator (ICOS), glucocorticoid-induced TNFR-related protein (GITR), and killer cell lectin-like receptor subfamily G member 1 (KLRG1). All of these effector

molecules contribute to the increased suppressive activity of effector T_{reg} cells (Smigiel *et al.*, 2014; Levine *et al.*, 2014; Vasanthakumar *et al.*, 2015; Dias *et al.*, 2017). KLRG1^{+} T_{reg} cells, for example, have been shown to exhibit greater suppressive capacity than their KLRG1^{-} counterparts *in vitro* (Cheng *et al.*, 2012; Yates *et al.*, 2018). Moreover, KLRG1^{+} T_{reg} cell numbers are positively correlated in numerous autoimmune diseases such as experimental autoimmune encephalomyelitis where their number increases with disease severity. They were also found to produce higher levels of interferon gamma (IFNy) and IL-10 (Tauro *et al.*, 2013).

Suppression mechanisms of T_{reg} cells include the secretion of immunosuppressive mediators as well as contact-dependent mechanisms. Secreted mediators include the anti-inflammatory cytokines IL-10 and TGF-β as well as perforin and the serine protease granzyme B, both of which induce apoptosis (Grossman *et al.*, 2004; Gondek *et al.*, 2005; Cao *et al.*, 2007; Schmidt *et al.*, 2012). Upregulation of CTLA4 leads to downregulation of CD80/CD86 on APCs and thereby indirectly to the inhibition of T_{conv} (Cederbom *et al.*, 2000; Oderup *et al.*, 2006; Onishi *et al.*, 2008).

Additionally, T_{reg} cells can upregulate the T_h-specific transcription factors T-bet (T_h1), GATA3 (T_h2), and RORyt (T_h17) which is associated with the suppression of the specific T_h subset. Absence of T-bet^{+} T_{reg} cells, for example, caused abnormal T_h1 activation without any effect on T_h2 and T_h17 cells (Levine *et al.*, 2017). In contrast, mice lacking GATA3^{+} T_{reg} cells exhibit severe skin inflammation characterised by an increased type 2 immune response (Wang *et al.*, 2011; Harrison *et al.*, 2018). Analysis of the specific subsets has revealed that T-bet is highly expressed in colonic T_{reg} cells (50-60 %) and to lower percentages (20-40 %) in T_{reg} cells of the lymphoid tissue, lung, liver, and small intestine (Koch *et al.*, 2009), whereas GATA3^{+} T_{reg} cells are mainly found in the skin (80 %) and colon (30 %) (Wohlfert *et al.*, 2011; Schiering *et al.*, 2014). RORyt T_{reg} cells are found in the colon (65 %) and small intestine (35 %). Interestingly, the majority of RORyt T_{reg} cells are considered Nrp1^{-} Helios1^{-} pTreg. They have been found to be involved in a broad spectrum of immune response impairments, depending on the environmental cues (Sefik *et al.*, 2015;

Ohnmacht *et al.*, 2015). T_{reg} cell-specific RORyt-deficient mice have been shown to have an accelerated T_h2 cell immune response under T_h2-inducing conditions (Ohnmacht *et al.*, 2015), elevated T_h17 cell and T_h1 cell cytokine production in the colon (Sefik *et al.*, 2015), and a critical role in suppression of T_h17 cell-dependent chronic gut inflammation (Xu *et al.*, 2017).

1.1.4 Chemokines and chemokine receptors

Chemokines are a large family of small, 8-10 kDa, secreted cytokines whose key feature is the recruitment (Luster, 1998; Zlotnik *et al.*, 2006; Sells and Hwang, 2010; Arimont *et al.*, 2017) and retention of leukocytes in both homeostasis and immune responses (Solari and Pease, 2015). Other cellular functions mediated by chemokines are cell spreading, proliferation, and cytokine secretion (Cronshaw *et al.*, 2004). Based on the positioning of their N-terminal cysteine residues, they can be classified into four subclasses: CC, CXC, C, and CX_3C chemokines (Clore *et al.*, 1990; Lodi *et al.*, 1994; Skelton *et al.*, 1995; Handel and Domaille, 1996; Kufareva *et al.*, 2015). The cysteine residues form disulfide-bonds and thereby determine the chemokine structure. Chemokines are further separated by their function and expression pattern. Inflammatory chemokines are induced at high levels in many different tissues or cell types upon stimulation or under pathological conditions. In contrast, homeostatic chemokines are constitutively secreted in discrete locations (Cronshaw *et al.*, 2004). So far, approximately 50 members of the chemokine family have been identified in humans and mice (Griffith *et al.*, 2014).

Chemokines signal through one or several of the approximately 20 G-protein coupled chemokine receptors (GPCRs) (Viney *et al.*, 2014; Griffith *et al.*, 2014) containing seven transmembrane domains (Fujimoto *et al.*, 2008) and being differentially expressed on leukocytes (Griffith *et al.*, 2014). Next to the conventional chemokine receptors, four atypical chemokine receptors (ACKR) have been identified. ACKR structurally resemble conventional chemokine receptors but are unable to initiate classical chemokine receptor signaling pathways (Hansell *et al.*, 2011). Due to their ability to internalise chemokines, ACKRs are also considered as

scavengers or decoy receptors. Their unconventional signaling properties cannot be explained by molecular or structural characteristics because all four ACKRs show no distinct sequence motifs (Nibbs and Graham, 2013).

In general, chemokine receptors are promiscuous in ligand-specificity meaning that one receptor can recognise many different chemokines and *vice versa* (Nibbs and Graham, 2013). Additionally, chemokines can bind to each other forming hetero- or homodimers further increasing the complexity of chemokine signaling (Von Hundelshausen *et al.*, 2017).

Overall, chemokines and their associated receptors are of great importance in a variety of diseases with an inflammatory component including asthma and rheumatoid arthritis (Koch *et al.*, 1992; Rathanaswami *et al.*, 1993; Koch *et al.*, 1994; Zlotnik *et al.*, 2006; Solari and Pease, 2015).

1.1.4.1 The CCL17/CCL22/CCR4-axis

CCR4 is expressed to varying degrees by T lymphocytes, especially the $CD4^+$ T cell subset (Bonecchi *et al.*, 1998; Wakugawa *et al.*, 2001; Solari and Pease, 2015), NK cells, macrophages, and DC (Poppensieker *et al.*, 2012; Ruland *et al.*, 2017). High CCR4 expression can further be found in skin-homing cutaneous lymphocyte antigen $(CLA)^+$ T cells (J. J. Campbell *et al.*, 1999). In patients suffering from severe atopic dermatitis, levels of both CCR4 and CLA were shown to be increased on the surface of peripheral blood $CD4^+$ T cells. Improvement of the symptoms led to a decrease in CCR4 expression (Wakugawa *et al.*, 2001). Up to date, CCR4 is the only known chemokine receptor for CCL17 and CCL22 (Santulli-Marotto, Boakye, *et al.*, 2013; Yoshie and Matsushima, 2015), although CCR8 is discussed as a second receptor for CCL17 in humans (Panina-Bordignon *et al.*, 2001).

Both chemokines are involved in the recruitment of T cells (Curiel *et al.*, 2004; Weber *et al.*, 2011; Wiedemann *et al.*, 2016; Fülle *et al.*, 2018), the facilitation of DC-T cell interaction (Semmling *et al.*, 2010; Rapp *et al.*, 2019) and sensitisation of DC migration (Stutte *et al.*, 2010; Bischoff *et al.*, 2015) (Figure 1.5). However, CCL17 and CCL22 differ in their distinct signaling pathways and functions, a phenomenon

that has been termed biased agonism (Rajagopal *et al.*, 2013; Anderson *et al.*, 2016).

CCL17, also known as thymus and activation-regulated chemokine (TARC), maintains localised inflammation through the recruitment of immune cells (Santulli-Marotto *et al.*, 2015; Fülle *et al.*, 2018), especially T_h1 and T_h2 cells as well as DC (Stutte *et al.*, 2010; Weber *et al.*, 2011). Additionally, CCL17 enhances the responsiveness of cutaneous DC to CCL19/20 and CXCL12, the ligands of CCR7 and CXCR4, respectively, promoting emigration from the skin (Stutte *et al.*, 2010). The chemokine was first found in the thymus (Lieberam and Förster, 1999) and subsequently in all major barrier organs and secondary lymphoid tissues, including the skin, lung, intestine and draining lymph nodes (Alferink *et al.*, 2003; Heiseke *et al.*, 2012; Solari and Pease, 2015). Within these tissues, CCL17 is not only produced by DC (Alferink *et al.*, 2003) and macrophages (Katakura *et al.*, 2004) but also blood endothelial cells (Achuthan *et al.*, 2016) and epidermal keratinocytes (Fujimoto *et al.*, 2008). In addition, *in vitro* stimulation of corneal and dermal fibroblasts with the T_h2 cell cytokines IL-4 and IL-13 caused CCL17 production (Fukuda *et al.*, 2003). CCL17 can interact with CCL5 increasing its potency. Further interaction partners are CCL21, CCL25, CCL26, CCL28, CXCL4, and CXCL17 (Von Hundelshausen *et al.*, 2017). CCL17 has been extensively studied in inflammatory and allergic diseases. It is associated with the enhancement of contact-hypersensitivity, atopic dermatitis, colitis, arthritis and atherosclerosis (Alferink *et al.*, 2003; Stutte *et al.*, 2010; Weber *et al.*, 2011; Heiseke *et al.*, 2012; Achuthan *et al.*, 2016). Similar to mice, CCL17 was also demonstrated to be upregulated in allergic contact dermatitis, atopic dermatitis and atherosclerosis in humans (Vestergaard *et al.*, 2000; Greaves *et al.*, 2001; Kamsteeg *et al.*, 2010).

In contrast, CCL22 or macrophage-derived chemokine (MDC) plays a more immunosuppressive role and is associated with the maintenance and recruitment of T_{reg} cells to inflammatory sites and the tumor microenvironment (Mizukami *et al.*, 2008; Li *et al.*, 2013; Chang *et al.*, 2016; Rapp *et al.*, 2019). The chemokine is predominantly produced by DC, although macrophages and B cells can also secrete

CCL22 (Schaniel *et al.*, 1998; Vulcano *et al.*, 2001; Rapp *et al.*, 2019). Under physiological conditions, CCL22 is expressed in the thymus, lymph nodes and PP. However, low levels could also be detected in the lung, spleen and colon (Rapp *et al.*, 2019). CCL22 promotes chemotaxis via two pathways: (i) the common Gαi-induced activation of the phosphoinositide 3-kinase (PI3K)/protein kinase B pathway and (ii) a unique β-arrestin-mediated activation of p38 mitogen-activated protein kinase (p38 MAPK) and Rho kinase (Cronshaw *et al.*, 2004; Santulli-Marotto *et al.*, 2015; Lin *et al.*, 2018; DeFea, 2018). CCL22-induced chemotaxis is distinctly reduced in β-arrestin-2-deficient mice. In addition, inhibition of PI3K in those mice completely abolishes chemotaxis, whereas some residual migration is observed in wild-type mice (DeFea, 2018; Lin *et al.*, 2018). Interestingly, dipeptidyl peptidase 4 (CD26) can cleave the N-terminal amino acids of CCL22 resulting in a truncated version that can still bind to and internalise the receptor without inducing agonist-specific signaling pathways (Ajram *et al.*, 2014). Like CCL17, CCL22 can interact with other chemokines including CCL14, CCL19, and CXCL4L1 modifying its activity (Von Hundelshausen *et al.*, 2017). Usage of CCL22 neutralising antibodies or artificial increase of CCL22 demonstrated the relevance of CCL22 in diverse pathologies such as autoimmunity and tumor growth (Curiel *et al.*, 2004; Bischoff *et al.*, 2015; Wiedemann *et al.*, 2016).

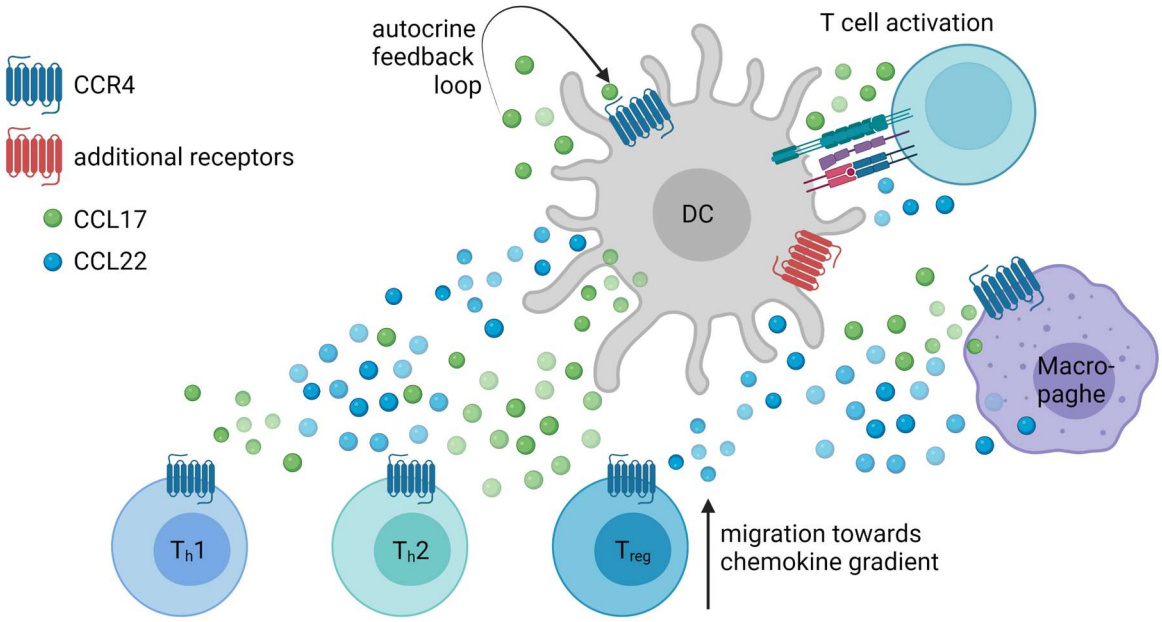

Figure 1.5: Source and functions of CCL17 and CCL22
CCL17 and CCL22 are primarily produced by DC and macrophages. Both induce chemotaxis and facilitate DC-T cell interaction, thereby promoting T cell activation. CCL17 and CCL22 share the chemokine receptor CCR4 which is expressed by various T cell subsets, including T_h1 cells, T_h2 cells, and T_{reg} cells but also on DC and macrophages themselves, inducing a positive autocrine feedback loop. (Figure created with BioRender)

CCL22 shows dominance over CCL17 regarding receptor-binding affinity, receptor internalisation and desensitisation (Viney *et al.*, 2014; Santulli-Marotto *et al.*, 2015). Both chemokines can induce calcium flux and desensitisation to a second identical stimulus. However, in heterologous desensitisation experiments it was shown that CCL22 desensitises the receptor for a second CCL17 stimulus, whereas a subsequent CCL22 stimulus to CCL17 still induces a calcium influx. Viney *et al.* (2014) characterised two different conformations of CCR4, which could explain these subtle differences. The major population can bind both chemokines. Meanwhile, the minor population is only able to be activated through CCL22. Therefore, CCL17 can only engage one receptor conformation, leaving the second population open to be activated by CCL22. In addition, the major population seems to rely upon K310, localised in helix VIII at the C-terminal region, for chemokine-induced activation.

Point mutations caused unresponsiveness towards CCL17 in chemotaxis assay but only reduced potency for CCL22. Both receptor states appear to be fixed and not interconvertible (Viney *et al.*, 2014).

The implication or involvement of the CCL17/CCL22/CCR4-axis in a variety of inflammatory and allergic diseases and cancer conditions (Vestergaard *et al.*, 2000; Thompson *et al.*, 2001; Cronshaw *et al.*, 2004; Wiedemann *et al.*, 2016) led to extensive research on anti-CCR4 biologics and small molecule antagonists for therapeutic approaches. Only one CCR4 antagonist has made it into clinical trials for the treatment of asthma but the study was later discontinued because of low target engagement (Ketcham *et al.*, 2018). On the contrary, the monoclonal CCR4-specific antibody Mogalizumab was approved for the treatment of relapsed or refractory adult T cell lymphoma in Japan in 2012 (Solari and Pease, 2015). Interestingly, treatment of cutaneous T cell lymphoma with Mogalizumab often caused skin rashes in patients (Trum *et al.*, 2022).

1.1.4.2 Atypical chemokine receptors

In contrast to the conventional chemokine receptors, ACKR are unable to initiate classical chemokine receptor signaling pathways (Hansell *et al.*, 2011). So far, there are four ACKRs characterised: ACKR1 or Duffy Antigen Receptor for Chemokines (DARC), ACKR2 or D6, ACKR3 or CC-chemokine receptor-like 1 (CCRL1), and ACKR4 or CXCR7. Their ligand specificity was defined using primary cells and immortalised cell lines expressing the exogenous ACKRs. ACKR1 binds to a broad range of CC- and CXC-chemokines (Gardner *et al.*, 2004; Novitzky-Basso and Rot, 2012). Human ACKR2 also shows a wide range for binding CC-chemokines, although the receptor has a more limited ligand repertoire in mice (Savino *et al.*, 2009; Bonecchi and Graham, 2016). ACKR3 and ACKR4 are more selective in their ligand-specificity, each only binding 2-3 chemokines (Balabanian *et al.*, 2005; Nibbs and Graham, 2013; Montpas *et al.*, 2018; Friess *et al.*, 2022). CCL17 can be sequestered by ACKR1 (Gardner *et al.*, 2004), whereas ACKR2 preferentially binds

to CCL22, although it regulates the activity of both chemokines (Santulli-Marotto, Boakye, *et al.*, 2013).

ACKR1 is strongly expressed on erythrocytes and can be found on blood vessel endothelial cells but not on leukocytes (Gardner *et al.*, 2004). Major function of the receptor is the internalisation of chemokines. Moreover, ACKR1-transfected polarised cells showed that internalised chemokines could be moved across the cells (transcytosis) where they are presented to leukocytes, thereby driving transmigration *in vitro*. This ability is exclusive for ACKR1 (Pruenster *et al.*, 2009). Additionally, experiments with ACKR1-deficient mice showed that the receptor functions as a blood-borne buffer of inflammatory cytokines ensuring the robust chemokine-driven recruitment and appropriate targeting of leukocytes (Fukuma *et al.*, 2003; Hansell *et al.*, 2011).

In mice, ACKR2 is predominantly expressed in innate-like B cells (Bordon *et al.*, 2009) and low level transcripts of the receptor could also be found in T cells, neutrophils, *in vitro*-derived DC, and mast cells. This is concomitant with expression patterns in humans where ACKR2 expression could be confirmed on some DC and monocytes through flow cytometry analysis of peripheral blood leukocytes. Furthermore, ACKR2 immunoreactivity could be found on tissue-resident mast cells (Mckimmie *et al.*, 2008; Nibbs and Graham, 2013). Upon chemokine interaction, the receptor gets rapidly internalised. In the endosome, the chemokine dislodges from the receptor due to low pH and later gets degraded in the lysosome while the receptor traffics back to the membrane (Weber *et al.*, 2004). Interestingly, β-arrestins bind to the receptor but are not needed for either internalisation or effective chemokine scavenging but rather for stabilisation and trafficking (Nibbs and Graham, 2013). ACKR2 can also regulate the activity of conventional chemokine receptors including CCR4 visualised by the suppression of CCR4-driven migration in transfected cells *in vitro* (Bonecchi *et al.*, 2004).

1.2 IL-33

IL-33 was identified in 2005 as a member of the IL-1 family (Schmitz *et al.*, 2005). It consists of two domains, the N-terminal nuclear localisation domain and the C-terminal IL-1-like cytokine domain (Carriere *et al.*, 2007). The nuclear localisation domain contains a chromatin-binding motif, promoting chromatin compaction and mediating interaction with histones (Roussel *et al.*, 2008). Additionally, *in vitro* studies using the human embryonic kidney (HEK) cell line HEK293RI revealed that the cytokine can inhibit nuclear factor 'kappa-light-chain-enhancer' of activated B-cells (NF-κB) transcriptional activity by binding to the p65 subunit of NF-κB (Ali *et al.*, 2011). IL-33 engagement with the receptor is mediated via the C-terminal IL-1-like domain; but unlike IL-1β or IL-18, cleavage of the N-terminal portion is not required for the release of IL-33 from the cell or its signaling via the receptor (Lüthi *et al.*, 2009; Talabot-Ayer *et al.*, 2009; Cayrol and Girard, 2014).

IL-33 is constitutively expressed but can be further upregulated during inflammation (Moussion *et al.*, 2008; Pichery *et al.*, 2012; Drake and Kita, 2017). Primary sources are non-haematopoietic cells, including epithelial cells from barrier organs (Schmitz *et al.*, 2005; Moussion *et al.*, 2008; Pastorelli *et al.*, 2010), fibroblastic reticular cells in lymphoid organs (Marvie *et al.*, 2010; Pichery *et al.*, 2012; Carlock *et al.*, 2014) and adipocytes (Moussion *et al.*, 2008; Wood *et al.*, 2009; Cayrol and Girard, 2014). In humans, IL-33 can also be produced by endothelial cells (Baekkevold *et al.*, 2003; Molofsky *et al.*, 2015). In contrast, endothelial IL-33 expression is restricted to the female reproductive system, liver, and adipose tissue (Marvie *et al.*, 2010; Pichery *et al.*, 2012; Carlock *et al.*, 2014). During inflammation and infection, however, activated immune cells such as DC, M2 macrophages, eosinophils, monocytes, mast cells, and B cells can also express IL-33 (Hsu *et al.*, 2010; Chang *et al.*, 2011; Wills-Karp *et al.*, 2012; Hardman *et al.*, 2013; Tjota *et al.*, 2013; Tjota *et al.*, 2014; Tashiro *et al.*, 2016). For example, TLR signaling in myeloid cells (Hardman *et al.*, 2013) and peritoneal macrophages (Polumuri *et al.*, 2012) stimulates IL-33 production. Nevertheless, non-haematopoietic cells remain the main source of IL-33 as levels in

epithelial cells are at least 10-fold higher compared to haematopoietic cells (Hardman *et al.*, 2013; Barlow *et al.*, 2013; Byers *et al.*, 2013).

In steady state, IL-33 localises to the nucleus (Moussion *et al.*, 2008; Pichery *et al.*, 2012). Upon inflammatory cues or tissue damage, the cytokine is rapidly and passively released through cell death by necrosis and/or necroptosis (Figure 1.6) (Garlanda *et al.*, 2013; Kaczmarek *et al.*, 2013; Molofsky *et al.*, 2015). IL-33 is thereby considered an alarmin, an intracellular alarm signal that is released upon cell injury. However, usage of a fluorescently-tagged IL-33, revealed not only the nuclear localisation of the cytokine but also its cytoplasmic presence within endothelial cells, fibroblasts, and mast cells (Kakkar *et al.*, 2012; Hsu and Bryce, 2012). Additionally, human bronchial epithelium exposed to *Alternaria*, a fungus and common pathogen in humans, and mechanically-stressed fibroblasts released IL-33 without cell death (Kouzaki *et al.*, 2011; Kakkar *et al.*, 2012). DC secreted IL-33 through perforin-2, a pore-forming protein, as perforin-2-deficiency in DC reduced IL-33 levels in the supernatant and impaired T_{reg} cell growth (Hung *et al.*, 2020; Glineur *et al.*, 2022).

Regulation of IL-33 is mediated by proteases (Figure 1.7). IL-33 is cleaved and subsequently inactivated by Caspase-3 and -7 during programmed cell death (apoptosis) to avoid unnecessary activation of the immune system (Lüthi *et al.*, 2009; Griesenauer and Paczesny, 2017). In contrast, cleavage of IL-33 through extracellular serine proteases that are secreted during inflammation, such as neutrophil elastase, neutrophil cathepsin G, and mast cell serine proteases, results in 10-30-fold increased bioactivity of IL-33 (Lefrançais and Cayrol, 2012; Lefrançais *et al.*, 2012; Lefrançais *et al.*, 2014).

Thus far, suppression of tumorgenicity 2 (ST2) is the only receptor described for IL-33. Constitutive overexpression of IL-33 or loss of nuclear localisation signals caused systemic inflammation in mice, which was abrogated by crossing onto the ST2-deficient background (Bessa *et al.*, 2014; Talabot-Ayer *et al.*, 2015). ST2 exists either in membrane-bound (ST2L) or soluble (sST2) form (Yanagisawa *et al.*, 1993) (Figure 1.6), although two additional isoforms have been described. Engagement of

IL-33 with ST2L recruits co-receptor IL-1 receptor accessory protein (IL-1RAcP) which is shared between the IL-1, IL-33, and IL-36 cytokine subfamilies (Fields *et al.*, 2019). The receptor complex initiates signaling by activating the transcription factors NF-κB and activator protein 1 (AP-1). Both NF-κB and AP-1 translocate into the nucleus and initiate gene transcription (Schmitz *et al.*, 2005; Andrade *et al.*, 2011). The soluble receptor form lacks the transmembrane domain and intracellular Toll-Interleukin-1 receptor (TIR) domain of the membrane-bound receptor but shares the extracellular cytokine-binding domain (Liu *et al.*, 2013). It functions primarily as a decoy receptor, removing free IL-33 from the extracellular environment, and potentially limiting deleterious effects of the cytokine. Hence, sST2 is upregulated in response to inflammatory stimuli. Indeed, sST2 was found to be upregulated in rheumatologic, cardiovascular, and allergic diseases (Yanagisawa *et al.*, 1993; Oshikawa *et al.*, 2002; Weinberg *et al.*, 2002; Hayakawa *et al.*, 2007; Polumuri *et al.*, 2012). Depending on the promotor region used, two additional splice variants of ST2 termed ST2V and ST2LV can be produced (Bergers *et al.*, 1994; Iwahana *et al.*, 1999). Little is known about either of the variants. ST2V seems to be highly expressed in the human GI tract (Tago *et al.*, 2001), while ST2LV is found during later stages of embryogenesis and in the eye, lung, heart, and liver tissue of chickens (Iwahana *et al.*, 2004).

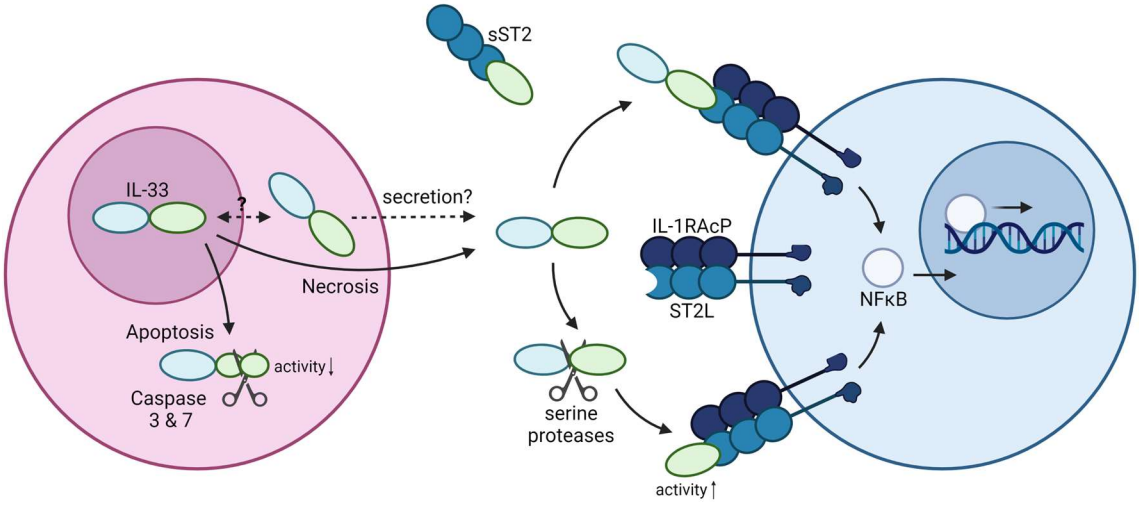

Figure 1.6: Molecular characteristics of IL-33
IL-33 is located in the nucleus but can be released into the extracellular environment. During apoptosis, Caspase-3 or -7 mediates the inactivation of IL-33 by cleavage. Extracellular IL-33 can be processed by proteases resulting in higher biological activity. Full-length and processed IL-33 bind to ST2L recruiting IL-1RacP and thereby inducing NF-κB signaling pathways that lead to activation and proliferation of the cell. Binding to sST2 reduced the availability of IL-33. (adapted from Molofsky et al., 2015, created with BioRender).

IL-33 demonstrates a pleiotropic spectrum not only in expression but also in function. The cytokine plays a role in both innate and adaptive immunity, and is involved in a variety of biological processes, ranging from tissue homeostasis (Moussion *et al.*, 2008; Pichery *et al.*, 2012), injury and wound-healing (Sanada *et al.*, 2007; Brunner *et al.*, 2011; Turnquist *et al.*, 2011; Liang *et al.*, 2013; Yin *et al.*, 2013) to type 2 immune responses (Yasuda *et al.*, 2012; Hardman *et al.*, 2013; Cayrol and Girard, 2014). Dysregulation of the ST2/IL-33-axis is implicated in numerous inflammatory diseases like asthma, inflammatory bowel disease (Beltrán *et al.*, 2010; Pastorelli *et al.*, 2010; Díaz-Jiménez *et al.*, 2011; Díaz-Jiménez *et al.*, 2016), graft-versus-host-disease (Vander Lugt *et al.*, 2013; Ponce *et al.*, 2015), cardiac disease (Weinberg *et al.*, 2003; Shimpo *et al.*, 2004), and type 2 diabetes (Miller *et al.*, 2012; Lin *et al.*, 2016). In humans, patients with chronic obstructive pulmonary disease and asthma show high IL-33 expression in airway epithelial cells (Préfontaine *et al.*, 2010; Byers

et al., 2013). Similarly, IL-33 levels are elevated and correlate with the extent of lung and skin fibrosis in patients suffering from systemic sclerosis (Yanaba *et al.*, 2011). In contrast, IL-33 improved cardiomyocyte survival and cardiac function after myocardial infarction (Seki *et al.*, 2009) and reduced atherosclerosis (Miller *et al.*, 2008).

The main cell populations, affected by IL-33 signaling, are associated with type 2 or regulatory immune responses (Cayrol and Girard, 2014). IL-33 can stimulate haematopoietic cells, including group 2 innate lymphoid cells (ILC2), eosinophils, basophils, mast cells, T_h2 cells, myeloid-derived suppressor cells, some DC and macrophage subsets and T_{reg} cells (Schmitz *et al.*, 2005; Garlanda *et al.*, 2013; Cayrol and Girard, 2014; Molofsky *et al.*, 2015). As cells expressing high ST2L levels, tissue-resident ILC, mast cells, and some T_{reg} cell populations comprise the initial targets for IL-33 signaling, although the primary target in most diseases are ILC2 (Moro *et al.*, 2010; Mchedlidze *et al.*, 2013; Brestoff *et al.*, 2015) which play a crucial role in type 2 immunity, eosinophil homeostasis, and allergic inflammation (Price *et al.*, 2010; Moro *et al.*, 2010; Nussbaum *et al.*, 2013; Cayrol and Girard, 2014). In a model of helminth infection with *Nippostrongylus brasiliensis,* the absence of IL-33 severely impaired worm clearance due to a defect in ILC2-mediated IL-13 production (Hung *et al.*, 2013). Additionally, IL-33 is necessary to restore airway epithelial integrity in an ILC2-dependent manner after influenza virus infection as inhibition of ST2 reduced ILC2 frequency and number in the lung during influenza infection, causing the loss of airway epithelial integrity, impaired respiratory tissue remodeling, and reduced lung function (Monticelli *et al.*, 2011). However, while ILC2 in the skin promote wound repair they can also drive atopic dermatitis-like inflammation in an IL-33-dependent manner (Salimi *et al.*, 2013; Imai *et al.*, 2013). Additionally, in a mouse model of liver injury, overexpression of IL-33 and subsequent overstimulation of ILC2 promoted liver fibrosis (Mchedlidze *et al.*, 2013). Hence, IL-33 signaling on ILC2 can be either harmful or beneficial depending on the tissue and disease state, highlighting the broad functional spectrum of IL-33.

IL-33 is also involved in the regulation of immune responses. Several studies have shown that the cytokine enhances the protective ability and stimulates the expansion of $ST2^+$ T_{reg} cells. T_{reg} cell expansion is promoted by IL-33 via NF-κB and p38 signaling either within the T_{reg} cells or indirectly through stimulating DC to produce IL-2 (Matta *et al.*, 2014). Additionally, *in vitro* studies showed that IL-33 enhances GATA3 expression in T_{reg} cells, leading to stabilised FoxP3 expression (Schiering *et al.*, 2014; Vasanthakumar *et al.*, 2015). The increase of T_{reg} cells after IL-33 treatment has great implications for transplantations. IL-33 treatment through i.p. injections increased T_{reg} cell numbers in the skin graft, increased IL-10 production, and decreased IFNy and IL-17 production, resulting in prolonged graft survival (Gajardo *et al.*, 2015). Similarly, mice receiving a heart transplant showed prolonged graft survival after IL-33 treatment, which led to the expansion of myeloid-derived suppressor cells and T_{reg} cells (Brunner *et al.*, 2011; Turnquist *et al.*, 2011). In a model of graft-vs-host-disease, IL-33-mediated expansion of $ST2^+$ T_{reg} cells prevented the accumulation of T_{conv} cells, leading to disease amelioration (Matta *et al.*, 2016). Overall, IL-33 has shown great potential for therapeutical applications in various diseases by improving the immunomodulatory function of T_{reg} cells.

1.2.1 Relevance in adipose tissue and obesity

The adipose tissue is a very complex organ, regulating adipogenesis, adipokine secretion and inflammatory responses. The main cell type regulating lipid uptake and release are mature adipocytes. However, they only comprise about 20 % of the resident cell types in adipose tissue. The remaining cells are adipocyte progenitor cells, preadipocytes, endothelial cells, fibroblasts, and immune cells (Norreen-Thorsen *et al.*, 2022; Emont *et al.*, 2022).

The adipose tissue can be divided into white adipose tissue (WAT), brown adipose tissue (BAT), and beige adipose tissue (Figure 1.7) (Garritson and Boudina, 2021). WAT is widely distributed throughout the body with major subcutaneous and visceral depots. Visceral WAT encloses vital organs within the rib cage and peritoneum, while subcutaneous WAT is located under the skin (Kwok *et al.*, 2016). The major function

of WAT is the storage of excess lipids and consequently the maintenance of energy homeostasis (Arner *et al.*, 2011; El Hadi *et al.*, 2019). Lipids are taken up and stored as triglycerides during positive energy balance (Fiorenza *et al.*, 2011; Wunderling *et al.*, 2023). At times of energy demand, lipids are released and converted into energy. Additionally, subcutaneous WAT is also important as a protector against external mechanical stress, a barrier against dermal infections and an insulator for preventing heat loss (Zhang *et al.*, 2015; Kwok *et al.*, 2016). Due to its prominent lipid storage function, it is characterised by unilocular, spherical, and lipid-filled adipocytes (Eto *et al.*, 2009).

BAT is found predominantly in rodents but also in human infants (Hatai, 1902; Urisarri *et al.*, 2021). It is involved in energy expenditure and heat production (El Hadi *et al.*, 2019; Copperi *et al.*, 2022) by utilising and dissipating lipid-derived energy. These effects are largely mediated by uncoupled protein 1 (UCP-1), which is located within the inner mitochondrial membrane (Ricquier and Kader, 1976; Golozoubova *et al.*, 2001). The adipocytes within the BAT are characterised by an elliptical morphology. Instead of storing one single lipid droplet like white adipocytes, brown adipocytes contain multiple small lipid droplets (Minokoshi *et al.*, 1986). Additionally, the tissue appears brown due to its dense vascularisation and high number of mitochondria (Kwok *et al.*, 2016). Due to its high metabolic activity, the BAT is rather associated with weight loss and leanness, whereas various health disorders such as obesity are linked to WAT expansion (Lowell *et al.*, 1993; Ghorbani *et al.*, 1997; Guerra *et al.*, 1998; Schmitz *et al.*, 2016; Raciti *et al.*, 2017; Maharjan *et al.*, 2021).

Lastly, beige adipose tissue derives from WAT but adopts BAT-like features such as the expression of UCP-1, increased mitochondria numbers, and vascularisation (Cousin *et al.*, 1992; Kwok *et al.*, 2016). Beige adipose tissue formation is induced upon cold exposure. The conversion of WAT to beige adipose tissue is known as adaptive thermogenesis, also termed browning (Harms and Seale, 2013; Gao *et al.*, 2018; Wang *et al.*, 2020).

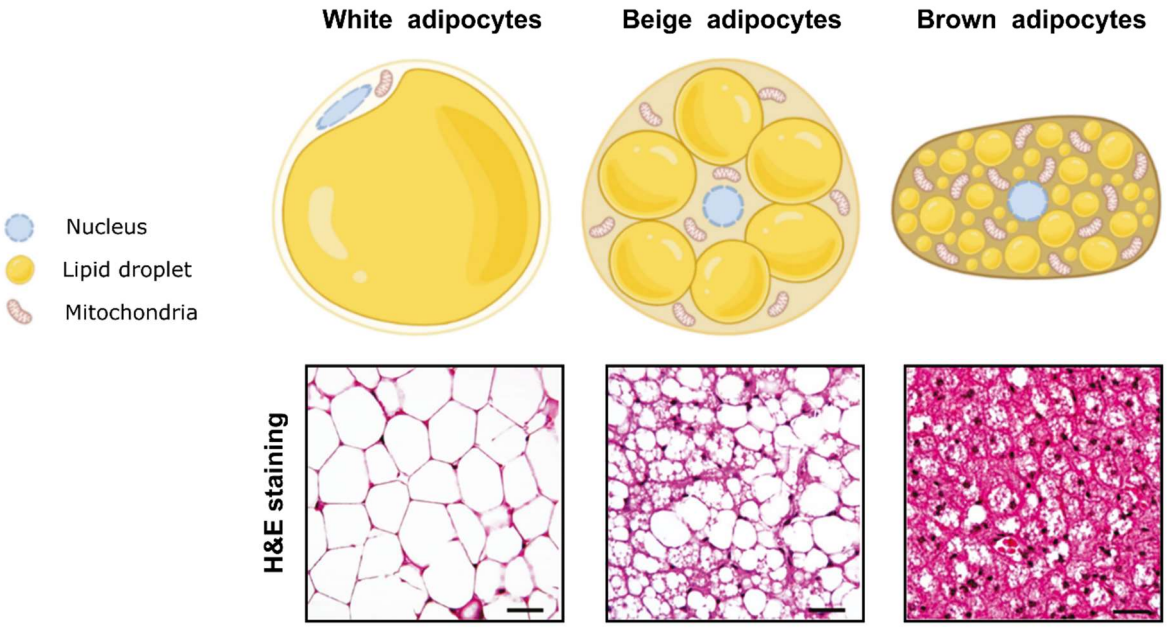

Figure 1.7: Characteristics of white, beige, and brown adipocytes
White adipocytes contain one large lipid droplet and a decentralised nucleus. Beige adipocytes derive from white adipocytes but have acquired characteristics of brown adipocytes due to stimuli like cold exposure. Brown adipocytes show an elliptical morphology and contain both multiple lipid droplets and mitochondria. Scale bar = 50 µM. (Images are adapted from Bargut et al., 2017 and Lee et al., 2021)

Several studies have highlighted the critical role of IL-33 in lipid metabolism as WAT is a source for both IL-33 and its receptor. Indeed, human preadipocytes and adipocytes produced ST2L and IL-33 at steady state *in vitro* (Wood *et al.*, 2009). In contrast, sST2 is expressed by subcutaneous and omental adipose tissue in humans (Zeyda *et al.*, 2013).

Mice lacking IL-33 or ST2 show increased obesity (Miller *et al.*, 2010; Brestoff *et al.*, 2015; Vasanthakumar *et al.*, 2015; Lee *et al.*, 2015). Additionally, ST2-deficient mice fed on high-fat diet (HFD) showed impaired glucose regulation and insulin secretion, increased fat mass, and body weight in comparison to wild type (wt) controls fed with HFD (Miller *et al.*, 2010). Concomitantly, treatment of genetically obese diabetic mice with IL-33 reduces adiposity and improved glucose and insulin tolerance (Miller *et al.*, 2010; Han *et al.*, 2015).

In *ob/ob* mice, a model of Type II diabetes, administration of IL-33 led to the accumulation of alternatively activated M2 macrophages and the improvement of glucose tolerance (Miller *et al.*, 2010). While classical activated M1 macrophages require T_h1 cytokines like tumor-necrose factor α (TNF-α) and IFNy, polarisation of M2 macrophages is associated with the release of T_h2 cytokines (Cardilo-Reis *et al.*, 2012; Wu *et al.*, 2015; Zhang *et al.*, 2017; Celik *et al.*, 2020; He *et al.*, 2020). Accumulation of M2 macrophages is linked to the improvement of obesity-induced insulin resistance and adipose tissue inflammation (Weisberg *et al.*, 2003; Xu *et al.*, 2003; Chawla *et al.*, 2011). Although M2 macrophages express ST2 on their cell surface, IL-33 can only indirectly influence their polarisation through the activation of ILC2 and the subsequent production of T_h2 cytokines by ILC2 (Kurowska-Stolarska *et al.*, 2008; Kurowska-Stolarska *et al.*, 2009; Li *et al.*, 2014). In fact, activation of ILC2 favours M2 polarisation, initiating reduced lipid storage as the downstream effect (Molofsky *et al.*, 2013).

Another immune cell subtype with protective functions in the adipose tissue are T_{reg} cells. Tissue-resident T_{reg} cells of the visceral adipose tissue (VAT) are required for tissue homeostasis (Feuerer *et al.*, 2009; Dwyer *et al.*, 2022) and constitutively express ST2 at high levels because IL-33 is required for their development, maintenance, and proliferation (Vasanthakumar *et al.*, 2015). Deletion of *St2* within T_{reg} cells significantly reduced VAT-T_{reg} cells, whereas lymphoid T_{reg} cells remained unaffected (Li *et al.*, 2018).

ST2-expressing T_{reg} cells are highly suppressive and express additional markers correlating to activation such as KLRG1, ICOS, and GITR (Vasanthakumar *et al.*, 2015; Siede *et al.*, 2016; Spath *et al.*, 2022). IL-33 injections induced expansion of $ST2^+$ T_{reg} cells, which significantly improved metabolic parameters in obese mice (Vasanthakumar *et al.*, 2015; Kolodin *et al.*, 2015).

Additionally, insulin resistance is strongly correlated with IL-33 levels. Increased insulin resistance was accompanied by reduced IL-33 levels in patients with diabetic nephropathy. Furthermore, this was associated with a shift towards enhanced T_h1 response, suppressing the T_h2 response (Anand *et al.*, 2014). As ST2 expression is

regulated by GATA3, the receptor is constitutively expressed on T_h2 cells. Indeed, IL-33 can activate T_h2 cells and induces their cytokine production (Xu *et al.*, 1998; Yin *et al.*, 2010). These findings suggest an involvement of the ST2/IL-33 axis in the T_h1/T_h2 balance. Indeed, IL-33 has shown a protective function in the pathogenesis of atherosclerosis (Miller *et al.*, 2008) as the shift from T_h1 cells to T_h2 cells reduced atherosclerosis development (Gupta *et al.*, 1997; De Boer *et al.*, 1999; Tu and Yang, 2019), suggesting a protective role of T_h2 cells within the adipose tissue.

Taken together, in the context of adipose tissue inflammation, IL-33 elicits protective functions through the activation of ILC2, M2 macrophage polarisation, direct and indirect $ST2^+$ T_{reg} cell expansion and T_h2 cell function.

1.2.2 Relevance in wound healing, tissue repair, and fibrosis

Tissue damage can be caused by various stimuli in the course of infections, autoimmune development, allergic responses, and tissue injury caused by toxins, radiation or mechanical injury (Wynn, 2008; Huang *et al.*, 2020).

During wound healing, inflammatory mediators facilitate the formation of provisional extracellular matrix (ECM) by triggering an anti-fibrinolytic coagulation cascade. Matrix-Metallo-Proteases, which are produced by myofibroblasts and epithelial and/or endothelial cells, cause the disruption of the basement membrane. Thereafter, inflammatory cells are recruited by cytokines and chemokines. Additional growth factors stimulate immune cell proliferation. Macrophages and neutrophils eliminate dead cells, tissue debris, and any invasive organism. Additionally, lymphocytes express pro-fibrotic cytokines and growth factors, leading to the activation of myofibroblasts. Activated fibroblasts develop into $\alpha\text{-SMA}^+$ myofibroblasts which are able to secrete collagen, migrate into the wound and promote wound contraction during which wound edges migrate towards the wound centre. Lastly, epithelial and/or endothelial cells proliferate over the basal layer and conclude the tissue regeneration (Kaviratne *et al.*, 2004; Wynn, 2008; García-de-Alba *et al.*, 2010; Dayer and Stamenkovic, 2015; Shinde *et al.*, 2017).

Excessive deposition of ECM components during wound healing can outbalance the degradation of collagens, leading to the abnormal development of excess connective tissue (Wynn, 2008; Huang *et al.*, 2020), increased tissue stiffness and associated disruption in function, for example reduced urinary filtration in the kidney or impaired gas exchange in the lung (Murray, 2016).

The involvement of IL-33 in wound healing and tissue repair is well described. In the context of fibrosis, the function of IL-33 is highly organ-specific. While IL-33 is strongly associated with the development of lung and liver fibrosis, the cytokine demonstrates cardioprotective and anti-fibrotic effects in cardiomyoctes.

IL-33 function in wound healing and tissue repair is mainly linked to its function in promoting type 2 $ST2^+$ cells, as type 2 cytokines are instrumental in the tissue repair process (Dwyer *et al.*, 2022). Several studies have demonstrated that the $CD4^+$ T_h2 cells and T_h2 cytokines are strongly linked to liver fibrosis (Wynn *et al.*, 1995; Chiaramonte *et al.*, 1999; Pesce *et al.*, 2006; Reiman *et al.*, 2006). Additionally, animals with T_h2-polarised inflammation showed upregulation of genes associated with wound healing and fibrosis (Sandler *et al.*, 2003)

In humans and mice, levels of IL-33 are upregulated in hepatic fibrosis (Marvie *et al.*, 2010; Mchedlidze *et al.*, 2013). It is proposed that IL-33 is secreted by stressed hepatocytes. As the main target cells of IL-33, ILC2 are recruited and activated to produce IL-13, triggering the profibrogenic activation of hepatic stellate cells, the major cell type to produce extracellular matrix (Mchedlidze *et al.*, 2013; Weiskirchen and Tacke, 2017; Tan *et al.*, 2018). Indeed, *in vitro* stimulation of activated hepatic stellate cells by IL-33 induced collagen expression (Tan *et al.*, 2018).

In a mouse model of bile duct ligation (BDL)-induced fibrosis, IL-33 levels are increased. Accordingly, ST2-deficient mice showed reduced inflammation, hepatic injury, and fibrosis in mouse models of toxic-, dietary- or BDL-induced fibrosis (Mchedlidze *et al.*, 2013; Y. Gao *et al.*, 2016; Tan *et al.*, 2018). Absence of ST2 was linked to reduced T_h1 cell, T_h2 cell, macrophage and neutrophil infiltrates in BDL-induced liver fibrosis. In line with these findings, ILC2 were increased and positively correlated to the upregulation of IL-33 in BDL (Tan *et al.*, 2018).

In a murine model of bleomycin (BLM)-induced lung injury, treated mice showed a significant accumulation of IL-33-producing cells within the lung. BLM induced IL-33 production in macrophages (Luzina *et al.*, 2013; Q. Gao *et al.*, 2016; Xu *et al.*, 2016). In turn, IL-33 promoted macrophages polarisation toward an M2 phenotype whose involvement in the acceleration of pulmonary fibrosis is well established (Li *et al.*, 2014; John *et al.*, 2016). Additionally, IL-33 promotes IL-13 production by T_h2 cells (Piehler *et al.*, 2016). IL-13 further supports M2 macrophage polarisation (Zhang *et al.*, 2017) and stimulates myofibroblast differentiation, thereby stimulating ECM production (John *et al.*, 2016; Kotsiou *et al.*, 2018). Inhibition of IL-33 or usage of ST2-deficient mice weakens fibrosis in BM-induced pulmonary fibrosis (Li *et al.*, 2014).

In contrast to the profibrogenic effect of IL-33 in chronic injury models, acute injury models are associated with a protective role of the cytokine. Administration of IL-33 upregulated anti-apoptotic genes while simultaneously repressing pro-apoptotic gene expression. Furthermore, IL-33-deficient mice showed more hepatic injury when receiving concanavalin A than their wt counterparts (Noel *et al.*, 2016).

During the healing process, ST2 promotes conversion of macrophages from an inflammatory to a non-inflammatory state, thereby promoting wound closure and reduced scarring (Lee *et al.*, 2016).

In addition, IL-33 shows protective functions in heart failure and cardiac fibrosis. IL-33 improved cardiac function and survival after myocardial infarction in ischemia-reperfused rats by reducing infarct size, fibrosis, and preventing cardyomyocyte apoptosis (Sanada *et al.*, 2007). Corresponding with its anti-apoptotic role, protein expression of anti-apoptotic B-cell lymphoma 2 (Bcl-2) and IL-33 are strongly correlated (Seki *et al.*, 2009). IL-33-deficiency in models of ischemic and non-ischemic heart failure resulted in impaired cardiac function and survival caused by amplified cardiac remodeling (Veeraveedu *et al.*, 2017).

Taken together, IL-33 functions in tissue remodelling and wound healing are highly context- and organ-dependent, eliciting both damaging and protective effects.

1.3 Salmonella

Salmonella are Gram-negative, rod-shaped, facultative anaerobic and enteroinvasive bacteria, leading to an acute intestinal inflammation in many mammalian and some avian species (Eberth, 1880; Small *et al.*, 1987; Griffin and McSorley, 2011; de Jong *et al.*, 2012). The bacteria are primarily transmitted through contaminated food or water and, thereby, considered a food-borne pathogen (Durham, 1898; Broz *et al.*, 2012). The genus *Salmonella* consists of two species, named *Salmonella enterica* and *Salmonella bongori* (Le Minor and Popoff, 1987; Reeves *et al.*, 1989; Brenner *et al.*, 2000). *Salmonella bongori* is generally regarded as an opportunist and restricted to cold-blooded animals (Dougan *et al.*, 2011). In contrast, *Salmonella enterica* shows a broad range of different cold- and warm-blooded hosts as well as habitats (Brenner *et al.*, 2000). This is illustrated by the fact that 99 % of *Salmonella* infections in humans and animals are caused by *Salmonella enterica* species (Kurtz *et al.*, 2017).

Salmonella enterica can be divided into 6 subspecies (Grimont and Weil, 2007; Wiedemann *et al.*, 2014). Subspecies can be further classified into serovars based on serological identification of the O (LPS), K (capsular), and H (flagella) antigens in accordance to the Kauffmann-White scheme (Salmonella Subcommittee of the Nomenclature Committee of the International Society for Microbiology, 1934; Dougan *et al.*, 2011). Through this method, over 2500 serovars were identified so far. Availability of sequence-based methods, however, started the process of replacing the classification based on historical phenotypic characteristics with a phylogenetic approach. *Salmonella* is now organised and clustered by genomic similarities (Achtman *et al.*, 2020; Chattaway *et al.*, 2021).

1.3.1 Salmonellosis and typhoid fever – disease outcome and treatment

Severity of *Salmonella* infections is influenced by a variety of factors including the host species, serovar, infecting dose, immunologic competence and gut flora. Therefore, the disease outcome clinically differs and ranges from asymptomatic carriage to potentially fatal (Dougan *et al.*, 2011).

Salmonellosis is a food-borne disease, predominantly acquired by ingesting contaminated food or water, and therefore, most prevalent in developing countries with poor water supply, sanitation and generally low-resource settings (Gordon, 2008; Stanaway *et al.*, 2019; Carey *et al.*, 2022). The major causes of gut-associated gastroenteritis are non-typhoidal *Salmonella* (NTS) serovars such as Typhimurium and Enteritidis. Human-restricted *Salmonella enterica* serovars Typhi (*S.* Typhi) and Paratyphi (*S.* Paratyphi), however, are causes of typhoid or paratyphoid fever, respectively, representing a severe systemic infection in some patients.

NTS is relatively short-lived with a short incubation period of 12-72 h, rapid disease onset and average duration of less than 10 days, while typhoid fever shows an asymptomatic incubation time between 5-9 days followed by persistent fever up to 3 weeks (Raffatellu, Wilson, *et al.*, 2008).

Typhoid fever can lead to gastrointestinal bleeding, intestinal perforation, septic shock and death when untreated (Butler *et al.*, 1990; Maskey *et al.*, 2006; Brosset Ugas *et al.*, 2016; Nurnaningsih *et al.*, 2022; World Health Organization, 2023). Annually, approximately 21 million new cases and more than 200,000 deaths in developing countries are reported (Harris and Brooks, 2012; Marchello *et al.*, 2019). Especially in south and southeast Asia as well as sub-Saharan Africa and Oceania, typhoid fever is the major cause of death and disability with the highest burden seen in infants and small children (Stanaway *et al.*, 2019; Meiring *et al.*, 2021; Garrett *et al.*, 2022).

NTS serovars are one of the major global causes of bacterial diarrhea leading annually to approximately 153 million cases and 57,000 deaths (CDC, 2023). In immunocompromised patients, however, non-typhoidal *Salmonella* causes invasive non-typhoidal Salmonellosis (iNTS). The incidence rate is highest in sub-Saharan Africa and especially in children under 5 years of age, immunocompromised or HIV-infected adults (Gordon, 2008; Reddy *et al.*, 2010; Strugnell *et al.*, 2014).

Generally, the treatment of sick individuals consists of therapy with effective antibiotics in combination with restoration of fluid and electrolyte balance (Parry *et al.*, 2002). A rising concern, however, is the spread of multidrug resistance (MDR)

against commonly used therapeutics like cephalosporins or fluoroquinolone (Klemm *et al.*, 2018; Carey *et al.*, 2022). Therefore, the development of vaccines against *Salmonella* infections has received increasing attention in recent years (Marchello *et al.*, 2019). Two vaccines, the Vi polysaccharide (Vi-PS) vaccine (Typhim Vi by Sanofi Pasteur or Typherix by GSK) and the live attenuated oral vaccine Ty21a (Crucell), are licenced for the prevention of typhoid fever (World Health Organization, 2019). However, both vaccines are not commonly used in typhoid endemic areas due to age restrictions (≥2 years for Vi-PS, ≥6 years Ty21a) (World Health Organization, 2019) and decreasing immunity after 2 years (Levine *et al.*, 1999; Khan *et al.*, 2012). A promising alternative are typhoid conjugate vaccines (TCV). Vi polysaccharide-tetanus toxoid (Vi-TT) conjugate Typbar-TCV (Bharat Biotech) and Vi-CRM197 conjugate TYPHIVEV (Biological E) showed safety and immunogenicity (Vadrevu *et al.*, 2021). Tybar-TCV and TYPHIVEV were pre-qualified by the WHO, meaning that they can be implemented into countries lacking a regulatory body such as Food and Drug Administration (FDA) and European Medicines Evaluation Agency (World Health Organization, 2023).

There are currently four TCV vaccine candidates with phase III clinical trials ongoing or completed: Vi polysaccharide conjugated to diphtheria toxoid BioTCV (PT Biofarma), Vi- CRM197 EuTYPH-C (EuBiologics), Vi-DT SKYTy-phoid (SK Bioscience), Vi-TT ZYVAC TCV (Zydus Cadila) (Carey *et al.*, 2022). All tested and licensed vaccines target *S.* Typhi, meaning there is no vaccine available against *S.* Paratyphi (World Health Organization, 2023).

Additionally, there are currently no licensed vaccines against iNTS but several vaccine candidates in preclinical or clinical phases. The attenuated vaccine WT05 (Microscience), which was tested in humans before 2019, showed a high anti-LPS antibody response and high tolerability but was ultimately discontinued due to prolonged faecal shedding of bacteria (Baliban *et al.*, 2020; World Health Organization, 2023). New approaches are being made in creating glycoconjugate vaccines against iNTS. iNTS COPS:FliC conjugate (University of Maryland Baltimore & Bharat Biotech International Ltd) is comprised of the purified core O-

polysaccharides (COPS) and the phase 1 flagellin protein (FliC), eliciting enhanced polysaccharide immunogenicity and engagement of $CD4^+$ T cell help (Baliban *et al.*, 2018). It is currently in phase 1 clinical trials (World Health Organization, 2023).
Development of *Salmonella* vaccines is still ongoing with many promising candidates but needs to be further promoted, especially with regard to increasing MDR in *Salmonella* serovar strains.

1.3.2 Pathogenicity

Salmonella in the vast majority of cases is transmitted via the faecal-oral route (Sfeir *et al.*, 2013). Following ingestion, the bacteria encounter the acidic environment and digestive enzymes of the stomach. However, contact with stomach acid induces an acid tolerance response (ATR) aiding in the survival of *Salmonella* spp. (Muller *et al.*, 2009; Palmer and Slauch, 2017). After reaching the intestinal lumen, *Salmonella* must compete with the resident gut microbiota. In a hostile take-over, the bacteria induce an intestinal inflammation through its virulence factors. The inflammatory immune response leads to the formation of new resources (Hallstrom and McCormick, 2011; Fàbrega and Vila, 2013). Formed reactive oxygen species (ROS) react with luminal sulfur compounds, thereby producing tetrathionate. *S.* Typhimurium, as one example, can utilise this product, whereas resident gut microbiota lack the associated metabolic pathway (Price-Carter *et al.*, 2001; Winter *et al.*, 2010). Furthermore, the number of resident microbiota decreases, leading to the availability of existing resources. Due to the induced dysbiosis, *S.* Typhimurium gains a growth advantage over the intestinal microbiota (Thiennimitr *et al.*, 2011; Broz *et al.*, 2012).
Using their flagella, *Salmonella* move towards intestinal epithelial cells and initiate attachment through adhesins and fimbriae (Edwards *et al.*, 2000; Wagner and Hensel, 2011; Suwandi *et al.*, 2019). Following adherence, *Salmonella* cross the epithelial barrier through several different mechanisms (Figure 1.8). The primary site of infection are M cells, preferentially in the distal ileum (Jones *et al.*, 1994). M cells are intestinal epithelial cells covering organised follicle-associated lymphoid tissue.

M cells are mainly concentrated in Peyer's Patches (PP) but can also be found in solitary intestinal lymphoid tissues (Owen and Jones, 1974; Hamada *et al.*, 2002). *Salmonella* can invade both lymphoid structures through transcytosis, although the main entry route is associated with the PP (Broz *et al.*, 2012). Furthermore, the pathogen can invade non-phagocytic enterocytes. For the invasion, *Salmonella* express a virulence-associated type III secretion system (T3SS) encoded by *Salmonella* Pathogenicity Island 1 (SPI-1) and *Salmonella* Pathogenicity Island 2 (SPI-2) (Francis *et al.*, 1992). The secretion apparatus forms a syringe-like structure, enabling the bacteria to inject a variety of effector proteins into the host cell. These proteins induce cytoskeletal and membranal rearrangements of the host cell, leading to bacterial engulfment and uptake (Hernandez *et al.*, 2004; Patel and Galán, 2006; Bakowski *et al.*, 2007; Bakowski *et al.*, 2010).

Alternatively, *Salmonella* can employ invasion-independent entry routes to cross the epithelial barrier. The lamina propria contains phagocyte populations, which can directly capture bacteria from the intestinal lumen. *In vitro* studies have shown that DC can capture bacteria from the apical cell surface by dendrites reaching through tight junctions of an epithelial monolayer (Rescigno *et al.*, 2001). Concomitantly, *in vivo* experiments with CX_3CR1^+ phagocytes of the lamina propria showed an extension of transepithelial dendrites into the intestinal lumen and an increasing frequency of those processes after *Salmonella* infections (Niess *et al.*, 2005). However, CX_3CR1^+ cells of the lamina propria seem unable to migrate. Therefore, the importance of the invasion-independent pathway is still unclear.

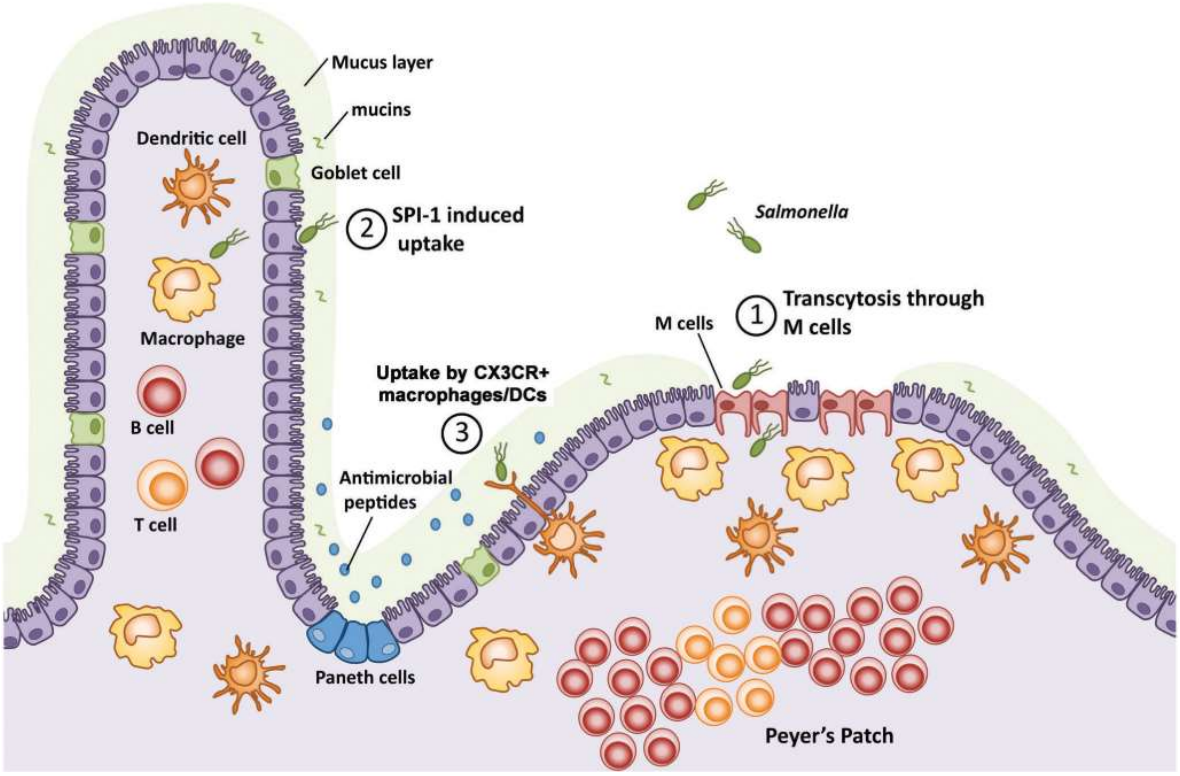

Figure 1.8: Schematic overview of the different entry routes for *Salmonella* to cross the intestinal mucosa.
The main invasion route is through M cells in PP. (B) Alternatively, *Salmonella* cross the intestinal mucosa by SPI-1 induced uptake by enterocytes. (C) Lastly, phagocytes can extend their dendrites through the epithelium and directly capture bacteria. (Figure adapted from Broz *et al.*, 2012).

After penetration of the PP, *Salmonella* encounters a lymphoid tissue structure rich in phagocytic cell populations. The bacteria are taken up by phagocytic immune cells and replicate within vacuolar compartments, labeled as *Salmonella*-containing vacuoles (SCV) (Hashim *et al.*, 2000). To evade degradation, *Salmonella* express a second T3SS, encoded on SPI-2 (Rathman *et al.*, 1997; Chakravortty *et al.*, 2005; Park *et al.*, 2018). This secretion complex interferes with the deposition of the reduced nicotinamide adenine dinucleotide phosphate (NADPH) oxidase complex within the phagosomal membrane in macrophages, preventing superoxide production (Buchmeier and Heffron, 1991; Vazquez-Torres, Xu, *et al.*, 2000). Furthermore, pathogenic *Salmonella* prevents the entry of reactive nitrogen and

oxygen intermediates in the phagosome and subsequently the oxidative burst, which consequentially improves survival of the bacteria (Vazquez-Torres, Jones-Carson, *et al.*, 2000; Mastroeni, Vazquez-Torres, *et al.*, 2000).

Salmonella disseminate to the draining mesenteric lymph node (mLN) through afferent lymphatics (Griffin and McSorley, 2011) and by infection of $CCR7^+$ $CD11b^+$ DC, which then migrate to the mLN (Voedisch *et al.*, 2009; Erazo *et al.*, 2021). Interestingly, *S.* Typhimurium is also able to migrate independently of phagocytes to the mLN where it is taken up by $CD64^+$ macrophages (Bravo-Blas *et al.*, 2019). From there on the bacteria traverse through efferent lymphatic vessels and colonise systemic sites like spleen and liver (Pham and McSorley, 2015).

1.3.3 Innate and adaptive immune responses against *Salmonella*

The interplay between innate response as first line of defence and the adaptive immune response is crucial for the clearance of and long-term immunity against *Salmonella.*

In a first line of defence, *Salmonella* has to overcome the acidic environment of the stomach and the thick mucous layer covering the mucosal epithelium. As previously mentioned, *Salmonella* has evolved an ATR which is induced upon slight or moderate exposure to acidic stress, increasing the resistance lethal pH (Foster and Hall, 1990; Wilmes-Riesenberg *et al.*, 1996). In the gut, intestinal epithelial cells form a tight physical as well as chemical barrier. Goblet cells and Paneth cells secrete mucus and antimicrobial peptides, respectively (Moe, 1953; Trier, 1963). Those antimicrobial peptides function as peptide antibiotics leading to the disruption of the bacterial cell membrane integrity (Broz *et al.*, 2012). To overcome this unfavourable environment, *Salmonella* has developed different strategies. For example, the PhoP-PhoQ signal transduction system increases the resistance towards these antimicrobial peptides (Guina *et al.*, 2000; Shi *et al.*, 2004). Indeed, *Salmonella* lacking either of the two components are severely attenuated (Miller *et al.*, 1989).

After overcoming the acidic and mucous challenges of the GIT, *Salmonella* crosses the epithelial barrier and encounters macrophages and DC of the GALT. Monocytic

cells can recognise PAMP through their PRR. The first PRRs to recognise *Salmonella* are TLR1/2/6 (lipoproteins), TLR4 (LPS), TLR5 (flagellin), and TLR9 (CpG-rich elements in DNA) (Medzhitov, 2001; Broz *et al.*, 2012). DC detect LPS via TLR4 and flagellin increases DC expression of MHC II, CD80, CD86, and CD40, which enables the cells to efficiently present antigens to naïve $CD4^+$ T cells in T cell areas of lymphoid tissues (McSorley *et al.*, 2002; Salazar-Gonzalez *et al.*, 2007).

In addition to extracellular and endosomal TLRs, the NLR family can sense cytosolic PAMP. NLRs containing a Caspase Recruitment Domain (CARD) recruit pro-Caspase-1 (Broz and Monack, 2011; Broz *et al.*, 2012). Activated Caspase-1 aids the clearance of *Salmonella* infections by pyroptotic cell death (Bergsbaken *et al.*, 2009; Miao *et al.*, 2010). Thereby, and regardless of whether the bacterium stays bound by the SCV, or enters the cytosol, the replicative niche of the pathogen is disturbed and the pathogen is also exposed to extracellular immune defenses (Miao *et al.*, 2010). Indeed, infected mice deficient for Caspase-1 showed a higher bacterial burden in systemic organs than wt mice (Lara-Tejero *et al.*, 2006; Raupach *et al.*, 2006).

Detection of PAMP through PRRs within the mucosa triggers an acute inflammation in the gut which leads to the activation of additional innate immune responses including the recruitment of neutrophils that delay the dissemination of the bacteria to systemic sites (Vassiloyanakopoulos *et al.*, 1998; Griffin and McSorley, 2011). Previous experiments have shown that the depletion of neutrophils causes an increase of the extracellular bacterial load within the liver (Conlan, 1996).

The cytokine interferon gamma (IFNγ) is crucial for the early control of *Salmonella* infections. Deficiencies in the IFNγ signaling cascade lead to an increased susceptibility to severe *Salmonella* infections in mice (Muotiala and Mäkelä, 1990; Kupz *et al.*, 2014). Additionally, patients with defects in the IFNγ receptor signaling pathway show recurrent dissemintated *Salmonella* infections (Nanton *et al.*, 2012). Main contributors to the IFNγ levels during the innate immune response are natural killer (NK) cells, especially $Thy1^+$ NK cells, although other IFNγ producing lymphocytes can compensate for the lack in IFNγ levels in the absence of NK cells

(Kupz *et al.*, 2013). IFNγ drives immunomodulatory and antiviral responses (Schoenborn and Wilson, 2007) by upregulating a variety of genes important for controlling antiviral, antimicrobial or apoptotic effects (MacMicking, 2012). Furthermore, IFNγ leads to the production of reactive nitrogen species (RNS) and ROS in phagocytes (Marchi *et al.*, 2014; Ingram *et al.*, 2017). While ROS are directly toxic to *Salmonella*, they can also induce activation of NF-κB. Among other things, NF-κB induces the expression of NLRP3 which leads to the activation of Caspase-1 (Morgan and Liu, 2011).

Although IFNγ is needed for the early control of *Salmonella* infections, $CD4^+$ T cells are required to clear the infection completely. Mucosal $CD11c^+$ $CCR6^+$ DC initiate the *Salmonella*-specific T cell response and drive the early clonal expansion of T cells within the PP (Salazar-Gonzalez *et al.*, 2006). $CD4^+$ T cell activation occurs within 3-6 hours after infection in the PP and 3 hours later in the mLN (Bumann, 2001; Salazar-Gonzalez *et al.*, 2006; Griffin and McSorley, 2011). The mLN is an important site for *Salmonella*-specific T cell activation. Experiments with mice in which the mLN was surgically removed showed elevated bacterial loads and immunopathology in the liver (Voedisch *et al.*, 2009). Therefore, the mLN appears to be essential for preventing the dissemination of *Salmonella*.

Several studies have demonstrated that the expansion of *Salmonella*-specific $CD4^+$ T cells and acquisition of T_h1 effector functions are crucial for clearance of *Salmonella* infection. Those $CD4^+$ T_h1 cells secrete anti-inflammatory cytokines such as IFNγ, TNFα, and IL-12, (Griffin and McSorley, 2011; Pham and McSorley, 2015) and can be activated by cognate and non-cognate stimuli (Pham *et al.*, 2017). Mice lacking $CD4^+$ T cells or T-bet^+ T_h1 cells succumb to primary *Salmonella* infection (Weintraub *et al.*, 1998; Ravindran *et al.*, 2005; Kupz *et al.*, 2014). Additionally, depletion of $CD4^+$ T cells prior to *Salmonella* challenge increases bacterial burden in systemic organs and eliminates protective functions in formerly vaccinated mice (Nauciel, 1990; Johanns *et al.*, 2010). It has been suggested that non-circulating or tissue resident lymphocytes are involved in the protective immunity mediated by attenuated *S.* Typhimurium strains. Adoptive transfer of liver-resident T_h1 cells,

acquired through vaccination, protected against virulent *Salmonella* challenge. Therefore, non-circulating memory T_h1 cells appear to be important in conveying immunity to *Salmonella* infections (Benoun *et al.*, 2018).

Another subset within the $CD4^+$ T cells are T_h17 cells, which are important for mediating the immunity to extracellular bacterial infections and recruitment of neutrophils. T_h17 produce the cytokines IL-17 and IL-22 that directly induce the production of antimicrobial peptides (Liang *et al.*, 2006). IL-17-deficient mice displayed a modest increase in bacterial dissemination after *Salmonella* infection proposing that the cytokine is involved in the maintenance of the mucosal barrier (Schulz *et al.*, 2008). Additionally, IL-17-deficient mice show defects in neutrophil recruitment to sites of infection upon *Salmonella* infection (Raffatellu, Santos, *et al.*, 2008). IL-22 leads to the production of antimicrobial peptides like lipocalin-2 by intestinal epithelial cells. However, *S.* Typhimurium has adapted to resist antimicrobial peptides by expressing the proteins necessary for the uptake and biosynthesis of salmochelin which promotes lipocalin-2 resistance (Santos *et al.*, 2009; Raffatellu *et al.*, 2009).

Involvement of T_{reg} cells has not been well described. Within the first three to four weeks after *Salmonella* infection, bacterial burden is strongly increased which may be ascribed to delayed effector T cell activation (Johanns *et al.*, 2010). At later time points, however, reduced bacterial burden and a robust effector T cell activation can be detected. This timetable correlates strongly with the suppressive potency of T_{reg} cells as their suppressive potency is increased at early time points of the infection but decreases 4-fold at later time points (Johanns *et al.*, 2010).

While the importance of $CD4^+$ T cells for the clearance of *Salmonella* infections is well described, their contribution to bacterial control in earlier stages of the infection is only minor. Indeed, CD4-deficient mice exhibited controlled bacterial growth (albeit the bacteria were not completely cleared) with three to four weeks post infection, which appeared to be the result of compensatory $CD8^+$ T cells since depletion of both $CD4^+$ and $CD8^+$ T cells resulted in a delayed death of the mice (Kupz *et al.*, 2014).

In contrast to $CD4^+$ T cells, the role of $CD8^+$ T cells in the defence against *Salmonella* is questionable. Mice lacking functional $CD8^+$ T cells are able to clear the infection similar to wt mice (Kupz *et al.*, 2014). Additionally, β2-microglobulin-deficient mice, lacking surface MHC I and subsequently functional $CD8^+$ T cells, can clear primary *Salmonella* infection (Hess *et al.*, 1996; Lo *et al.*, 1999). However, those mice also lack expression of CD1 and might express free MHC class. Indeed, mice lacking only MHC I indicated a modest protective function for $CD8^+$ T cells in clearing primary *Salmonella* infection (Lee *et al.*, 2012).

As with $CD8^+$ T cells, the involvement of B cells in the defence against *Salmonella* is not well understood. While absence of B cells does not interfere with the clearance of primary infection with attenuated *Salmonella* strain, immunised, B cell-deficient mice cannot be protectively immunised and succumb to secondary infection with virulent *Salmonella* (McSorley and Jenkins, 2000; Mittrücker *et al.*, 2000; Mastroeni, Simmons, *et al.*, 2000). Interestingly, B cell-deficient mice immunised with attenuated *Salmonella* show reduced numbers of T_h1 cells which was antibody-independent as the T_h1 population in mice, lacking all secreted antibodies, was comparable to control wt mice (Nanton *et al.*, 2012). Overall, the relevance of antibodies in *Salmonella* immunity remains controversial (Mastroeni and Rossi, 2020). Neither mucosal immunoglobulins nor IgA are necessary for protective function against *Salmonella* (Wijburg *et al.*, 2006; Strugnell and Wijburg, 2010; Nanton *et al.*, 2012). However, serum from *Salmonella* treated mice was able to provide protection against secondary infection in vaccinated B cell-deficient mice (McSorley and Jenkins, 2000). Some studies have also suggested a role of B cells in secretion of inflammatory cytokines and antigen-presentation to *Salmonella*-specific T_h1 cells, contributing to the control of *Salmonella* infections.

Taken together, IFNγ is crucial for early control of bacterial burden as mice lacking the cytokine are unable to control the infection and succumb within 4 weeks (Kupz *et al.*, 2014). In contrast, $CD4^+$ T cells, especially T_h1 $CD4^+$ cells, are required for the clearance of *Salmonella* infection and long-term protection. While $CD8^+$ T cells and

B cells play no major role in clearing infections by (attenuated) Salmonellae, they are likely to contribute to long-term immunity against *Salmonella* infections.

1.3.4 Mouse models

S. Typhi is an exclusively human pathogen (de Jong *et al.*, 2012) and naturally avirulent in mice (Strugnell *et al.*, 2014). In contrast, *S.* Typhimurium is a generalist, adapted to a wide range of hosts (Palmer and Slauch, 2017). In humans, *S. Typhimurium* causes gastroenteritis; in mice, however, the pathogen leads to a systemic infection showing many characteristics to human typhoid fever (Pham and McSorley, 2015; Benoun *et al.*, 2018).

Infection outcome is highly dependent on host genes that are necessary for the immune response against intracellular pathogens such as natural resistance-associated macrophage protein 1 (*Nramp1*) or Toll-like receptor 4 (*TLR4*) (Chapes *et al.*, 2001; Higginson *et al.*, 2016).

The *Nramp1* gene encodes for a metal transporter that is important in iron metabolism and indirectly in pathogen resistance (Vidal *et al.*, 1995; Govoni *et al.*, 1996; Goswami *et al.*, 2001). Many mouse strains used for the study of *Salmonella* infections such as C57BL/6 or Balb/c mice show a single nucleotide polymorphism (SNP) in Nramp1. The SNP renders the protein non-functional. Consequently, bacteria, including *Salmonella, Leishmania,* and *Mycobacteria,* proliferate uncontrollably as phagocytic cells fail to deprive the SCV of metal ions (Vidal *et al.*, 1995). Nramp1$^{-/-}$ mice are therefore more susceptible to virulent *Salmonella* strains and succumb within three weeks (Plant and Glynn, 1979; Johanns *et al.*, 2010). In contrast, Nramp1$^{+/+}$ mouse strains (129 Sv, DBA) survive the infection (Govoni *et al.*, 1996; Monack *et al.*, 2004) although similar lethality can be achieved by infecting Nramp1$^{+/+}$ mouse strains with increased bacterial doses (10^5 colony-forming units (CFU) intraperitoneally or intravenously or by oral infection with higher doses (10^8 CFU) (Higginson *et al.*, 2016).

Recently, humanised mouse models for *S.* Typhi infection have been developed. The transfer of human haematopoietic stem cells into immunodeficient mice leads

to susceptibility of the mice to *S.* Typhi by allowing dissemination of bacteria through liver, spleen and gallbladder (Mian *et al.*, 2011). Although humanised mice seem promising, they carry high costs and labor in generation as well as maintenance, and intrinsic variability from the grafting process. Furthermore, human BM is highly heterogeneous subjecting humanised mice to biological variability (Mian *et al.*, 2011).

Although the *S.* Typhimurium mouse model is imperfect as the pathogen causes gastroenteritis instead of a systemic infection in humans, implying different pathogenicity and immune responses (Palmer and Slauch, 2017), most of our knowledge concerning *Salmonella* infections and immunity, however, is derived from studies in mice (Dougan *et al.*, 2011).

1.4 Aim of the thesis

CCL17 and CCL22 are two chemokines primarily expressed by DC and macrophages under homeostatic and inflammatory conditions (Schaniel *et al.*, 1998; Vulcano *et al.*, 2001; Alferink *et al.*, 2003; Katakura *et al.*, 2004; Rapp *et al.*, 2019). Both chemokines facilitate the interaction between DC and T cells (Semmling *et al.*, 2010; Rapp *et al.*, 2019), induce migration (Curiel *et al.*, 2004; Weber *et al.*, 2011; Wiedemann *et al.*, 2016; Fülle *et al.*, 2018), and sensitise DC for migration (Stutte *et al.*, 2010; Bischoff *et al.*, 2015). Although CCL17 and CCL22 share the chemokine receptor CCR4 (Santulli-Marotto, Boakye, *et al.*, 2013; Yoshie and Matsushima, 2015), they show different functions in immune regulation, a phenomenon which is called biased agonism (Rajagopal *et al.*, 2013; Anderson *et al.*, 2016). CCL17 is involved in the migration and activation of T_h1 and T_h2 cells as well as DC migration and has been particularly studied in the pathogenesis of allergic and inflammatory diseases (Alferink *et al.*, 2003; Stutte *et al.*, 2010; Weber *et al.*, 2011; Heiseke *et al.*, 2012; Achuthan *et al.*, 2016). In contrast, CCL22 is rather associated with T_{reg} cell recruitment and appears to play a more immunosuppressive role (Curiel *et al.*, 2004; Santulli-Marotto *et al.*, 2015; Bischoff *et al.*, 2015; Mohamed *et al.*, 2016; Wiedemann *et al.*, 2016; Ketcham *et al.*, 2018).

Both chemokines were studied in a variety of allergic and inflammatory diseases as well as tumorigenesis. However, not much is known about their importance in infection and in building a $CD4^+$ T cell immunity against infectious diseases. Hence, I aimed to investigate the role of CCL17 and CCL22 in the adaptive T cell immunity against *Salmonella* infection using a vaccine/challenge model with $CCL17^{E/E}$ $CCL22^{-/-}$ and $CCR4^{-/-}$ mice.

In the context of *Salmonella* infection, IL-33 deficiency in mice was shown to be detrimental, as $IL\text{-}33^{-/-}$ mice exhibited severe destruction of the gut and higher susceptibility to the infection (Mahapatro *et al.*, 2016). Intestinal stromal cells and DC upregulate IL-33 in response to bacterial ligands, such as flagellin (Owens *et al.*, 2013). IL-33 signaling and function on intestinal stromal cells was directly protective against *Salmonella* infection (Owens *et al.*, 2013; Mahapatro *et al.*, 2016). Moreover, IL-33 stimulates CCL17 and CCL22 production by DC (Besnard et al., 2011; Kurokawa et al., 2013), which likely aids immune cell recruitment into sites of inflammation and indicates a connection between the IL-33 signaling pathway and the CCL17/CCL22/CCR4-axis. Thus, the present thesis focused on investigating the role of CCL17 and CCL22 in IL-33-mediated immune responses in lymphoid organs associated with *Salmonella* dissemination and beyond.

Additionally, previously generated data using a 2,4-dinitro-1-fluorobenzene (DNFB)-induced contact hypersensitivity assay (CHS) mouse model showed that $CCR4^{-/-}$ mice developed an exaggerated immune response, whereas $CCL17^{E/E}$ $CCL22^{-/-}$ mice were protected (Fülle, 2018). These findings suggested the existence of a third player, either ligand or receptor, in the CCL17/CCL22/CCR4-axis. Therefore, the last part of the thesis aimed to gather more evidence for, and ultimately identify, the second putative receptor for CCL17 and CCL22. For that purpose, methods such as a chemokine-based receptor staining and a Pull Down Assay needed to be established.

Chapter 2: Materials and Methods

2.1 Materials

2.1.1 Equipment

Table 2.1: Equipment

Equipment	Article – (Company)
Automatic tissue processor	Leica ASP300 (Leica Microsystems, Wetzlar, Germany)
Cell Counting Chamber	Neubauer improved (La Fontaine via Labotec, Göttingen, Germany)
Centrifuges	5415R (Eppendorf, Hamburg, Germany) 5810R (Eppendorf, Hamburg, Germany) Allegra® X-15R Centrifuge (Beckman Coulter, Brea, USA)
Centrifuge Concentrator	Concentrator plus (Eppendorf, Hamburg, Germany)
Cryostat	Leica CM3050 S (Leica Microsystems, Wetzlar, Germany)
Dewar Carrying Flasks	26B (KGW-Isotherm, Karlsruhe, Germany)
Electrophoresis Power Supply	Power Source™ 300V (VWR International, Radnor, USA)
Electrophoresis System	XCell SureLock (Invitrogen, Waltham, USA)
ELISA washer	CAPP wash 12 (CAPP, Odense, Germany)
Flow Cytometer	BD LSR II Flow (BD Biosciences, Heidelberg, Germany) BD FACS Symphony ™ (BD Biosciences, Heidelberg, Germany) BD FACS Aria™ III (BD Biosciences, Heidelberg, Germany)

Forceps	FV126-115, vedena® feine anatomische Pinzette SEMKEN, 155 mm (6‘‘) (Medical Highlights Germany GmbH, Rohrdorf, Germany)
Freezer (-20 °C)	Comfort (Liebherr, Biberach, Germany)
Freezer (-80 °C)	New Brunswick Ultra-Low Temperature Freezer (Eppendorf, Hamburg, Germany)
Fridge (+4 °C)	MediLine LKUexv1610 (Liebherr, Biberach, Germany)
Fume Hood	System DELTA 30 laboratory fume cupboards (Wesemann International GmbH, Wangen im Allgäu, Germany)
Gel documentation system	Odyssey (Li-Cor Bioscience, Bad Homburg, Germany)
Gel electrophoresis	PerfectBlue Gel System (Peqlab, Erlangen, Germany)
Hamilton syringe	Model 1750 RN (Hamilton Company, Reno, USA)
Heating devices	TS1 Thermo Shaker (Biometra, Göttingen, Germany) Heating block Thermostat TH21 (HLC BioTech, Bovenden, Germany) Water bath WNB 22 (Memmert, Schwabach, Germany)
Ice machine	Scotsman Flockeneisbereiter AF200 (Hubbard Systems, Birmingham, USA)
Incubator	CB 150 (Binder, Tuttlingen, Germany) ECOCELL (MMM Group, Planegg/München, Germany) Memmert INE 500 (Memmert GmbH + Co.KG, Schwabach, Germany) ECOCELL (MMM Group, Planegg/München, Germany)

Incubator shaker	New Brunswick Innova® 44/44R (Eppendorf, Hamburg, Germany) Stuart orbital incubator SI500 (Cole-Parmer, Stone, UK)
Laminar flow workbench	BDK Laminar Flow (BDK, Sonnenbrühl, Genkingen, Germany)
Magnetic stirrer	IKA RCT basic (IKA-Werke GmbH & Co. KG, Staufen, Germany)
Mass spectrometer	Q Exactive™ Plus (Thermo Fisher Scientific, Waltham, Germany)
Measuring cylinder	250 mL, 500 mL, 1000 mL, 2000 mL (VWR, Wayne, USA)
Microscope	BZ 9000 Keyence (KEYENCE DEUTSCHLAND GmbH, Neu-Isenburg, Germany) Olympus BX50 (Olympus Corporation, Tokyo, Japan) Eclipse TS100 (Nikon Instruments Inc., Melville, NY, USA)
Microtome	Leica RM2255 (Leica Microsystems, Wetzlar, Germany)
Microwave	NN-E235M (Panasonic, Osaka, Japan)
Paraffin Embedding Station	Leica EG1150 H (Leica Microsystems, Wetzlar, Germany)
pH meter	FiveEasy FE20-Basic (Mettler Toledo, Columbus, USA)
Photometer	Bio-Photometer 6131 (Eppendorf, Hamburg, Germany)
Pipettes	10 µL, 20 µL, 100 µL, 200 µL, 1000 µL (Eppendorf, Hamburg, Germany)

Rocking Plattform Shaker	Duomax 1030 (Heidolph Instruments GmbH & Co.KG, Schwabach, Germany
Scales	440-35A (Kern & Sohn, Balingen, Germany)
	ABJ 220-4M (Kern & Sohn, Balingen, Germany)
Scissors	EV107-110, Vedena® Feine Schere IRIS, spitz-spitz, gerade, 110 mm (4 ¼'') (Medical Highlights Germany GmbH, Rohrdorf, Germany)
	EV118-115, Vedena® chirurgische Schere, spitz-stumpf, gerade, 115 mm (4 ½'') (Medical Highlights Germany GmbH, Rohrdorf, Germany)
Sonicator bath	Sonorex Digitec (Bandelin, Berlin, Germany)
Spectrophotometer	EL 800 (BioTek, Winooski, USA)
Syringe Pump	Fusion 101 (Chemyx Inc., Stafford, US)
Thermal cycler	T100TM (BioRad, Hercules, USA)
	T1 Thermocycler (Biometra, Göttingen, Germany)
Threaded bottles	100 mL, 250 mL, 500 mL, 1000 mL (Schott, Mainz, Germany)
Tissue homogeniser	IKA® T10 basic (IKA®-Werke GmbH & Co.KG, Staufen, Germany)
Transilluminator	Biostep Dark Hood DH-40/50 (biostep, Burkhaltsdorf, Germany)
Vortex Shaker	Vortex Genie 2 (Scientific Industries, New York, USA)
Water Bath	Leica HI1210 (Leica Microsystems, Wetzlar, Germany)

2.1.2 Consumables

Table 2.2: Consumables

Item	Company
Cell strainer nylon (70µm, 100µm)	VWR International, Radnor, US Starlab International GmbH, Hamburg, Germany
Cover slips (24x60 mm)	Epredia, Kalamazoo, USA
CryoPure Tube 1.8 ml	Sarstedt, Nümbrecht, Germany
Crytome blades	A. Hartenstein GmbH, Würzburg, Germany
Culture plates (6-well/ 24-well/ 48-well/ 96- well, flat bottom)	Greiner, Kremsmünster, Austria
ELISA plate (half-area, 96 K)	Greiner, Kremsmünster, Austria
Embedding cassettes	Carl Roth GmbH + Co.KG, Karlsruhe, Germany
Filter tips	Sarstedt, Nümbrecht, Germany
Flow cytometry tubes	Sarstedt, Nümbrecht, Germany
Glass Reagent/Media Bottles (10 mL, 50 mL, 200 mL, 500 mL)	VWR International, Radnor, USA
ImmEDGE™ hydrophobic barrier pen	Vector Laboratories, Burlingame, USA
Measuring beakers	Sigma-Aldrich, St. Louis, USA
Measuring cylinders (10 mL, 100 mL, 500 mL)	VWR International, Radnor, USA
Micro tube 1.1ml Z-Gel	Sarstedt, Nümbrecht, Germany
Microscope slides (Superfrost plus)	Thermo Fisher Scientific, Waltham, USA
Microtome blades	
NativeMark™ Protein Standard	Invitrogen, Waltham, USA
NativePAGE™ 3-12 % Bis-Tris Gel (1.0 mm)	Invitrogen, Waltham, USA

NativePAGE™ Sample Buffer (4x)	Invitrogen, Waltham, USA
Parafilm®	American National Cam, Greenwich, USA
PCR tubes	Sarstedt, Nümbrecht, Germany
Petri dishes	Greiner, Kremsmünster, Austria
Precision wipes	Kimberly-Clark, Reigate, UK
Reaction tubes (15ml, 50ml)	Greiner, Kremsmünster, Austria
Safe seal reaction tubes (0,5, 1.5ml, 2.0ml)	Sarstedt, Nümbrecht, Germany
Serological pipettes (5 mL, 10 mL, 25 mL)	Greiner, Kremsmünster, Austria
Sterican needles (1.20x40 mm; 18Gx1½, 0.90x40mm; 19G x 1½ 0.90x40 mm; 20Gx1½, 0.40x20 mm; 27Gx¾)	Braun, Melsungen, Germany
Syringes Inject-F Tuberkulin (1ml)	Braun, Melsungen, Germany
Syringes Inject® (2ml, 5ml, 10ml, 20ml)	Braun, Melsungen, Germany
Tissue-Tek® Cryomold (15x15x5 mm)	Sakura Finetek USA, Inc., Torrance, USA
UVette® (220 nm – 1.600 nm)	Eppendorf, Hamburg, Germany
Micro Bio-Spin™ 6 Columns	Bio-Rad Laboratories Inc., Hercules, USA
Cell culture flasks (T25, T75, T175)	Greiner Bio-One, Kremsmünster, Austria

2.1.3 Chemicals and reagents

Table 2.3: Chemicals and reagents

Chemical/reagents	Company
100bp DNA Ladder	New England BioLabs, Ipswich, USA
10x TAE buffer	Invitrogen, Waltham, USA

16 % Formaldehyde Solution (w/v), methanol-free	Thermo Fisher Scientific, Waltham, USA
2-mercaptoethanol	Sigma-Aldrich, St. Louis, USA
2,2,2-trifluorethanol (TFE)	Acros organics, Waltham, USA
Acetic acid	Sigma-Aldrich, St. Louis, USA
Acetone	VWR International, Radnor, Germany
Ammonium acetate (MS-grade)	Sigma-Aldrich, St. Louis, USA
Bacto™ Agar	BD Bioscience, Franklin Lakes, USA
BisTris	Sigma-Aldrich, St. Louis, USA
BLOXALL® Endogenous Blocking Solution	Vector Laboratories Inc., California, USA
Bovine serum albumin (BSA)	SERVA Electrophoresis GmbH, Heidelberg, Germany
Chloroform	Merck KGaA, Darmstadt, Germany
Collagenase D	SERVA Electrophoresis GmbH, Heidelberg, Germany
Complete protease inhibitor mix	Roche, Basel, Switzerland
Coomassie-G250	Sigma-Aldrich, St. Louis, USA
DABCO	Sigma-Aldrich, St. Louis, USA
DAPI	Sigma-Aldrich, St. Louis, USA
Deoxynucleotide (dNTP) Solution Mix	Peqlab, Erlangen, Germany
DNase I	Merck, Darmstadt, Germany
Dulbecco's Modified Eagle Medium (DMEM)	Thermo Fisher Scientific, Waltham, USA
Dulbecco’s phosphate-buffered saline (PBS)	Sigma-Aldrich, St. Louis, USA
Dynabeads™ MyOne™ Streptavidin C1	Invitrogen, Waltham, USA
Eosin	Merck, Darmstadt, Germany
Ethanol 70% (methylated)	Roth, Karlsruhe, Germany

Ethylenediaminetetraacetic acid (EDTA)	Sigma-Aldrich, St. Louis, USA
EZ-Link™ Sulfo-NHS-LC-Biotin	Thermo Fisher Scientific, Waltham, USA
FACS Clean Solution	BD Bioscience, Franklin Lakes, USA
FACS Rinse Solution	BD Bioscience, Franklin Lakes, USA
Fetal Bovine Serum	PAN-Biotech GmbH, Aidenbach, Germany
Fixable Viability Dye eFluor 780	eBioscience, San Diego, US
Gelatine from porcine skin	Sigma-Aldrich, St. Louis, USA
Gentamicin	Gibco by Life Technologies, Carlsbad, USA
Glycerol	Roth, Karlsruhe, Germany
Hank's Balanced Salt Solution (HBSS) (10x)	Gibco by Life Technologies, Carlsbad, USA
Haemalaun solution accid according to Mayer	Roth, Karlsruhe, Germany
N-2-hydroxyethylpiperazine-N-2-ethane sulfonic acid (HEPES)	Sigma-Aldrich, St. Louis, USA
Horseradish Peroxidase	Sigma-Aldrich, St. Louis, USA
Hydrochloric acid (HCl)	Sigma-Aldrich, St. Louis, USA
Iscove's Modified Dulbecco's Medium (IMDM)	Thermo Fisher Scientific, Waltham, USA
Isopropanol (MS-grade)	Thermo Fisher Scientific, Waltham, USA
Luria-Bertani (LB) Broth, high salt	Sigma-Aldrich, St. Louis, USA
LC-MS Grade Water	Thermo Fisher Scientific, Waltham, USA
L-Glutamine	Gibco by Life Technologies, Carlsbad, USA

Liberase™	Merck, Darmstadt, Germany
Methanol (MS-grade)	VWR International, Radnor, USA
Micro Bio-Spin™ 6 Columns	Bio-Rad Laboratories Inc., Hercules, USA
Mouse BD Fc Block™ (purified rat anti-mouse CD16/CD32)	BD Bioscience, Franklin Lakes, USA
Mowiol®	Sigma-Aldrich, St. Louis, USA
OMICS internal standard mix	AG Thiele, LIMES Insitute, University of Bonn, Germany
OneTaq Quick-Load 2X Master Mix with Standard Buffer	New England Biolabs, Ipswich, USA
Paraformaldehyde (PFA)	Merck, Darmstadt, Germany
Penicillin-Streptomycin	Gibco by Life Technologies, Carlsbad, USA
peqGOLD Universal Agarose	Peqlab, Erlangen, Germany
Phosphate Buffered Saline Dulbecco	Merck, Darmstadt, Germany
Poly-D-lysine	Invitrogen, Waltham, USA
Ponceau S	Thermo Fisher Scientific, Waltham, USA
Potassium bicarbonate ($KHCO_3$)	Merck, Darmstadt, Germany
Precision Plus Protein Dual Color Standards	Bio-Rad Laboratories Inc., Hercules, USA
Proteinase K	Sigma-Aldrich, St. Louis, USA
RBC Lysis Buffer (10x)	BioLegend, San Diego, USA
Roswell Park Memorial Institute (RPMI) 1640	Thermo Fisher Scientifc, Waltham, USA
Sodium chloride (NaCl)	Sigma-Aldrich, St. Louis, USA
Sodium deoxycholate	Sigma-Aldrich, St. Louis, USA
Sodium fluoride	Sigma-Aldrich, St. Louis, USA

Sodium orthovanadate	Sigma-Aldrich, St. Louis, USA
SPHERO™ Blank Calibration Particles (6.0 – 6.4 µm)	BD Bioscience, Franklin Lakes, USA
Sterile Water for cell culture	PAN-Biotech, Aidenbach, Germany
Streptomycin sulfate	Roth, Karlsruhe, Germany
Sucrose	Sigma-Aldrich, St. Louis, USA
Sulfuric acid (H_2SO_4)	Roth, Karlsruhe, Germany
TG standard mix	AG Thiele, LIMES Insitute, University of Bonn, Germany
Tissue-Tek Freezing Medium	A. Hartenstein GmbH, Würzburg, Germany
TMB Plus2®	Kementec Solutions A/S, Taastrup, DK
Tricine	Sigma-Aldrich, St. Louis, USA
Triethylammoniumbicarbonat (TEAB)	Sigma-Aldrich, St. Louis, USA
Tris Buffered Saline	Merck, Darmstadt, Germany
Tris(2-carboxyethyl)phosphine (TCEP)	Thermo Fisher Scientific, Waltham, USA
Tri-sodium citrate dihydrate	Sigma-Aldrich, St. Louis, USA
Trypan Blue	Sigma-Aldrich, St. Louis, USA
Trypsin	Sigma-Aldrich, St. Louis, USA
Tween-20	Roth, Karlsruhe, Germany
UltraPure™ Distilled Water, DNase/RNase Free	Invitrogen, Waltham, USA
VectaMount® Permanent Mounting Medium	Vector Laboratories Inc., Burlingame, USA
Xylene	Roth, Karlsruhe, Germany

2.1.4 guideRNA and primer

Table 2.4: guideRNAs and primer

guideRNA/primer	Sequence	Company
guideRNAs for CCR4 knockout	GGTTACAAGCGTAGAGATAA ACGTCACTCATGGATAGATG	Integrated DNA Technologies, Inc., Coralville, USA
Primer CCR4 (framing)	CCAAAGGTCCCCAGTCACTC GCACCGACGAGCTTCTTCTA	Integrated DNA Technologies, Inc., Coralville, USA
Primer CCR4 (intern)	CTCCCAGGCCTCTTGTTCAG CTGTAGCCTGGATGGCGTAG	Integrated DNA Technologies, Inc., Coralville, USA

2.1.5 Chemokines and cytokines

Table 2.5: Chemokines and cytokines

Chemokines/cytokines	Company
Murine MDC (CCL22)	Peprotech, Cranbury, USA
Recombinant mouse CCL17/TARC	BioLegend, San Diego, USA
Recombinant murine IL-33	Peprotech, Cranbury, USA
Recombinant murine KC (CXCL1)	Peprotech, Cranbury, USA

2.1.6 Solutions and buffers

Table 2.6: Solutions and buffers

Solutions/buffers	Content
Binding buffer (chemokine-tetramer)	RPMI 1640 10 % heat-inactivated fetal bovine serum (FCS) 2 mM L-Glutamine 100 U/ml Penicillin 100 µg/ml Streptomycin

	0.05 mM 2-mercaptoethanol 20 mM HEPES
Blocking buffer (immunofluorescence)	1 % BSA 2 % goat-serum PBT (0.4 %)
BMDC medium	RPMI 1640 10 % heat-inactivated FCS 2 mM L-Glutamine 100 U/ml Penicillin 100 µg/ml Streptomycin 1.43 mM mM 2-mercaptoethanol 2 % GM-CSF
BW5147.3 media	RPMI 1640 10 % heat-inactivated FCS 2 mM L-Glutamine 100 U/ml Penicillin 100 µg/ml Streptomycin 1.43 µM mM 2-mercaptoethanol
Citrate buffer (10mM, pH 6)	2.94 g Tri-sodium citrate dihydrate 0.05 % Tween-20 in 1000 mL ddH_2O
Digestion buffer (spleen)	PBS 1 mg/mL Col D 0.1 mg/mL DNase I
Digestion buffer (PP)	RPMI 1640 5 % heat-inactivated FCS 100 U/ml Liberase 5 U/ml DNase I
Extraction Mix	14,7 mL Methanol

	2,53 mL $CHCl_3$ 720 µL OMICS internal standard mix 50,4 µL TG standard mix
FACS buffer	PBS 2 mM EDTA 0.5 % heat-inactivated FCS
HEK cell medium	DMEM 10 % heat-inactivated FCS 2 mM L-Glutamine 100 U/ml Penicillin 100 µg/ml Streptomycin 1.43 µM mM 2-mercaptoethanol
MutuDC medium	IMDM 10 % heat-inactivated FCS 10 mM HEPES 50 U/ml Penicillin 50 µg/ml Streptomycin 50 µM mM 2-mercaptoethanol
Native cathode buffer (20x)	1 g Coomassie G-250 in 200 mL ultrapure H_2O
Native dark blue buffer	1x native running buffer 1x native cathode buffer In 200 mL ultrapure H_2O
Native light blue buffer	1x native running buffer 0.1x native cathode buffer In 200 mL ultrapure H_2O
Native running buffer (20x, pH 6.8)	50 mM BisTris 50 mM Tricine
Native sample buffer (pH 7.2)	50 mM BisTris

	6 N HCl 50 mM NaCl 10 % w/v Glycerol 0.001 % Ponceau S
PFA (4 %)	4g PFA in 100 ml PBS, pH 7.4
RIPA lysis buffer	50 mM Tris-HCl, pH 7.3 150 mM NaCl 0.1 mM EDTA 1 % (w/v) sodium deoxycholate 1 % (v/v) Triton X-100 0.2 % (w/v) sodium fluoride 100 µM sodium orthovanadate Complete protease inhibitor mix
RIPA wash buffer	50 mM Tris-HCl, pH 7.3 150 mM NaCl 0.1 mM EDTA 0.2 % (w/v) sodium fluoride 100 µM sodium orthovanadate
SK11AeαIL18 medium	RPMI 1640 10 % heat-inactivated FCS 2 mM L-Glutamine 100 U/ml Penicillin 100 µg/ml Streptomycin 1.43 µM mM 2-mercaptoethanol
Spray buffer	16 mL Isopropanol 10 mL Methanol 1720 µL MS-grade water 10 mM ammonium acetat

Starvation medium	RPMI 1640 0.5 % heat-inactivated FCS 100 U/ml Penicillin 100 µg/ml Streptomycin
Wash buffer PBT (immunofluorescence)	0.4 % Triton X-100 PBS

2.1.7 Kits and assays

Table 2.7: Kits and assays

Kits/assays	Company
DuoSet® ELISA Mouse CCL17/TARC	R&D Systems, Minneapolis, USA
DuoSet® ELISA Mouse CCL22/MDC	R&D Systems, Minneapolis, USA
eBioscience™ Foxp3 / Transcription Factor Staining Buffer Set	eBioscience, Inc., San Diego, USA
ImmPress® Goat Anti-Rat IgG Polymer Kit, Peroxidase	Vector Laboratories Inc., Burlingame, USA
ImmPACT® DAB Substrate Kit, Peroxidase	Vector Laboratories Inc., Burlingame, USA
SuperSignal® West Pico Chemiluminescent Substrate	Thermo Fisher Scientific, Waltham, USA

2.1.8 Antibodies

Table 2.8: Flow cytometry antibodies

Antigen	Clone	Conjugate	Dilution	Company
B220	RA3-6B2	APC-Cy7	1:200	BioLegend
CCR4	2G12	BV421	1:100	BioLegend
CD103	2E7	PerCP-Cy5.5	1:200	BioLegend
CD105	MJ7/18	PE	1:200	BioLegend
CD11b	M1/70	BV605	1:300	BioLegend

CD11b	M1/70	PE-Cy7	1:200	eBioscience
CD11c	N418	BV510	1:200	BioLegend
CD11c	HL3	BUV395	1:300	BD Bioscience
CD16/32	S17011E	APC-R700	1:100	BioLegend
CD133	315-2C11	PE/Dazzle	1:200	BioLegend
CD150	TC15-12F12.2	BV51	1:200	BioLegend
CD172α	P84	PE/Dazzle	1:200	BioLegend
CD19	6D5	BV650	1:200	BioLegend
CD25	PC61	PE-Cy7	1:200	BioLegend
CD3	145-2C11	APC-Cy7	1:200	BioLegend
CD34	SA376A4	PE-Cy7	1:200	BioLegend
CD4	GK1.5	BUV564	1:200	BD Bioscience
CD41	MWReg30	BUV563	1:200	BD Bioscience
CD44	IM7	BV570	1:300	BioLegend
CD45	30-F11	BUV661	1:200	BD Bioscience
CD45	30-F11	BV510	1:200	BioLegend
CD62L	MEL-14	APC-R700	1:200	BD Bioscience
CD69	H1.2F3	BV711	1:200	BioLegend
CD71	RI7217	BV421	1:200	BioLegend
CD8	YTS156.7.7	PerCP-Cy5.5	1:200	BioLegend
c-kit	2B8	PerCP-Cy5.5	1:200	BioLegend
F4/80	BM8	APC-Cy7	1:200	BioLegend
F4/80	BM8	BV786	1:200	BioLegend
FoxP3	FJK-16s	PE	1:100	eBioscience
GATA3	TWAJ	PE-eFluor610	1:50	eBioscience
IL7Rα	A7R34	BV711	1:200	BioLegend
KLRG1	2F1	BUV395	1:100	BD Bioscience
Ly6C	HK1.4	BV711	1:200	BioLegend
Ly6G	1A8	BUV563	1:200	BD Bioscience

MHC II	M5/114.15.2	APC-Cy7	1:200	BioLegend
MHC II	M5/114.15.2	BV650	1:200	BioLegend
MHC II	M5/114.15.2	PE-Cy7	1:200	BioLegend
NK1.1	PK136	PE	1:200	BD Bioscience
Nrp1	3E12	APC	1:100	BioLegend
RORγt	Q31-378	BV421	1:100	BD Bioscience
Sca-1	E13-161.7	BUV35	1:20	BioLegend
ST2	U29-93	BV605	1:100	BD Bioscience
T-bet	4B10	BV786	1:100	BioLegend
TCRβ	H57-597	BUV737	1:200	BD Bioscience
Ter119	TER-119	APC	1:200	BioLegend

Table 2.9: Fluorphore-coupled streptavidins

Conjugate	Concentration used	Company
BV421	2.5 µg/mL or 100 µg/mL	BioLegend
PE	100 µg/mL	BioLegend

Table 2.10: Histological antibodies

Antigen	Clone	Conjugate	Host	Dilution	Company
GFP	polyclonal	unconjugated	rabbit	1:200	Life Technologies
CD45	30-F11	unconjugated	rat	1:300	BioLegend
Rabbit IgG	polyclonal	AlexaFluor 488	goat	1:200	Life Technologies

2.1.9 Bacterial strains

Table 2.11: *Salmonella* Typhimurium strains

Strain	Resistance	Characteristics	Source/Reference
SL1344	Streptomycin	Wild type strain rpsL hisG	(Wray and Sojka, 1978)
TAS2010	Streptomycin	Living, attenuated strain (∆edd ∆pfkA ∆pfkB)	(Kupz *et al.*, 2013)

Table 2.12: Software

Software	Company
BioRender	BioRender, Toronto, Canada
BZ-II Analyzer	Keyence, Montabaur, Germany
Explore Q Exactive Plus Tune	Thermo Fisher Scientific, Waltham, USA
FACS Diva	BD, Franklin Lakes, USA
FlowJo 10.5.3	TreeStar, Inc., Ashland, USA
GraphPad Prism 9.2.0	GraphPad, La Jolla, USA
ImageJ (Fiji)	Rasband, W.S., ImageJ, U. S. National Institutes of Health, Bethesda, USA
Inkscape 1.2.1	Harrington, B. et al, Inkscape
ImageLab 6.01	Bio-Rad Laboratories Inc., Hercules, USA
LipidXplorer	Lipidomics Informatics for Life Sciences
Mendeley Software	Elsevier, Amsterdam, Netherlands
Microsoft Office 2016	Microsoft, Redmond, USA
PEAKS Studio 11	Bioinformatics Solutions Inc., Waterloo, ON, Canada

2.2 Methods

2.2.1 Animal experiments

2.2.1.1 Mice housing conditions

Mice were housed under specific pathogen-free (SPF) conditions in the Genetic Resources Center (GRC) of the Life & Medical Sciences Institute, University of Bonn, Germany. Mice were maintained in individually ventilated cages under conventional laboratory conditions (12h/12h light/dark cycle, 22 °C), with *ad libitum* access to food and water. Genotypes were defined through polymerase-chain reaction (PCR.) All animal experiments were performed with age- and sex-matched mice, indicated in the specific animal experiment sections, using wild-type (wt) C57BL/6JRcc, $CCL17^{E/E}$, $CCL22^{-/-}$, $CCL17^{E/E}$ $CCL22^{-/-}$ or $CCR4^{-/-}$ mice. Both $CCL17^{E/E}$ and $CCL17^{E/E}$ $CCL22^{-/-}$ mice express the enhanced green fluorescent protein (EGFP) under the control of the endogenous *Ccl17* promoter. All animal experiments were approved by the government of North Rhine-Westphalia (Az 81-02.04.2018.A094). Mice were killed by cervical dislocation.

Mouse line	**Genetic background**	**Reference**	**Supplier**
Wild type	C57BL/6JRcc	-	GRC
$CCL17^{E/E}$	C57BL/6JRcc	(Alferink *et al.*, 2003)	I. Förster
$CCL22^{-/-}$	C57BL/6JRcc	I. Förster (unpublished)	I. Förster
$CCL17^{E/E}$ $CCL22^{-/-}$	C57BL/6JRcc	I. Förster (unpublished)	I. Förster
$CCR4^{-/-}$	C57BL/6JRcc	(Chvatchko *et al.*, 2000)	I. Förster

2.2.1.2 *Salmonella* Typhimurium infection

2.2.1.2.1 Bacterial growth of *Salmonella* Typhimurium and oral gavage

Salmonella enterica serovar Typhimurium (STM) strains were grown overnight at 37 °C either on LB agar plates or shaking in LB broth. Both were supplemented with 50 µg/mL streptomycin.

For oral infection of mice, the required STM strains were streaked on LB agar plates and grown overnight. One colony was picked and cultured in 10 mL LB broth overnight. On the next day, the overnight culture was diluted 1:100 with LB broth and cultured for an additional 5 h shaking at 37 °C. Bacteria were harvested by centrifugation (3700 rpm, room temperature, 10 min) and washed two times with steril phosphate-buffered saline (PBS). The bacterial concentration was determined through the optical density at 600 nm. To reach the appropriate STM concentration ($2.5x10^9$ CFU/mL TAS2010, $1x10^9$ CFU/mL SL1344), bacteria were diluted in sterile LB broth/10 % potassium bicarbonate solution (1:1 ratio).

2.2.1.2.2 Preparation and storage of STM glycerol stocks

For long-term storage of STM stocks, 500 µL overnight STM culture was mixed with LB broth/glycerol mix (1:1 ratio) and stored at -80 °C.

2.2.1.2.3 Oral infection of mice

Each mouse received either 200 µL LB broth/10 % potassium bicarbonate solution or 200 µL STM solution through a 1 mL syringe with a metal feeding needle. For vaccination experiments, male and female mice between 12-14 weeks were infected with $2.5x10^9$ CFU attenuated STM strain TAS2010 and challenged after 12 weeks with $1x10^9$ CFU wt STM strain SL1344. Body weight of each mouse was measured three times a week for three weeks and afterwards once per week. Mice were monitored up to 15 weeks.

2.2.1.3 IL-33 treatment

WT, CCL17$^{E/E}$, CCL22$^{-/-}$, CCL17$^{E/E}$ CCL22$^{-/-}$, and CCR4$^{-/-}$ mice (18-21 weeks, male) were intraperitoneally (i.p.) injected with 0.5 µg of recombinant murine IL-33 in 100 µL PBS every second day (d0, 2, 4, and 6). Body weight of each mouse was measured on the same days as the i.p. injections. All mice were monitored until the end of the experiment on day 8.

2.2.2 Flow cytometry and analysis of cell populations

2.2.2.1 Preparation of single cells – thymus, mesenteric lymph nodes and spleen

Thymus, mLN and spleen were collected in ice-cold PBS. Remaining fat tissue was removed from all organs. To generate single cell suspension, organs were gently pushed through a 70 µm cell strainer (T cells). For myeloid cells, organ was dissected into small pieces using scissors and incubated with digestion buffer (1 mg/mL Col D/0.1 mg/mL DNase I in PBS) for 30 min at 37 °C. Afterwards, the tissue suspension was gently pushed through a 100 µm cell strainer. All single cell suspensions (T cells, myeloids) were washed in PBS for 5 min at 400x*g* and 4 °C. Supernatant was removed, the pellet was resuspended in 2 mL red blood cell (RBC) lysis and incubated for 5 min at room temperature to lyse erythrocytes. Afterwards, RBC lysis was stopped by adding 10 mL ice-cold PBS. Cells were washed in PBS for 5 min at 400x*g* and 4 °C, resuspended and transferred into a 96 well plate for staining with fluorescently labeled antibodies. For staining of erythrocytes and their progenitors RBC lysis was skipped.

2.2.2.2 Preparation of single cells – Peyer's patches

Small intestines were collected in ice-cold HBSS with 10 % FCS. Intestines were flushed and PP were isolated using scissors. Thereafter, PP were digested in digestion buffer (RPMI 1640 with 5 % FCS 100 U/mL Liberase, 5 U/mL DNase) for 20 min shaking at 37 °C. To generate a single cell suspension, digested tissue was gently pushed through a 70 µm cell strainer. Cells were washed for 5 min at 400x*g*

and 4 °C and resuspend in FACS buffer. Cell suspension was transferred into a 96 well plate for staining.

2.2.2.3 Preparation of single cells – blood

Mice were killed by cervical dislocation. Immediately after, blood was taken from the cheek of each mouse and collected in EDTA-coated tubes containing 450 µL FACS buffer. The blood was later further diluted (1:10) in FACS buffer and either stained with antibodies for flow cytometry or measured with the ADVIA® 2120i Haematology system to assess blood parameters.

2.2.2.4 Preparation of single cells – bone marrow

In preparation, a 0.5 mL collection tube was carefully pierced at the bottom using a 20G (0.90 x 40 mm) needle. The tube was placed inside a 1.5 mL collection tube with an added volume of 100 µL PBS. Hind legs were collected in ice-cold PBS. After removing remaining muscle and fat tissue, epiphyses were cut off and the bones were placed inside the 0.5 mL collection tube. The bones were centrifuged at 1,000x*g* and 4 °C for 20 s and later discarded. The pellet was resuspended in the pre-layed 100 µL PBS and either stained with antibodies for flow cytometry or measured with the ADVIA® 2120i Haematology system.

2.2.2.5 Flow Cytometry

2.2.2.5.1 Chemokine-based receptor staining

2.2.2.5.1.1 Biotinylation of chemokines

Chemokines were mixed with a 3-fold molar excess of EZ-Link-Sulfo-NHS-LC-Biotin (Biotin) and incubated first at 4 °C followed by an incubation period at room temperature each for 30 min. Meanwhile, a Micro Bio-Spin 6 Chromatography Column was rebuffered and the biotinylated samples were added following manufacturer's instructions. Purified biotinylated chemokines were stored at -20 °C and used within 2-3 months minimizing the number of thawing-freezing cycles. 2 µL were used for determination of concentration via NanoDrop Spectrophotometer. The

optimal staining concentration was titrated after every biotinylation via flow cytometry.

2.2.2.5.1.2 Staining with pre-formed chemokine-streptavidin-tetramer

The staining was done in accordance to Springer Protocols - Chemokines and Protocols (Ford *et al.*, 2013). Biotinylated chemokines were pre-incubated with fluorophore-coupled streptavidin in PBS or binding buffer (6 µg/mL biotinylated chemokine: 100 µg/mL streptavidin) and incubated in the dark for 45 min at room temperature. Meanwhile, $1x10^6$ cells were transferred into each well of a round-bottomed 96-well plate and spun down (400x*g*, 5 min, room temperature). Pre-assembled chemokine-streptavidin-tetramer was added and incubated for 1 h in the dark at 37 °C, unless otherwise indicated. Afterwards, samples were washed twice with FACS buffer (400x*g*, 5 min, 4 °C) and incubated with 50 µL antibody mixture for 15 min at 4 °C. Finally, samples were washed twice in FACS buffer, resuspended in 300 µL FACS buffer and measured using flow cytometry.

2.2.2.5.1.3 Staining with biotinylated chemokines

Single cell suspensions were transferred to 96-well round-bottom plate, centrifuged (400x*g*, 5 min, 4 °C) and incubated with 10 µg/mL biotinylated chemokine, unless otherwise determined via titration of optimal concentration. Cells were stained for 30 min on ice. Afterwards, cells were washed twice in PBS (400x*g*, 5 min, 4 °C) followed by the addition of 2.5 µg/mL fluorophore-coupled streptavidin. Streptavidin was incubated for 30 min at room temperature. Subsequently, cells were washed twice with PBS (400x*g*, 5 min, 4 °C) and stained for surface or intracellular antigens with antibodies.

2.2.2.5.2 Surface staining with antibodies

Single cell suspensions were transferred to 96-well round-bottom plate, centrifuged (400x*g*, 5 min, 4 °C) and incubated with 50 µL antibodies against surface markers either for immune cell populations (Table 2.13) or cell culture cells (Table 2.14). Each antibody mixture contained Fc-block™ to block non-specific binding. Cells were stained for 30 min on ice. After the incubation, cells were washed in PBS (400x*g*, 5 min, 4 °C) and resuspended in 150 µL PBS. Before acquisition, $5x10^3$ counting beads were added to each sample to calculate cell counts. Total cell counts were calculated following manufacturer's instruction (Equation 2.1). Compensation was done with BD compensation beads. Data were collected with BD FACSSymphony™ cell analyser or BD LSR II flow cytometer and analysed with FlowJo™ software.

Equation 2.1: Counting beads-based calculation of absolute cell count

$$\text{Absolute count}\left(\frac{\text{cells}}{\mu\text{L}}\right) = \frac{\text{cell count} \times \text{V (counting beads)}}{\text{counting beads count x V(cells)}} \times \text{counting beads concentration}\left(\frac{\text{beads}}{\mu\text{L}}\right)$$

Table 2.13: Antibody staining panel for immune cell characterisation in PP, mLN, and spleen. Details of antibodies are listed in Table 2.8

T cells	Myeloid, B cells, NK cells	Erythrocytes and progenitors
CCR4 (surface, optional)	CD103	CD105 (surface)
CD25 (surface)	CD11b (surface)	CD133 (surface)
CD4 (surface)	CD11c (surface)	CD150 (surface)
CD44 (surface)	CD172α (surface)	CD16/32 (surface)
CD45 (surface)	CD19 (surface)	CD34 (surface)
CD62L (surface)	CD45 (surface)	CD41 (surface)
CD69 (surface)	F4/80 (surface)	CD45 (surface)
CD8 (surface)	LiveDead/Lineage (CD3)	CD71 (surface)
FoxP3 (intracellular)	Ly6C (surface)	c-kit (surface)
GATA3 (intracellular)	Ly6G (surface)	IL7Rα (surface)
KLRG1 (surface)	MHC II (surface)	LiveDead/Lineage (F4/80, B220, MHC II)
LiveDead/Lineage (F4/80, B220, MHC II)	NK1.1 (surface)	Sca-1 (surface)
Nrp1(surface)		ST2 (surface)
RORγt (intracellular)		Ter119 (surface)
ST2 (surface)		
T-bet (intracellular, optional)		
TCRβ (surface)		

Table 2.14: Antibody staining panel for characterising cell culture cells. Details of antibodies are listed in Table 2.8

BW5147.3	**HEK**	**MutuDC cDC1/cDC2**	**SK11AEαIL18**
CD44 (surface)	LiveDead	CD11b (surface)	B220 (surface)
LiveDead		CD11c (surface)	LiveDead
		LiveDead	
		MHC II (surface)	

2.2.2.5.3 Intracellular staining

Intracellular proteins were stained following staining of surface markers (section 2.2.2.5.2). Cells were fixed and permeabilised using the eBioscience™ FoxP3/transcription factor staining buffer set according to manufacturer's instructions. Antibodies were stained overnight in 50 µL permeabilisation buffer shaking at 4 °C. The next day, cells were washed first in permeabilisation buffer and afterwards in PBS (400x*g*, 5 min, 4 °C). For measurement, cells were resuspended in 150 µL PBS.

2.2.3 Histology

2.2.3.1 Organ treatment and embedding

Organ samples of the inguinal white adipose tissue (iWAT) and brown adipose tissue (BAT) for histology were fixed in 4 % PFA for at least 4 hours. Subsequently, the PFA was removed and the organs were placed into a paraffin histology strainer. Using the Tissue Processor, the samples were dehydrated and infiltrated with paraffin (Table 2.15). Finally, all samples were embedded in paraffin.

Table 2.15: **Paraffin infiltration protocol from the Tissue Processor.**

Step	Reagent	Incubation time
1	70 % Ethanol (EtOH)	1 hour
2	70 % EtOH	1 hour
3	80 % EtOH	1 hour
4	80 % EtOH	1 hour
5	90 % EtOH	1 hour
6	96 % EtOH	1 hour
7	100 % EtOH	1 hour
8	100 % EtOH	1 hour
9	Xylene	1 hour
10	Xylene	1 hour
11	Paraffin	1 hour
12	Paraffin	1 hour

2.2.3.2 Gelatin embedding

Adipose tissues from naïve mice were fixed and dehydrated in 2 % PFA/30 % sucrose in PBS overnight at 4 °C. Afterwards, tissue samples were washed three times with 30 % sucrose in PBS and incubated in fresh 30 % sucrose solution at 4 °C overnight. Subsequently, tissue samples were equilibrated in gelatin solution for 1-2 h at 37 °C. For embedding, tissue samples were placed in the middle of a cryomold. The cryomold was filled to 50 % with gelatin solution and incubated for 20 min at 4 °C until gelatin solution was solidified. Cryomold was filled to the top with gelatin solution and again incubated for 20 min at 4 °C. All samples were stored at -80 °C.

2.2.3.3 Sectioning

All paraffin-embedded iWAT and BAT samples were pre-cooled for sectioning with the microtome. Slices of 5 µm thickness were prepared and placed on glass slides.

The sectioned samples were air-dried overnight and later stored at room temperature.

Gelatin-embedded iWAT and BAT samples were sectioned in the cryostat. Before sectioning, the cryostat temperature was adjusted to the lowest possible temperature setting (-35 °C). Tissue samples were taken from storage at -80 °C and immediately sliced with the machine. The iWAT was sliced at 10 µm thickness and the BAT at 7 µm thickness. Slices were stored at -20 °C.

2.2.3.4 Haematoxylin and eosin (H&E) staining

Paraffin-embedded sections were incubated for 20 min at 65 °C. Then samples were deparaffinated, dehydrated and stained following the protocol from Table 2.16. Finally, sections were embedded with Entellan and dried overnight at room temperature.

Table 2.16: H&E staining protocol

Step	Reagent	Incubation time	Purpose
1	Xylene	10 min	Deparaffinisation
2	Xylene	10 min	
3	100 % EtOH	5 min	Rehydration
4	100 % EtOH	5 min	
5	96 % EtOH	3 min	
6	90 % EtOH	3 min	
7	80 % EtOH	3 min	
8	70 % EtOH	3 min	
9	H_2O [dest.]	3 min	
10	Haemalaun	3 min	Staining
11	H_2O [dest.]	2 min (rinsing)	
12	Eosin	3 min	Counterstaining
13	H_2O [dest.]	Short rinse	
14	70 % EtOH	1 min	Dehydration
15	80 % EtOH	1 min	
16	90 % EtOH	1 min	
17	96 % EtOH	1 min	
18	100 % EtOH	1 min	
19	100 % EtOH	1 min	
20	Xylene	5 min	Clearing
21	Xylene	5 min	

2.2.3.5 Picrosirius red staining

For Picrosirius red staining, paraffin-embedded sections of iWAT and BAT were incubated twice in xylene for 10 min to remove the paraffin. Afterwards, sections were rehydrated in a series of ethanol dilutions, starting from two times 100 % ethanol, followed by 96 %, 90 %, 80 %, and 70 % ethanol with 3 min per incubation step. Rehydrated samples were washed for 1 min in ddH_2O and incubated in

Picrosirus red staining solution for 1 h. Excess staining was carefully removed by first rinsing with ddH_2O and then with 0.5 % acetic acid. Samples were quickly dehydrated in 100 % ethanol and finally embedded with Euparal. Slides were dried overnight at room temperature.

Table 2.17: Picrosirius red staining protocol

Step	Reagent	Incubation time	Purpose
1	Xylene	10 min	Deparaffinisation
2	Xylene	10 min	
3	100 % EtOH	5 min	Rehydration
4	100 % EtOH	5 min	
5	96 % EthOH	3 min	
6	90 % EtOH	3 min	
7	80 % EtOH	3 min	
8	70 % EtOH	3 min	
9	H_2O [dest.]	1 min	
10	Picrosirius red	60 min	Staining
11	ddH_2O	Short rinse	Wash
12	0.5 % acetic acid	Short rinse	
13	100 % EtOH	Short rinse	Dehydration

2.2.4.6 Immunohistology

Paraffin-embedded sections were incubated for 20 min at 65 °C. Deparaffinisation was performed by incubating slides two times in xylene for 6 min. Sections were rehydrated in a series of ethanol dilutions, starting from two times 100 % ethanol, followed by 96 %, 90 %, 80 %, and 70 % ethanol with 3 min per incubation step. Afterwards, slides were air-dried.

For antigen retrieval, slides were transferred into pre-heated citrate buffer and incubated at 85 °C for 50 min. Slides were cooled down at room temperature for a

few minutes, before cooling them under running tap water for 1 min. Subsequently, slides were dipped into 100 % ethanol for a few seconds, air-dried and sections were surrounded by a hydrophic barrier ImmEdge pen.

In a humidified chamber, samples were first blocked with BloxAll Blocking Solution for 10 min at room temperature, washed with ddH_2O for 1 min and again blocked with 2.5 % goat serum from the ImmPRESS Goat Anti-Rat IgG Polymer Kit for 30 min at room temperature. The blocking solution was discarded and sections were either stained with primary antibody in 2.5 % goat serum or only 2.5 % goat serum (antibody control) overnight at 4 °C. After washing the slides in wash buffer (0.05 % Tween/PBS) for 5 min, secondary antibody solution (goat-anti-rat-IgG-HRP) was added and incubated for 30 min at room temperature. Following another washing step, 100 µL of freshly prepared peroxidase substrate (ImmPACT DAB Substrate Kit, 1 drop of solution in 1 mL washing buffer) was added. Slides were stained for a maximum of 5 min. Substrate was washed away with ddH_2O and slides were dehydrated in a reversed series of ethanol dilutions (70 %, 80 %, 90 %, 96 %, and 100 %) and xylene each for 1 min. Lastly, samples were embedded with VectaMount® Permanent Mounting Medium and dried overnight at room temperature.

2.2.4.7 Immunfluorescence staining

Gelatin-embedded tissue sections were taken from the -20 °C freezer and equilibrated to room temperature. Glass slides were rinsed two times with 0.05 % Tween20 in PBS and one time with 0.4 % PBT (0.4 % Triton in PBS) to wash away most of the gelatin. Afterwards, sections were blocked using blocking buffer (1 % BSA in 0.4 % PBT and 2 % NGS) for 30 min at room temperature. Subsequently, sections were incubated with 100 µL primary antibody (rabbit-anti-GFP, 1:200) in blocking buffer overnight at 4 °C. Sections were washed with 0.4 % PBT two times for 5 min and incubated with the secondary antibody (goat-anti-rabbit-AlexaFluor488, 1:200) for 2 h at room temperature. Slides were washed two times with 0.4 % PBT and one time with 0.4 % PBT containing 0.2 µg/mL DAPI. Finally,

slides were mounted using Mowiol® containing triethylenediamine (DABCO) and dried for at least 24 h at room temperature.

2.2.4.8 Microscopy

Microscopy and analysis of H&E, Picrosirius red staining, and immunohistology were performed with the BZ-9000 (Keyence) microscope in the Brightfield-Channel using 4x, 10x and 20x magnification. Immunofluorescence staining of gelatin-embedded iWAT and BAT samples was also analysed with the BZ-9000 (Keyence) microscope.

2.2.4.9 Image analysis

Images were processed using Fiji software ImageJ.

2.2.5 Lipidomics

2.2.5.1 Lipid extraction

Lipidome analysis of frozen BAT samples was done via mass spectrometry (MS). For each sample, approximately 4 mg wet tissue weight was obtained and transferred into original 2 mL Eppendorf tubes. 1 mL of MS-grade ddH_2O was added to the sample. The tissue was homogenised with a tissue homogeniser and further diluted by adding 500 µL of MS-grade ddH_2O. To accomplish complete homogenisation the samples were sonicated for 20 min. For lipid extraction, 20 µL of pre-diluted homogenate (1:4 in MS-grade ddH_2O) were mixed with 500 µL MS Extraction Mix. Afterwards, the samples were centrifuged for 2 min at 20,000x*g*. The complete supernatant was transferred into a new original 2 mL Eppendorf tube, followed by adding 200 µL chloroform and 800 µL 1 % acetic acid. The suspension was mixed thoroughly and subsequently centrifuged for 2 min at 20,000x*g*. Afterwards, the entire lower phase, containing the purified lipids, was collected and transferred into a new original 1.5 mL Eppendorf tube. Using a centrifuge concentrator (45 °C, 20 min), the solvent was evaporated. Lipids were dissolved in 1 mL spray buffer (2-propanol:methanol:water at 8:5:1 + 10 mM ammonium acetate) and sonicated for 5 min. Samples can be directly measured or stored at -20 °C.

2.2.5.2 Mass spectrometry (MS)

All MS measurements were done under the supervision and in agreement with Dr. Klaus Wunderling from the Thiele group. Recording of mass spectra was done on a Thermo Q Exactive Plus spectrometer with a standard heated electrospray ionisation ion source. For injection, BAT lipid extracts were diluted 1:10 with spray buffer and taken up with a Hamilton syringe. Injection from a Hamilton syringe was driven by a syringe pump controlled by the Tune instrument control software. All samples were sprayed at flow rates between 2-10 µL min^{-1} and following parameters: sheath gas flow rate 6, aux gas flow rate 2, sweep gas flow rate 0, gas heating off, spray voltage positive mode 4.1 kV, negative mode 3.2 kV and ion transfer capillary temperature of 280 °C.

MS1 spectra were recorded between 400-1200 *m/z* segmented in ranges of 100 *m/z* for 1 min, followed by MS2 spectra recording first between 1200-1600 *m/z* in three 100 *m/z* steps and then between 240-400 *m/z* for 0.6 min. Afterwards, MS3 spectra was recorded by data independent acquisition for 9.4 min. Subsequently, MS4 spectra was recorded between 380-431 *m/z* for 0.2 min before final recording of MS5 spectra by data independent acquisition for 0.4 min. All scan parameters are noted down in Table 2.18.

.

Table 2.18: MS scan parameters for lipidomics of BAT

MS1 scans	Automatic gain control target	$3x10^6$
	Maximum ion time	2000 ms
	Resolution	280,000
	Peak mode	Centroid
MS2 scans	Automatic gain control target	$3x10^6$
	Maximum ion time	2000 ms
	Resolution	280,000
	Peak mode	Centroid
MS3 scans	Automatic gain control target	$2x10^5$
	Maximum ion time	400 ms
	Resolution	70,000
	Spectral multiplexing	no
	First mass	dynamic
	Isolation window	1.0 *m/z*
	Stepped normalised collision energy (NCE)	10, 25, 40
	Spectrum data type	Centroid
MS4 scans	Automatic gain control target	$2x10^5$
	Maximum ion time	2000 ms
	Resolution	140,000
	Peak mode	Centroid
MS5 scans	Automatic gain control target	$2x10^5$
	Maximum ion time	automatic
	Resolution	140,000
	Spectral multiplexing	no
	First mass	300 *m/z*
	Isolation window	1.2 *m/z*
	Stepped normalised collision energy (NCE)	10, 12, 14

2.2.5.3 Identification of lipids

To analyse the data, generated raw spectrum files were converted to .mzml files using MSConverter and imported into LipidXplorer. Molecular fragment query language (.mfql), identifying the respective species by the presence of a peak corresponding to the expected mass, was used to identify the lipids. The example below identifies triacylglycerides (TAG):

```
QUERYNAME = TAG;
DEFINE PR1 = 'C[40..70] H[70..130] N[1] O[6]' WITH DBR = (1.5,12), CHG = 1;

IDENTIFY
PR1 IN MS1+

SUCHTHAT
isOdd(PR1.chemsc[C]) AND
isEven(PR1.chemsc[H])
#AND PR1.intensity > 20

REPORT
NAME = "TAG(%d:%d)" % ((PR1.chemsc[C] - 3), (PR1.chemsc[db] - 1));
CLASS = "TACG";
SAMPLE = "1";
IS = "0";
chemsc = PR1.chemsc;
C = "%d" % (PR1.chemsc[C] - 3);
db = "%d" % (PR1.chemsc[db] - 1);
MASS = "%4.4f" % "(PR1.mass)";
ERROR = "%2.2f ppm" % "(PR1.errppm)";
ISpmol = 427.1;
INT = PR1.intensity; ;
```

2.2.6 Haematological analysis

Haematological parameters, haematological indices as wells as leukocyte cell counts of diluted blood and bone marrow samples were examined using the ADVIA® 2120i haematology system. The machine was calibrated before each measurement according to manufacturer's instruction. For each sample 300 µL were measured.

2.2.7 Identification of the second receptor for CCL17 and/or CCL22

2.2.7.1 Generation of CCR4-deficient BW5147.3 cell lines

Generation of CCR4-deficient BW5147.3 cell lines was performed following the IDT genome editing protocol "Alt-R CRISPR-Cas9 System: Delivery of ribonucleoprotein complexes into Jurkat T cells using the Neon® Transfection System". Briefly, 44 µM of fluorescently labeled guideRNA was mixed with 36 µM Alt-R Cas9 protein in nuclease-free IDTE buffer and assembled at room temperature for 20 min. Afterwards, the Cas9-gRNA RNP complex was mixed with Alt-R Cas9 Electroporation Enhancer according to the manufacturer's protocol. $5x10^5$ BW5147.3 cells were electroporated with 1.8 µM gRNA, 1.5 µM Cas9 and 1.8 µM Alt-R Cas9 Electroporation Enhancer. Transfection was performed using the Neon® Transfection System at 1600 V and 10 ms pulse width (3 pulses). After electroporation, fluorescent cells were single-cell sorted in flat-bottomed 96-well plates using the cell sorter Aria II and cultured at 37 °C and 5 % CO_2. CCR4-deficient clones were validated through PCR, flow cytometry (CCR4 staining) and sequencing by Eurofins, previously GATC.

2.2.7.2 Pull Down Assay

2.2.7.2.1 Preparation of beads

Washing and preparation of magnetic Dynabeads™ MyOne™ Streptavidin C1 was performed according to the manufacturer's instructions.

2.2.7.2.2 Pull Down Assay

Pull Down Assay was performed using biotinylated CCL17 and CCL22. As negative chemokine, not binding to the target cells, biotinylated CXCL1 was applied. BW5147.3 cells (positive control), CCR4-deficient BW5147.3 cell clones and SK113AE-4 hybridoma cells (αIL18) (negative control) cells were used.

After cell harvest, $2x10^6$ cells were transferred into sterile, lidded FACS tubes. Following centrifugation (400x*g*, 5 min, 4 °C) and aspiration of the supernatant, 10 µg/mL of the respective biotinylated chemokines were added. All samples were incubated for 30 min at 4 °C. Subsequently, cells were washed twice with PBS and incubated with 100 µg/mL Dynabeads™ MyOne™ Streptavidin C1 for 30 min at room temperature. Cells were washed again twice with PBS and magnetic Pull Down was done as described by the manufacturer. Therefore, the FACS tubes, containing the samples, were placed in a magnet and supernatant was discarded after 2-3 min. Samples were washed three times in washing buffer (0.01 % (w/v) BSA in PBS) before proceeding with the cell lysis.

2.2.7.2.3 Cell lysis

For the cell lysis, samples were incubated with radioimmunoprecipitation assay (RIPA) lysis buffer for 20 min at 4 °C. Afterwards, RIPA lysis buffer was discarded and the sample was washed 4 times with RIPA wash buffer using the magnet. After last washing step, bead-bound cells were transferred into 1.5 mL tubes and centrifuged (400x*g*, 5 min, 4 °C). Supernatant was discarded before proceeding with the trypsin digest.

2.2.7.2.4 Trypsin digest

The sample was digested overnight at 37 °C. The digestion mix contained 2,2,2-trifluorethanol (TFE), tris(2-carboxyethyl)phosphine (TCEP), trypsin and triethylammoniumbicarbonat (TEAB) as described in Table 2.19. Importantly, TFE had to be less than or equal to 10 % of the final volume. After overnight digestion,

samples were centrifuged at 14,000x*g* for 10 min and 50 % of the volume was transferred into MS tubes. Samples were stored at 4 °C until measurement.

Table 2.19: Composition of digestion mix.

Step	Volume	Reagent	Purpose
1	3 µL	TFE	unfolds proteins
2	1 µL	TCEP	bond-breaker
3	10 µL	2.5 mg/mLTrypsin	cuts protein after lysine and arginine
4	16 µL	50 mM TEAB	buffer

2.2.7.2.5 MS analysis

Samples were measured by the Melbourne Mass Spectrometry and Proteomics Facility under the guidance of Prof. Nicholas Williamson. Recording of mass spectra was done on a Thermo Q Exactive Plus spectrometer. Acquired data files were processed using Peaks Studio 11 software using the paramters noted in Table 2.20.

Table 2.20: Parameters for Peaks Studio 11 analysis

Parameter	Specification
Enzyme	Trypsin
Instrument	Orbitrap (Orbi Orbi)
Fragmentation method	High-collision (HCD)
Acquisition method	Data-dependent (DDA)
Database	Mouse-july-2022
Precursor mass	10.0 ppm
Fragment ion	0.05 Da
Post-translational modifications	Oxidation, acetylation

2.2.8 Cell culture

2.2.8.1 Cell lines

BW5147.3 T cell lymphoma cell line was purchased from ATCC (TIB-47). CCR4-deficient BW5147.3 cells were generated from the original cell line using

CRISPR/Cas9 technology (see 2.2.7.1). SK113AE-4 αIL18 hybridoma cell line was generated by Matthias Lochner in the lab of Prof. Irmgard Förster at the Technical University in Munich (Lochner *et al.*, 2002). Lymphoma and hybridoma cell lines were cultured in RPMI-1640 supplemented with 10 % heat-inactivated FCS, 100 U/mL penicillin, 100 µg/mL streptomycin, 2 mM L-glutamine, and 1.43 µM β-mercaptoethanol.

Murine tumor dendritic cell lines (MutuDC) cDC1 and cDC2 were given by Hans Acha-Orbea (Fuertes Marraco *et al.*, 2012). The cell lines were cultured in IMDM supplemented with 10 % heat-inactivated FCS, 10 mM HEPES, 50 U/mL penicillin, 50 µg/mL streptomycin and 50 µM β-mercaptoethanol. For harvest, cells were incubated in non-enzymatic 5 mM EDTA/PBS buffer.

Human embryonic kidney cell line HEK293 and CCR4-expressing HEK293 cells (HEK:mCCR4) were provided by Leonor Kremer (Centro Nacional de Biotecnología, Madrid, Spain). Cells were cultured in DMEM supplemented with 10 % heat-inactivated FCS, 100 U/mL penicillin, 100 µg/mL streptomycin, 2 mM L-glutamine, and 1.43 µM β-mercaptoethanol.

All cell lines were cultured at 37 °C and 5 % CO_2 in a humidified incubator. For long-time storage, they were frozen in their respective full media containing 10 % dimethyl sulfoxide (DMSO) and stored in a nitrogen tank.

2.2.8.2 Generation and stimulation of bone marrow-derived DC (BMDC)

Mice were sacrificed by cervical dislocation and hind legs were collected in ice-cold PBS. Remaining muscle and fat tissue was removed. Tibia and femur were separated and opened by cutting of the epiphysis on both sides. BM was flushed out with sterile PBS using a syringe with a 27G¾ needle and filtered through a 100 µm cell strainer into a 50 mL falcon. Cell suspension was centrifuged at 1500 rpm for 5 min at 4 °C. Supernatant was discarded and pellet was resuspended in RPMI supplemented with 2 % GM-CSF (BMDC medium). $5x10^5$ cells in 10 mL BMDC medium were seeded in non-tissue-culture-treated petri dishes (94 mm x 16 mm). On day 3, 10 mL of fresh BMDC media was added to each petri dish. BMDC were

differentiated on day 6 and were stimulated with 20 µg/mL IL-33. Therefore, old media was removed and fresh medium without supplement or containing IL-33 was added. Cells were cultured for an additional 24 h before supernatant was taken for determination of chemokine concentrations.

2.2.9 Transwell Migration Assay

2.2.9.1 Transwell Migration Assay with BW5147.3 cells

BW5147.3 cells were thawed one day prior to performance of the assay procedure. On the day of the Transwell Migration Assay, cells were harvested by centrifugation (400x*g*, 5 min), adjusted to $6.7x10^5$ cells/mL in starvation media, and starved for 3.5 h at 37 °C. Lower chambers of the 96 transwell plates were filled with 235 µL of starvation media without supplement or containing either 100 ng/mL recombinant murine CCL17 or CCL22. After starvation, upper chambers were filled with 75 µL of cell suspension ($5x10^4$ cells/mL). Cells migrated for 2.5 h at 37 °C. Following migration, transmigrated cells in the lower chambers were harvested and cell numbers were measured using flow cytometry. All results are displayed as migrated cells.

2.2.9.2 Transwell Migration Assay with primary T cells

For migration of primary T cells, mice were sacrificed by cervical dislocation and the thymus was harvested. To generate single cell suspensions, the thymus was homogenised through a 70 µm cell strainer using a syringe plunger. After centrifugation (400x*g*, 5 min, 4 °C), the cell suspension was stained with suitable antibody mixture and incubated for 20 min at 4 °C. Stained cells were washed with FACS buffer and sorted into distinct cell subsets (Table 2.21) using the cell sorter Aria III. Following sorting, cells were washed (400x*g*, 5 min, 4 °C), adjusted to $1x10^6$ cells/mL in starvation media, and starved for 2 h at 37 °C. The lower chambers of the 6-well transwell plates were filled with 600 µL starvation media containing either no supplement, 100 ng/mL recombinant murine CCL17 or CCL22. The upper chambers were loaded with 100 µL of the starved cell suspension ($1x10^5$ cells/mL).

Following migration for 3 h at 37 °C, transmigrated cells in the lower chambers were harvested and numbers were measured using flow cytometry. All results are displayed as migrated cells.

Table 2.21: Sorted cell populations for Transwell Migration Assay

Population	Marker
Immature CD4+ T cells	$LD^-/Lin^-/CD45^+/CD8^-/CD4^+/CD69^+$
Mature CD4+ T cells	$LD^-/Lin^-/CD45^+/CD8^-/CD4^+/CD69^-$
CD8+ T cells	$LD^-/Lin^-/CD45^+/CD8^+/CD4^-$

2.2.10 Enzyme Linked Immunosorbent Assay

Chemokine or cytokine production was measured by Enzyme Linked Immunosorbent Assay (ELISA) according to the manufacturer's instructions.

2.2.11 Blue Native Polyacrylamide Gel Electrophoresis (BN-PAGE)

NativePAGE™ 4-16 % Bis-Tris Gels were placed in an electrophoresis running chamber and 400 mL or 200 mL of cold native running buffer was added to the outer and inner chamber respectively. Biotinylated or unlabeled murine recombinant chemokines or chemokine mixtures were mixed with an appropriate amount of cold 4x native sample buffer. Afterwards, samples or 5 µL of native marker were loaded in the respective wells. Native running buffer was removed from the inner chamber and replaced by ice-cold 200 mL Dark Blue Cathode Buffer. BN-PAGE was run at 4 °C first for 45 min with a constant voltage of 150 V and then paused to exchange Dark Blue Cathode Buffer against Light Blue Cathode Buffer. Afterwards, the run was continued with a constant voltage of 250 V for 45 min. The gel was removed from the electrophoresis chamber and carefully placed in a container with fixing solution. Following fixation of proteins, the gel was stained with Coomassie Blue. For optimal staining, the gel was microwaved at 800 W for 45 s before incubating at room temperature for 20 min. Subsequently, the gel was destained by adding destaining solution, microwaving (800 W, 45 s) and shaking at room temperature. This process

was repeated 2-3 times to speed up the destaining process. Gel was imaged using the Odyssey gel documentation system.

2.2.12 Statistical analysis

All statistical analyses were performed with GraphPad Prism 9.2.0 using unpaired *t*-test, one-way or two-way ANOVA with Tukey's post-hoc test for multiple comparisons. Survival studies were analysed using Log-rank (Mantel-Cox) test. *P*-values were calculated to determine statistical significance. A *p*-value of ≤ 0.05 was considered significant (*p < 0.05, **p < 0.01, ***p < 0.001 and ****p<0.0001). Data are presented as mean values ± standard deviation, unless otherwise specified.

Chapter 3: The influence of CCL17 and CCL22 on *Salmonella* infection

CCL17 and CCL22 are two chemokines expressed under homeostatic and in inflammatory conditions (Vulcano *et al.*, 2001; Alferink *et al.*, 2003). Both chemokines facilitate the interaction between DC and T cells (Alferink *et al.*, 2003; Semmling *et al.*, 2010; Rapp *et al.*, 2019). Nevertheless, CCL17 and CCL22 also show differential functions in immune regulation. While CCL17 is associated with T_h2/T_h1 cell migration (Weber *et al.*, 2011) as well as DC migration (Stutte *et al.*, 2010), CCL22 is associated with T_{reg} cell recruitment and thought to play a more immunosuppressive role (Curiel *et al.*, 2004; Mohamed *et al.*, 2016; Rapp *et al.*, 2019). However, both chemokines share the receptor CCR4, which is expressed on a variety of T cell subsets including T_h1 cells, T_h2 cells, and T_{reg} cells (Imai *et al.*, 1998; Imai *et al.*, 1999; Sebastiani *et al.*, 2001; Yoshie and Matsushima, 2015). Signal transduction via the CCR4 receptor appears to be different for the two chemokines, a phenomenon that has been termed biased agonism (Rajagopal *et al.*, 2013; Anderson *et al.*, 2016). Thus, only CCL22 leads to the recruitment of β-arrestin and, consequently, to internalisation and recycling of CCR4 (Lin *et al.*, 2018). Both chemokines have been extensively studied in allergic and inflammatory diseases, including CHS, atopic dermatitis, and artherosclerosis (Vestergaard *et al.*, 2000; Alferink *et al.*, 2003; Stutte *et al.*, 2010; Heiseke *et al.*, 2012; Achuthan *et al.*, 2016), as well as autoimmunity and tumor growth (Curiel *et al.*, 2004; Bischoff *et al.*, 2015; Wiedemann *et al.*, 2016; Ketcham *et al.*, 2018). Their involvement in infectious diseases, however, is not well described so far. Hence, this study aimed to address if CCL17-, CCL22- or CCR4-deficiency would interfere with the adaptive immune response against an infectious disease. Therefore, wt, $CCL17^{E/E}$ $CCL22^{-/-}$, and $CCR4^{-/-}$ mice were analysed in a murine vaccine/challenge model for *Salmonella* Typhimurium (STM). In this model, C57BL/6 mice are vaccinated using an attenuated STM strain described as TAS2010 (Kupz *et al.*, 2013). Mice are able to clear the infection within 7 to 10 weeks and develop protective immunity against

secondary challenge with virulent STM, in this case SL1344 (Kupz *et al.*, 2014). Unvaccinated mice, however, typically succumb to the infection with SL1344 within 5 to 8 days, depending on the bacterial dose that is administered. The advantage of the TAS2010, or similar, vaccination model is the possibility to simultaneously study the primary and secondary T cell response after vaccination and challenge, respectively. Overall, it was hypothesised that the absence of the chemokines or their receptor would have a negative impact on the clearance of *Salmonella* infections.

3.1 Vaccinated CCL17$^{E/E}$ CCL22$^{-/-}$ and CCR4$^{-/-}$ mice show reduced survival after challenge with virulent *Salmonella*

As CCL17 and CCL22 are involved in a variety of immune responses, mainly recruiting and activating immune cells, the absence of one or both of the chemokines could potentially interfere with the vaccine efficacy, thereby affecting the survival of vaccinated mice against *Salmonella* infections.

To test this hypothesis, wt, CCL17$^{E/E}$ CCL22$^{-/-}$, and CCR4$^{-/-}$ mice were orally vaccinated with 2.5x10^{9} CFU attenuated STM TAS2010 and monitored over 12 weeks. All strains showed similar weight loss curves (Figure 3.1A). Wt and CCL17$^{E/E}$ CCL22$^{-/-}$ mice lost 3-5 % of their body weight within the first week after vaccination. CCR4$^{-/-}$ mice did not obviously lose weight within the first week, but this was not significantly different form the other mouse strains. Afterwards, all mice continuously gained weight. Wt mice showed the highest weight gain, followed by CCR4$^{-/-}$ and lastly CCL17$^{E/E}$ CCL22$^{-/-}$ mice. The differences in weight gain seen in wt mice were significant compared with the chemokine and chemokine receptor knockout mice (Figure 3.1A).

Mice were then challenged with 1x10^{9} CFU of virulent STM SL1344 and monitored for an additional three weeks to assess vaccine efficacy. Unvaccinated wt mice served as procedural controls. As previously described, unvaccinated wt mice succumbed to the infection within 4-7 days post-challenge (Figure 3.1B). Vaccination clearly prolonged the survival of mice for all strains analysed. Vaccinated CCL17$^{E/E}$

$CCL22^{-/-}$ and $CCR4^{-/-}$ mice, however, showed a survival rate of approximately 67 %, whereas vaccinated wt mice survived 100 %.

A *Salmonella* challenge experiment, performed by Adrian Semeniuk, in the animal facility of the Life & Medical Sciences Institute in Bonn showed similar results (Figure 3.1C). Unvaccinated wt mice succumbed to the infection within two to six days while their vaccinated counterparts survived the *Salmonella* challange with a survival rate of 100 %. $CCL17^{E/E}$ $CCL22^{-/-}$ and $CCR4^{-/-}$ mice were less protected, showing survival rates of 50 % each. Notably, the three $CCL22^{-/-}$ mice included in the experiment were unable to clear the infection and all succumbed within 16 days after challenge. Due to the low number of $CCL22^{-/-}$ mice in the study, this result has to be interpreted with caution.

The findings of this study suggested that CCL17 and CCL22 are important for the improved survival of vaccinated mice to *Salmonella* challenge.

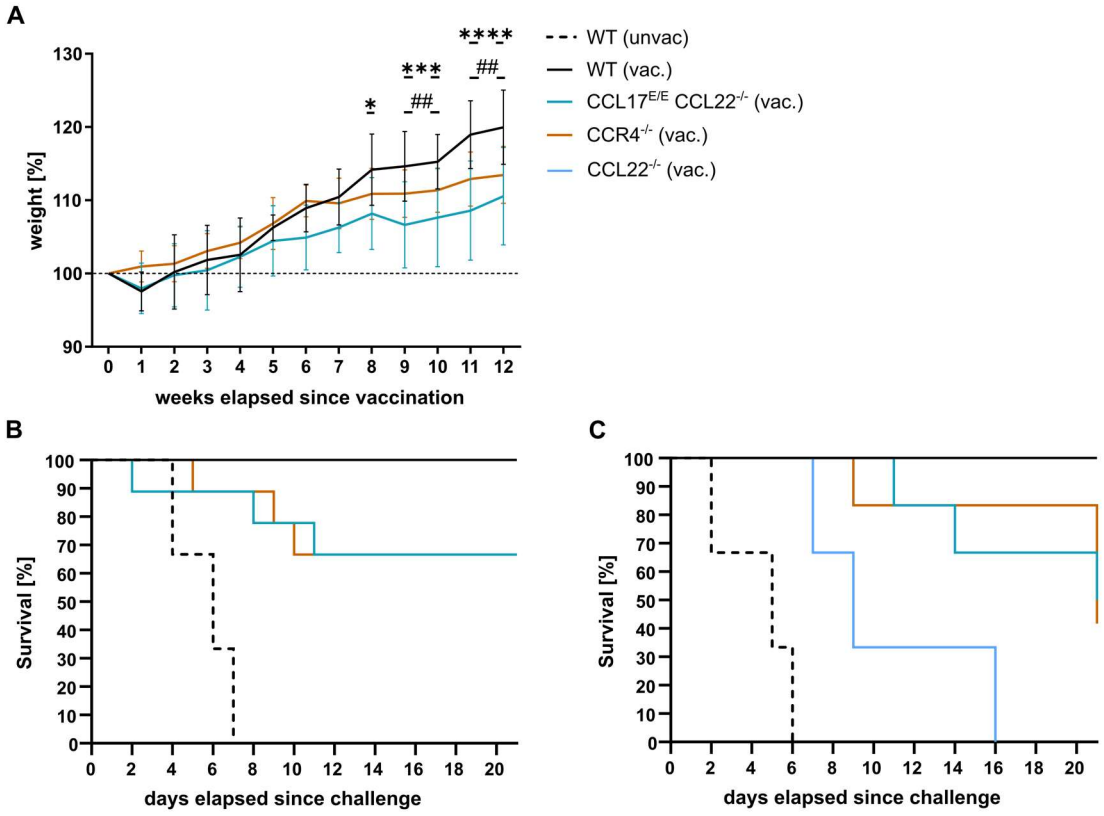

Figure 3.1: Survival of *Salmonella*-vaccinated and challenged mice
Wt, CCL17$^{E/E}$ CCL22$^{-/-}$, and CCR4$^{-/-}$ mice were orally vaccinated (vac.) with 2.5x10^{9} CFU TAS2010. 12 weeks post-vaccination mice were orally challenged with 1x10^{9} CFU SL1344. Mice were monitored over 21 days for their health status according to animal ethics. (A) Changes in whole body weight over the course of the experiment. Recorded weights were normalised to day 0 (pre-vaccination). (n=8-9 mice, one experiment, identical to the experiment shown in (B); (B-C) Survival curves of two independent experiments; (B) n=3 unvaccinated mice, n=8-9 vaccinated mice, one experiment; (C) n=3 unvaccinated mice, n=3-6 vaccinated mice, one experiment performed by Adrian Semeniuk). Statistical significance was tested using (A) two-way ANOVA with multiple comparison (* wt vs CCL17$^{E/E}$ CCL22$^{-/-}$; # wt vs CCR4$^{-/-}$) or (B-C) curve comparison with Logrank (Mantel-Cox test).

3.2 Differences in $CD4^+$ T cells and T_{reg} cells do not appear to be responsible for differential survival in wt, $CCL17^{E/E}$ $CCL22^{-/-}$, and $CCR4^{-/-}$ mice

$CD4^+$ T cells, especially T_h1 T cells, are crucial for the immune response against and clearance of *Salmonella* infections (Griffin and McSorley, 2011; Kupz *et al.*, 2013). An impaired T cell recruitment due to absence of the chemokines and a subsequent altered T cell composition of either T_{conv} or T_{reg} cells, which are clearing the infection or controlling the immune response, respectively, could explain the differential survival rates in wt, $CCL17^{E/E}$ $CCL22^{-/-}$, and $CCR4^{-/-}$ mice. Hence, the analysis focused on $CD4^+$ T cells in the PP, mLN, and spleen.

To assess if the deficiency of the chemokines or the chemokine receptor might have altered T cell composition in the steady state, naïve wt, $CCL17^{E/E}$ $CCL22^{-/-}$, and $CCR4^{-/-}$ mice were analysed. All genotypes were analysed between 11-12 weeks of age, which correlates to the age where mice received the vaccination with the attenuated *Salmonella* strain TAS2010.

The gating strategy (Figure 3.2) started with lymphoid cells which were selected based on their SSC and FSC properties. Doublet cells were excluded and viable $CD45^+$ cells were analysed. $CD45^+$ $TCR\beta^+$ cells were then divided into $CD4^+$ and $CD8^+$ T cells. $CD4^+$ T cells were further separated into $FoxP3^-$ T_{conv} cells and $FoxP3^+$ T_{reg} cells. From the $FoxP3^+$ compartment, $KLRG1^+$ T_{reg} cells were selected and analysed for ST2 expression. In parallel, $FoxP3^+$ T_{reg} cells were separated into thymic $Nrp1^+$ (Yadav *et al.*, 2012) and peripheral $ROR\gamma t^+$ T_{reg} cells (Yang *et al.*, 2016; Kim *et al.*, 2017). Thymic T_{reg} cells originate in the thymus. Peripheral T_{reg} cells, however, develop from pre-existing T_{conv} cells after exposure to antigens in peripheral organs (Modigliani *et al.*, 1996; Cobbold and Waldmann, 1998; Maloy and Powrie, 2001; Yadav *et al.*, 2013).

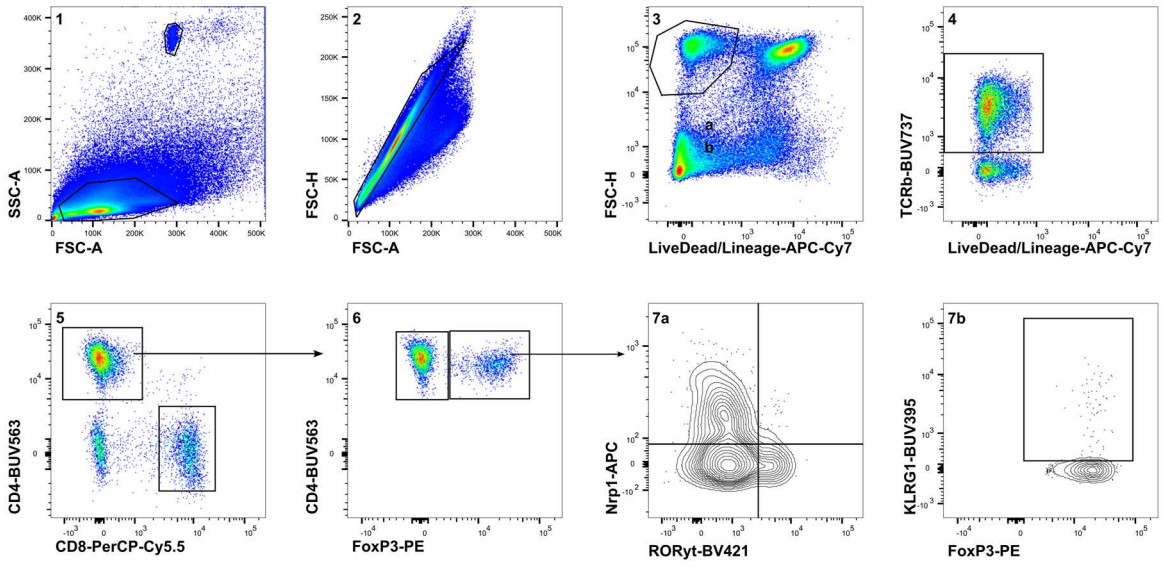

Figure 3.2: Gating strategy of T cell FACS analysis
Gating strategy was also used for naïve, unvaccinated wt, CCL17$^{E/E}$ CCL22$^{-/-}$, and CCR4$^{-/-}$ mice. Wt, CCL17$^{E/E}$ CCL22$^{-/-}$, and CCR4$^{-/-}$ mice were orally vaccinated (vac.) with 2.5x10^{9} CFU TAS2010. 12 weeks post-vaccination mice were orally challenged with 1x10^{9} CFU SL1344. Mice were monitored over 21 days for their health status according to animal ethics. PP, mLN, and spleen were isolated and analysed via flow cytometry. Lymphoid cells were selected based on their FSC and SSC properties (1). Doublet cells were excluded (2). Viable CD45^{+} immune cells were selected (3). CD45^{+} TCRβ^{+} cells (4) were further separated into CD4^{+} and CD8^{+} T cells (5). CD4^{+} FoxP3^{+} T cells were identified as T$_{reg}$ cells (6) and either investigated for their origin as thymic or peripheral T$_{reg}$ cells (7a) or for their KLRG1 expression (7b). Representative gating of mLN cells from an infected wt mouse.

In the naïve state, overall T cell composition between wt, CCL17$^{E//E}$ CCL22$^{-/-}$, and CCR4$^{-/-}$ mice showed no significant differences (data not shown). KLRG1^{+} T$_{reg}$ cells, however, were significantly reduced in CCL17$^{E/E}$ CCL22$^{-/-}$ mice and CCR4$^{-/-}$ mice compared to wt mice in the PP (Figure 3.3A; left panel). Consequently, the ratio of KLRG1^{+} T$_{reg}$ cells to FoxP3^{-} T$_{conv}$ cells was significantly decreased in naïve CCL17$^{E/E}$ CCL22$^{-/-}$ and CCR4$^{-/-}$ mice compared to wt mice (Figure 3.3; left panel). In the mLN, both frequencies of KLRG1^{+} T$_{reg}$ cells and the ratio of KLRG1^{+} T$_{reg}$ cells to FoxP3^{-} T$_{conv}$ cells (Figure 3.3A, B; middle panel) were comparable between the three genotypes in naïve state. Similar to the mLN, frequencies of KLRG1^{+} T$_{reg}$ cells and the ratio of KLRG1^{+} T$_{reg}$ cells to FoxP3^{-} T$_{conv}$ cells (Figure 3.3A, B; right panel) were

unchanged between wt and CCL17$^{E/E}$ CCL22$^{-/-}$ naïve mice in the spleen. KLRG1^{+} T_{reg} cell frequency and the ratio of KLRG1^{+} T_{reg} cells to FoxP3^{-} T_{conv} cells of CCR4$^{-/-}$ mice, however, were significantly decreased compared to CCL17$^{E/E}$ CCL22$^{-/-}$ and wt mice.

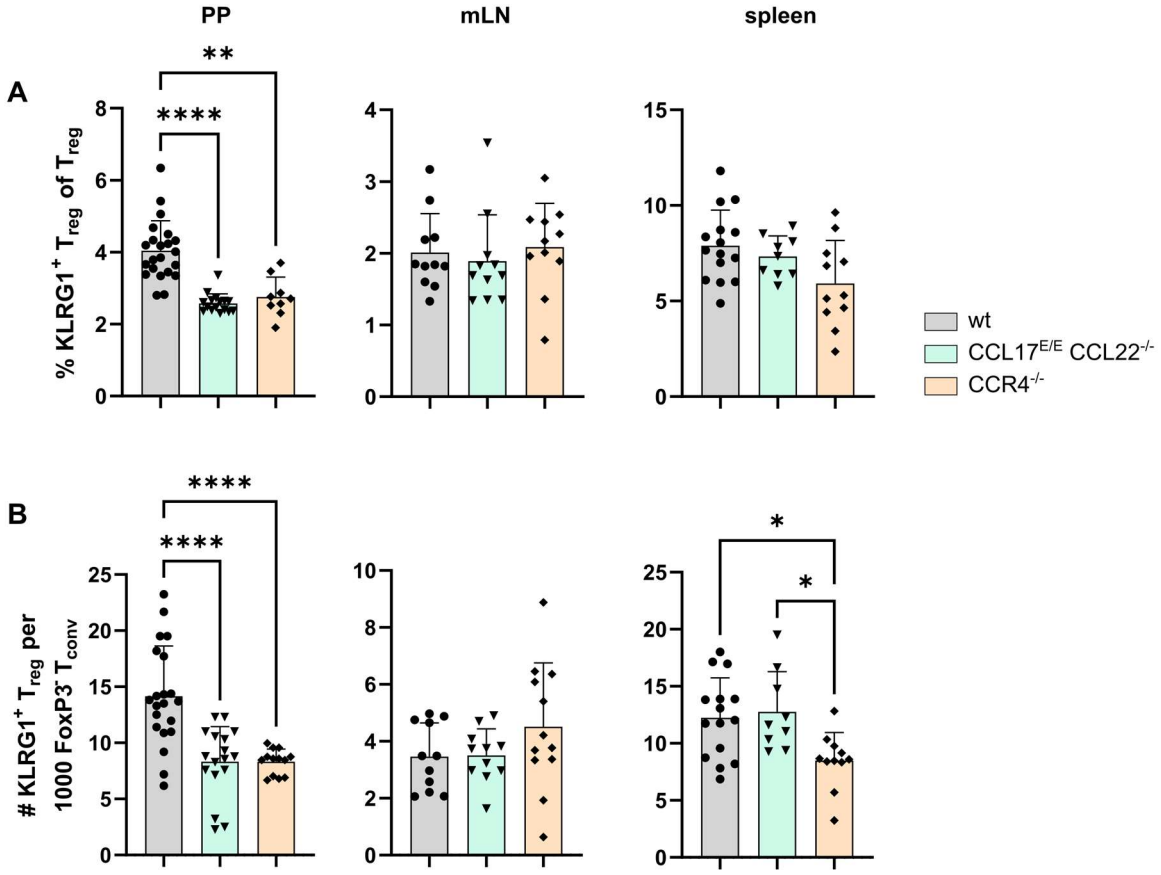

Figure 3.3: T cell FACS analysis of naïve mice – KLRG1^{+} T_{reg} cells
PP, mLN and spleen from naïve wt, CCL17$^{E/E}$ CCL22$^{-/-}$, and CCR4$^{-/-}$ mice were isolated and analysed. A) Frequencies of KLRG1^{+} T_{reg} cells. (B) Ratio of KLRG1^{+} T_{reg} cells to FoxP3^{-} T_{conv} cells. Symbols represent individual mice (PP: n=9-22, pooled from four (CCR4$^{-/-}$), seven (CCL17$^{E/E}$ CCL22$^{-/-}$), and nine (wt) independent experiments; mLN: n=11, pooled from four independent experiments; spleen: n=9-15, pooled from four or six (wt) independent experiments). Statistical significance was tested using one-way ANOVA with Tukey's test for multiple comparison. Data are presented as mean with SD.

The reduction of KLRG1$^+$ T_{reg} cells in the PP, the main entry point for *Salmonella* (Broz *et al.*, 2012), might impact the effective pathogen clearance by failing to control excessive immune responses. To assess how T cell composition is changed by STM infection, mice were analysed 21 days post STM challenge. All data from STM challenged mice 21 days post infection was compared to naïve mice prior to vaccination to assess STM-caused alterations to the T cell compartment. As wt, CCL17$^{E/E}$ CCL22$^{-/-}$, and CCR4$^{-/-}$ mice were similar in naïve state regarding T cell frequencies and counts, except KLRG1$^+$ T_{reg}, only naïve wt mice were depicted.

After STM challenge, KLRG1$^+$ T_{reg} cell frequencies were significantly increased in wt and CCR4$^{-/-}$ mice compared to naïve wt mice (Figure 3.4A, left panel). Interestingly, the differences of KLRG1$^+$ T_{reg} cell frequencies observed in naïve state between the genotypes were no longer visible, although CCL17$^{E/E}$ CCL22$^{-/-}$ still showed a tendency to be reduced. Subsequently, the ratio of KLRG1$^+$ T_{reg} cells to FoxP3$^-$ T_{conv} cells reflects the distribution of the KLRG1$^+$ T_{reg} cell frequency after STM challenge (Figure 3.4B, left panel). Strikingly, ratio of KLRG1$^+$ T_{reg} cells to FoxP3$^-$ T_{conv} cells was unaffected after STM challenge in all genotypes compared to naïve wt mice. In the mLN, both frequencies of KLRG1$^+$ T_{reg} cells (Figure 3.4A; middle panel) and the ratio of KLRG1$^+$ T_{reg} cells to FoxP3$^-$ T_{conv} cells (Figure 3.4B; middle panel) were significantly increased compared to naïve wt mice before vaccination and STM challenge. Although KLRG1$^+$ T_{reg} cell frequency and KLRG1$^+$ T_{reg} cell to FoxP3$^-$ T_{conv} cell ratio were mostly comparable between the three STM challenged wt, CCL17$^{E/E}$ CCL22$^{-/-}$, and CCR4$^{-/-}$ mice, CCR4$^{-/-}$ mice showed a significantly higher ratio of KLRG1$^+$ T_{reg} cells to FoxP3$^-$ T_{conv} cells compared to CCL17$^{E/E}$ CCL22$^{-/-}$ mice (Figure 3.4B; middle panel).

In contrast, frequencies of KLRG1$^+$ T_{reg} cells and ratio of KLRG1$^+$ T_{reg} cells to FoxP3$^-$ T_{conv} cells were significantly decreased in CCL17$^{E/E}$ CCL22$^{-/-}$, but not CCR4$^{-/-}$, mice compared to challenged wt mice. Similar to the PP and mLN, STM challenge increased the KLRG1$^+$ T_{reg} cell frequency and ratio of KLRG1$^+$ T_{reg} cells to T_{conv} cells in all genotypes, which was significant for wt and CCR4$^{-/-}$ mice.

Overall, KLRG1$^+$ T_{reg} cell frequencies were altered in all genotypes after STM challenged compared to their respective naïve mice. KLRG1$^+$ T_{reg} cell frequency reduction in the naïve PP was mostly abolished. In contrast, previously similar KLRG1$^+$ T_{reg} cell frequencies in wt, CCL17$^{E/E}$ CCL22$^{-/-}$, and CCR4$^{-/-}$ mice were changed after STM challenge and revealed a frequency reduction in CCL17$^{E/E}$ CCL17$^{E/E}$ CCL22$^{-/-}$, but not CCR4$^{-/-}$, mice.

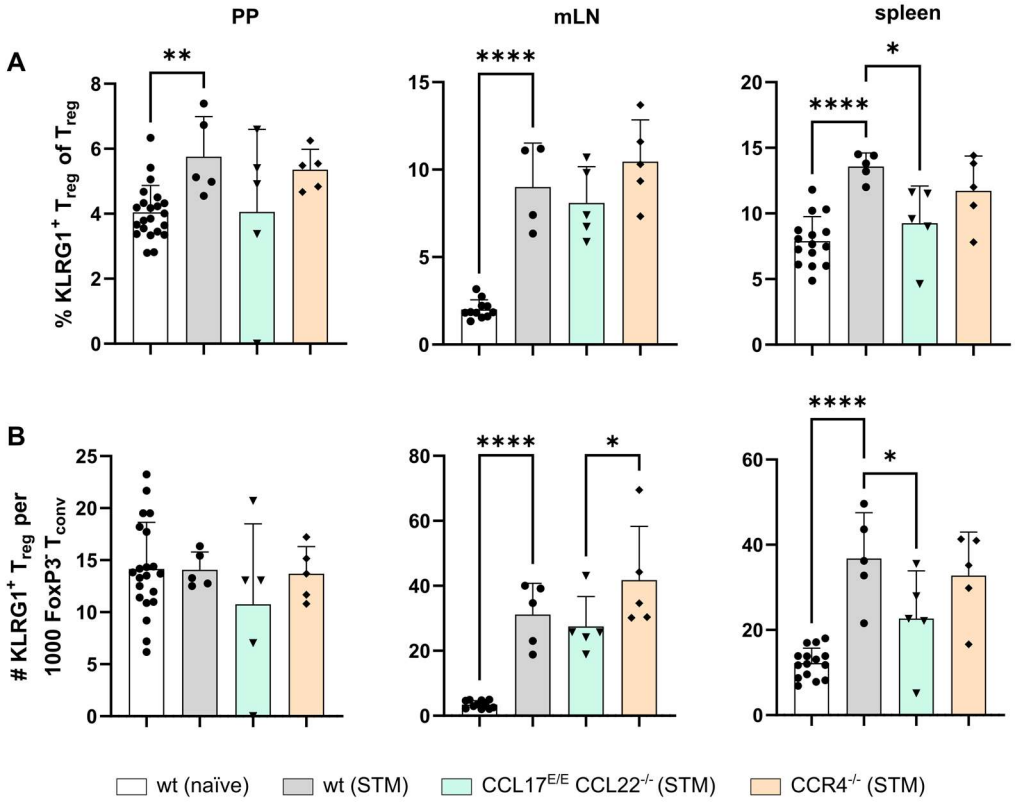

Figure 3.4: T cell FACS analysis of naïve and STM challenged mice – KLRG1$^+$ T_{reg} cells

Wt, CCL17$^{E/E}$ CCL22$^{-/-}$, and CCR4$^{-/-}$ mice were orally vaccinated (STM) with 2.5x10^9 CFU TAS2010. 12 weeks post-vaccination mice were orally challenged with 1x10^9 CFU SL1344. PP, mLN and spleen were isolated and analysed. (A) Frequencies of KLRG1$^+$ T_{reg} cells. (B) Ratio of KLRG1$^+$ T_{reg} cells to FoxP3$^-$ T_{conv} cells. Naïve wt mice (11-12 weeks) were used as controls. Symbols represent individual mice (naïve: for PP n=9-22, pooled from nine independent experiments; for mLN n=11, pooled from four independent experiments; for spleen n=9-15, pooled from six independent experiments; STM challenge: n=4-5, one experiment; for naïve mice n=12-15, pooled from six independent experiments). Statistical significance was tested using one-way ANOVA with Tukey's test for multiple comparison. Data are presented as mean with SD.

As slight changes in KLRG1$^+$ T_{reg} frequencies were visible, even 21 days after infection, CD4$^+$ T cells and the T_{reg} cell compartment were analysed.

Analysis of CD4$^+$ T cell frequency revealed no differences between STM challenged mice in the PP (Figure 3.5A, left panel). Furthermore, there were no significant changes between naïve wt mice and STM challenged wt, CCL17$^{E/E}$ CCL22$^{-/-}$, or CCR4$^{-/-}$ mice with respect to the percentage of CD4$^+$ T cell in the PP or mLN but there were significant differences between the groups in the splenic lymphocyte population. Interestingly, FoxP3$^+$ T_{reg} cell frequencies were significantly reduced in STM challenged mice compared with naïve wt mice (Figure 3.5B; left panel). Frequencies within the STM challenged cohorts, however, were comparable. Frequencies of CD4$^+$ T cell in mLN were unaffected by STM challenge compared to naïve wt mice and showed no differences between the different genotypes challenged with STM (Figure 3.5A; middle panel). The FoxP3$^+$ T_{reg} cell frequency was increased after STM challenged in the mLN in comparison to naïve wt mice. Again, no significant differences between the different genotypes challenged with STM were visible (Figure 3.5B; middle panel). In the spleen, however, both CD4$^+$ T cell and FoxP3$^+$ T_{reg} cell frequencies were significantly increased in STM challenged mice compared to naïve wt mice (Figure 3.5A and B; right panel). Interestingly, frequencies of CD4$^+$ T cells were significantly increased in STM challenged CCL17$^{E/E}$ CCL22$^{-/-}$ and CCR4$^{-/-}$ mice compared to STM wt mice (Figure 3.5A; right panel).

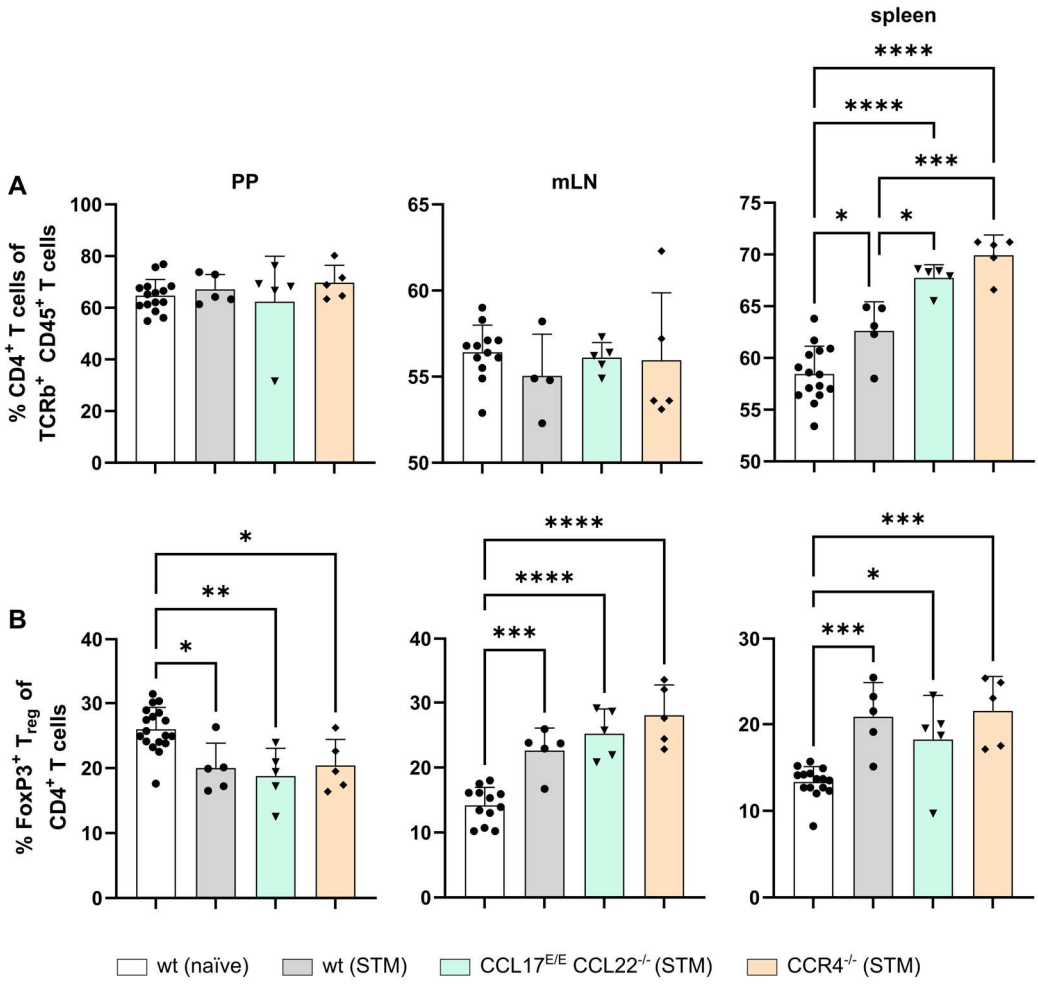

Figure 3.5: T cell FACS analysis of naïve and *Salmonella* challenged mice – frequencies of CD4$^+$ T cells and FoxP3$^+$ T$_{reg}$ cells

Wt, CCL17$^{E/E}$ CCL22$^{-/-}$, and CCR4$^{-/-}$ mice were orally vaccinated (STM) with 2.5x10^9 CFU TAS2010. 12 weeks post-vaccination mice were orally challenged with 1x10^9 CFU SL1344. PP, mLN and spleen were isolated and analysed. Frequencies of (A) CD4$^+$ T cells and (B) FoxP3$^+$ T$_{reg}$ cells. Naïve wt mice (11-12 weeks) were used as controls. Symbols represent individual mice (n=4-5, one experiment; for naïve mice n=12-15, pooled from six independent experiments). Statistical significance was tested using one-way ANOVA with Tukey's test for multiple comparison. Data are presented as mean with SD.

Although $CD4^+$ T cell frequencies were increased in the PP of STM challenged mice, overall $FoxP3^+$ T_{reg} cell frequencies were decreased. Strikingly, however, $KLRG1^+$ T_{reg} cell frequency was increased after STM challenge. Opposing results were obtained for the mLN, where $CD4^+$ frequencies after STM challenge were similar to naïve wt mice prior to the vaccination, but $FoxP3^+$ T_{reg} cell frequencies were significantly increased after STM challenge. Both findings suggested frequency shifts in the T_{reg} cell subpopulations. Hence, $Nrp1^+$ thymic tT_{reg} cells and $ROR\gamma t^+$ peripheral pT_{reg} cells were investigated.

In the PP, $Nrp1^+$ T_{reg} cell frequencies revealed no significant differences between STM challenged mice in the PP (Figure 3.6A; left panel) and between naïve wt mice and STM challenged wt, $CCL17^{E/E}$ $CCL22^{-/-}$, or $CCR4^{-/-}$ mice. Frequencies of $RORyt^+$ T_{reg} cells in PP were slightly decreased in STM challenged wt and $CCR4^{-/-}$ mice but significantly decreased in STM challenged $CCL17^{E/E}$ $CCL22^{-/-}$ mice compared to naïve wt mice (Figure 3.6B; left panel). However, STM challenged wt, $CCL17^{E/E}$ $CCL22^{-/-}$, and $CCR4^{-/-}$ mice were comparable regarding their $RORyt^+$ T_{reg} cell frequency. Similar results were obtained for the mLN. Frequencies of $Nrp1^+$ and $ROR\gamma t^+$ T_{reg} cells in mLN were unaffected by STM challenge compared to naïve wt mice and showed no differences between the different genotypes challenged with STM (Figure 3.6A, B; middle panels). In the spleen, $Nrp1^+$ T_{reg} cell frequencies were unchanged between naïve wt and infected mice (Figure 3.6A; right panel), while $RORyt^+$ T_{reg} cells were significantly reduced in $CCL17^{E/E}$ $CCL22^{-/-}$ mice compared to naïve wt mice (Figure 3.6B, right panel). Interestingly, the $RORyt^+$ T_{reg} cell frequency in STM challenged $CCL17^{E/E}$ $CCL22^{-/-}$ mice was also significantly decreased compared to STM challenged $CCR4^{-/-}$ mice.

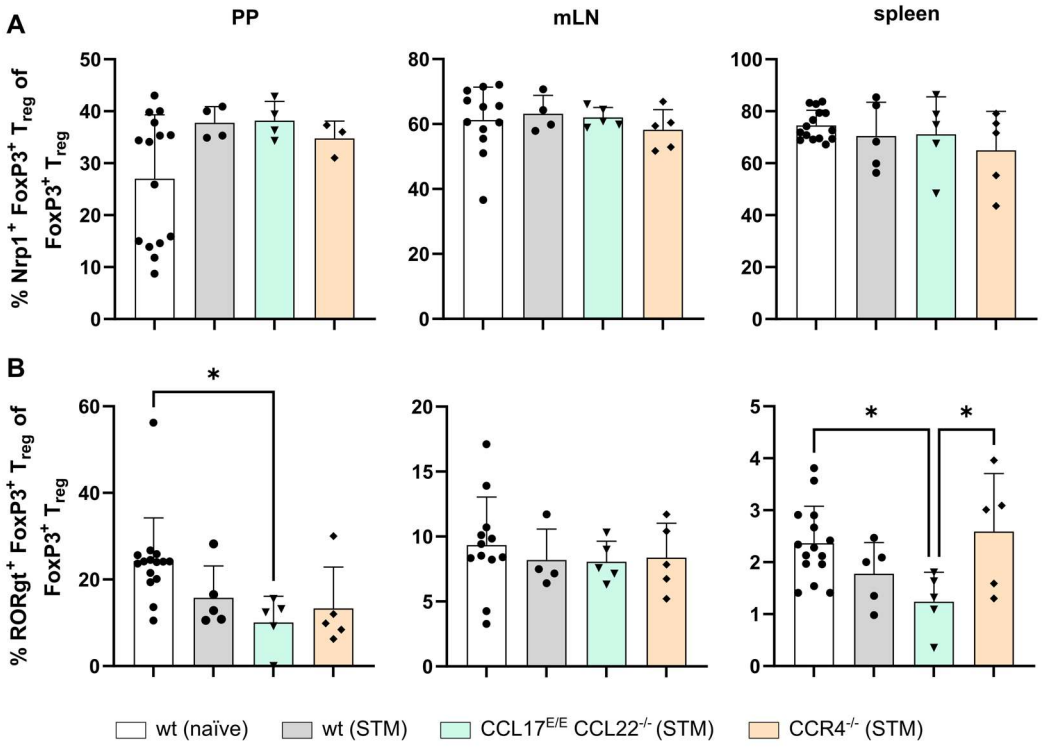

Figure 3.6: T cell FACS analysis of naïve and *Salmonella* challenged mice – frequencies of Nrp1$^+$ T_{reg} cells and RORγt$^+$ T_{reg} cells
Wt, CCL17$^{E/E}$ CCL22$^{-/-}$, and CCR4$^{-/-}$ mice were orally vaccinated (STM) with 2.5x10^9 CFU TAS2010. 12 weeks post-vaccination mice were orally challenged with 1x10^9 CFU SL1344. PP, mLN and spleen were isolated and analysed. Frequencies of (A) Nrp1$^+$ T_{reg} cells and (B) RORγt$^+$ T_{reg} cells. Naïve wt mice (11-12 weeks) were used as controls. Symbols represent individual mice (n=4-5, one experiment; for naïve mice n=12-15, pooled from six independent experiments). Statistical significance was tested using one-way ANOVA with Tukey's test for multiple comparison. Data are presented as mean with SD.

Interestingly, all mice challenged with virulent SL1344 showed a significant increase in spleen weight compared with naïve wt mice even on day 21 after challenge (Figure 3.7A). Spleen weight between infected mice of different genotypes, however, was comparable. As splenomegaly can be caused by excessive lymphocyte migration, T cells counts in the spleen were calculated.

In correlation with the frequency data, absolute cell counts of CD4$^+$ T cells were significantly increased in STM challenged CCR4$^{-/-}$ mice compared to naïve wt mice (Figure 3.7B). There were no significant differences in the CD4$^+$ cell numbers in STM

challenged wt and CCL17$^{E/E}$ CCL22$^{-/-}$ mice compared with naïve wt mice. The FoxP3^{+} T_{reg} cell counts were also increased in infected mice compared with naïve wt mice, which was significant for wt and CCR4$^{-/-}$ mice (Figure 3.7C). Similar to CD4^{+} T cells, Nrp1^{+} T_{reg} cells (Figure 3.7D) were slightly increased in infected mice compared with naïve wt mice. This increase was again only significant for CCR4$^{-/-}$ mice. RORγt^{+} T_{reg} cells were significantly increased in CCR4$^{-/-}$ mice compared with infected wt and CCL17$^{E/E}$ CCL22$^{-/-}$ as well as naïve wt mice (Figure 3.7E). Lastly, KLRG1^{+} T_{reg} cell counts in infected wt and CCR4$^{-/-}$ mice were significantly increased compared to naïve wt mice (Figure 3.7F).

Overall, and although frequencies of the analysed T cell subsets in the spleen showed some differences between infected wt and knockout mice, the counts of T cell populations in the spleen remained unchanged between the infected genotypes (Figure 3.7B-F) with the exception of RORγt^{+} T_{reg} cells (Figure 3.7E) which were significantly increased in CCR4$^{-/-}$ mice compared with CCL17$^{E/E}$ CCL22$^{-/-}$ mice, but not wt mice, after STM challenge.

Taken together the data showed that 21 days after *Salmonella* challenge the largest differences in T cell subsets between the genotypes were observed in the spleen. Absolute cell counts of CD4^{+} T cells and KLRG1^{+} T_{reg} cells were similarly increased, leading to a comparable ratio of KLRG1^{+} T_{reg} cells to T_{conv} cells in all genotypes. Interestingly, significant differences in KLRG1^{+} T_{reg} cell frequencies and KLRG1^{+} T_{reg} cell to T_{conv} cell ratios between the genotypes was observed in naïve mice, but these differences were resolved 21 days after *Salmonella* challenge. The CD4^{+} T cell and T_{reg} cell frequency data could not explain the differential survival outcomes in vaccinated wt and chemokine or chemokine receptor knockout mice.

.

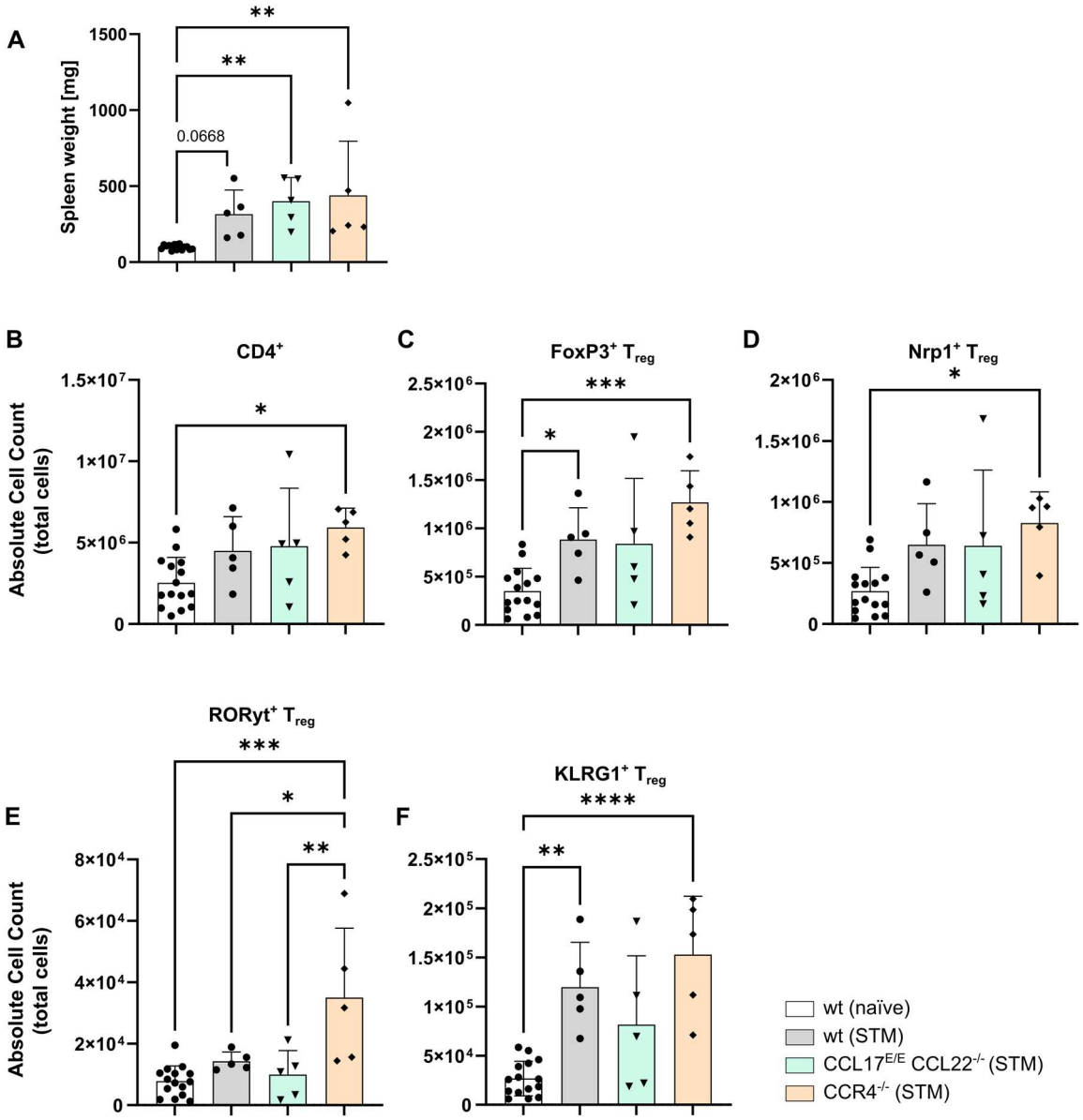

Figure 3.7: T cell FACS analysis of naïve and *Salmonella* challenged mice – absolute counts in the spleen

Wt, CCL17$^{E/E}$ CCL22$^{-/-}$, and CCR4$^{-/-}$ mice were orally vaccinated (vac.) with 2.5x10^9 CFU TAS2010. 12 weeks post-vaccination mice were orally challenged with 1x10^9 CFU SL1344. Spleens were isolated and analysed. (A) Spleen weight of naïve and infected mice. Absolute cell counts of (B) CD4$^+$ T cells, (C) FoxP3$^+$ T_{reg} cells, (D) Nrp1$^+$ T_{reg} cells, (E) RORγt$^+$ T_{reg} cells, and (F) KLRG1$^+$ T_{reg} cells. Naïve wt mice (11-12 weeks) were used as controls. Symbols represent individual mice (n=4-5, one experiment, for naïve mice n=12-15, pooled from six independent experiments). Statistical significance was tested using one-way ANOVA with Tukey's test for multiple comparison. Data are presented as mean with SD.

3.3 Discussion

The chemokines CCL17 and CCL22 are primarily expressed by DC and macrophages. As ligands of CCR4, both chemokines are involved in the recruitment of T cells (Curiel *et al.*, 2004; Weber *et al.*, 2011; Wiedemann *et al.*, 2016; Fülle *et al.*, 2018), facilitate the DC-T cell interaction (Semmling *et al.*, 2010; Rapp *et al.*, 2019) and the sensitisation for DC migration (Stutte *et al.*, 2010; Bischoff *et al.*, 2015). Although CCL17 and CCL22 share many functions, several studies have highlighted their differential relevance or association in various diseases. CCL17 is associated with T_h2/T_h1 polarisation (Weber *et al.*, 2011) and is well described in the context of allergic and inflammatory diseases such as CHS (Alferink *et al.*, 2003; Fülle *et al.*, 2018) and atopic dermatitis (Vestergaard *et al.*, 2000; Stutte *et al.*, 2010). In contrast, CCL22 is associated with T_{reg} cell recruitment and thought to play a more immunosuppressive role (Curiel *et al.*, 2004; Mohamed *et al.*, 2016; Rapp *et al.*, 2019). While both chemokines are extensively studied in the tumor-microenvironment (Curiel *et al.*, 2004; Wiedemann *et al.*, 2016), allergic and inflammatory diseases (Alferink *et al.*, 2003; Stutte *et al.*, 2010), and the steady-state, less is known about their involvement in infectious diseases. In the context of *Salmonella*, acquired knowledge is important in the translational research of vaccine development. Hence, this thesis focused on the function of CCL17 and CCL22 in the adaptive immune response against *Salmonella* infection.

The *Salmonella* infection studies, performed in this study, showed that absence of the CCL17/CCL22/CCR4-axis impaired survival to *Salmonella* challenge. Vaccinated wt mice were protected from STM challenge, while the survival of $CCL17^{E/E}$ $CCL22^{-/-}$ and $CCR4^{-/-}$ mice was decreased (Figure 3.1B, C). However, a similar study performed by Anna Erazo observed the opposite result (Erazo, 2020). In this study, vaccinated $CCL17^{E/E}$ $CCL22^{-/-}$ showed better survival after *Salmonella* challenge compared to single-deficient or wt mice. Additionally, $KLRG1^+$ T_{reg} cell frequency and the ratio of $KLRG1^+$ T_{reg} cells to T_{comv} cells was significantly reduced in $CCL17^{E/E}$ $CCL22^{-/-}$ mice. She, therefore, hypothesised that the reduction in $KLRG1^+$ T_{reg} cells promotes an enhanced STM-specific T_h1 immune response as

T_h1 cells expanded during STM challenge. In conjunction with fewer suppressive KLRG1$^+$ T_{reg} cells, this may create a more effective environment to fight *Salmonella* challenge.

One possible explanation for the different experimental outcomes could be the mouse facility where the experiments took place and the resulting impact on the gut microbiome of the mice utilised. Experiments of Anna Erazo were performed in the quarantine room at the Peter Doherty Institute in Melbourne (Australia), while the experiments of this study were performed at the Life & Medical Sciences Institute in Bonn (Germany).

The GI tract contains a highly complex and variable microbiome (Grzymajlo, 2022) including bacteria, archaea, protozoa, and fungi (Caruso *et al.*, 2019). This diversity is influenced by genetics, age, diet, general lifestyle and pharmacological treatments (Vasquez *et al.*, 2018; Zhang *et al.*, 2018). The microbes present influence the uptake and metabolism of nutrients (Rowland *et al.*, 2018; Skrypnik and Suliburska, 2018), hormone secretion (Neuman *et al.*, 2015), maintenance of the gut barrier function (Cani *et al.*, 2009; Chelakkot *et al.*, 2018) but also the protection against pathogen infections by colonisation resistance (Ducarmon *et al.*, 2019). Such colonisation resistance is mediated by species composition and richness in the gut microbiome. While a healthy intestinal microbiome protects against pathogenic infections (Huttenhower *et al.*, 2012) and supports an optimal immune system to develop, alterations of the gut microbiota (i.e. a dysbiosis) favors infection by various pathogens, for example *Salmonella* (Grzymajlo, 2022). Interestingly, *Salmonella* as well as other enteric pathogens can interact with the intestinal microbiota leading to dysbiosis and changes in the infection outcome (Sekirov *et al.*, 2008; Grzymajlo, 2022).

Similar to humans, mouse strains differ in their intestinal microbiota composition (Ferreira *et al.*, 2011). In specific experiments that may be location-dependent, the 129S1/SvImJ mouse strain, for example, showed an overrepresentation of *Bacteroidetes* which, while related to better protection against inflammation, did not affect the colonisation levels of *Salmonella* (Ferreira *et al.*, 2011). Commensals

promote colonisation resistance by priming and modulating the host immune systems, competing with pathogens for nutrients or directly targeting the pathogens with metabolites (Vasquez *et al.*, 2018). For example, *Lactobacillus casei* produces linoleic acid, limiting the growth of *S.* Typhimurium (Peng *et al.*, 2018), and commensal *Escherichia coli* may produce indole which leads to the downregulation of SPI-1 T3SS gene expression of *S.* Typhimurium (Nikaido *et al.*, 2012). In contrast, fucose, galactose, and sialic acid, produced by *Bacteroides thetaiotaomicron* can enhance the growth of *S.* Typhimurium (Chow and Lee, 2008; Pacheco *et al.*, 2012; Ng *et al.*, 2013). Additionally, intestinal microbiota are also directly involved in the clearance of pathogens by stimulating the mucosal immune system which may also reduce pathogen numbers (Stecher *et al.*, 2005).

The composition of the gut microbiota can be influenced by various factors including the uptake of microbiota from the mother during birth, age of the mice, housing, diet, handling and the institution. All mice utilised in this thesis shared the same genetic background (C57BL/6JRcc) as the mice used in previous studies in Melbourne were transferred from Germany. However, the gut microbiota can differ between isogenic mice depending on the environment (Stecher *et al.*, 2010; Franklin and Ericsson, 2017; Velazquez *et al.*, 2019). Although the gut microbiota is highly strain-specific, such strain-specific differences disappear when embryos are transferred from different mothers into a single dam suggesting that pups develop the gut microbiome of the birth mother regardless of the strain. Consequently, microbiota between littermates is highly analogous. Given experimental mice are often birthed in isolation, even keeping animals in the same diet and raising them in the same cage does not guarantee homogeneity between the gut microbiomes (Sait *et al.*, 2003). Moreover, the similarities remain present across generations as similar microbiota can be found in litters from mice that are sisters. In contrast, litters of mice differing in their maternal origin develop different gut microbiota (Ley *et al.*, 2005; Hufeldt *et al.*, 2010). Additionally, the type of housing, diet and treatment of animal feed and water are important factors to consider and might have influenced the experimental set-up. In one study, germ-free mice, inoculated with the same defined microbiome,

developed different gut microbiota depending on being single-housed in microisolator or ventilated cages (Lundberg *et al.*, 2017) though mice within the same cage demonstrate significantly less variations in their gut microbiota compared to mice housed in different cages (Deloris Alexander *et al.*, 2006). Dietary modifications can shift gut microbiota within 48 h (Llewellyn *et al.*, 2018). Diversity of gut microbiota can be increased with diets containing the soluble plant fiber psyllium, while casein-high diets reduce the diversity of the microbiome (Leystra and Clapper, 2019). Lastly, sterilisation of water and mouse chow impacts the composition of the gut microbiota. Irradiated chow reduces species diversity compared with autoclaving or no treatment of the chow (Rausch *et al.*, 2016). In contrast, autoclaved water decreases microbial diversity compared to sterilisation by H_2SO_4 acidification (Leystra and Clapper, 2019). Taken together those findings highlight that the gut microbiome is likely to be different between mice, especially in different locations and the impact of this difference on experimental findings is very hard to determine. In short, differences in the two institutes regarding mouse husbandry could have contributed to the differential results in the survival against STM challenge.

Similar observations were reported for $IL10^{-/-}$ mice that exhibit severe enterocolitis. Under SPF conditions, $IL10^{-/-}$ mice showed decreased colitis compared with mice housed under conventional conditions (Kühn *et al.*, 1993). However, while some institutions reported the colitis phenotype of $IL10^{-/-}$ mice, mice of the same genotype in other institutes failed to develop colitis (Dieleman *et al.*, 2000; Yang *et al.*, 2013). Therefore, it may be important to analyse and compare the gut microbiome of mice housed at the Peter Doherty Institute and the Life & Medical Sciences Institute to explain why very different phenotypes were observed. Moreover, the gut microbiome between the wt and knockout mice should be considered as the absence of the chemokines CCL17 and CCL22 or the receptor CCR4 might also have a differential impact on the gut microbiota. For example, Tanabe *et al.* (2021) showed that CCL17 levels in cord blood at 32 weeks of gestation were positively associated with microbiota diversity and inversely correlated with *Firmicutes* diversity.

Firmicutes belongs to one of the two dominant bacterial phyla within the human gut microbiome (Magne *et al.*, 2020).

The results of Erazos study indicated that the absence of CCL22 lead to an impaired recruitment and activation of T_{reg} cells resulting in less immunosuppressive environment and a promoted STM-specific T_h1 response more effective to clear *Salmonella* (Erazo, 2020). Indeed, treatment of mice with an anti-CCL22 antibody reduces T_{reg} cell migration to tumors (Curiel *et al.*, 2004) and CCL22-deficiency results in decreased cell-cell-contacts and contact time between DC and T_{reg} cells (Rapp *et al.*, 2019) which are required for optimal immunosuppressive function (Takahashi *et al.*, 1998; Thornton and Shevach, 1998b; Onishi *et al.*, 2008). Based on her findings, Erazo suggested that there was an essential role for CCL22 and a minor role for CCL17 in the protection against *Salmonella* infection as $CCL22^{-/-}$ and $CCL17^{E/E}$ $CCL22^{-/-}$ mice demonstrated increased survival after STM challenge compared to $CCL17^{E/E}$ and wt mice (Erazo, 2020). This was also supported by the fact that CCL22 is the dominant chemokine as seen in competitive binding experiments to CCR4 (Imai *et al.*, 1998).

The results presented here indicate an overall impairment in the recruitment or activation of effector T cells in the chemokine-deficient animals. Pre-incubation of colon cancer cells with an anti-CCR4 antibody or an agonist for CCR4 inhibited CCL17-induced cell migration (Al-Haidari *et al.*, 2013) and blocking of CCL17 by RNA aptamers (Fülle *et al.*, 2018) inhibited CCL17-dependent cell migration. In a mouse mode of atopic dermatitis, CCL17-deficient Langerhans cells showed impaired emigration from the skin after contact sensitiser exposure (Stutte *et al.*, 2010). Similarly, application of CCL22 aptamers ameliorated the immune response and reduced cell migration in a model of DNFB-induced CHS (unpublished data). In addition, T_{reg} cell trafficking to tumors is significantly reduced in mice treated with an anti-CCL22 antibody (Curiel *et al.*, 2004; Wiedemann *et al.*, 2016).

The absence of the chemokines could also directly impair activation of DC which are needed for priming of T cells, and in the subsequent induction of the adaptive immune response. Indeed, CCL17 has been shown to induce a direct autocrine or

paracrine effect on DC, influencing their activation and enhancing TLR-induced cytokine expression. Absence of CCL17 or CCR4 significantly reduced IL-12 and IL-23 expression in BMDC compared to wt BMDC. Furthermore, whereas CCL17 itself does not drive IL-12 production, co-stimulation with low doses of LPS induced IL-12 production that was further enhanced by CCL17 in a dose-dependent manner, highlighting a positive feedback loop for DC (Heiseke *et al.*, 2012). Co-culture of $CD4^+$ $CD62L^+$ OT-II T cells and OVA-pulsed wt or $CCL17^{E/E}$ BMDC in the presence of LPS showed higher levels of IFNy production and induction of IFNy-producing T cells, which correlated with higher T-bet mRNA expression, when the transgenic T cells were co-cultured with wt BMDC (Heiseke *et al.*, 2012).

In the context of *Salmonella* infections, absence of CCL17 or its receptor could reduce the differentiation of T-bet^+ T_h1 cells, impairing the clearance of *Salmonella* as several studies have shown that mice lacking $CD4^+$ T cells or T-bet^+ T_h1 cells are much more sensitive to *Salmonella* infection than wt mice (Weintraub *et al.*, 1998; Ravindran *et al.*, 2005; Kupz *et al.*, 2014). Moreover, overall deficiency in CCL17 results in T_{reg} cell expansion within the mLN or lamina propria (Weber *et al.*, 2011; Heiseke *et al.*, 2012), potentially impairing the effective immune response against *Salmonella*. The suppressive potency of T_{reg} cells is increased within the first three to four weeks after *Salmonella* infection, correlating with increased bacterial burden and delayed effector T cell activation (Johanns *et al.*, 2010). The expansion of T_{reg} cells paired with reduced T_h1 differentiation in the absence of CCL17 might lead to a less effective environment to fight STM challenge, resulting in an increased bacterial burden and, ultimately, enhanced lethality.

For future experiments it would be important to analyse the cellular composition early after STM challenge (as done by Anna Erazo). A time point around 5 days post STM challenge would be relevant, as vaccinated $CCL17^{E/E}$ $CCL22^{-/-}$ and $CCR4^{-/-}$ mice started to succumb to the infection from day 5 onwards. After 12 or 14 days, *Salmonella* infection appeared to be mostly cleared, apart from the limited number of $CCL22^{-/-}$ mice (data shown here, experiment conducted by Adrian Semeniuk). In line, 21 days post STM challenge T cell frequencies and counts in the STM

challenged mice were similar between the genotypes. Minor differences were observed in the investigated T cell populations between STM challenged mice, but these differences do not adequately explain the decreased survival of CCL17$^{E/E}$ CCL22$^{-/-}$ and CCR4$^{-/-}$ mice after STM challenge. Therefore, the impact of CCL17, CCL22, and CCR4 on *Salmonella* immunity remains less than fully resolved.

Interestingly, the frequencies of CD4$^+$ T cells, FoxP3$^+$ T_{reg} cells and KLRG1$^+$ T_{reg} cells remained elevated in the spleen 21 days after STM challenge, compared with naïve mice (Figure 3.5-Figure 3.7). Frequencies of KLRG1$^+$ T_{reg} cells were also increased in STM challenged mice in PP and mLN. This could indicate that the immune response is not yet complete. It should be noted, however, that naïve control mice and STM challenged mice were not age matched. While control mice were between 11 to 12 weeks of age, correlating to the age at which mice were first vaccinated, STM challenged mice were between 26 to 29 weeks old at the time of analysis.

Although the cellular composition in immune organs can change with age, it is unlikely that the increase in CD4$^+$ T cell, T_{reg} cell, and KLRG1$^+$ T_{reg} cell frequencies and numbers observed in the spleen was due to aging. Rather than increasing, number of classical T cells decrease in aged mice (Decman *et al.*, 2012; Deshpande *et al.*, 2015). Krishnarajah *et al.* (2022) showed in a cytometry-based high parametric analysis, mapping tissue-specific immune cell patterns in young and old mice, that CD4$^+$ T cells are steadily decreasing and decrease 2- to 4-fold within the small intestine and mLN, while being nearly non-existing in the spleen in mice 18-20 months of age.

Overall, further experiments are required to assess the stark differences between the contrasting results regarding the *Salmonella* vaccine efficacy in wt and CCL17$^{E/E}$ CCL22$^{-/-}$ mice after vaccination and challenge with *Salmonella*. Next to gut microbiome analysis, the analysis of T cell populations using antigen-specific reagents (e.g. tetramers), as well as other adaptive and innate immune cell populations, is crucial to understanding the different outcomes observed between the genotypes. Such studies will help to further resolve the importance of CCL17, CCL22, and CCR4 in the immune response against *Salmonella*.

Chapter 4: Function of CCL17 and CCL22 in IL-33-induced immune responses

The cytokine IL-33 plays a role in both innate and adaptive immunity and is involved in a variety of biological processes, ranging from tissue homeostasis (Moussion *et al.*, 2008; Pichery *et al.*, 2012), injury and wound-healing (Sanada *et al.*, 2007; Brunner *et al.*, 2011; Turnquist *et al.*, 2011; Liang *et al.*, 2013; Yin *et al.*, 2013) to type 2 immune responses (Yasuda *et al.*, 2012; Hardman *et al.*, 2013; Cayrol and Girard, 2014). In steady state, IL-33 is constitutively expressed by non-haematopoietic cells, like epithelial and endothelial cells (Moussion *et al.*, 2008). As a consequence IL-33 is especially important in barrier organs, including the skin, the lung, or the gastrointestinal tract (Schmitz *et al.*, 2005; Pastorelli *et al.*, 2010). However, macrophages and DC also seem to produce IL-33 when activated under specific conditions (Schmitz *et al.*, 2005; Chang *et al.*, 2011; Tjota *et al.*, 2013).

Thus far, ST2 is the only receptor described for IL-33 (Tominaga, 1989; Bessa *et al.*, 2014; Griesenauer and Paczesny, 2017). Next to non-haematopoietic cells, haematopoietic cells associated with type 2 immune responses are known to basally express and upregulate the receptor expression in an inflammatory context (Griesenauer and Paczesny, 2017).

Concerning the gut, IL-33 has been observed to elicit host-protective or pathogenic functions (Liew *et al.*, 2010). In the context of *Salmonella* infection, IL-33-deficiency in mice resulted in severe destruction of the gut and increased susceptibility to the infection (Mahapatro *et al.*, 2016). Bacterial ligands such as flagellin were shown to induce IL-33 expression in intestinal stromal cells and DC (Owens *et al.*, 2013). Additionally, pericryptal fibroblasts, located in the small intestine, can also secrete IL-33 (Mahapatro *et al.*, 2016). IL-33 signaling by these pericryptal fibroblasts promoted differentiation of intestinal epithelial cells, including goblet and Paneth cells, which are important for anti-bacterial repsonses and directly protected against *Salmonella* infections (Mahapatro *et al.*, 2016). Moreover, IL-33 stimulates CCL17

and CCL22 production by DC (Besnard *et al.*, 2011; Kurokawa *et al.*, 2013), which likely aids immune cell recruitment into sites of inflammation.

Hence, this chapter aimed to investigate and characterise the role of CCL17 and CCL22 in IL-33-mediated immune responses in lymphoid organs associated with *Salmonella* distribution and beyond. We hypothesised that IL-33, a prominent alarmin, and the CCL17/CCL22/CCR4-axis are interconnected, with IL-33 promoting CCL17- and CCL22-induced cell migration as well as both chemokines being important in mediating IL-33-induced immune responses. Therefore, mice were intraperitoneally injected with 0.5 µg of recombinant murine IL-33 every second day (days 0, 2, 4, and 6) and analysed on day 8 using published protocols (Vasanthakumar *et al.*, 2015).

4.1 IL-33 stimulates production of CCL17 and CCL22 in BMDC

Stimulation of BMDC with IL-33 leads to the upregulation of activation markers and increased CCL17 production in a dose-dependent manner (Besnard *et al.*, 2011). Furthermore, whereas OVA-induced allergic airway inflammation causes an increase of CCL17 in the lung of wt mice, the levels were significantly reduced in ST2-deficient mice (Besnard *et al.*, 2011), showing that IL-33 can be important for CCL17 production. Additionally, one study has described that IL-33 can induce CCL22 production by DC (Kurokawa *et al.*, 2013).

Based on the literature, it was proposed that CCL17 and CCL22 are upregulated in BMDC after IL-33 stimulation. To investigate this question, wt BMDC were generated and stimulated with 20 ng/mL IL-33. Chemokine levels of CCL17 and CCL22 in the supernatant were assessed 24 h later by ELISA.

Stimulation with IL-33 increased CCL17 (Figure 4.1A) and CCL22 production (Figure 4.1B) significantly. Therefore, IL-33 is not only capable to induce CCL17 but also CCL22 production.

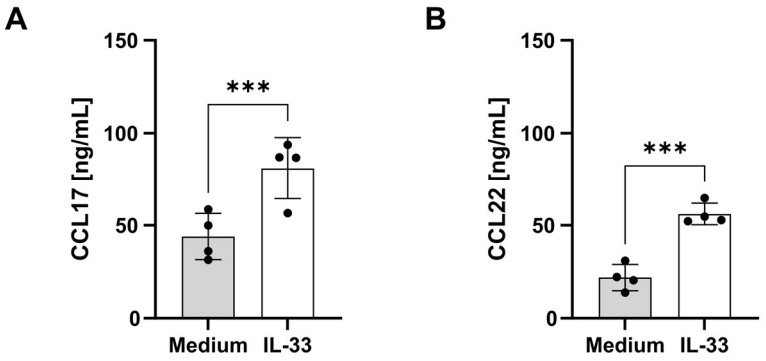

Figure 4.1: **IL-33 induces production of CCL17 and CCL22 in BMDC *in vitro*.** BM cells were harvested from tibia and femur of wt mice and cultured in RPMI medium containing 2 % GM-CSF. On day 6, BMDC were stimulated with 20 ng/mL IL-33 for 24 hours. Supernatant was taken and chemokine concentration for (A) CCL17 and (B) CCL22 was analysed using ELISA. Symbols represent individual samples (n=4, pooled from two independent experiments). Statistical significance was tested using unpaired t-test. Data are presented as mean with SD.

4.2 T_{reg} cells of PP, mLN, and spleen express ST2

IL-2 is essential for the survival of T cells, including T_{reg} cells (Kelly *et al.*, 2007; Cheng *et al.*, 2012). But effector T_{reg} cells are mainly found outside of T cell zones, thus needing different survival signals. Indeed, effector T_{reg} cells show high levels of ST2 expression and IL-33 is required for their maintenance and proliferation. $ST2^+$ effector Treg cells are more abundant in visceral adipose tissue (VAT) but rare in lymphoid organs (Vasanthakumar *et al.*, 2015).

To assess, if $KLRG1^+$ T_{reg} in the PP, mLN and spleen, organs associated with *Salmonella* distribution, could show responsiveness towards IL-33; wt, chemokine and chemokine receptor knockout mice were analysed for ST2 expression. Therefore, the following gating strategy was used (Figure 4.2A): lymphoid cells were selected based on their SSC and FSC properties. Doublet cells were excluded and viable $CD45^+$ cells selected. $CD45^+$ $TCR\beta^+$ cells were divided into $CD4^+$ and $CD8^+$ T cells. $CD4^+$ T cells were further separated into $FoxP3^-$ T_{conv} cells and $FoxP3^+$ T_{reg} cell. From the $FoxP3^+$ compartment, $KLRG1^+$ T_{reg} cells were selected and analysed for ST2 expression.

Frequencies of ST2 expression in KLRG1$^+$ T_{reg} cells showed no significant differences between CCL17$^{E/E}$, CCL22$^{-/-}$, CCL17$^{E/E}$ CCL22$^{-/-}$, and CCR4$^{-/-}$ mice in PP, mLN, and spleen compared to wt mice (Figure 4.2B). The highest frequencies were found in spleen (30-40 %), while ST2$^+$ KLRG1$^+$ T_{reg} cells in PP and mLN reached frequencies between 10-20 %. These results show that some KLRG1$^+$ effector T_{reg} cells express ST2 but these ST2 expressing cells are a minority within the KLRG1$^+$ effector T_{reg} population in PP, mLN, and spleen, consistent with the literature (Vasanthakumar *et al.*, 2015).

Frequencies of KLRG1$^+$ T_{reg} cells are comparable between naïve wt, CCL17$^{E/E}$ and CCL22$^{-/-}$ mice in PP but significantly reduced in CCL17$^{E/E}$ CCL22$^{-/-}$ and CCR4$^{-/-}$ mice (Figure S.1A). Comparable frequencies were observed in mLN (Figure S.1B). In spleen, CCL22$^{-/-}$ mice showed significantly reduced frequencies of KLRG1$^+$ T_{reg} cells compared to wt, CCL17$^{E/E}$, and CCL17$^{E/E}$ CCL22$^{-/-}$ mice (Figure S.1C). Frequencies of KLRG1$^+$ T_{reg} cells in all other mouse strains were comparable to each other.

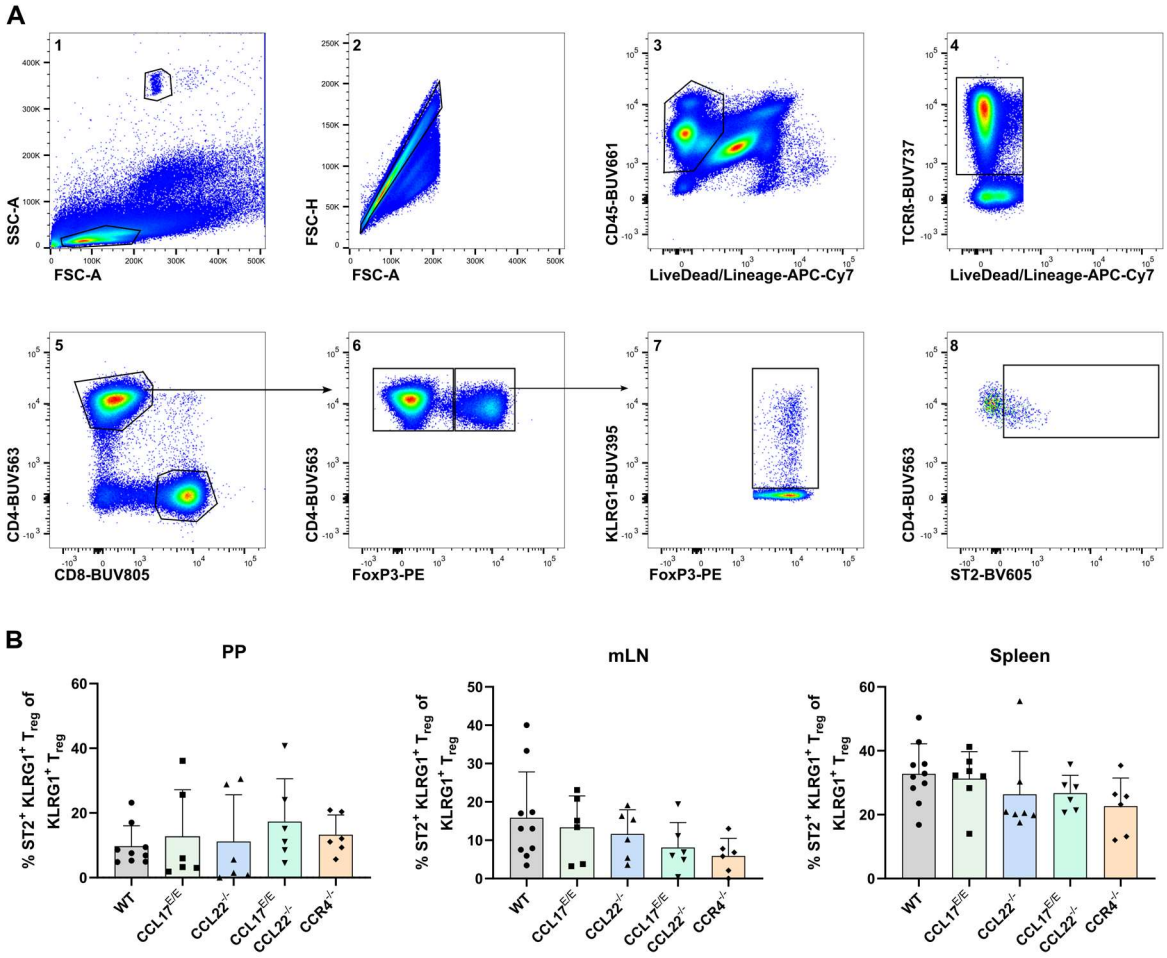

Figure 4.2: KLRG1$^+$ T_{reg} cells express ST2 in PP, mLN, and the spleen
(A) Gating strategy of T cell FACS analysis in lymphoid organs of naïve WT, CCL17$^{E/E}$, CCL22$^{-/-}$, CCL17$^{E/E}$ CCL22$^{-/-}$, and CCR4$^{-/-}$ mice. PP, mLN, and spleen were isolated and analysed via flow cytometry. Lymphoid cells were selected based on their FSC and SSC properties (1). Doublet cells were excluded (2). Viable CD45$^+$ immune cells were selected (3). For T cells, TCRβ$^+$ cells were identified (4) and further separated into CD4$^+$ and CD8$^+$ T cells (5). CD4$^+$ FoxP3$^+$ cells were identified as T_{reg} cells (6) and analysed for their KLRG1 expression (7). KLRG1$^+$ T_{reg} cells were further analysed for their ST2 expression (8). Representative gating of the spleen from a naïve wt mouse. (B) The frequency of ST2$^+$ KLRG1$^+$ T_{reg} cells in wt (grey), CCL17$^{E/E}$ (green), CCL22$^{-/-}$ (blue), CCL17$^{E/E}$ CCL22$^{-/-}$ (turquoise), and CCR4$^{-/-}$ (orange) mice in PP, mLN, and spleen. Symbols represent individual mice (n=6-7 mice; pooled from three independent experiments; for wt n=8-10; pooled from 6 independent experiments). Statistical significance was tested using one-way ANOVA with Tukey's test for multiple comparison. Data are presented as mean with SD.

4.3 Addition of IL-33 leads to expansion of KLRG1$^+$ T_{reg} cells in PP, mLN, and spleen

KLRG1$^+$ T_{reg} cells express ST2 and are responsive to IL-33, leading to proliferation in *in vitro* and *in vivo* settings (Vasanthakumar *et al.*, 2015). Therefore, a hallmark of IL-33 treatment should be the expansion of KLRG1$^+$ T_{reg} cells.

Wt, CCL17$^{E/E}$, CCL22$^{-/-}$, CCL17$^{E/E}$ CCL22$^{-/-}$, and CCR4$^{-/-}$ mice were injected with 0.5 µg IL-33 or PBS intraperitoneally. A similar gating strategy as was described in Section 4.2 and Figure 4.2A was used to assess IL-33-mediated T_{reg} cell expansion and its influence on other T cell subsets (Figure 4.3). In parallel, FoxP3$^+$ T_{reg} cells were also separated into thymic Nrp1$^+$ (Yadav *et al.*, 2012) and peripheral RORγt$^+$ T_{reg} cells (Yang *et al.*, 2016; Kim *et al.*, 2017).

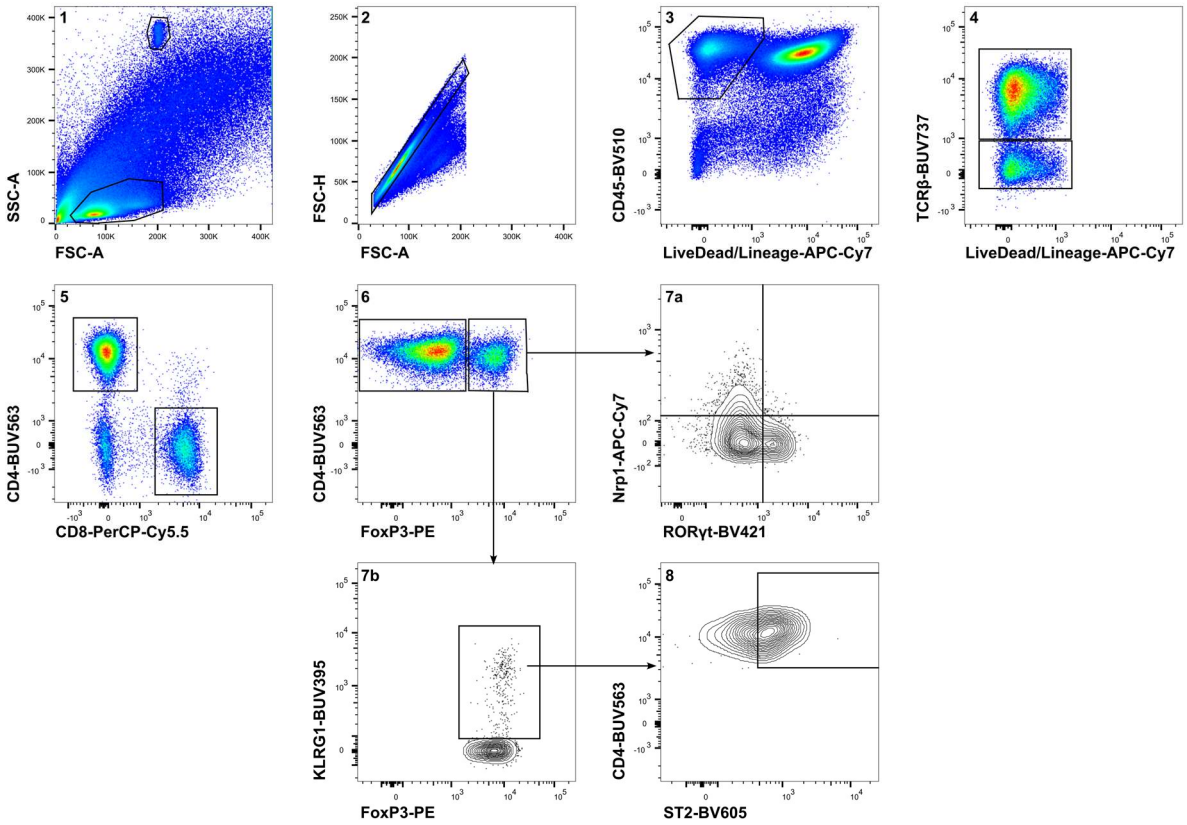

Figure 4.3: Gating strategy of T cell FACS analysis of IL-33 injected mice
Wt, CCL17$^{E/E}$, CCL22$^{-/-}$, and CCL17$^{E/E}$ CCL22$^{-/-}$-deficient mice were intraperitoneally injected with 100 µL PBS (control) or 0.5 µg IL-33/100 µL PBS every second day (day 0, 2, 4 and 6) and analysed on day 8. Mice were monitored every second day for their health status according to animal ethics. PP, mLN, and spleen were isolated and analysed via flow cytometry. Lymphoid cells were selected based on their FSC and SSC properties (1). Doublet cells were excluded (2). Viable CD45$^+$ immune cells were selected (3). For T cells, TCRβ$^+$ cells were identified (4) and further separated into CD4$^+$ and CD8$^+$ T cells (5). CD4$^+$ FoxP3$^+$ cells were identified as T_{reg} cells (6) and either investigated for their origin as thymic or peripheral T_{reg} cells (7a) or their KLRG1 expression (7b). KLRG1$^+$ T_{reg} cells were then addressed for their ST2 expression (8). Representative gating of PP from a PBS-treated wt mouse.

CD45^{+} immune cell numbers in the PP were significantly decreased in IL-33-treated CCL17$^{E/E}$ and CCL17$^{E/E}$ CCL22$^{-/-}$ mice, but did not affect other genotypes (Figure 4.4A). On the other hand, immune cell numbers were moderately but not significantly increased in the mLN (Figure 4.4B), or were unaffected in the spleen (Figure 4.4C), following IL-33 treatment. Absolute cell counts of CD45^{+} immune cells were comparable in PBS-treated mice of all genotypes and across all organs (Figure 4.4A-C).

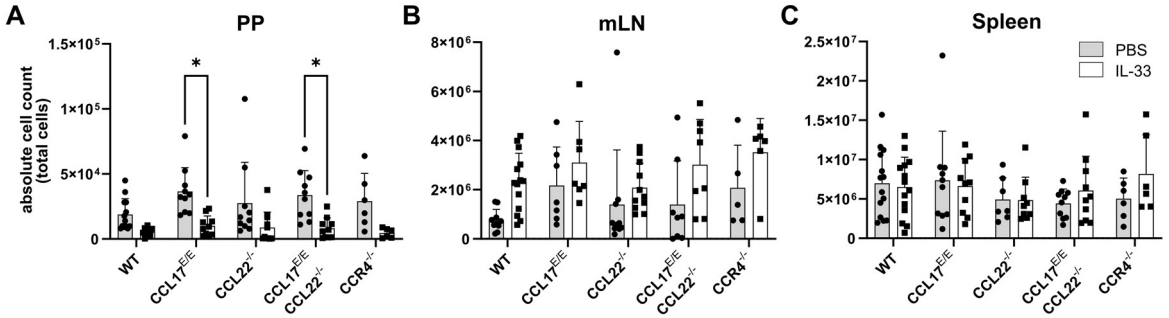

Figure 4.4: FACS analysis of PBS- and IL-33-treated mice – counts of CD45^{+} immune cells

Wt, CCL17$^{E/E}$, CCL22$^{-/-}$, CCL17$^{E/E}$ CCL22$^{-/-}$, and CCR4$^{-/-}$ mice were intraperitoneally injected with PBS (grey) or 0.5 µg IL-33 (white) every second day. On day 8, absolute cell counts of CD45^{+} cells in (A) PP, (B) mLN, and (C) spleen were analysed. Symbols represent individual mice (n=10-14; pooled from three (CCL22$^{-/-}$), four (CCL17$^{E/E}$ and CCL17$^{E/E}$ CCL22$^{-/-}$) or six (wt) independent experiments; for CCR4$^{-/-}$ n=6; from two independent experiments). Absolute cell counts were calculated using counting beads. In case of the PP, cell counts were normalised to the number of isolated PP. Statistical significance was tested using two-way ANOVA with Tukey's test for multiple comparison. Data are presented as mean with SD.

Absolute counts of $CD4^+$ T cells were decreased in IL-33-treated mice compared to PBS-treated mice in the PP, which was significant for $CCL17^{E/E}$ and $CCL17^{E/E}$ $CCL22^{-/-}$ mice only (Figure 4.5A, left row). $CD4^+$ T cells were moderately increased after IL-33 treatment in the mLN (Figure 4.5A, middle row) but unchanged between IL-33-treated and control groups in the spleen (Figure 4.5A, right row). Interestingly, frequencies of $CD4^+$ T cells in the PP were significantly increased for wt, $CCL17^{E/E}$ and $CCR4^{-/-}$ mice after IL-33 treatment, but not for $CCL22^{-/-}$ and $CCL17^{E/E}$ $CCL22^{-/-}$ mice, although a tendency was visible (Figure 4.5B, left row). Frequencies of $CD4^+$ T cells were unchanged in the mLN after IL-33 treatment (Figure 4.5B, middle row). In the spleen, however, frequencies were significantly increased for $CCL17^{E/E}$ $CCL22^{-/-}$ and $CCR4^{-/-}$ mice (Figure 4.5B, right row).

Similar results were obtained for the absolute cell count and frequency of $FoxP3^+$ T_{reg} cells. Absolute cell count of $FoxP3^+$ T_{reg} cells were reduced in IL-33-treated mice, which was significant for $CCL17^{E/E}$ mice (Figure 4.5C, left row), but the frequency was unchanged between IL-33-treated and control groups (Figure 4.5D, left row). In the mLN, both $FoxP3^+$ T_{reg} cell counts and frequencies were slightly increased (Figure 4.5C, D; middle rows). Only $CCL17^{E/E}$ $CCL22^{E/E}$ mice treated with IL-33 showed significance for the increase in frequency of $FoxP3^+$ T_{reg} cells. Lastly, absolute cell counts of $FoxP3^+$ T_{reg} cells were unchanged in the spleen between control and IL-33-treated mice (Figure 4.5C, right row). Interestingly, $FoxP3^+$ T_{reg} cell counts were significantly higher in IL-33-treated $CCR4^{-/-}$ mice compared to IL-33-treated wt and $CCL22^{-/-}$ mice. Additionally, the frequency of $FoxP3^+$ T_{reg} cell was significantly increased for all genotypes after IL-33 treatment and treated $CCR4^{-/-}$ mice showed the highest frequencies compared to wt, $CCL17^{E/E}$, and $CCL22^{-/-}$ mice, treated with IL-33 (Figure 4.5D, right row).

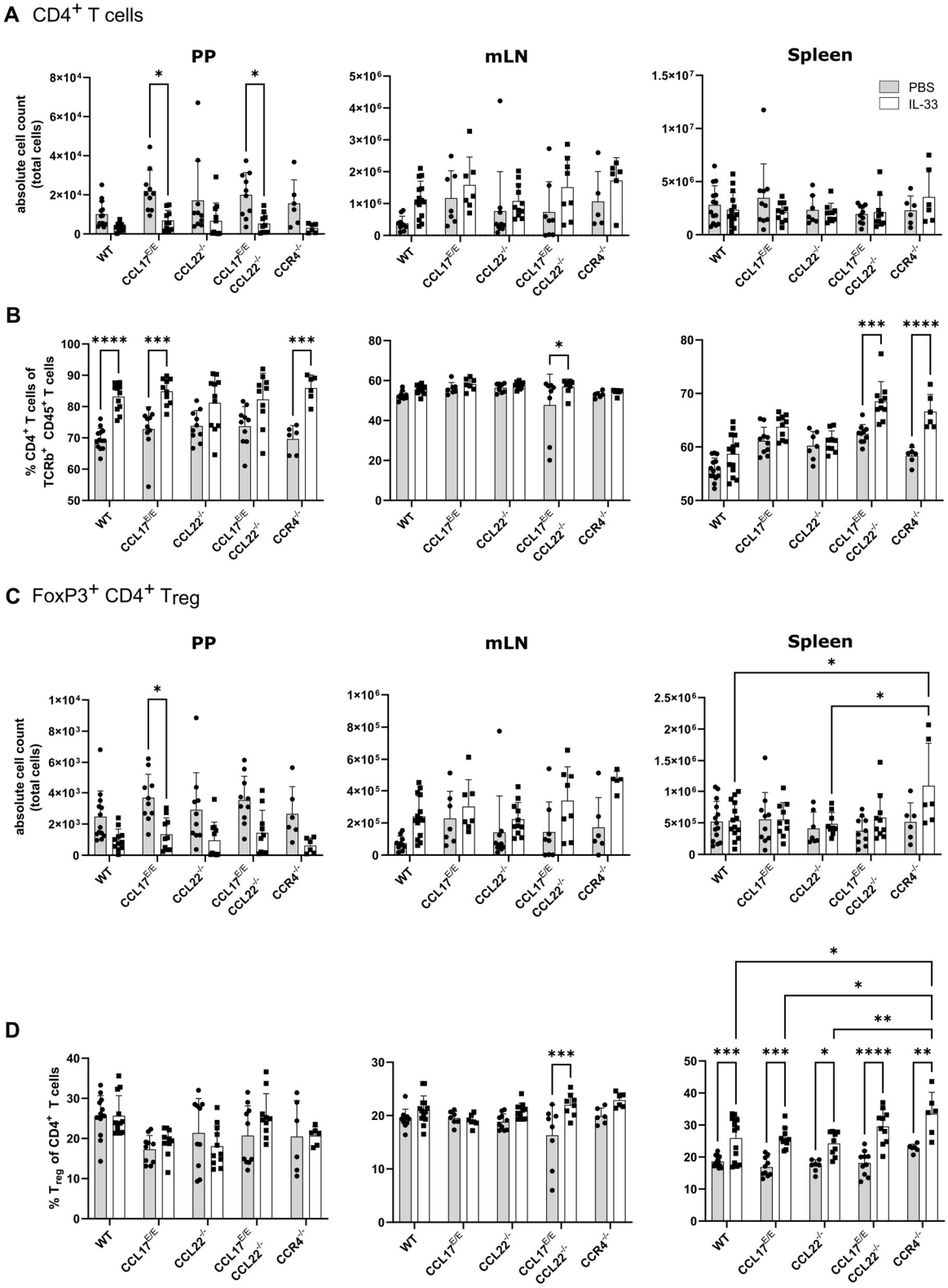
A CD4+ T cells
PP
mLN
Spleen
PBS
IL-33
absolute cell count (total cells)
B
% CD4+ T cells of TCRb+ CD45+ T cells
C FoxP3+ CD4+ Treg
D
% Treg of CD4+ T cells
WT
CCL17E/E
CCL22-/-
CCL17E/E CCL22-/-
CCR4-/-

Figure 4.5: FACS analysis of PBS- and IL-33-treated mice – $CD4^+$ T cells and $FoxP3^+$ T_{reg} cells
Wt, $CCL17^{E/E}$, $CCL22^{-/-}$, $CCL17^{E/E}$ $CCL22^{-/-}$, and $CCR4^{-/-}$ mice were intraperitoneally injected with PBS (grey) or 0.5 µg IL-33 (white) every second day. $CD4^+$ T cells (A) absolute cell counts and (B) frequencies as well as $FoxP3^+$ (C) absolute cell counts and (D) frequencies in PP (left), mLN (middle), and spleen (right) were analysed. Symbols represent individual mice (n=10-14; pooled from three ($CCL22^{-/-}$), four ($CCL17^{E/E}$ and $CCL17^{E/E}$ $CCL22^{-/-}$) or six (wt) independent experiments; for $CCR4^{-/-}$ n=6; from two independent experiments). Absolute cell counts were calculated using counting beads. In case of the PP, cell counts were normalised to the number of isolated PPs. Statistical significance was tested using two-way ANOVA with Tukey's test for multiple comparison. Data are presented as mean with SD.

Furthermore, whereas absolute counts of $KLRG1^+$ T_{reg} cells were unaffected in the PP (Figure 4.6A, left row), their counts were significantly increased in the mLN after IL-33 treatment (Figure 4.6A, middle row). They were also increased in the spleen, most significantly in the $CCR4^{-/-}$ mice but not in $CCL22^{-/-}$ mice (Figure 4.6A, right row).

Application of IL-33 significantly increased the frequency of $KLRG1^+$ T_{reg} cells in all three organs independent of the genotype. However, the increase was less pronounced in $CCL17^{E/E}$ $CCL22^{-/-}$ and $CCR4^{-/-}$ mice for PP and mLN and in $CCL22^{-/-}$ mice in the spleen (Figure 4.6B).

Subsequently, the ratio of $KLRG1^+$ T_{reg} cells to $FoxP3^-$ T_{conv} cells was determined and found significantly increased after IL-33 treatment across all organs and genotypes, except in $CCL22^{-/-}$ and $CCR4^{-/-}$ mice in the PP (Figure 4.6C). $CCL22^{-/-}$ mice only showed a significant increase in the mLN, although a tendency was visible for PP and spleen. In $CCR4^{-/-}$-deficient mice the ratio was significantly changed for mLN and spleen. In PP the ratio of $KLRG1^+$ T_{reg} cells to $FoxP3^-$ T_{conv} cells of $CCR4^{-/-}$ mice was significantly decreased compared to wt mice in the IL-33-treated cohort. In contrast, the ratio in $CCR4^{-/-}$ mice after IL-33 treatment was significantly increased compared to wt, $CCL17^{E/E}$ and $CCL22^{-/-}$ mice in spleen.

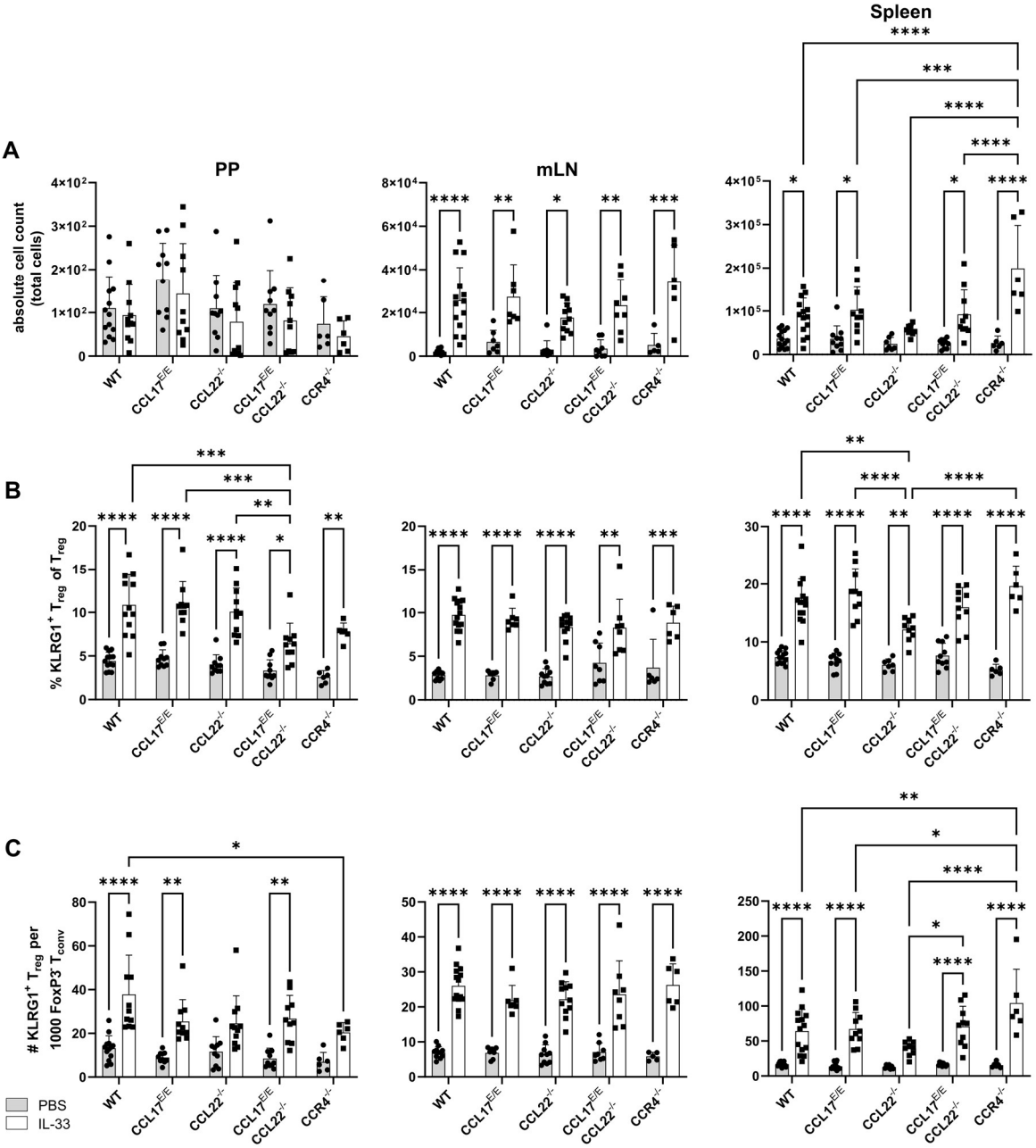

Figure 4.6: FACS analysis of PBS- and IL-33-treated mice – KLRG1$^+$ T_{reg} cells
Wt, CCL17$^{E/E}$, CCL22$^{-/-}$, CCL17$^{E/E}$ CCL22$^{-/-}$, and CCR4$^{-/-}$ mice were intraperitoneally injected with PBS (grey) or 0.5 µg IL-33 (white) every second day. On day 8, PP (left), mLN (middle), and spleen (right) were analysed. (A) Absolute cell counts and (B) frequencies of KLRG1$^+$ T_{reg} cells. Additionally, the ratio of KLRG1$^+$ T_{reg} cells to FoxP3$^-$ T_{conv} cells was calculated (C). Symbols represent individual mice (n=10-14; pooled from three (CCL22$^{-/-}$), four (CCL17$^{E/E}$ and CCL17$^{E/E}$ CCL22$^{-/-}$) or six (wt) independent experiments; for CCR4$^{-/-}$ n=6; from two independent experiments).

Absolute cell counts were calculated using counting beads. In case of the PP, cell counts were normalised to the number of isolated PPs. Statistical significance was tested using two-way ANOVA with Tukey's test for multiple comparison. Data are presented as mean with SD.

Within the T_{reg} cell compartment, thymic $Nrp1^+$ and peripheral $ROR\gamma t^+$ T_{reg} cells were analysed (Figure 4.7). Overall, cell numbers and frequencies for these T_{reg} cell subsets were mostly unaffected across all organs after IL-33 treatment. The exception was the number of peripheral T_{reg} cells in the PP which was significantly reduced compared to the control groups (Figure 4.7C). However, thymic T_{reg} cell numbers in the PP also showed a tendency to be decreased.

Taken together, administration of IL-33 expanded $KLRG1^+$ effector T_{reg} cells, consistent with previous research (Vasanthakumar *et al.*, 2015). Because IL-33-mediated expansion was exclusively targeting $KLRG1^+$ effector T_{reg} cells but not $FoxP3^-$ T cells, the ratio of $KLRG1^+$ T_{reg} cells to $FoxP3^-$ T_{conv} cells was shifted upwards, making IL-33 injections a suitable tool for creating a more immunosuppressive environment.

Interestingly, absolute cell counts of overall immune cells and underlying T cell subsets were decreased in the PP; one possible explanation for this phenomenon is migration of these cells to other organs.

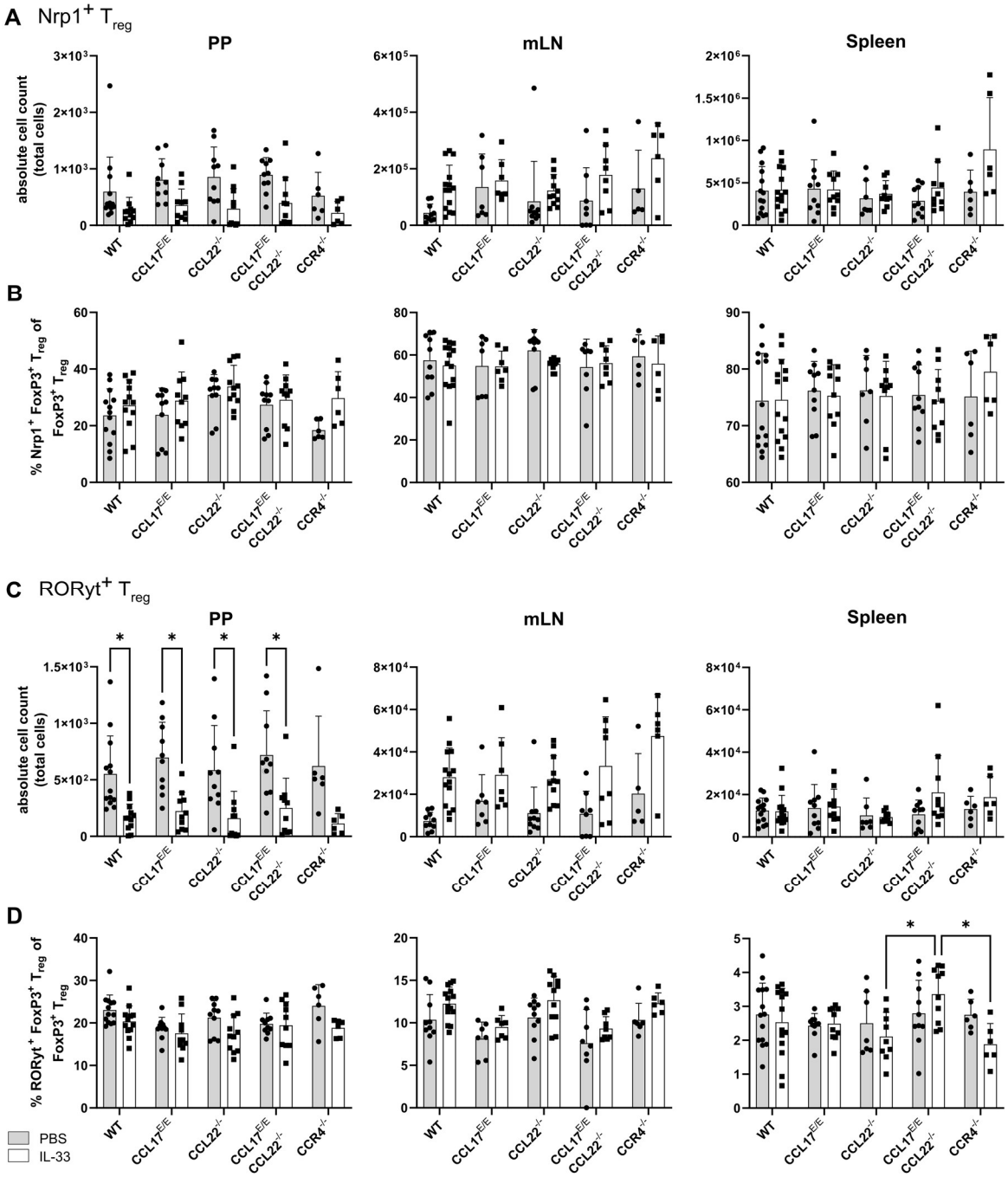

Figure 4.7: FACS analysis of PBS- and IL-33-treated mice – tT_{reg} and pT_{reg} cells
Wt, $CCL17^{E/E}$, $CCL22^{-/-}$, $CCL17^{E/E}$ $CCL22^{-/-}$, and $CCR4^{-/-}$ mice were intraperitoneally injected with PBS (grey) or 0.5 µg IL-33 (white) every second day. On day 8, PP (left), mLN (middle), and spleen (right) were analysed. (A) Absolute cell counts and (B) frequencies of $Nrp1^+$ tT_{reg} cells, (C) absolute cell counts and (D) frequencies of $ROR\gamma t^+$ pT_{reg} cells. Symbols represent individual mice (n=10-14; pooled from three ($CCL22^{-/-}$), four ($CCL17^{E/E}$ and $CCL17^{E/E}$ $CCL22^{-/-}$) or six (wt) independent

experiments; for CCR4$^{-/-}$ n=6; from two independent experiments). Absolute cell counts were calculated using counting beads. In case of the PP, cell counts were normalised to the number of isolated PPs. Statistical significance was tested using two-way ANOVA with Tukey's test for multiple comparison. Data are presented as mean with SD.

4.4 IL-33 causes splenomegaly independently of CCL17 and CCL22

Treatment of naïve mice with IL-33 causes increased production of Th2 cytokines, severe inflammation and splenomegaly (Schmitz *et al.*, 2005). Splenomegaly could also be observed in the IL-33 model used in this thesis independently of the genotype (Figure 4.8). Although KLRG1$^+$ T_{reg} cell numbers were significantly increased (Figure 4.6), overall T cell numbers remained unaffected (Figure 4.5, Figure 4.7), raising the question if other immune cell populations might be increased and causing the significant increase in spleen weight.

Hence, a second antibody panel and gating strategy were designed to assess this question. The gating strategy was set as follows (Figure 4.9): Immune cells were selected based on their FSC and SSC properties. Following exclusion of doublet cells, viable CD45$^+$ cells were analysed. From the CD45$^+$ immune cell compartment neutrophils were first excluded by their Ly6G expression. Second and third, NK cells and B cells were selected. Remaining cells that were negative for the previous markers (Ly6G, NK1.1 and CD19) were separated by their F4/80 and CD11b expression. Double positive cells were identified as macrophages. Double negative cells, however, were further selected based on their CD11c expression. CD11c$^+$ cells were identified as DC and further separated into CD172α$^-$ cDC1 and CD172α$^+$ cDC2. From the previous gate, CD11c$^-$ cells were divided into Ly6C$^-$ and Ly6C$^+$ monocytes.

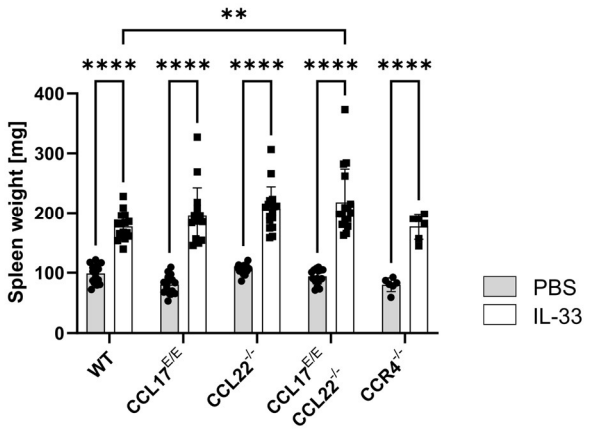

Figure 4.8: IL-33 causes splenomegaly independent of CCL17 and CCL22
Wt, CCL17$^{E/E}$, CCL22$^{-/-}$, CCL17$^{E/E}$ CCL22$^{-/-}$, and CCR4$^{-/-}$ mice were intraperitoneally injected with PBS (grey) or 0.5 µg IL-33 (white) every second day. Spleen weight was determined for control and treated groups on day 8. Symbols represent individual mice (n=16; from five or six (wt) independent experiments; for CCR4$^{-/-}$ n=6; from two independent experiments). Statistical significance was tested using two-way ANOVA with Tukey's test for multiple comparison. Data are presented as mean with SD.

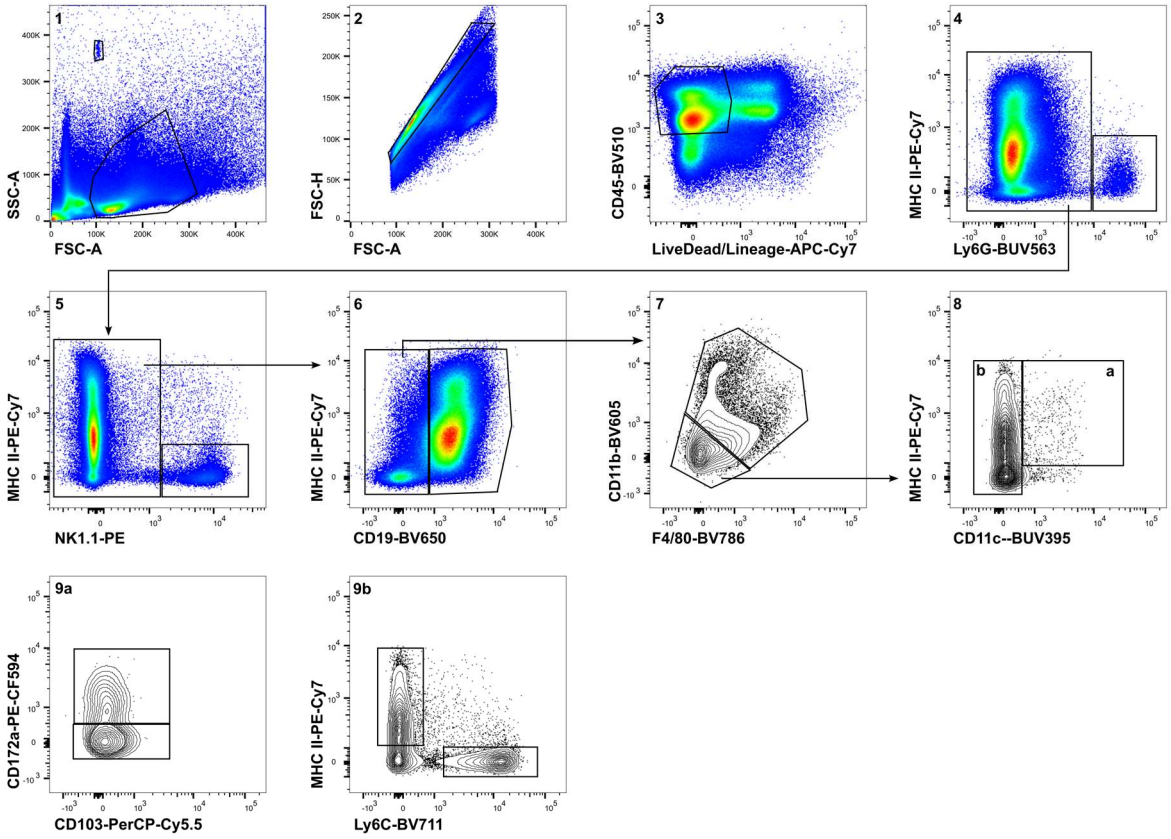

Figure 4.9: Gating strategy of myeloid cell, NK cell, and B cell FACS analysis of IL-33 injected mice

Wt, CCL17$^{E/E}$, CCL22$^{-/-}$, CCL17$^{E/E}$ CCL22$^{-/-}$, and CCR4$^{-/-}$ mice were intraperitoneally injected with PBS (grey) or 0.5 µg IL-33 (white) every second day and analysed on day 8. Mice were monitored every second day for their health status according to animal ethics. Spleen was isolated and analysed via flow cytometry. Immune cells were selected based on their FSC and SSC properties (1). Doublet cells were excluded (2). Viable CD45^{+} immune cells were selected (3). From the CD45^{+} immune cell compartment neutrophils (4), NK cells (5), B cells (6), macrophages (7), and DC (8) were selected. DC were further separated into CD172α^{-} cDC1 and CD172α^{+} cDC2 (9a). Remaining cells, negative for all previous markers, were divided into Ly6C^{-} and Ly6C^{+} monocytes (9b). Representative gating of spleen cells from a PBS-treated wt mouse

Overall, IL-33 injections did not increase the frequency of B cells, NK cells, neutrophils, macrophages, monocytes, and DC populations cDC1 and cDC2 compared to control groups (Figure 4.10). Of note, $CCL17^{E/E}$ mice showed a significant decrease in B cells (Figure 4.10A) after IL-33 administration as well as tendencies of increased NK cells (Figure 4.10B) and neutrophils (Figure 4.10C). Absolute cell counts of all populations were also unaffected by IL-33 treatment (Figure 4.11).

Overall, the immune cell populations investigated, including myeloid cells, B cells, and NK cells, were unaffected by IL-33 treatment, thereby not contributing to the observed splenomegaly. These results are consistent with the previous observation that $CD45^{+}$ cell numbers were unchanged between control and treated groups in the spleen (Figure 4.4). Therefore, the splenomegaly is probably caused by non-immune cells.

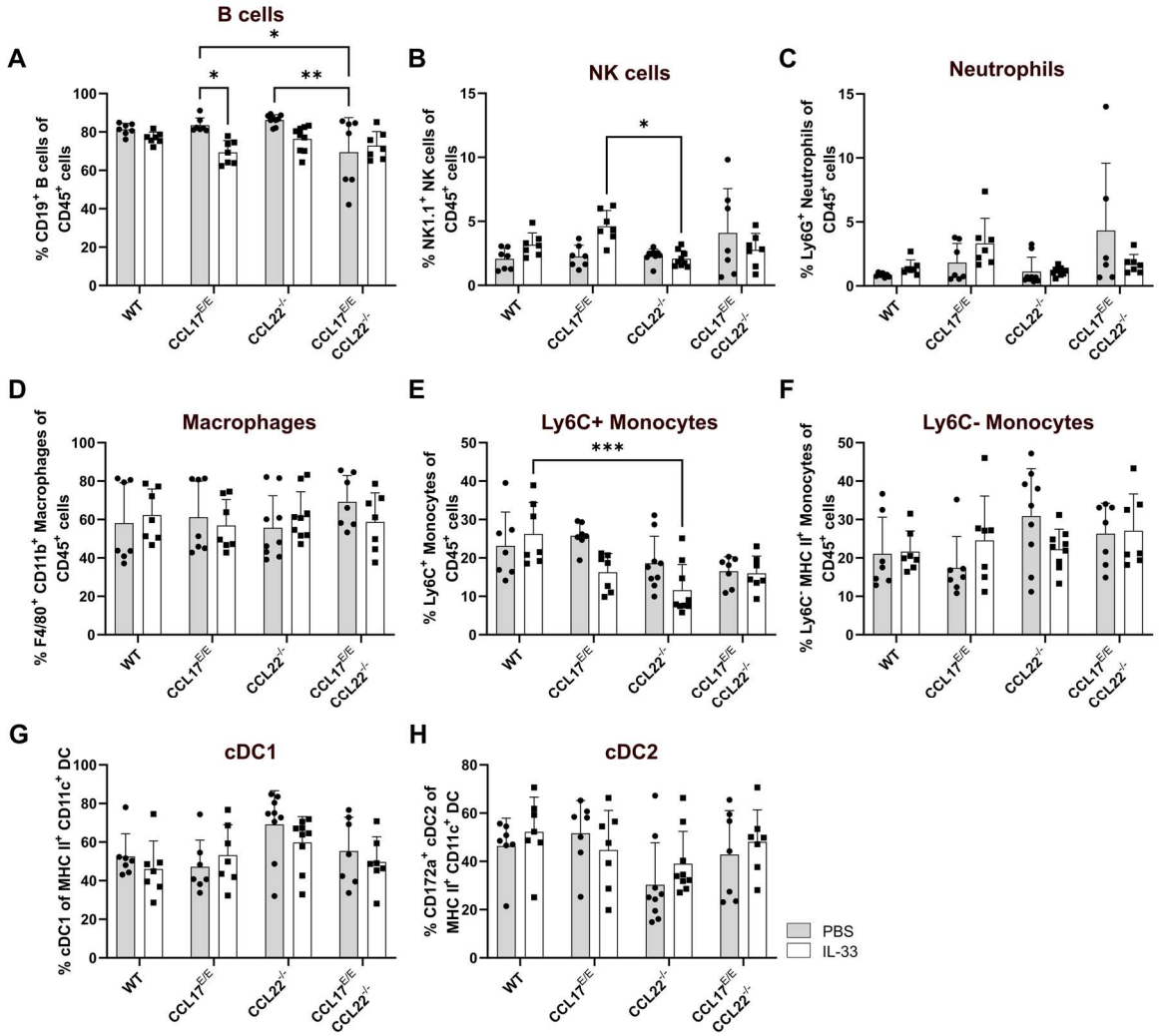

Figure 4.10: FACS analysis of PBS- and IL33-treated mice – frequency of splenic myeloid cells, B cells and NK cells

Wt, CCL17$^{E/E}$, CCL22$^{-/-}$, and CCL17$^{E/E}$ CCL22$^{-/-}$ mice were intraperitoneally injected with PBS (grey) or 0.5 µg IL-33 (white) every second day. Spleen was isolated and analysed on day 8. Frequencies of (A) B cells, (B) NK cells, (C) neutrophils, (D) macrophages, (E) Ly6C^{+} monocytes, (F) Ly6C^{-} monocytes, (G) cDC1, and (H) cDC2. Symbols represent individual mice (n=7-8; from two (CCL22$^{-/-}$) or three independent experiments). Statistical significance was tested using two-way ANOVA with Tukey's test for multiple comparison. Data are presented as mean with SD.

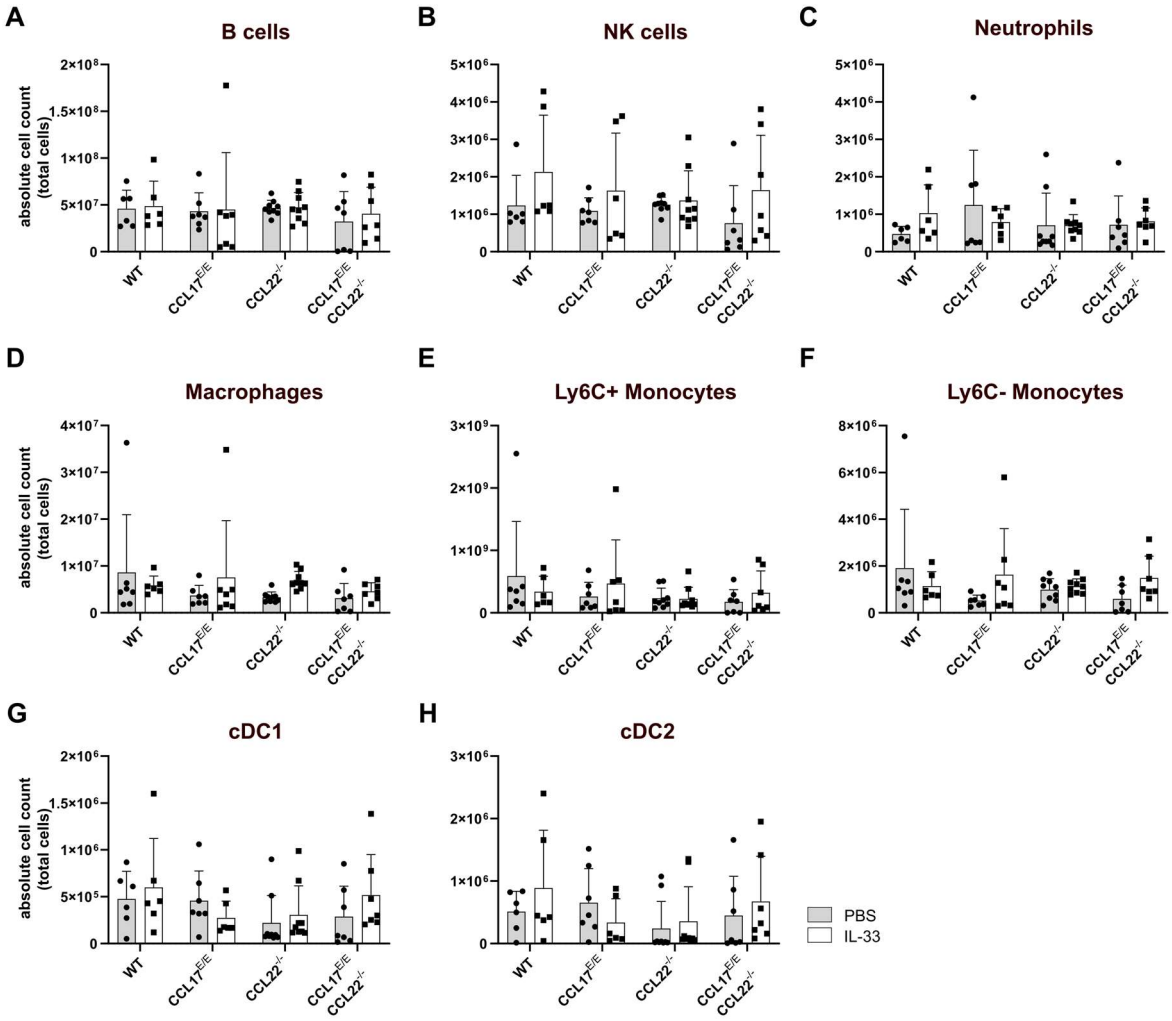

Figure 4.11: FACS analysis of PBS- and IL33-treated mice – absolute counts of splenic myeloid cells, B cells and NK cells

Wt, CCL17$^{E/E}$, CCL22$^{-/-}$, and CCL17$^{E/E}$ CCL22$^{-/-}$ mice were intraperitoneally injected with PBS (grey) or 0.5 µg IL-33 (white) every second day. Spleen was isolated and analysed on day 8. Absolute cell counts of (A) B cells, (B) NK cells, (C) neutrophils, (D) macrophages, (E) Ly6C^{+} monocytes, (F) Ly6C^{-} monocytes, (G) cDC1, and (H) cDC2. Symbols represent individual mice (n=7-8; from two (CCL22$^{-/-}$) or three independent experiments). Absolute cell counts were calculated using counting beads. Statistical significance was tested using two-way ANOVA with Tukey's test for multiple comparison. Data are presented as mean with SD.

4.5 IL-33 influences extramedullary erythropoiesis

The BM is the primary site for erythropoiesis. During inflammation, however, erythropoiesis can also occur in the spleen (Jing *et al.*, 2021). To assess if erythrocytes or their progenitor cells are contributing to the IL-33 induced splenomegaly a new gating strategy was established (Figure 4.12) and the gating strategy was set as follows: haematopoietic cells were selected based on their FSC and SSC properties. Following the exclusion of doublet cells and autofluorescent (AF) cells, viable cells were analysed for their CD71 and Ter119 expression. $CD71^+$ $Ter119^-$ cells were identified as pro-erythrocytes. $Ter119^+$ cells were further gated based on their levels of CD71 and their FSC properties, separating them into three populations (Koulnis *et al.*, 2011; Koulnis *et al.*, 2012). $CD71^+$ $Ter119^+$ FSC^{high} cells were defined as basophilic erythroblasts maturing into polychromatic erythroblasts ($CD71^+$ $Ter119^+$ FSC^{low}) and later into orthochromatic erythroblasts and reticulocytes ($CD71^-$ $Ter119^+$ FSC^{low}) (Koulnis *et al.*, 2012; Yeo *et al.*, 2019).

The double negative population ($CD71^-$ $Ter119^-$) was separated by Sca-1 expression. Sca-1 expressing cells were identified as $CD105^+$ $CD150^+$ HSC and $CD105^-$ $CD150^-$ MPP. From the previous gate ($Sca\text{-}1^-$ cells), $CD41^+$ $CD150^{int}$ MkP and $FcyRII/III^+$ GMP were excluded and remaining cells were separated by their CD105 and CD150 expressions into ($Sca\text{-}1^-$ $CD41^-$ $FcyRII/III^-$) $CD105^+$ $CD150^-$ CFU-E, $CD105^+$ $CD150^+$ pre-CFU-E, and $CD105^-$ $CD150^+$ pre-MegE.

Absolute cell counts of basophilic erythroblasts ($CD71^+$ $Ter119^+$ FSC^{high}) were significantly increased in $CCL22^{-/-}$ and $CCL17^{E/E}$ $CCL22^{-/-}$ mice (Figure 4.13A). The same was true for their frequency, although in this case $CCL17^{E/E}$ and $CCR4^{-/-}$ mice also showed a significant increase. Polychromatic erythroblasts ($CD71^+$ $Ter119^+$ FSC^{low}) and orthochromatic erythroblasts ($CD71^-$ $Ter119^+$ FSC^{low})/reticulocytes were largely unaffected (Figure 4.13B, C), although $CCL17^{E/E}$ $CCL22^{-/-}$ mice showed a significant decrease in the frequency of orthochromatic erythroblasts/reticulocytes after IL-33 treatment.

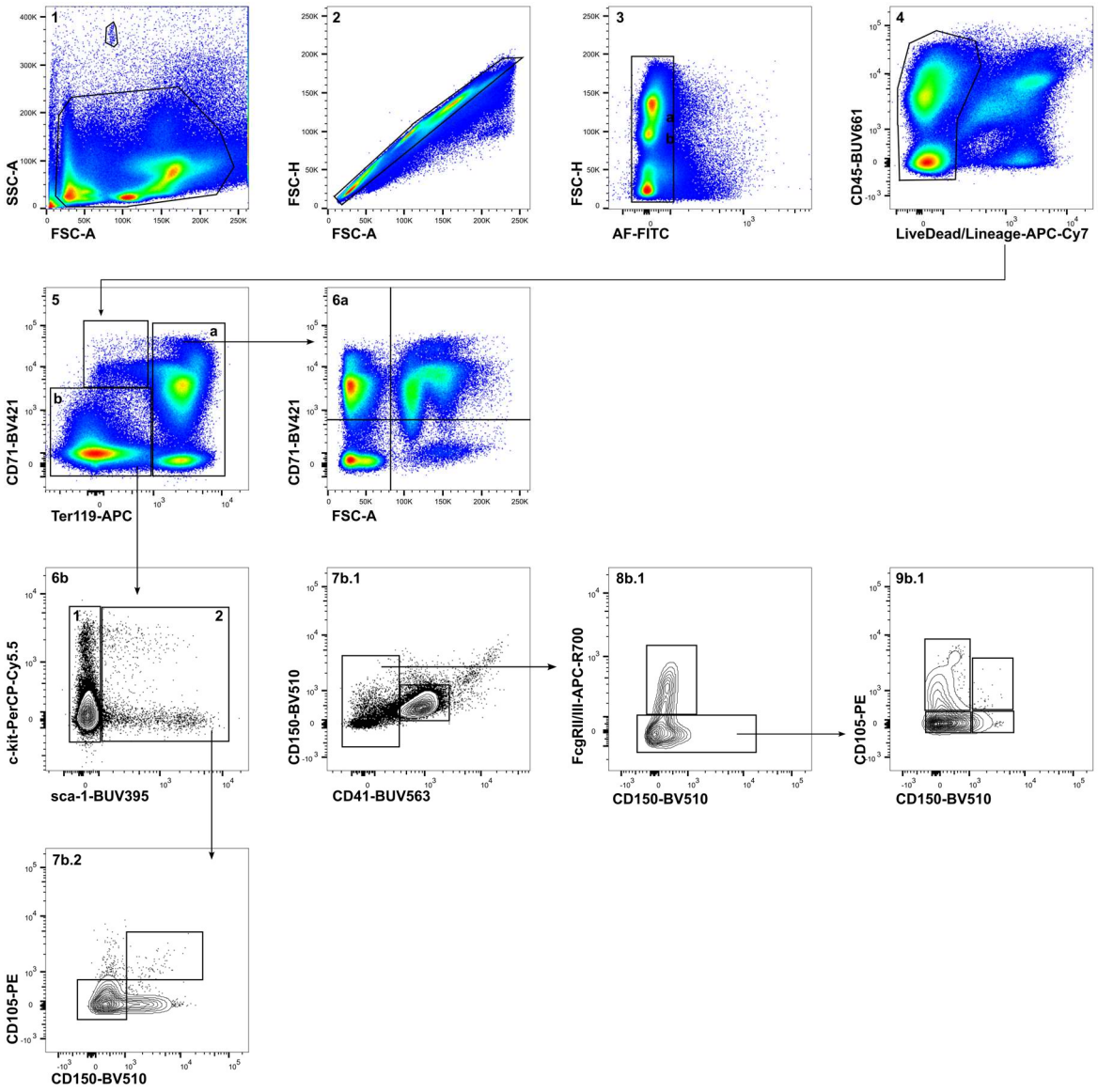

Figure 4.12: Gating strategy of erythroid progenitor cells FACS analysis of IL-33 injected mice

Wt, CCL17$^{E/E}$, CCL22$^{-/-}$, CCL17$^{E/E}$ CCL22$^{-/-}$, and CCR4$^{-/-}$ mice were intraperitoneally injected with PBS (grey) or 0.5 µg IL-33 (white) every second day and analysed on day 8. Mice were monitored every second day for their health status according to animal ethics. Blood, BM and spleen were isolated and analysed via flow cytometry. Haematopoietic cells were selected based on their FSC and SSC properties (1). Doublet cells (2) and autofluorescent cells (3) were excluded. Viable cells were selected (4) and separated through their CD71 and Ter119 expression (5). CD71^{+} Ter119^{-} were characterised as pro-erythrocytes (5 unlabeled). Ter119^{+} cells (5a) were further characterised by their levels of CD71 and their FSC properties, determining basophilic erythroblasts (CD71^{+} Ter119^{+} FSC^{high}), polychromatic

erythroblasts (CD71$^+$ Ter119$^+$ FSC^{low}), and orthochromatic erythroblasts (CD71$^-$ Ter119$^+$ FSC^{low})/reticulocytes (6a). From the CD71$^-$ Ter119$^-$ cells (5b), sca-1$^+$ cells (6b.2) were selected and determined as CD105$^+$ CD150$^+$ HSC and CD105$^-$ CD150$^-$ MPP (7b.2). Sca-1$^-$ cells (6b.1), excluding CD41$^+$ CD150^{int} MkP (7b.1) and FcyRII/III$^+$ GMP (8b.1), were separated by their CD105 and CD150 expressions into (Sca-1$^-$ CD41$^-$ FcyRII/III$^-$) CD105$^+$ CD150$^-$ CFU-E, CD105$^+$ CD150$^+$ pre CFU-E, and CD105$^-$ CD150$^+$ pre MegE (9b.1). Representative gating of spleen cells from a PBS-treated wt mouse

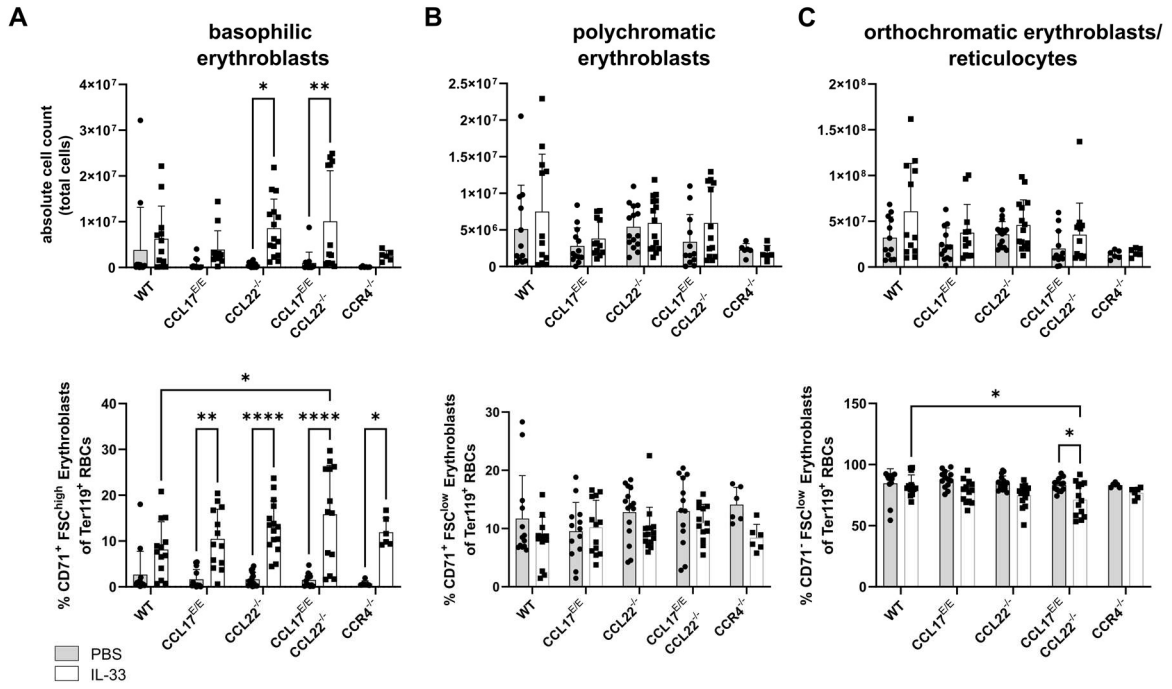

Figure 4.13: Basophilic erythroblasts are increased in CCL22$^{-/-}$ and CCL17$^{E/E}$ CCL22$^{-/-}$ mice after IL-33 treatment in the spleen

Wt, CCL17$^{E/E}$, CCL22$^{-/-}$, and CCL17$^{E/E}$ CCL22$^{-/-}$ mice were intraperitoneally injected with PBS (grey) or 0.5 µg IL-33 (white) every second day. Spleen was isolated and analysed on day 8. Absolute cell counts (upper row) and frequencies (lower row) of (A) basophilic erythroblasts, (B) polychromatic erythroblasts, and (C) orthochromatic erythroblasts/reticulocytes. Symbols represent individual mice (n=6-12; pooled from two (CCR4$^{-/-}$) or three independent experiments). Absolute cell counts were calculated using counting beads. Statistical significance was tested using two-way ANOVA with Tukey's test for multiple comparison. Data are presented as mean with SD.

Counts of haematopoietic stem cells (HSC) in the spleen were unchanged between control and IL-33-treated mice for all genotypes (Figure 4.14A). Notably, control CCL22$^{-/-}$ mice showed the highest HSC counts. This increase was significant compared to CCL17$^{E/E}$ CCL22$^{-/-}$ mice. Similarly, absolute cell counts of multipotent progenitors (MPP), granulocyte-monocyte progenitors (GMP), promegakaryocytes (pre-MegE), megakaryocyte progenitors (MkP), and pre-colony-forming unit-erythroid cells (pre CFU-E) remained unaffected by IL-33 (Figure 4.14B-F). In contrast, CFU-E were increased in the spleen in all genotypes after IL-33 treatment, significantly for CCL17$^{E/E}$ CCL22$^{-/-}$ mice (Figure 4.14G). Lastly, counts of proerythroblasts (pro-Erys) were also increased for all genotypes after treatment (Figure 4.14H) and significance was reached for chemokine single knockouts or double knockouts.

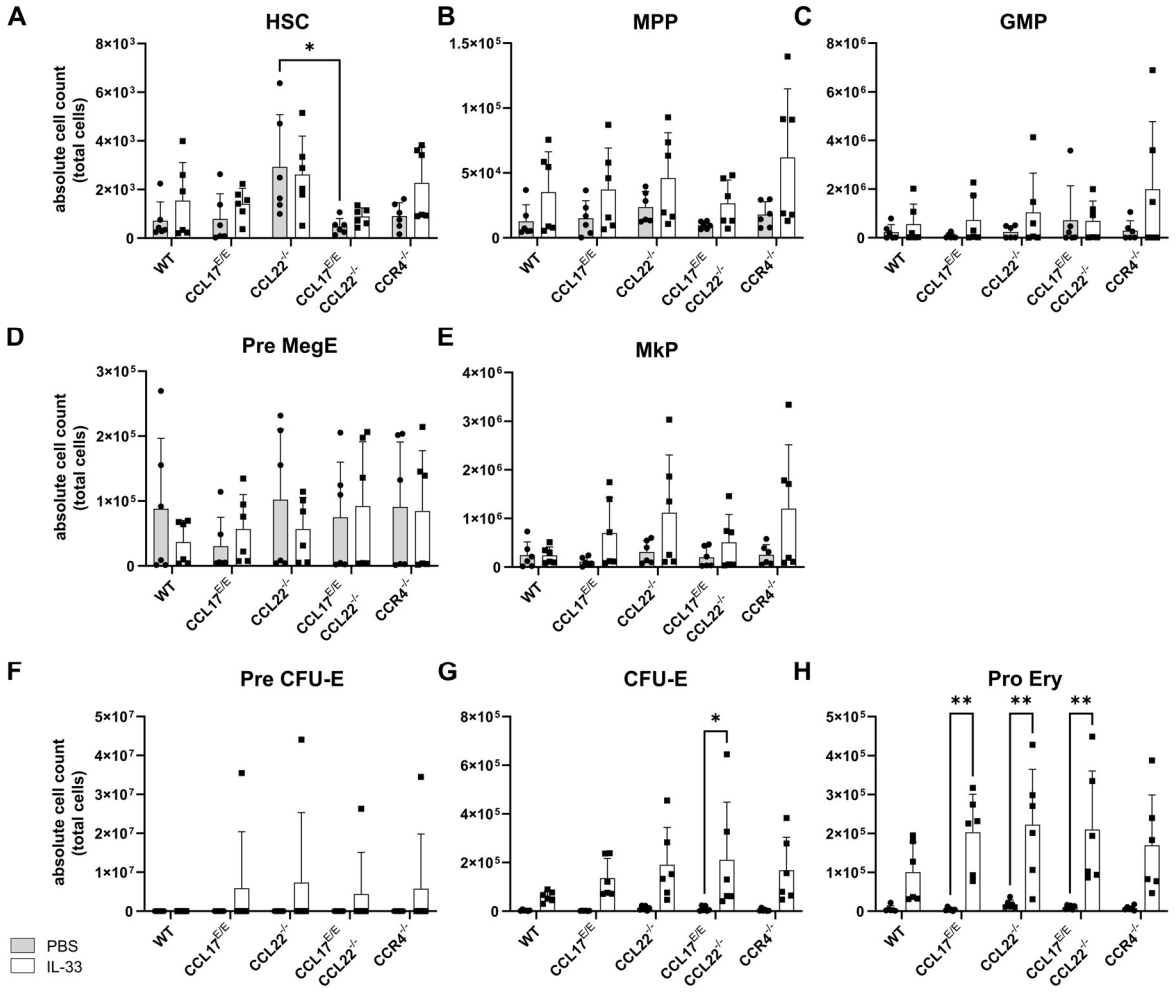

Figure 4.14: Splenic progenitors of erythrocytes are increased in chemokine-knockout mice after IL-33 treatment

Wt, CCL17$^{E/E}$, CCL22$^{-/-}$, and CCL17$^{E/E}$ CCL22$^{-/-}$ mice were intraperitoneally injected with PBS (grey) or 0.5 µg IL-33 (white) every second day. Spleen was isolated and analysed on day 8. Absolute cell counts of (A) HSC, (B) MPP, (C) GMP, (D) pre-MegE, (E) MkP, (F) pre-CFU-E, (G) CFU-E, and (H) pro-Ery. Symbols represent individual mice (n=6; from two independent experiments). Absolute cell counts were calculated using counting beads. Statistical significance was tested using two-way ANOVA with Tukey's test for multiple comparison. Data are presented as mean with SD.

Administration of IL-33 resulted in the accumulation of immature erythroblasts, particularly in CCL22$^{-/-}$ and CCL17$^{E/E}$ CCL22$^{-/-}$ mice. However, in previous studies, injections with IL-33 twice per week for 4 weeks in SKG mice, which spontaneously develop chronic autoimmune arthritis and are used as a human rheumatoid arthritis model (Sakaguchi *et al.*, 2006), led to a reduction in frequency and numbers of Ter119^{+} erythroid cells in the BM, while erythroid progenitors in the spleen remained unchanged (Swann *et al.*, 2020). Thus, absence of CCL22 and perhaps CCL17 could have a direct or indirect influence on erythropoiesis and might facilitate extramedullary haematopoiesis.

To investigate IL-33-mediated effects on erythropoiesis and the involvement of CCL17 and CCL22, blood and BM were also analysed via flow cytometry using the gating strategy described above (Figure 4.12).

The absolute counts of basophilic erythroblasts were unaffected in blood (Figure **4.15**A), but significantly decreased in BM (Figure 4.15C) of IL-33-treated mice. The exception were BM cells of CCL22$^{-/-}$ mice, although a moderate reduction was visible also in this genotype. A similar observation could be made for polychromatic erythroblasts. Lastly, orthochromatic erythroblasts and reticulocytes were unaffected in blood and BM by IL-33 treatment. Interestingly, a significant difference between IL-33-treated CCL17$^{E/E}$ and CCR4$^{-/-}$ mice across all three types of erythroblasts and reticulocytes was observed in the blood.

Similar results were obtained for the frequencies of erythroblast populations. In the blood, frequencies remained unaffected by IL-33 treatment (Figure 4.15B). In the BM, frequencies of basophilic and polychromatic erythroblasts were significantly decreased after IL-33 treatment in line with their decreased absolute numbers (Figure 4.15D). In contrast, counts of orthochromatic erythroblasts and reticulocytes were significantly increased after IL-33 treatment for all genotypes.

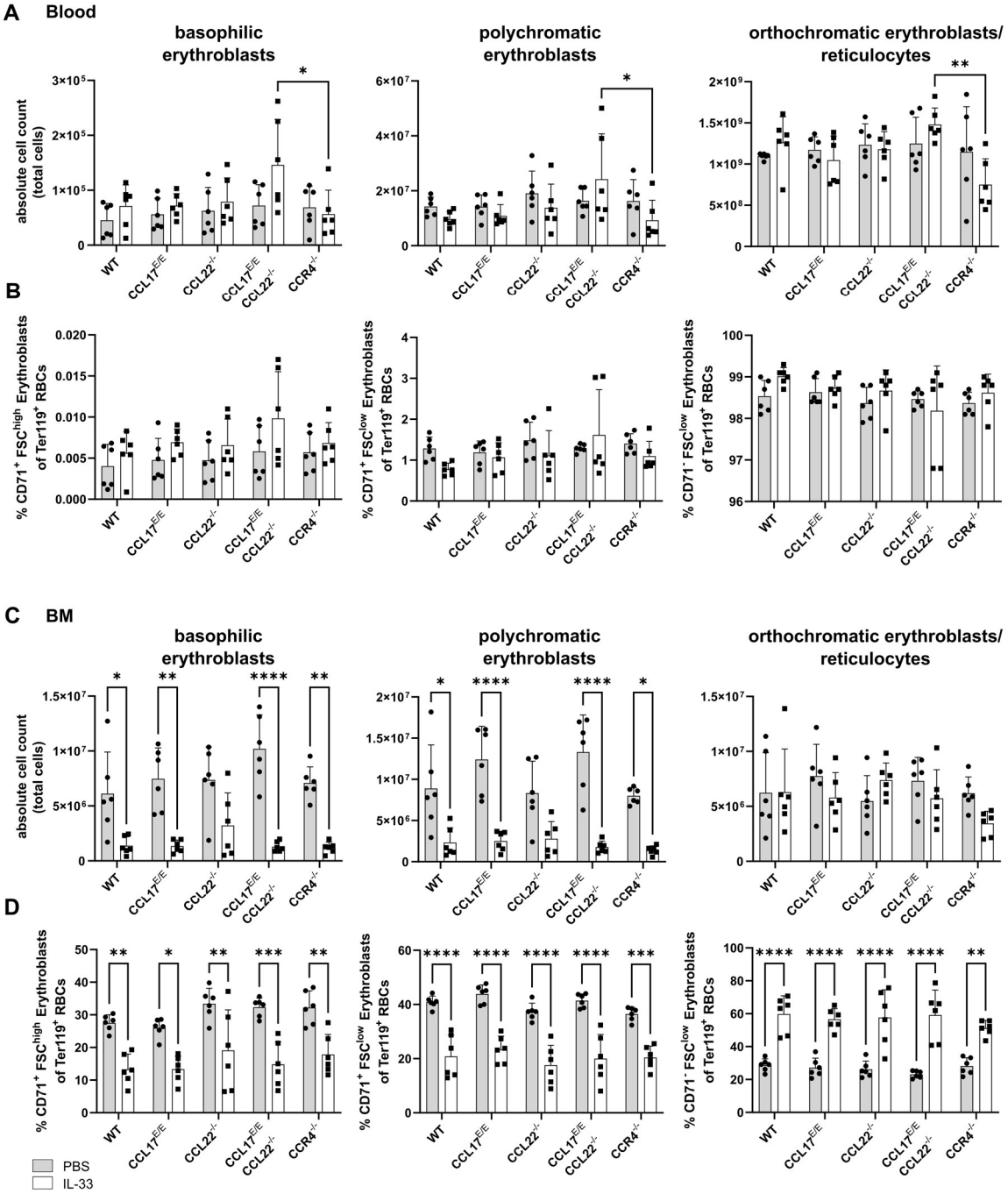

Figure 4.15: Absolute cell counts and frequencies of erythroid progenitor cells are altered in IL-33-treated mice

Wt, CCL17$^{E/E}$, CCL22$^{-/-}$, CCL17$^{E/E}$ CCL22$^{-/-}$, and CCR4$^{-/-}$ mice were intraperitoneally injected with PBS (grey) or 0.5 µg IL-33 (white) every second day. Blood and BM were isolated and analysed on day 8. (A) Absolute cell counts and (B) frequencies of basophilic erythroblasts (left panel), polychromatic erythroblasts (middle panel),

and orthochromatic erythroblasts/ reticulocytes (right panel) in the blood. (C) Absolute cell counts and (D) frequencies of basophilic erythroblasts (left panel), polychromatic erythroblasts (middle panel), and orthochromatic erythroblasts/ reticulocytes (right panel) in the BM. Symbols represent individual mice (n=6; pooled from two independent experiments). Absolute cell counts were calculated using counting beads. Statistical significance was tested using two-way ANOVA with Tukey's test for multiple comparison. Data are presented as mean with SD.

Counts of HSC in the BM were unchanged between control and IL-33-treated mice for all genotypes. Notably, BM HSC counts in IL-33-treated wt and CCR4$^{-/-}$ mice were significantly decreased compared to CCL22$^{-/-}$ mice (Figure 4.16A). MPP and GMP counts also remained unaffected by IL-33 (Figure 4.16B, C). Counts of pre-MegE were significantly increased only in the BM of IL-33-treated CCL17$^{E/E}$ mice (Figure 4.16D). The increase was also significant compared to IL-33-treated CCL22$^{-/-}$ and CCR4$^{-/-}$ mice. In the case of MkP, only treated CCL22$^{-/-}$ mice showed a significant increase, although a tendency was also visible for CCL17$^{E/E}$ mice (Figure 4.16E). Additionally, MkP counts in IL-33-treated wt and CCR4$^{-/-}$ mice were significantly decreased compared to IL-33-treated CCL22$^{-/-}$ mice. Pre-CFU-E were decreased after IL-33 treatment (Figure 4.16F). This decrease was significant in wt and CCL22$^{-/-}$ mice. Interestingly, pre-CFU-E counts in control mice were already significantly lower in CCL17$^{E/E}$, CCL17$^{E/E}$ CCL22$^{-/-}$ and CCR4$^{-/-}$ mice compared to CCL22$^{-/-}$ mice and in the case of CCL17$^{E/E}$ mice even to wt mice. Administration of IL-33 also lead to a decrease of CFU-E (colony-forming unit-erythroid) in the BM which was significant in CCL17$^{E/E}$ CCL22$^{-/-}$ mice (Figure 4.16G), contrasting the findings obtained for the spleen (Figure 4.14G). Absolute cell counts of pro-Erys were also decreased in IL-33-treated mice (Figure 4.16H). Significance was reached only for CCL17$^{E/E}$ CCL22$^{-/-}$ mice.

Taken together, IL-33 strongly impacts erythropoiesis in both BM and spleen. Immature progenitors of erythrocytes, starting from pre-CFU-E, were significantly decreased in counts and frequencies in BM after IL-33 treatment. However, absolute cell counts of orthochromatic erythroblasts/reticulocytes were unchanged, suggesting that IL-33 promotes maturation of erythrocytes. Reticulocytes are later

sent into the bloodstream where they finalise their maturation. The maturation of erythrocytes in the BM appeared to be independent of CCL17, CCL22, and CCR4. Additionally, IL-33 also induced extramedullary erythropoiesis in the spleen as basophilic erythroblast counts were increased. This increase was strongest in the absence of CCL22, hinting for a direct or indirect role of the chemokine in splenic erythropoiesis.

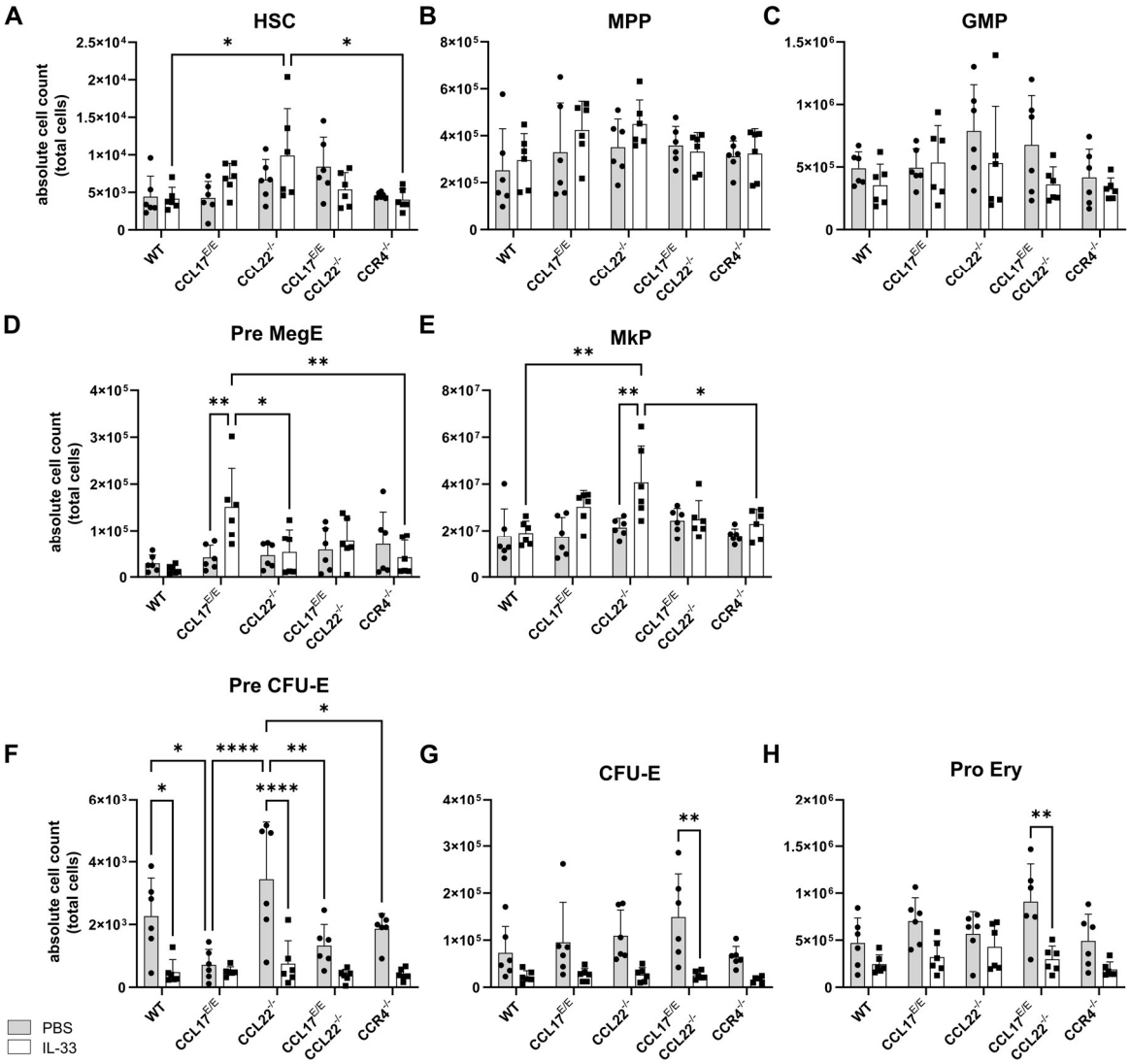

Figure 4.16: FACS analysis of PBS- and IL33-treated mice – progenitor cells in the BM

Wt, CCL17$^{E/E}$, CCL22$^{-/-}$, and CCL17$^{E/E}$ CCL22$^{-/-}$ mice were intraperitoneally injected with PBS (grey) or 0.5 µg IL-33 (white) every second day. BM was isolated and analysed on day 8. Absolute cell counts of (A) HSC, (B) MPP, (C) GMP, (D) pre-MegE, (E) MkP, (F) pre-CFU-E, (G) CFU-E, and (H) pro-Ery. Symbols represent individual mice (n=6; from two independent experiments). Absolute cell counts were calculated using counting beads. Statistical significance was tested using two-way ANOVA with Tukey's test for multiple comparison. Data are presented as mean with SD.

4.6 IL-33 causes eosinophilia in blood and bone-marrow

The IL-33-induced impairment of the erythropoiesis in the BM could be indicative of a haematologic disorder. The haematology system ADVIA® 2120i is frequently used in medical settings to analyse blood parameters in the context of checking the health status of an individual. Common parameters measured are the haemoglobin concentration, the haematocrit, the mean corpuscular volume (MCV), the mean corpuscular haemoglobin (MCH), and the mean corpuscular haemoglobin concentration (MCHC). Haemoglobin is expressed by red blood cells and is needed for supplying the tissue with oxygen. The haematocrit indicates the percentage of the red blood cell volume within the total blood volume (Billett, 1990). MCV measures the average red blood cell size, MCH shows the average haemoglobin amount in each red blood cell, while MCHC shows the average haemoglobin concentration in the red blood cells in relation to the cell size (Sarma, 1990). Deviations from the average values are indicators of haematologic disorders. As IL-33 treatment impaired erythropoiesis in the BM, it was hypothesised that the common blood-specific parameters are also altered.

Analysis of the blood showed no difference between control and treated groups regarding the red blood cell count, the haematocrit, the MCV, haemoglobin concentration, MCH, and MCHC (Figure 4.17A-F). However, CCL17$^{E/E}$ CCL22$^{-/-}$ mice already displayed a higher MCV compared to wt mice and CCL22$^{-/-}$ mice in the control groups and these differences were also visible after IL-33 treatment. The frequency of reticulocytes showed no significant differences (Figure 4.17G) although reticulocyte numbers after IL-33 treatment were slightly reduced (Figure 4.17H). Interestingly, reticulocyte counts of IL-33-treated CCL17$^{E/E}$ CCL22$^{-/-}$ mice were significantly higher compared to treated wt mice.

In contrast, the number of white blood cells increased after IL-33 treatment in the chemokine-deficient mice, which was significant for CCL17$^{E/E}$ CCL22$^{-/-}$ mice (Figure **4.18**A). While the frequency of lymphocytes showed a slight tendency to be reduced, the opposite was true for lymphocyte counts (Figure 4.18B, C) mainly due to the overall increased white blood cell counts. In the case of eosinophils, IL-33 treatment

led to significantly increased frequency and total cell count in all chemokine- or CCR4-deficient genotypes, but not in wt mice (Figure 4.18D, E). Furthermore, comparison between the IL-33-treated groups showed that both the frequency and the absolute number of eosinophils were significantly higher in $CC22^{-/-}$ mice compared to wt mice.

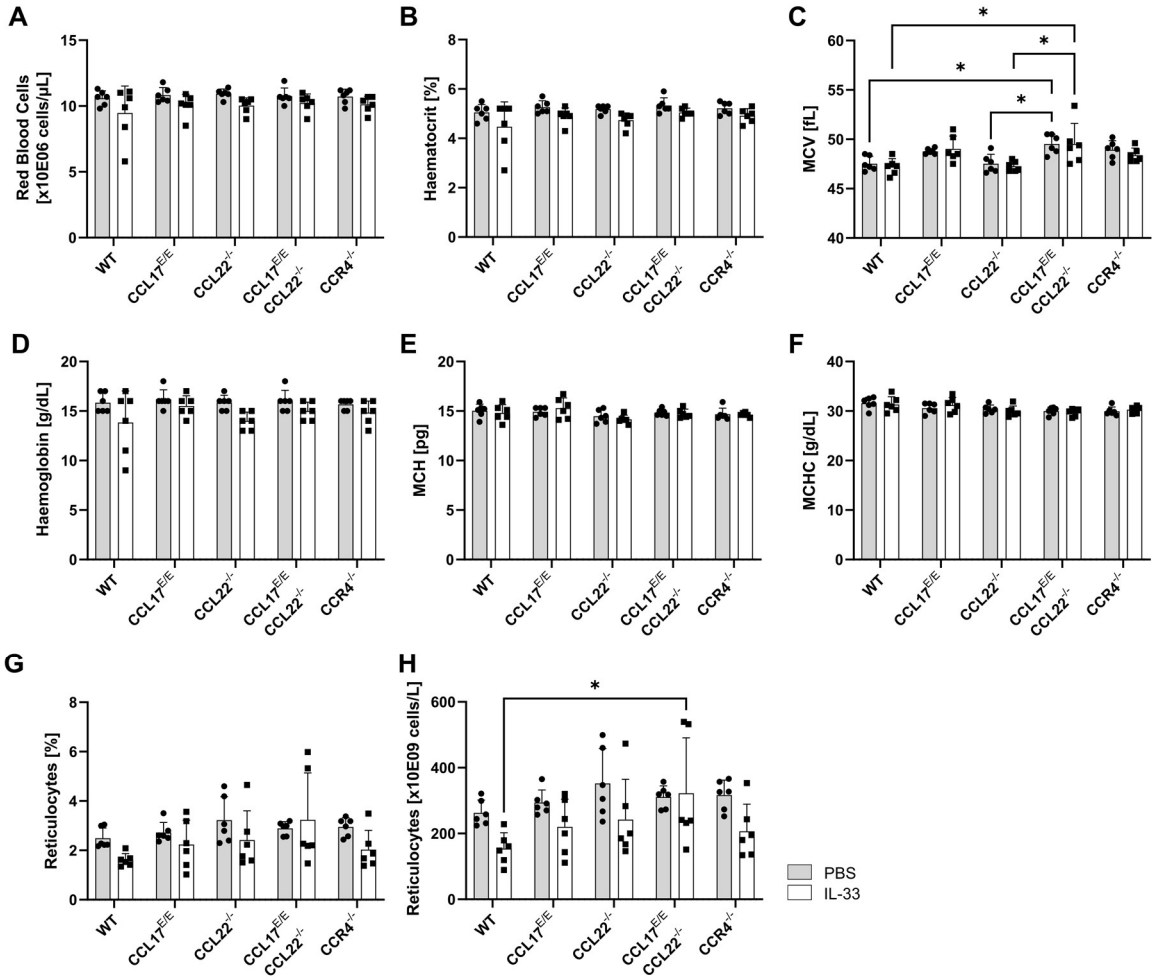

Figure 4.17: Haematologic analysis of the blood after IL-33 treatment – blood parameters

Wt, CCL17$^{E/E}$, CCL22$^{-/-}$, CCL17$^{E/E}$ CCL22$^{-/-}$, and CCR4$^{-/-}$ mice were intraperitoneally injected with PBS (grey) or 0.5 µg IL-33 (white) every second day. On day 8, blood was isolated and measured with the haematology system ADVIA® 2120i. Analysis of (A) red blood cell count, (B) haematocrit, (C) mean corpuscular volume MCV, (D) hemoglobin concentration, (E) mean corpuscular hemoglobin MCH, (F) mean corpuscular hemoglobin concentration MCHC, (G) frequency, and (H) absolute cell count of reticulocytes. Symbols represent individual mice (n=6; from two independent experiments). Statistical significance was tested using two-way ANOVA with Tukey's test for multiple comparison. Data are presented as mean with SD.

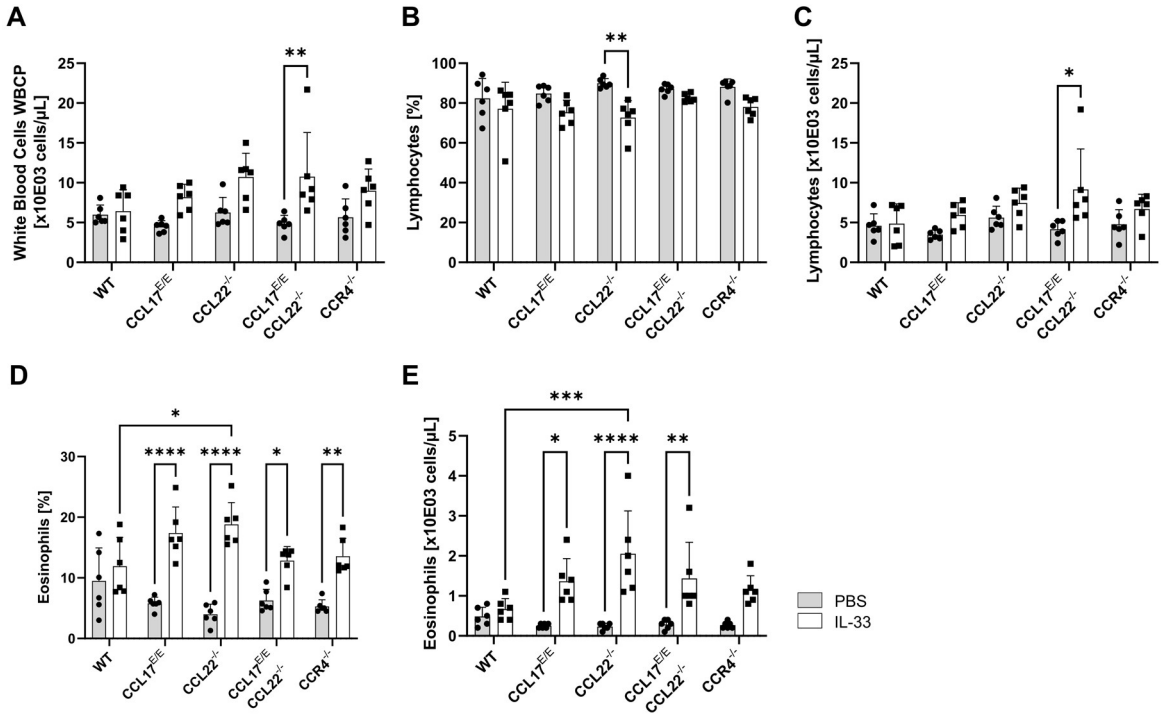

Figure 4.18: Haematologic analysis of the blood after IL-33 treatment – white blood cells, lymphocytes and eosinophils

Wt, CCL17$^{E/E}$, CCL22$^{-/-}$, CCL17$^{E/E}$ CCL22$^{-/-}$, and CCR4$^{-/-}$ mice were intraperitoneally injected with PBS (grey) or 0.5 µg IL-33 (white) every second day. On day 8, blood was isolated and measured with the haematology system ADVIA® 2120i. Analysis of (A) white blood cell count, (B) frequency, and (C) absolute cell count of lymphocytes. Additionally, (D) frequency, and (E) absolute cell count of eosinophils was measured. Symbols represent individual mice (n=6; from two independent experiments). Statistical significance was tested using two-way ANOVA with Tukey's test for multiple comparison. Data are presented as mean with SD.

In the BM, the MCV remained unaffected by IL-33 treatment (Figure 4.19A). Furthermore, frequency and count of reticulocytes were also unaffected (Figure 4.19B, C). In contrast to the blood, the number of red blood cells in the BM was decreased for all genotypes after IL-33 treatment, but this was significant only for $CCL17^{E/E}$ mice (Figure 4.19D). White blood cell counts were unchanged between control and IL-33-treated groups (Figure 4.19E). Lymphocyte frequencies and counts, however, were significantly reduced after IL-33 treatment independent of the genotype (Figure 4.19F, G). Large unstained cells, identified as activated lymphocytes and peroxidase-negative cells (Vanker and Ipp, 2014), were also reduced after IL-33 treatment (Figure 4.19H, I). Lastly, eosinophils were increased in the IL-33-treated groups for all genotypes including wt mice (Figure 4.19J, K). This change was significant for the frequency, but a tendency towards increased eosinophil counts was visible as well.

Overall, IL-33 induced eosinophilia in the blood and BM. While this appeared to be independent of the chemokines or their receptor in the BM, absence of CCL17, CCL22, and CCR4 significantly increased eosinophils in the blood after IL-33 treatment compared to wt mice. This suggests that CCL17 and CCL22 are dispensable for IL-33-driven eosinophil maturation (Johnston and Bryce, 2017), whereas mature eosinophils in the blood potentially fail to migrate towards inflammatory sites due to missing chemokine signals and are therefore retained and accumulated in the blood.

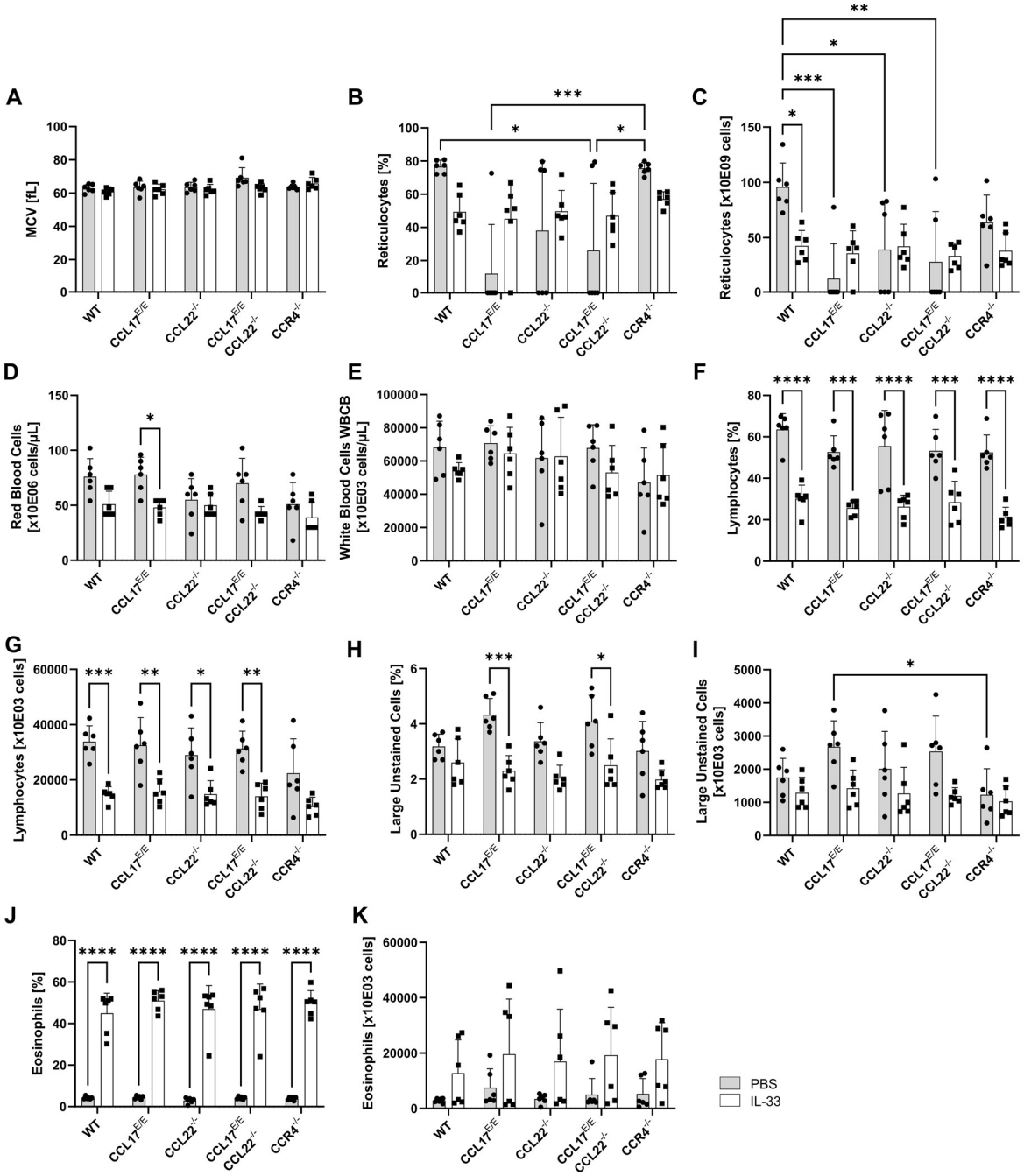

Figure 4.19: Haematologic analysis of the BM after IL-33 treatment
Wt, CCL17$^{E/E}$, CCL22$^{-/-}$, CCL17$^{E/E}$ CCL22$^{-/-}$, and CCR4$^{-/-}$ mice were intraperitoneally injected with PBS (grey) or 0.5 µg IL-33 (white) every second day. On day 8, BM was isolated and measured with the haematology system ADVIA® 2120i. Analysis of (A) MCV, (B) frequency and (C) absolute cell count of reticulocytes, (D) red blood cell count, (E) white blood cell counts. Additionally, frequency and absolute cell count of (F,G) lymphocytes, (H,I) large unstained cells, and (J,K) eosinophils were

measured. Symbols represent individual mice (n=6; from two independent experiments). Statistical significance was tested using two-way ANOVA with Tukey's test for multiple comparison. Data are presented as mean with SD.

4.7 CCR4-deficiency delays or impairs IL-33-induced weight loss

The function of IL-33 has been intensively studied in the context of obesity. While the cytokine is known to limit obesity by improving metabolic parameters, such as visceral fat weight; glucose and insulin tolerance; as well as liver steatosis, overall body weight gain remained unaffected between wt and IL-33-treated mice fed with HFD (Kai *et al.*, 2021) or in *ob/ob* mice (Ashley M Miller *et al.*, 2010).

Interestingly, WT, CCL17$^{E/E}$, CCL22$^{-/-}$, and CCL17$^{E/E}$ CCL22$^{-/-}$ mice lost on average between 5-8 % of body weight within 8 days of IL-33 treatment (Figure 4.20A-D). This change in body weight was significant from day 6, and in the case of wt mice even from day 4, onwards. In contrast, CCR4$^{-/-}$ mice showed no significant weight loss after IL-33 treatment, not even on day 8 of the experiment (Figure 4.20E, F). This suggests that absence of CCR4 either delays or protects against IL-33-induced weight loss. Interestingly, CCL17$^{E/E}$ CCL22$^{-/-}$ and CCR4$^{-/-}$ mice differed regarding the extent of IL-33-induced weight loss (Figure 4.20D-F), hinting that there might be a third player, either a third ligand for CCR4 or a second receptor for CCL17 and CCL22, involved.

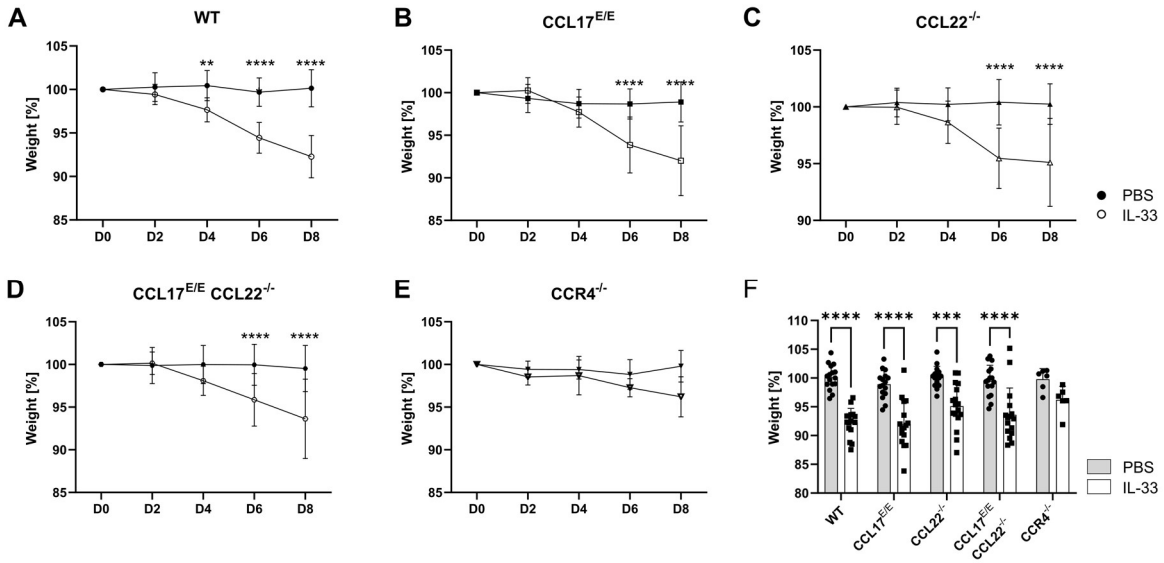

Figure 4.20: Absence of CCR4 delays or impairs IL-33 induced weight loss
Wt, CCL17$^{E/E}$, CCL22$^{-/-}$, CCL17$^{E/E}$ CCL22$^{-/-}$, and CCR4$^{-/-}$ mice were intraperitoneally injected with PBS (grey) or 0.5 µg IL-33 (white) every second day and analysed on day 8. Weight was monitored every second day prior to IL-33 injections. (A-E) Weight curves of control and treated groups of indicated genotypes. (F) Weight on day 8. All recorded weights were normalised to day 0 (pre-injection). (n=16; pooled from four (CCL22$^{-/-}$), five (CCL17$^{E/E}$, and CCL17$^{E/E}$ CCL22$^{-/-}$) or six (wt) independent experiments; for CCR4$^{-/-}$ n=6; pooled from two independent experiments). Statistical significance was tested using two-way ANOVA with Tukey's test for multiple comparison. Data are presented as mean with SD.

4.8 Absence of CCL22 protects from development of fibrosis in adipose tissue

The severe weight loss observed in IL-33-treated mice might be caused by changes within, and size reduction of, the adipose tissue depots. Therefore, inguinal white adipose tissue (iWAT) and brown adipose tissue (BAT) were further analysed and compared between the genotypes. The morphology of the adipose tissue depots was assessed through haematoxylin and eosin staining, while Picrosirius Red staining was used to evaluate fibrosis. This dye stains collagens, a component of connective tissue replacing parenchymal tissue in the process of fibrosis, leading to tissue damage and remodeling (Wynn, 2008; Vogel *et al.*, 2015).

With both H&E and Picrosirius Red staining iWAT of control mice showed a confluent layer of large spherical cells representing adipocytes (Figure 4.21). After IL-33

treatment the adipocyte cell layer was disrupted by extensive collagen depositions as indicated by the Picrosirius Red staining. Accumulation of collagen was localised around the AT lobules (perilobular fibrosis) and within the adipocyte area (pericellular fibrosis). Images of the Picrosirius red staining (four per condition) were blinded and scored for severity of perilobular and pericellular fibrosis after Lassen *et al*. (Lassen *et al.*, 2017). Depicting the average score of each animal revealed that fibrosis was especially severe in wt, $CCL17^{E/E}$, $CCL17^{E/E}$ $CCL22^{-/-}$, and $CCR4^{-/-}$ mice (Figure 4.22). Interestingly, $CCL22^{-/-}$ mice already showed signs of fibrosis in the control mice but fibrosis was not further exacerbated upon IL-33 treatment.

In BAT, administration of IL-33 leads to a higher density of the BAT cells, especially in wt mice. This effect was less pronounced in $CCL17^{E/E}$ and $CCL22^{-/-}$ mice. It should be noted, however, that $CCL22^{-/-}$ mice already exhibited a much denser brown adipocyte cell layer in the PBS-treated control group (Figure 4.21).

Taken together, CCL22-deficiency clearly protected from or delayed IL-33-induced fibrosis in iWAT. In contrast, $CCL17^{E/E}$ $CCL22^{-/-}$ mice still showed signs of fibrosis. This indicates i) a detrimental role of CCL22 that promotes fibrosis and ii) a beneficial function of CCL17.

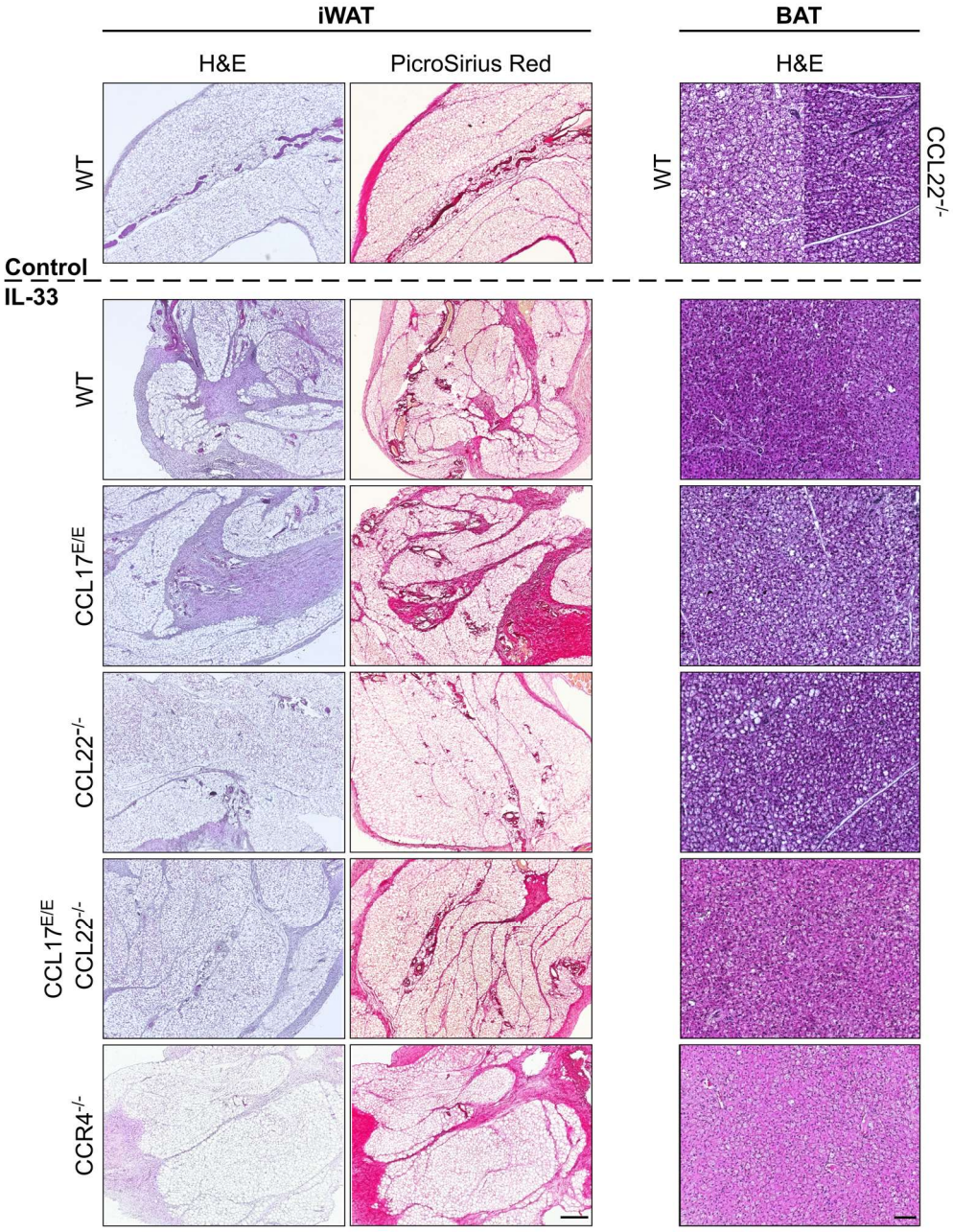

Figure 4.21: Histological analysis of mice after treatment with IL-33
Wt, CCL17$^{E/E}$, CCL22$^{-/-}$, CCL17$^{E/E}$ CCL22$^{-/-}$, and CCR4$^{-/-}$ mice were intraperitoneally injected with PBS (grey) or 0.5 µg IL-33 (white) every second day and analysed on day 8. iWAT and BAT were isolated and embedded in paraffin for histological staining. H&E (left) and Picrosirius red (middle) staining of iWAT. H&E staining of BAT (right). Sections from indicated genotypes. Images were prepared using confocal microscopy. iWAT: scale bar is 500 µm, 4x magnification. BAT: scale bar 200 µm, 20x magnification. Representative images are shown (n = 4-6, two independent experiments).

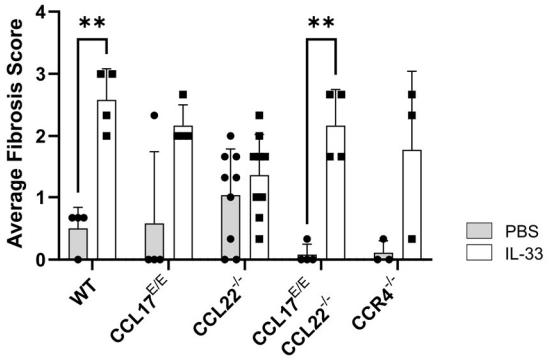

Figure 4.22: Scoring of iWAT Picrosirius red staining
Wt, CCL17$^{E/E}$, CCL22$^{-/-}$, CCL17$^{E/E}$ CCL22$^{-/-}$, and CCR4$^{-/-}$ mice were intraperitoneally injected with PBS (grey) or 0.5 µg IL-33 (white) every second day and analysed on day 8. iWAT and BAT were isolated and embedded in paraffin for histological staining. Images from Picrosirius red staining were blinded and distributed to collegues for scoring from 0-3 after Lassen *et al*. (Lassen *et al.*, 2017). Symbols represent the average score of each mouse. (n=4 images per group; from two independent experiments). Statistical significance was tested using two-way ANOVA with Tukey's test for multiple comparison. Data are presented as mean with SD.

4.9 IL-33 leads to immune cell infiltration within the adipose tissue

Administration of IL-33 resulted in a higher cell density of the brown adipocyte tissue (Figure 4.21). It was unclear, however, whether this observation was caused by infiltrating immune cells as a result of IL-33 treatment (Pastille *et al.*, 2019; Tran *et al.*, 2022) or a loss of lipid droplets within the brown adipocytes. Furthermore, IL-33 induced fibrosis in iWAT (Figure 4.21, Figure 4.22). The development of fibrosis can be influenced by numerous mechanisms, cell types, and mediators. The most prominent cell types in areas of fibrosis are fibroblasts and myofibroblasts, cells that are involved in wound healing and tissue repair (Murray, 2016). Interestingly, adipocytes can adopt a fibroblast-like phenotype and acquire fibrogenic features (Jones *et al.*, 2020), potentially promoting fibrosis in chronic HFD. To address the question, whether IL-33 causes immune cell infiltration into the AT, immunohistochemistry stainings were performed and sections of iWAT and BAT were stained for CD45^{+} cells.

In control mice, only a few or no $CD45^+$ cells could be detected in iWAT and BAT respectively (Figure 4.23, top). But after the IL-33 treatment, an influx of $CD45^+$ cells was visible, most strongly in the iWAT (Figure 4.23, bottom). Additionally, at higher magnification it was apparent that $CD45^+$ cells in iWAT primarily accumulated at sites of fibrosis (Figure 4.24A, B). In some cases, $CD45^+$ cells surrounded the white adipocytes (Figure 4.24C) and formed crown-like structures (Figure 4.24D). In BAT, $CD45^+$ cells were distributed throughout the brown adipocyte tissue (Figure 4.23, Figure 4.24E, F). Again $CCL22^{-/-}$ mice showed less immune cell infiltration compared to the other genotypes.

Overall, IL-33 induces immune cell infiltration into the iWAT and BAT. Nevertheless, the densification of brown adipocyte tissue was not solely explainable by infiltrating $CD45^+$ immune cells. Reduced lipid storage within the brown adipocytes might be an additional phenotypic change caused by IL-33.

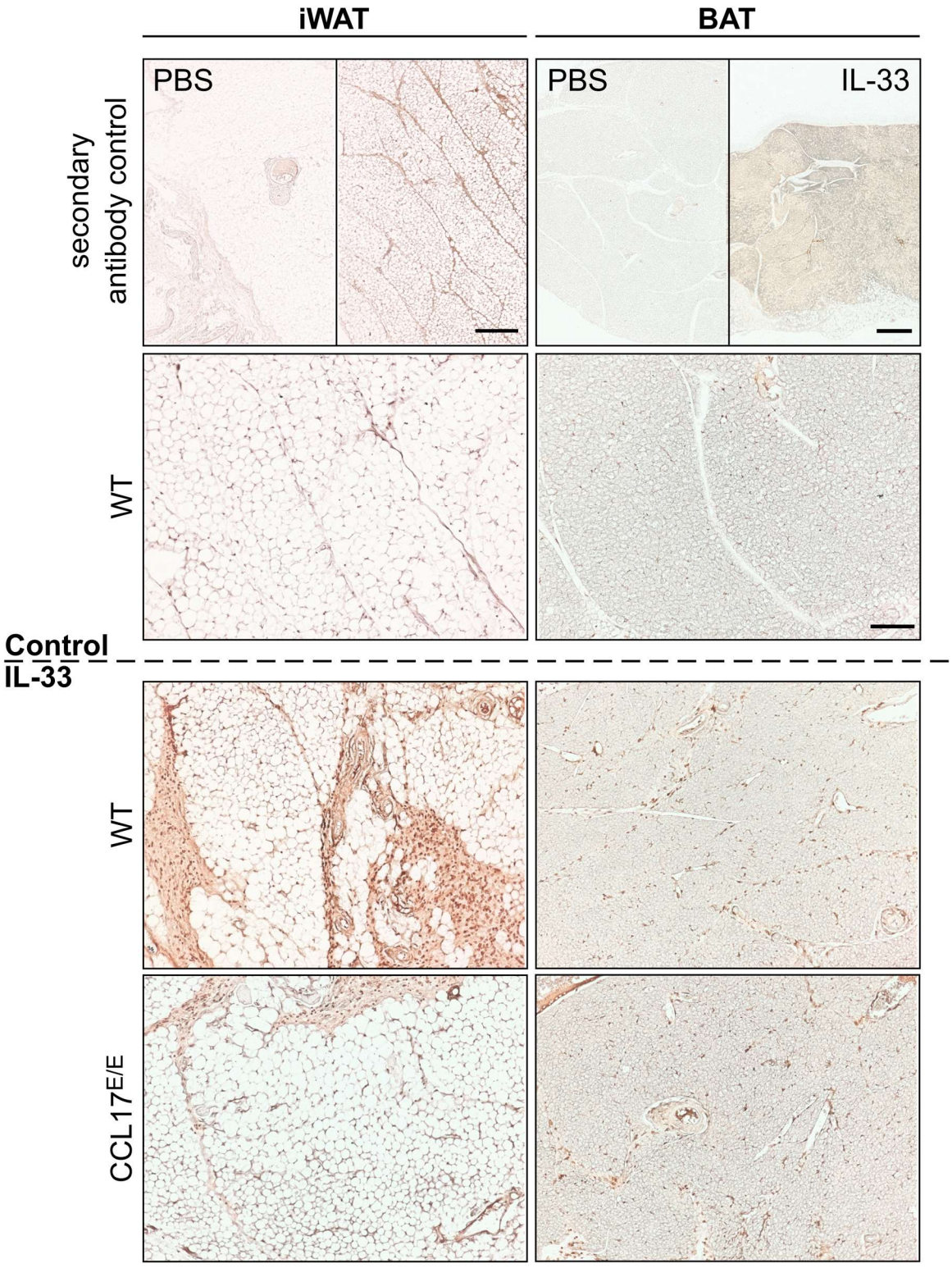
iWAT
BAT
PBS
PBS
IL-33
secondary antibody control
WT
Control
IL-33
WT
CCL17E/E

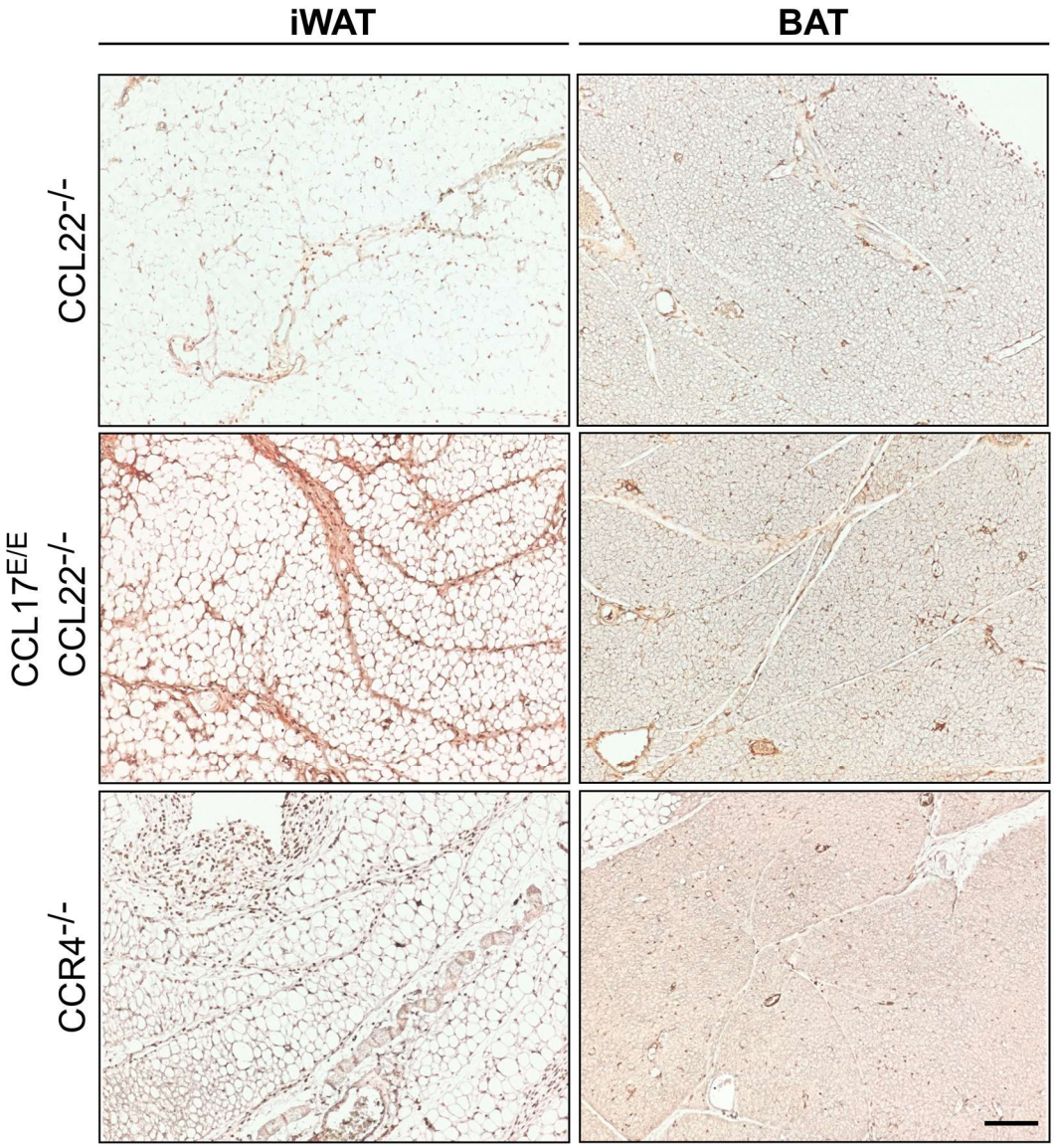

Figure 4.23: Immune cell infiltration in iWAT and BAT caused by IL-33 treatment

Wt, CCL17$^{E/E}$, CCL22$^{-/-}$, CCL17$^{E/E}$ CCL22$^{-/-}$, and CCR4$^{-/-}$ mice were intraperitoneally injected with PBS or 0.5 µg IL-33 every second day and analysed on day 8. iWAT and BAT were isolated and embedded in paraffin for further analysis. Immunohistochemistry staining of CD45^{+} immune cell of iWAT (left panel) and BAT (right panel) using rat-anti-mouse CD45 primary antibody, goat-anti-rat-IgG-HRP secondary antibody, and peroxidase substrate solution to visualise signal. Vertical sections from indicated genotypes and conditions. Images were prepared using confocal microscopy. Secondary antibody control: scale bar is 1000 µm, 4x magnification. Images of CD45^{+} cell staining: scale bar is 500 µm, 10x magnification. Representative images are shown. (n = 4-6, two independent experiments).

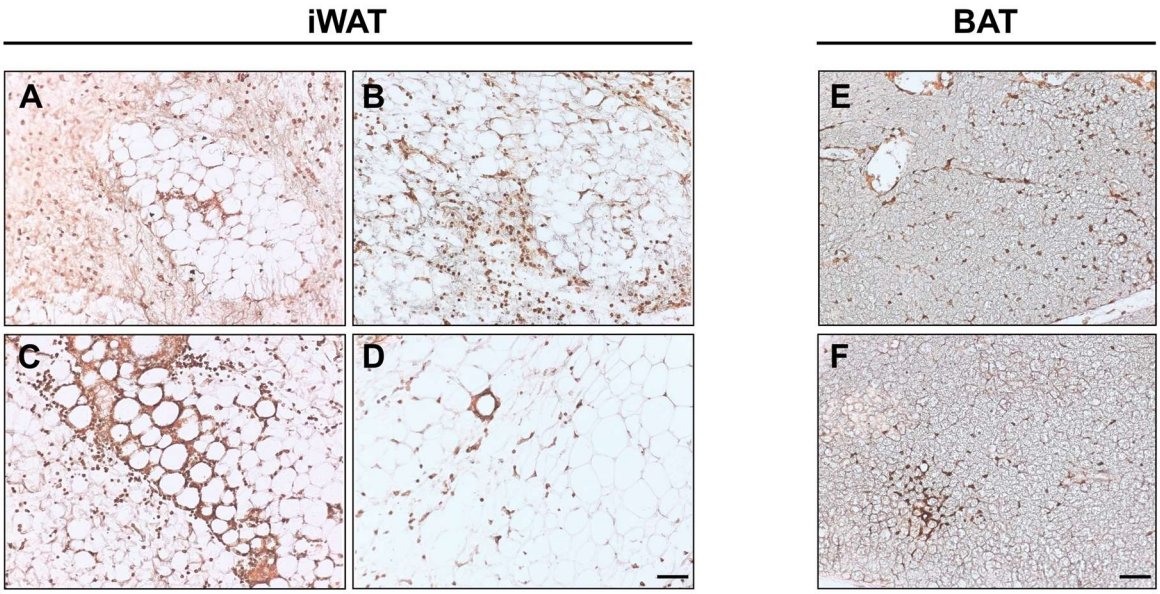

Figure 4.24: Immunhistochemistry staining of CD45+ cells in iWAT and BAT after IL-33 treatment

Wt, CCL17$^{E/E}$, CCL22$^{-/-}$, CCL17$^{E/E}$ CCL22$^{-/-}$, and CCR4$^{-/-}$ mice were intraperitoneally injected with PBS or 0.5 µg IL-33 every second day and analysed on day 8. iWAT and BAT were isolated and embedded in paraffin for further analysis. CD45^{+} cells in iWAT are found (A, B) at sites of fibrosis and (C, D) surrounding adipocytes, forming crown-like structures. (E, F) CD45+ cells are found throughout BAT. Sections from (A) CCL17$^{E/E}$ mice, (B) CCL17$^{E/E}$ CCL22$^{-/-}$ mice, (C) CCL22$^{-/-}$ mice, (D) CCR4$^{-/-}$ mice, and (E, F) wt mice after IL-33 treatment. Images were prepared using confocal microscopy. Scale bar 200 µm, 20x magnification. Representative images are shown. (n = 4-6, two independent experiments).

4.10 CCL17 is expressed in the inguinal white adipose tissue

In the absence of CCL22, mice are protected from IL-33-induced fibrosis in the iWAT, suggesting either a detrimental role of CCL22 or a beneficial role of CCL17. CCL17 might also be involved in adipocyte homeostasis in naïve mice. Therefore, transcription of the *Ccl17* gene locus in the iWAT and BAT was assessed using the $CCL17^{E/E}$ reporter line compared to wt mice. Adipose tissue sections from wt mice were used as negative control. Additionally, adipose tissues from $CCL17^{E/E}$ mice were also stained with the secondary antibody only (secondary antibody control), serving as a second negative control. Both controls were used to assess the specificity of the staining. EGFP signal was enhanced by staining against GFP. Furthermore, nuclei were stained to visualise the localisation of cells.

A CCL17-EGFP signal could only be detected in the iWAT where it was located off-site to the DAPI signal, suggesting that the EGFP protein was located in the cytoplasm as expected (Figure 4.25). In BAT, no specific CCL17-EGFP signal could be detected (Figure 4.26). The signal in the representative image shown for $CCL17^{E/E}$ mice was an uncommon occurrence and thereby considered as staining artefact.

These finding suggest that CCL17 could indeed be involved in signaling processes in the white adipocytes and in IL-33-mediated fibrosis. However, it remains unclear if CCL17 levels increase after IL-33 administration and if CCL22 is also expressed in the iWAT.

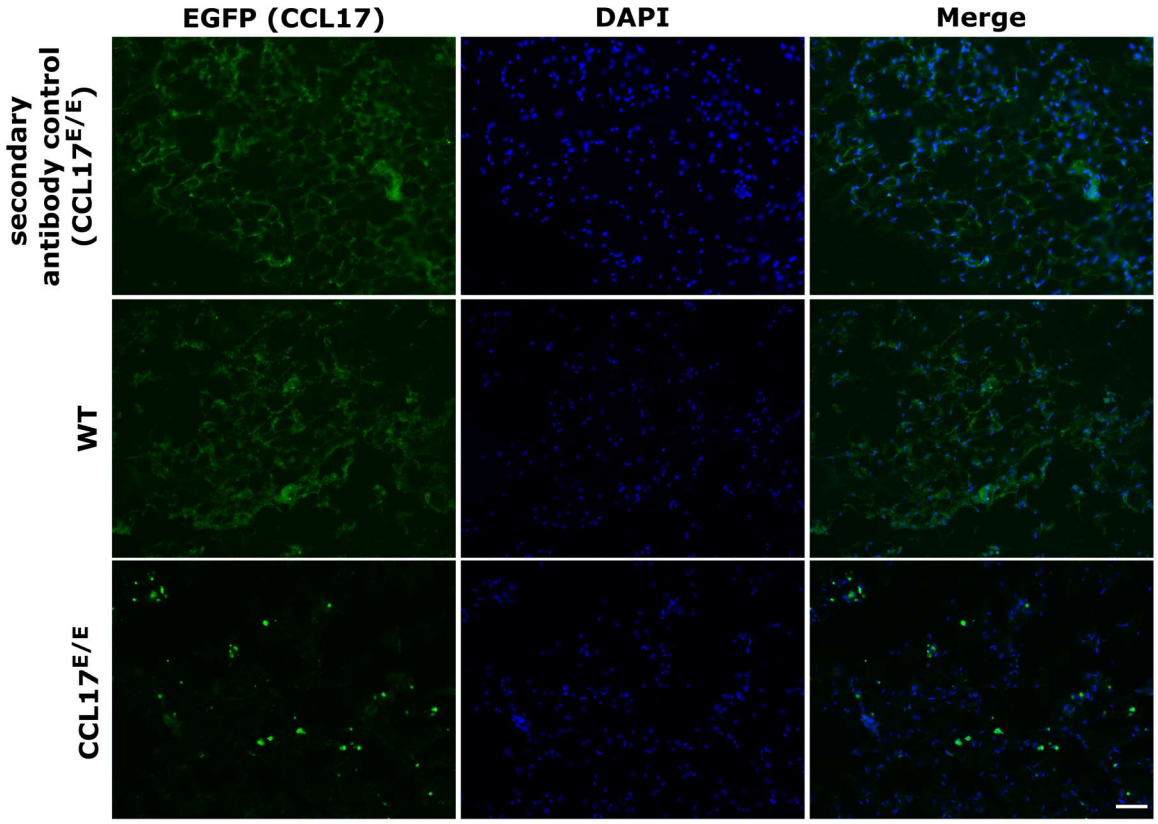

Figure 4.25: CCL17/EGFP reporter is expressed in the iWAT
iWAT sections from naïve wt and CCL17$^{E/E}$ mice were embedded in gelatin and stained for EGFP (green, left panel) and counterstained with DAPI (blue, middle panel). Secondary antibody control was performed on BAT slides from CCL17$^{E/E}$ mice. Images were prepared using confocal microscopy. Scale bar 200 µm, 20x magnification. Representative images are shown (n=2, two independent experiments).

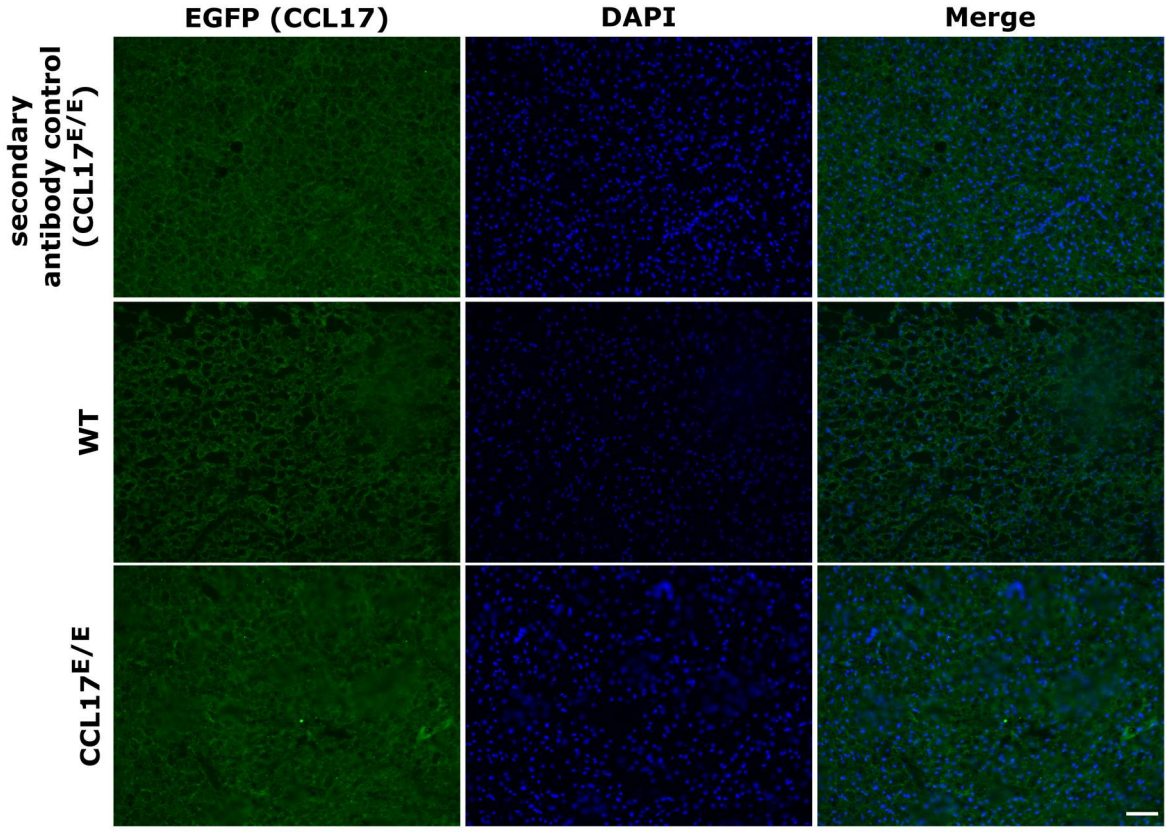

Figure 4.26: CCL17 is not expressed in the BAT
BAT sections from naïve wt and CCL17$^{E/E}$ mice were embedded in gelatin and stained for EGFP (green, left panel) and counterstained with DAPI (blue, middle panel). Secondary antibody control was performed on BAT slides from CCL17$^{E/E}$ mice. Images were prepared using confocal microscopy. Scale bar 200 µm, 20x magnification. Representative images are shown (n=2, two independent experiments).

4.11 Triacylglycerols are reduced upon IL-33 treatment in wt mice

In addition to weight loss, BAT morphology was influenced by IL-33 treatment with the BAT apparently becoming denser. As this cannot be explained by immune cell infiltration only, this increased density phenomenon was investigated to determine if IL-33 treatment leads to loss of lipids in the brown adipocytes. To assess if the storage of lipid droplets was impaired, BAT weight and lipid composition were measured and analysed.

BAT weight was significantly reduced in IL-33-treated wt mice compared to control mice (Figure 4.27A). In contrast, only slight tendencies of reduced BAT weight were visible in $CCL17^{E/E}$, $CCL17^{E/E}$ $CCL22^{-/-}$, and $CCR4^{-/-}$ mice. Furthermore, BAT weight in $CCL22^{-/-}$ and $CCR4^{-/-}$ mice was already significantly decreased compared to wt mice in control groups.

Next, lipids were extracted and lipidomics using MS was performed. In the following analysis, names of lipid species are replaced by abbreviations. The nomenclature used for fatty acids (FAs) indicates the number of C-atoms and double bonds, meaning a FA with 36 C-atoms and four double bonds will be noted as 36:4;Y. Additional triple bonds are indicated by the suffix ";Y" (Wunderling *et al.*, 2021).

The analysis showed that most lipid classes remained unaffected by IL-33 treatment (Figure 4.27B-N). Most notably, IL-33 injections lead to a significant decrease of triacylglycerides (TAGs) in wt mice but not in the other genotypes (Figure 4.27M). All tested genotypes displayed a variety of TAG species, although wt mice depicted the highest amount in each species (Figure 4.28, Figure 4.29). Administration of IL-33 decreased TAG species in wt mice, most notably 46:1;Y, 48:2;Y to 48:0;Y, 50:3;Y to 50:1;Y, 52:3;Y and 52:2;Y. Knockout mice also showed a decrease within the TAG species after IL-33 treatment. However, shifts were minor compared to wt mice.

Phosphatidylinositols (PIs) and phosphatidylserines (PS) were also reduced in wt mice upon IL-33 administration (Figure 4.27J,K). The shift in PI after IL-33 administration was due to changes in PI 34:1;Y which was decreased in wt and $CCR4^{-/-}$ mice and slightly in $CCL17^{E/E}$ mice (Figure 4.30). Wt mice showed more PS species compared to chemokine and chemokine receptor knockout mice even in the

control group (Figure 4.31). Upon IL-33 administration, PS species 38:2;Y, 40:2;Y, and 40:1;Y were lost and remaining species were decreased. Next to wt mice, $CCL17^{E/E}$ mice showed the second most PS species. 38:4;Y and 40:5,Y were lost in IL-33-treated mice but in contrast to wt mice, remaining PS species remained unaffected. $CCL17^{E/E}$ $CCL22^{-/-}$ and $CCR4^{-/-}$ mice showed the lowest numbers and amounts of different PS species. Only the PS species 36:1;Y was present in all genotypes and conditions.

Interestingly, diacylglycerol (DAG) was slightly increased in wt mice after IL-33 treatment, however, the variation was large (Figure 4.27). Wt mice in the IL-33-treated group showed the highest increase in DAG species 34:0;Y, 36:3;Y, 36:2;Y, and 36:0;Y (Figure 4.32). Minor increases were also visible in the other DAG species. 34:0;Y was also increased in $CCL17^{E/E}$ and $CCL22^{-/-}$ mice after IL-33 treatment, but remained unaffected in $CCL17^{E/E}$ $CCL22^{-/-}$ and $CCR4^{-/-}$ mice. Overall, DAG in knockout mice displayed only minor shifts or remained unaffected after IL-33 injections. The exception were $CCL17^{E/E}$ mice that also showed a strong increase in DAG species 36:3;Y and 36:2;Y compared to control mice.

Taken together, densification of brown adipocyte tissue (Figure 4.21) by IL-33 was likely caused by loss of lipids, especially the lipid classes TAG, PI, and PS. This was most apparent in wt mice which also showed the strongest densification of BAT and reduction in BAT weight. Lipid composition in chemokine and chemokine receptor knockout mice were already altered in PBS-treated control mice compared to wt control mice. This basal difference might explain the less severe outcome of IL-33 treatment in the different knockout genotypes.

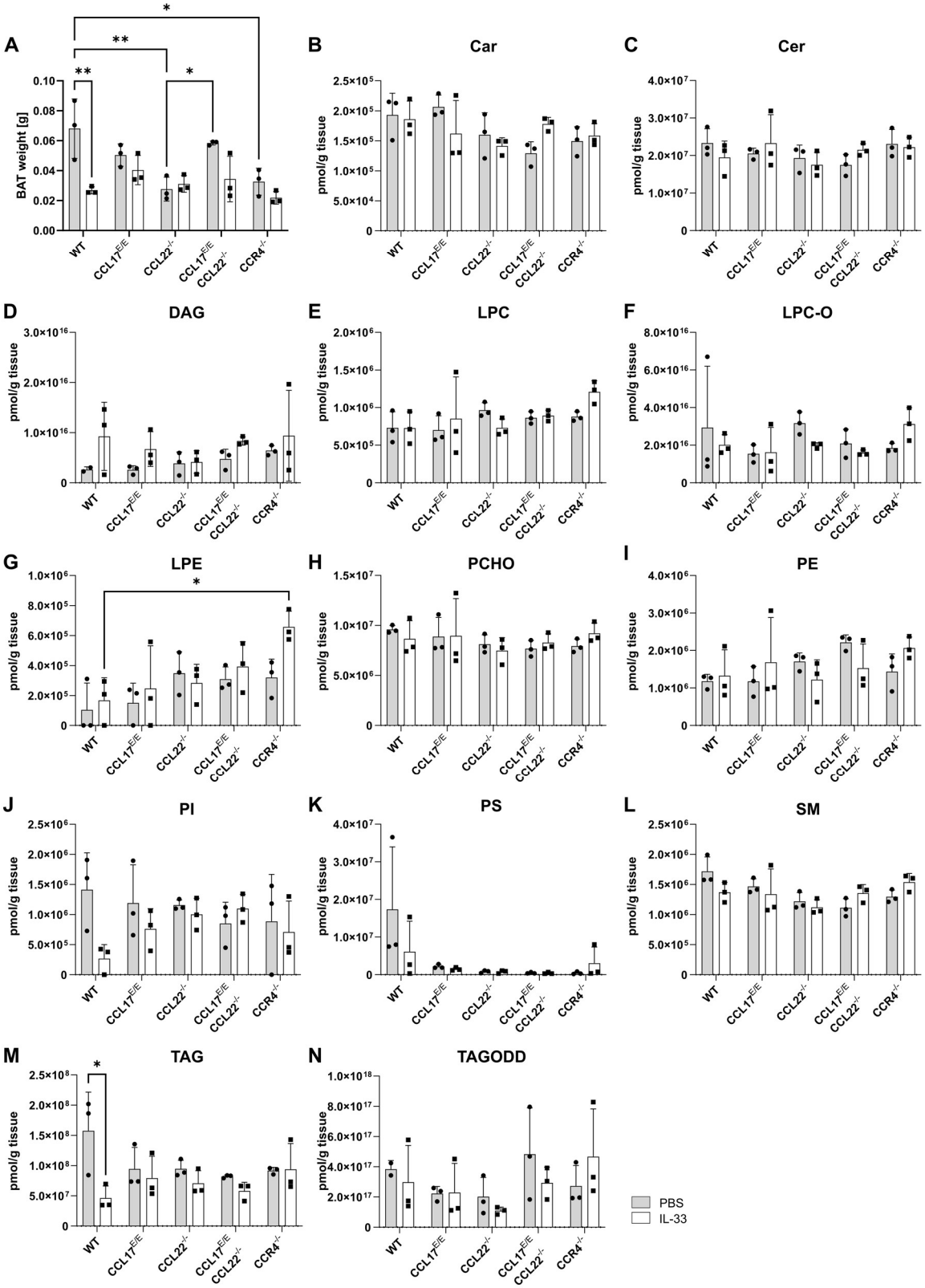
A
BAT weight [g]
B
Car
C
Cer
D
DAG
E
LPC
F
LPC-O
G
LPE
H
PCHO
I
PE
J
PI
K
PS
L
SM
M
TAG
N
TAGODD
pmol/g tissue
WT
CCL17E/E
CCL22-/-
CCL17E/E CCL22-/-
CCR4-/-
PBS
IL-33

Figure 4.27: IL-33 leads to reduction of lipid classes TAG, PI, and PS in wt mice
Wt, CCL17$^{E/E}$, CCL22$^{-/-}$, CCL17$^{E/E}$ CCL22$^{-/-}$, and CCR4$^{-/-}$ mice were intraperitoneally injected with PBS (grey) or 0.5 µg IL-33 (white) every second day and analysed on day 8. BAT was harvested. BAT weight was measured and lipidomics were performed. (A) BAT weight of control and IL-33-treated mice. (B-N) concentration of indicated lipid classes detected by MS. Symbols represent individual mice (n=3, one experiment). Statistical significance was tested using two-way ANOVA with Tukey's test for multiple comparison. Data are presented as mean with SD.

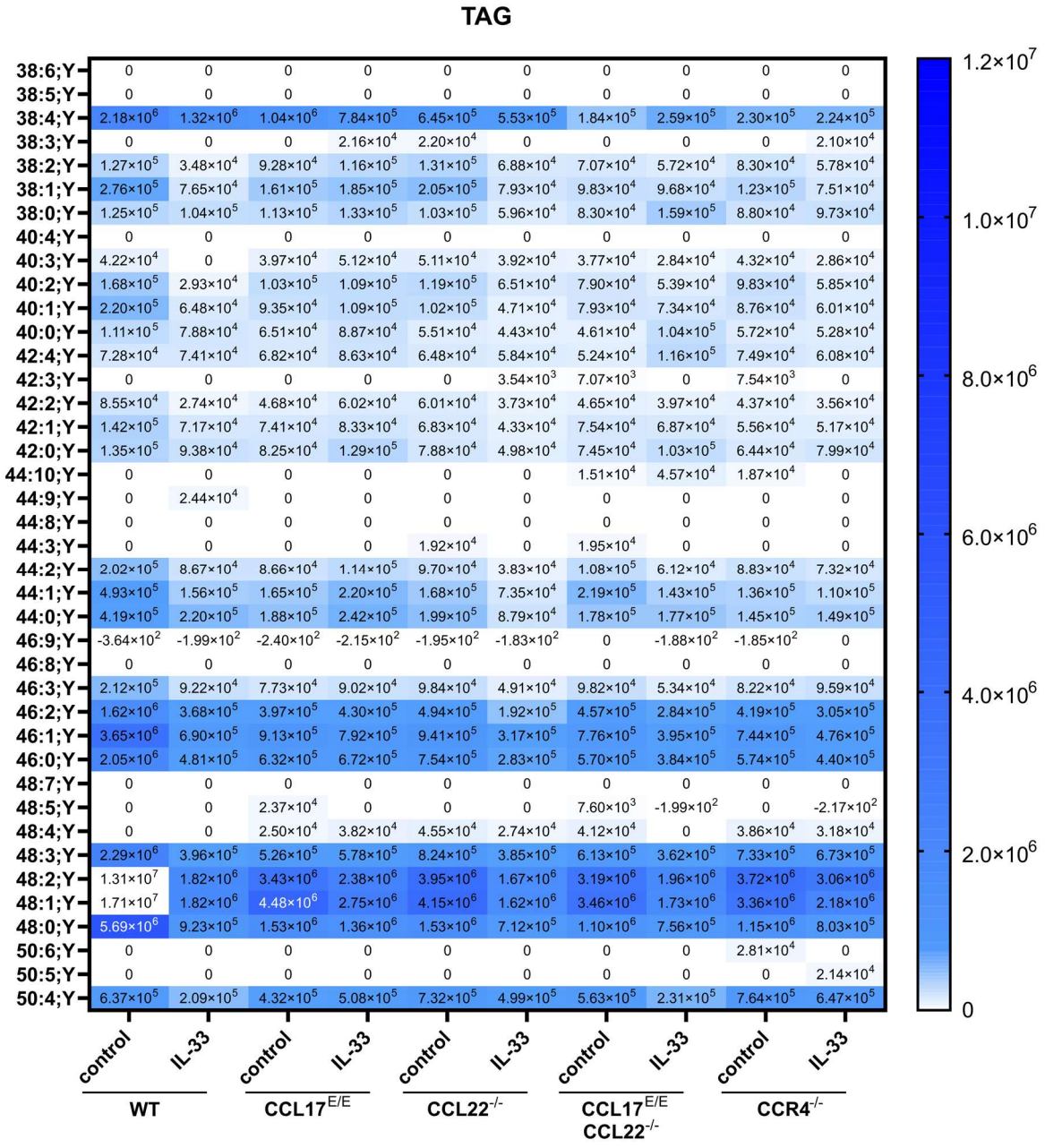

Figure 4.28: MS analysis of TAG species in BAT of PBS- and IL-33-treated mice

Wt, CCL17$^{E/E}$, CCL22$^{-/-}$, CCL17$^{E/E}$ CCL22$^{-/-}$, and CCR4$^{-/-}$ mice were intraperitoneally injected with PBS (grey) or 0.5 µg IL-33 (white) every second day and analysed on day 8. Lipids from the BAT were extracted. Absolute amounts of the lipid species are shown in pmol. The data represent the mean values of three individual mice (n=3).

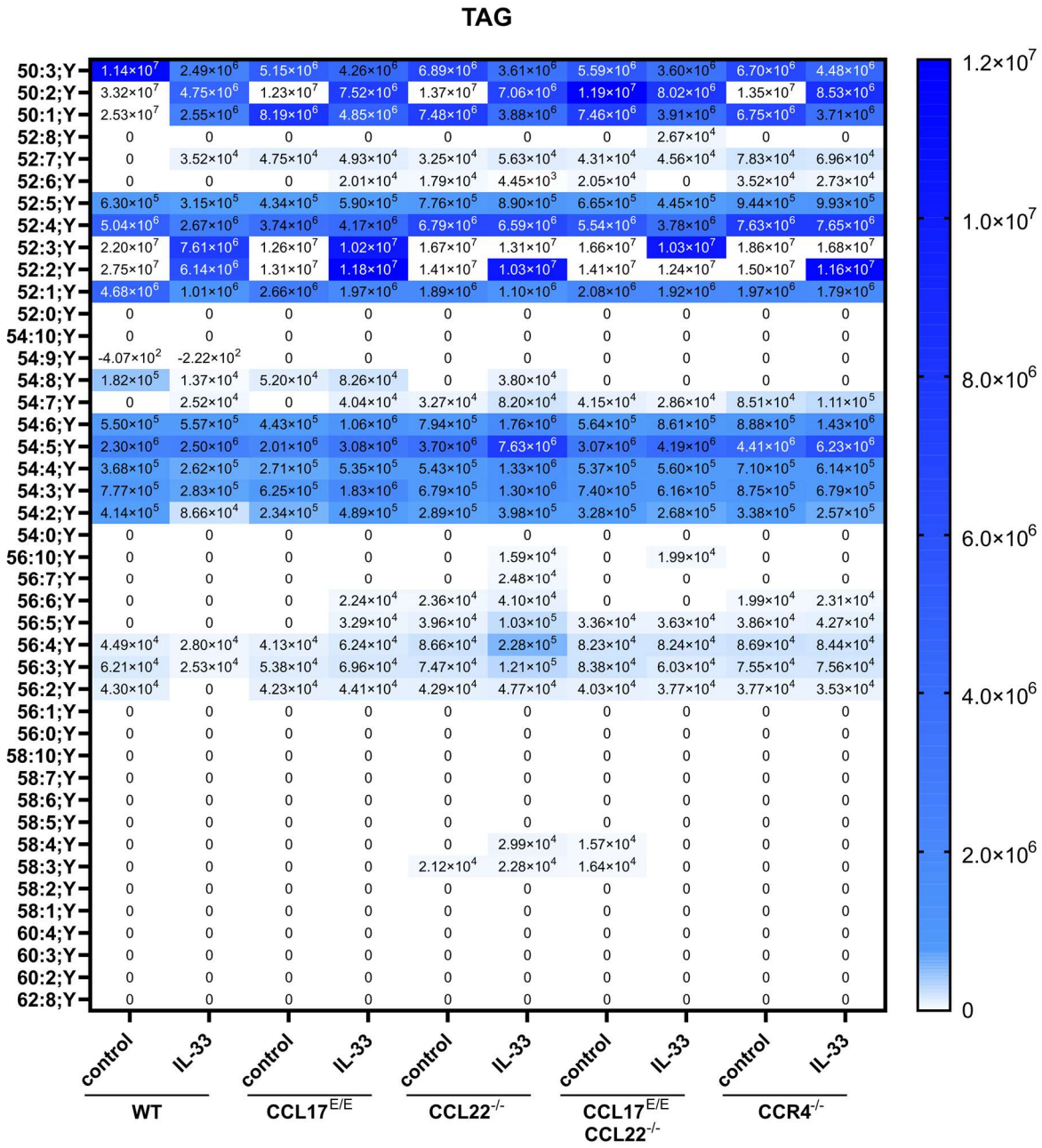

Figure 4.29: MS analysis of TAG species in BAT of PBS- and IL-33-treated mice

Wt, CCL17$^{E/E}$, CCL22$^{-/-}$, CCL17$^{E/E}$ CCL22$^{-/-}$, and CCR4$^{-/-}$ mice were intraperitoneally injected with PBS (grey) or 0.5 µg IL-33 (white) every second day and analysed on day 8. Lipids from the BAT were extracted. Absolute amounts of the lipid species are shown in pmol. The data represent the mean values of three individual mice (n=3).

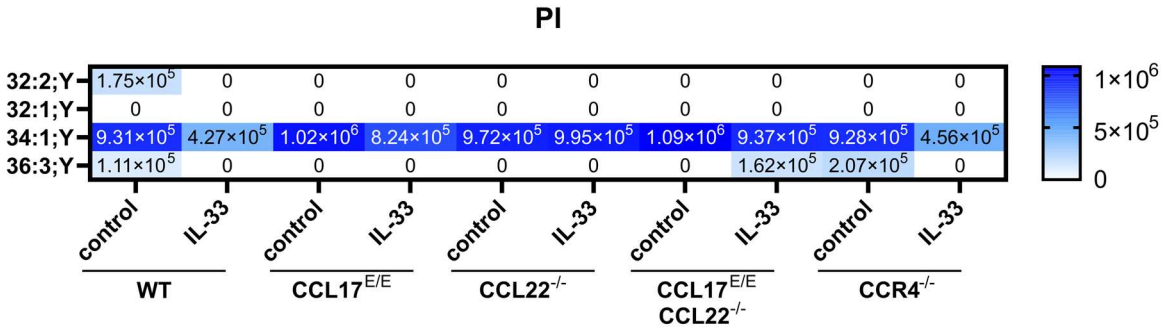

Figure 4.30: MS analysis of PI species in BAT of PBS- and IL-33-treated mice
Wt, CCL17$^{E/E}$, CCL22$^{-/-}$, CCL17$^{E/E}$ CCL22$^{-/-}$, and CCR4$^{-/-}$ mice were intraperitoneally injected with PBS (grey) or 0.5 µg IL-33 (white) every second day and analysed on day 8. Lipids from the BAT were extracted. Absolute amounts of the lipid species are shown in pmol. The data represent the mean values of three individual mice (n=3).

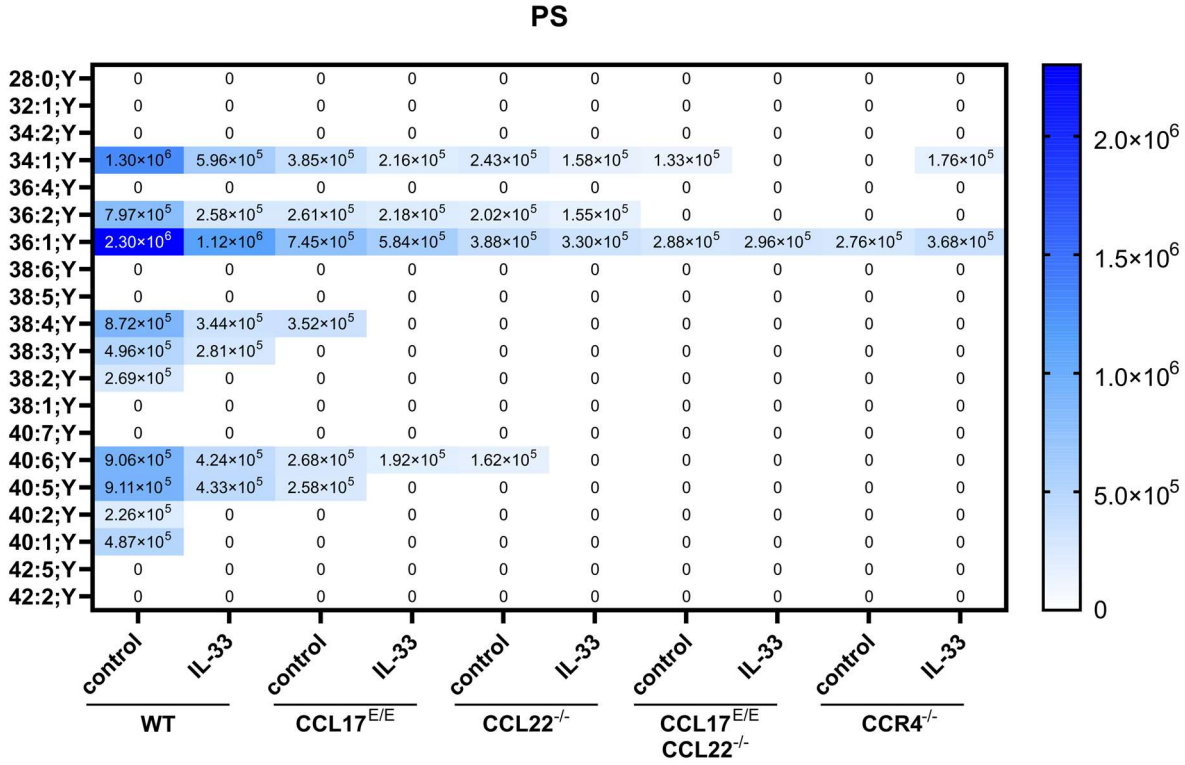

Figure 4.31: MS analysis of PS species in BAT of PBS- and IL-33-treated mice
Wt, CCL17$^{E/E}$, CCL22$^{-/-}$, CCL17$^{E/E}$ CCL22$^{-/-}$, and CCR4$^{-/-}$ mice were intraperitoneally injected with PBS (grey) or 0.5 µg IL-33 (white) every second day and analysed on day 8. Lipids from the BAT were extracted. Absolute amounts of the lipid species are shown in pmol. The data represent the mean values of three individual mice (n=3).

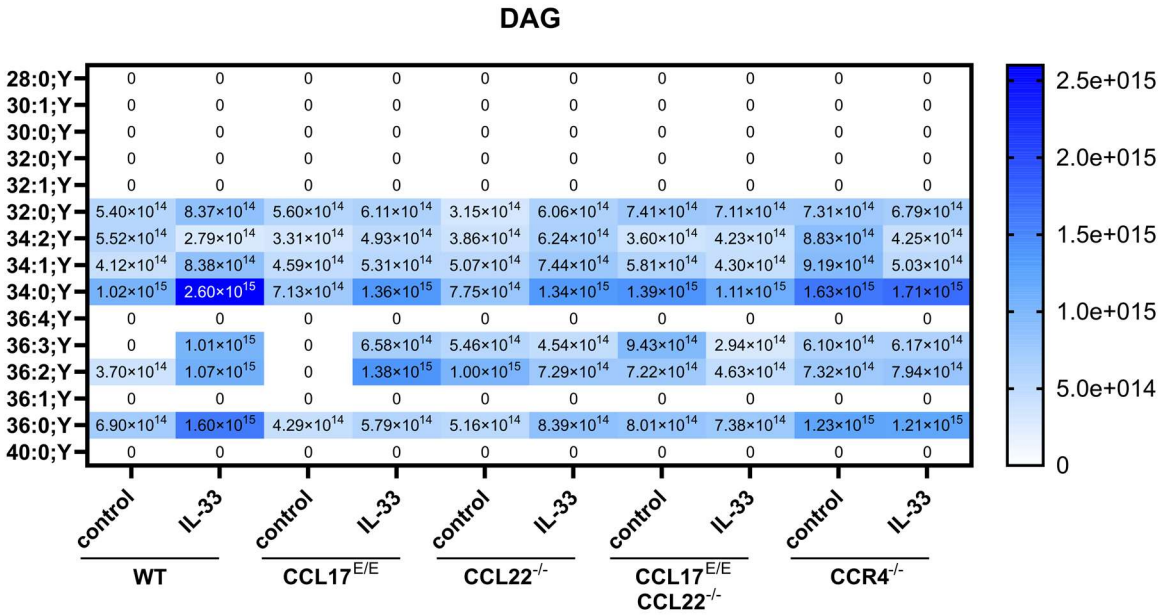

Figure 4.32: MS analysis of DAG species in BAT of PBS- and IL-33-treated mice
Wt, CCL17$^{E/E}$, CCL22$^{-/-}$, CCL17$^{E/E}$ CCL22$^{-/-}$, and CCR4$^{-/-}$ mice were intraperitoneally injected with PBS (grey) or 0.5 µg IL-33 (white) every second day and analysed on day 8. BAT was harvested and lipid composition was measured through MS. Values represent the mean of three individual mice (n=3).

4.12 Discussion

IL-33 is a pleiotropic cytokine and, as a mediator of both the innate and adaptive immune response, is involved in numerous biological processes including tissue homeostasis (Moussion *et al.*, 2008; Pichery *et al.*, 2012), tissue remodeling (Sanada *et al.*, 2007; Brunner *et al.*, 2011; Turnquist *et al.*, 2011), and type 2 immune responses (Yasuda *et al.*, 2012; Hardman *et al.*, 2013; Cayrol and Girard, 2014). IL-33 is constitutively expressed by non-haematopoietic cells, like epithelial and endothelial cells (Moussion *et al.*, 2008), although activated immune cells were shown to contribute to IL-33 levels during inflammation and infection (Hsu *et al.*, 2010; Chang *et al.*, 2011; Wills-Karp *et al.*, 2012; Hardman *et al.*, 2013; Tjota *et al.*, 2013; Tjota *et al.*, 2014; Tashiro *et al.*, 2016). IL-33 is considered an alarmin, which is expressed in the nucleus under steady state conditions but rapidly released upon tissue damage or inflammatory cues (Moussion *et al.*, 2008; Pichery *et al.*, 2012;

Garlanda *et al.*, 2013; Kaczmarek *et al.*, 2013; Molofsky *et al.*, 2015). So far, ST2 is the only receptor described for IL-33. The membrane-bound form induces a signaling cascade within the respective cell, while the soluble form functions primarily as a decoy receptor, removing free IL-33 from the extracellular environment (Yanagisawa *et al.*, 1993). Although IL-33 primarily affects cell populations associated with type 2 immune responses (Cayrol and Girard, 2014), the main targets of the cytokine are tissue-resident ILC2 and T_{reg} cells (Schmitz *et al.*, 2005; Moro *et al.*, 2010; Garlanda *et al.*, 2013; Mchedlidze *et al.*, 2013; Cayrol and Girard, 2014; Brestoff *et al.*, 2015). As one of the first signals in response to tissue injury, infection, and various other stimuli, it drives inflammation by activating immune cells and promoting their effector functions. In response to IL-33, DC, for example, produce the chemokines CCL17 and CCL22, which in turn initiate lymphocyte recruitment (Besnard *et al.*, 2011; Kurokawa *et al.*, 2013). With regard to CCL17 and CCL22, chemokine levels were shown to positively correlate with IL-33 expression in BALB/c mice treated with aeorosolised ovalbumin-treated or infected with Respiratory Syncytial Virus-A2 (Warren *et al.*, 2021).

In this thesis, new insights into IL-33 biology were provided by investigating the interaction between IL-33-mediated functions and the CCL17/CCL22/CCR4-axis in various tissues. In this process, a novel role of CCL17 and CCL22 was observed in mediating adipose tissue homeostasis and IL-33-induced adipose tissue fibrosis.

4.12.1 IL-33-induced an increase in KLRG1$^+$ T_{reg} cells in PP, mLN, and spleen

IL-33 was shown to be involved in the regulation of immune responses by targeting T_{reg} cells. Extensive studies have revealed the ability of IL-33 to enhance the protective effect of ST2$^+$ T_{reg} cells as well as stimulating their expansion and stabilising their FoxP3 expression via GATA3 (Schiering *et al.*, 2014; Vasanthakumar *et al.*, 2015; Matta and Turnquist, 2016). ST2 expression positively correlates with the activation status of T_{reg} cells (Vasanthakumar *et al.*, 2015; Siede *et al.*, 2016; Spath *et al.*, 2022). As shown by Vasanthakumar *et al.,* effector KLRG1$^+$ T_{reg} cells are mainly located outside the T cell zone as visualised by

immunofluorescence staining of the mLN. Therefore, effector KLRG1$^+$ T_{reg} cells are less dependent on IL-2, which is primarily provided by T cells, but gain responsiveness to IL-33 via ST2. IL-33 becomes a crucial factor for effector T_{reg} cell development, maintenance, and proliferation. Interestingly, while T_{reg} cells showed high ST2 expression in the VAT, the majority of T_{reg} cells in the small intestine, lamina propria, lymph nodes, and spleen showed no or low ST2 expression (Vasanthakumar *et al.*, 2015).

The present study confirmed a low frequency of ST2$^+$ KLRG1$^+$ T_{reg} cells in the PP and mLN (between 10-20 %) and slightly higher levels (20-35 %) in the spleen (Figure 4.2B). Nevertheless, IL-33 was able to expand the frequency of KLRG1$^+$ T_{reg} cells for all three organs (Figure 4.6A, B) consistent with previous reports in the literature (Brunner *et al.*, 2011; Vasanthakumar *et al.*, 2015; Gajardo *et al.*, 2015; Matta *et al.*, 2016).

Interestingly, in the PP, counts of KLRG1$^+$ T_{reg} cells were unaffected by IL-33 treatment and similar to the counts in PBS-treated mice, while counts of KLRG1$^+$ T_{reg} cells in the mLN and spleen were significantly and drastically increased after IL-33 treatment. It should be noted, however, that the counts of all CD45$^+$ cells and of all T cells were significantly reduced in the PP after IL-33 treatment (Figure 4.4). Therefore, the expansion of KLRG1$^+$ T_{reg} cells was still successful.

Although KLRG1$^+$ T_{reg} cell counts were increased in the mLN and spleen of IL-33-treated mice, the counts of overall FoxP3$^+$ T_{reg} cells were unaffected (Figure 4.5C). A possible explanation could be that the expansion is not due to actual proliferation but upregulation of KLRG1 within the FoxP3$^+$ T_{reg} cell compartment. An upregulation of KLRG1 would also be in line with the observed increase in KLRG1$^+$ T_{reg} cell frequency. A contributing factor to upregulation of KLRG1 instead of cell proliferation could also be the low levels of ST2$^+$ KLRG1$^+$ T_{reg} cells, providing fewer IL-33 responsive T_{reg} cells in comparison to previous studies in the VAT (Vasanthakumar *et al.*, 2015). In future studies, it should be addressed whether IL-33 induces proliferation or induces an effector state of T_{reg} cells by KLRG1$^+$ upregulation in the PP, mLN, and spleen.

The KLRG1$^+$ T_{reg} cells compartment seemed to be exclusively affected by IL-33 in comparison to the T cell subsets investigated. However, the increased frequency of overall CD4$^+$ T cells in the PP could also indicate an expansion of T_h2 cells. T_h2 cells express ST2 (Löhning *et al.*, 1998; Xu *et al.*, 1998) and according to the literature, the ST2 receptor expression is highly GATA3-dependent. It was shown that the *in vitro* administration of IL-33 activates and stimulates cytokine production in T_h2 cells (Schmitz *et al.*, 2005). However, an expansion of T_h2 cells by IL-33 has not been described.

Administration of IL-33 leads to a reduction of overall CD45$^+$ immune cells in the PP. As an alarmin, IL-33 induces a variety of biological processes including the activation of non-haematopoietic and haematopoietic cells, which subsequently perform effector functions such as cytokine or chemokine production (Molofsky *et al.*, 2015; Griesenauer and Paczesny, 2017). Chemokines are chemoattractants inducing the recruitment of immune cells (Sells and Hwang, 2010). It is therefore possible that the immune cells from the PP are migrating to other organs, probably the mLN as both organs are connected through lymphatic vessels (Mason *et al.*, 2008). The finding that overall immune cells in the mLN were increased supports this hypothesis. Furthermore, this increase in immune cell numbers cannot simply be explained by the expansion of KLRG1$^+$ T_{reg} cells because i) it is most likely that the expansion is only due to IL-33-induced upregulation of KLRG1 and ii) cell counts of overall CD45$^+$ immune cells in the spleen where not increased although similar KLRG1$^+$ T_{reg} cell frequency and count trends were visible.

The IL-33-mediated increase of KLRG1$^+$ T_{reg} cells was independent of CCL17, CCL22, and CCR4. While some differences between the genotypes were visible such as a lower increase of KLRG1$^+$ T_{reg} cell counts in IL-33-treated CCL22$^{-/-}$ mice compared to the other IL-33-treated mice, the overall trends were similar and differences were mainly caused by outliers.

4.12.2 IL-33 impairs erythropoiesis in the BM and drives accumulation of erythroid progenitors in the spleen

Recent studies have observed an involvement of IL-33 in the life cycle of erythrocytes. For example, IL-33 is critical for the development of iron-recycling red pulp macrophages, which are important for the elimination of senescent erythrocytes because phagocytosis of those cells frees the ferrous haemoglobin required for transporting oxygen from the lung to the tissue (Lu *et al.*, 2020). Iron-recycling red pulp macrophages are therefore important regulators of iron metabolism (Lu *et al.*, 2020). Interestingly, red blood cells themselves express IL-33 (Wei *et al.*, 2015; Lu *et al.*, 2020), thereby promoting the development of iron-recycling red pulp macrophages. Additionally, erythroid progenitors express high levels of ST2, especially after lineage commitment, suggesting a role for IL-33 in erythropoiesis (Swann *et al.*, 2020).

The data obtained within this thesis confirmed the effect of IL-33 on erythropoiesis in the BM and erythroid progenitors in the spleen. Administration of IL-33 significantly decreased counts of erythroid progenitors in the BM, starting from pre CFU-E (including MEP and B-CFU-E) but excluding orthochromatic erythroblasts and reticulocytes (Figure 4.15C, D; Figure 4.16). This suggests a suppressive effect of IL-33 on erythropoiesis in the BM. Indeed, IL-33 was observed to directly inhibit terminal erythroid differentiation (Swann *et al.*, 2020). *In vitro* cultures of CFU-E in proerythroid medium, containing erythropoietin and other stem cell factors, for four days revealed that CFU-E retained their morphology when cultured with IL-33, indicating that their differentiation is halted. Additionally, administration of IL-33 to CFU-E cultures significantly reduces Ter119^{+} cell frequency, also indicative of the absence of a maturation process. Similar to the model used in this thesis, IL-33 injections over 1 week decreased the absolute count of erythroid progenitors in the BM of SKG mice (Swann *et al.*, 2020). Taken together, IL-33 shows an inhibiting effect on erythropoiesis.

Interestingly, orthochromatic erythroblasts and reticulocytes in the BM were unaffected or only slightly affected by IL-33 treatment. These cell types might be

unresponsive to IL-33. Though PreCFU-E and CFU-E show high ST2 levels, expression decreases with maturation (Swann *et al.*, 2020). It could be possible that, although differentiation from PreCFU-E to polychromatic erythroblast is directly inhibited by IL-33 via ST2 signaling, differentiation from polychromatic to orthochromatic erythroblasts is unaffected and continues even in the presence of IL-33. Until existing pools of polychromatic erythroblast are depleted, normal orthochromatic erythroblast levels and subsequent reticulocytes could be maintained. This hypothesis is supported by the findings by Swann *et al.* showing that prolonged IL-33 administration over 4 weeks reduced $Ter119^{+}$ erythroid cell frequency in the BM (Swann *et al.*, 2020). It is possible that a similar observation could be made if the IL-33 treatment model used in this thesis was extended to 4 weeks.

When BM erythropoiesis is impaired, erythropoiesis can also occur in the spleen (Millot *et al.*, 2010; Greenwald *et al.*, 2019; Jing *et al.*, 2021). Additionally, while inflammation can suppress BM erythropoiesis, it can also promote extramedullary erythropoiesis. For example, *Salmonella* infection can induce extramedullary erythropoiesis through the upregulation of erythropoietin (Jackson *et al.*, 2010). In the presented study, counts of CFU-E, ProEry, and basophilic erythroblasts were increased in the spleen after IL-33 treatment (Figure 4.13, Figure 4.14). As counts of basophilic erythroblasts were unaffected in the blood of IL-33-treated mice (Figure 4.15A, B), accumulation of this cell population was not due to retainment from the blood but rather extramedullary erythropoiesis. Interestingly, however, Swann *et al*. observed that the frequencies of splenic erythroid progenitors were unaffected by either short or prolonged exposure to IL-33 (Swann *et al.*, 2020). This is partially contradicting the presented data as counts of CFU-E, ProEry, and basophilic erythroblast were increased after IL-33 treatment. An increase of CFU-E, ProEry, and basophilic erythroblast counts was most strongly observed in knockout mice, especially in the absence of CCL22 (basophilic erythroblasts). This suggests an involvement of the chemokines, CCL17 and CCL22, and their receptor in the regulation of IL-33-induced extramedullary haematopoiesis. T_{reg} cells could likely be

involved in regulating extramedullary haematopoiesis as they are also involved in the regulation of stress erythropoiesis, which is induced by impairment of BM erythropoiesis and anemic stress (Fraser *et al.*, 2018). Fraser *et al*. showed that stress erythropoiesis is associated with anti- and pro-inflammatory signals. Indeed, pro-inflammatory factors secreted in response to *Citrobacter rodentium* infection simultaneously inhibited BM erythropoiesis and induced stress erythropoiesis. Factors like BMP4 and GDF15 regulate stress erythropoiesis and induce T_{reg} cell development, implicating a role for T_{reg} cells in the regulation of stress erythropoiesis (Fraser *et al.*, 2018). Additionally, CCL22, in contrast to CCL17, is associated with T_{reg} cell recruitment (Santulli-Marotto *et al.*, 2015; Mohamed *et al.*, 2016; Ketcham *et al.*, 2018); in the absence of CCL22, it is possible that T_{reg} cells do not migrate into the spleen and therefore cannot suppress or regulate extramedullary haematopoisis. This hypothesis is supported by the observation that the number of KLRG1$^+$ T_{reg} cells in the spleen is reduced in IL-33-treated mice (Figure 4.6). However, the number of KLRG1$^+$ T_{reg} cells was comparable between IL-33-treated CCL17$^{E/E}$ CCL22$^{-/-}$ mice and IL-33-treated wt mice. Since IL-33 treatment led to a slight but visible increase of basophilic erythroblasts in wt mice, together these data suggest that T_{reg} cells are not the only regulator of extramedullary haematopoisis. Additionally, counts of CFU-E and ProEry were similarly increased between the IL-33-treated knockout mice. As early stages of erythroid progenitors still express high levels of ST2, IL-33 might directly promote their differentiation, counteracting the regulatory function of T_{reg} cells and additional cell types. However, in this case, IL-33 would induce counteracting functions by directly inhibiting BM erythropoiesis but promoting splenic extramedullary erythropoiesis. On the other hand, extramedullary erythropoiesis might be delayed in time, which would explain why only the earliest erythroid progenitors were affected. In line, while *Plasmodium berghei* infection induced granulocyte-macrophage progenitors in the BM within the first week, these progenitors were not expanded in the spleen until the end of the second week of infection (Mungyer *et al.*, 1983), highlighting the different kinetics between BM and spleen. Possible differences in kinetics are also supported by the fact that

extramedullary erythropoiesis is often induced after the BM is impaired or inhibited (Millot *et al.*, 2010; Jackson *et al.*, 2010; Chou *et al.*, 2012; Greenwald *et al.*, 2019; Jing *et al.*, 2021).

Overall, the present study showed that IL-33 treatment inhibits BM erythropoiesis, independent of CCL17, CCL22, and CCR4 expression. IL-33-induced extramedullary erythropoiesis, however, was partially increased. In the absence of the chemokines or CCR4, the counts of CFU-E and ProEry were further increased, while CCL22-deficiency drove enhanced expansion of basophilic erythroblasts, possibly due to impaired migration of T_{reg} cells contributing to the regulation of extramedullary erythropoiesis.

4.12.3 IL-33-induced eosinophilia might contribute to splenomegaly

Eosinophils, together with neutrophils and basophils, are classified as granulocytes due to the presence of granules in the cytoplasm (Fettrelet *et al.*, 2021). During steady state, eosinophils are primarily circulating in the bloodstream but can also reside in various organs including the lung, thymus, adipose tissue, spleen, and the lamina propria after engagement with chemokines, such as CCL5, CCL11, and CCL24 (Kato *et al.*, 1998; Wen and Rothenberg, 2017; Jacobs *et al.*, 2021). Eosinophils mediate immune responses through both cell-cell-contact and cytokine secretion, and are involved in T cell recruitment (Jacobsen *et al.*, 2008), T_h2 polarisation (Spencer *et al.*, 2009; Wen and Rothenberg, 2017), and antigen presentation (Pozo *et al.*, 1992; Padigel *et al.*, 2007; Garro *et al.*, 2011). Mice lacking eosinophils exhibited reduced recruitment of effector T cells (Jacobsen *et al.*, 2008). Activation of eosinophils triggers degranulation of pre-formed and stored cytotoxic mediators, thus facilitating a much faster response to pro-inflammatory signals than other cell populations (McBrien and Menzies-Gow, 2017). Eosinophils are involved in a variety of infectious, autoimmune, and allergic diseases (Fettrelet *et al.*, 2021). Coincidentally, immune cells linked to allergy, including eosinophils, express ST2 in high levels on their cell surface (Kitaura *et al.*, 1996), indicating responsiveness to IL-33.

The present study demonstrated that administration of IL-33 induced eosinophilia in the BM and blood (Figure 4.18D, E; Figure 4.19J, K), which was probably due to enhanced lineage commitment towards eosinophils instead of a generalised increase in haematopoiesis as the counts of HSC and GMP were not increased. Indeed, IL-33 was shown to contribute to eosinophil development. IL-33 administration caused eosinophil progenitor expansion in the BM (Johnston *et al.*, 2016). Moreover, the cytokine also modulates IL-5Rα expression, increasing surface levels on eosinophil progenitors and thereby enhancing IL-5 responsiveness as well as eosinophil lineage commitment. Overexpression of IL-5 revealed increased eosinophil counts in BM, blood, and tissues, indicating an essential role of the cytokine in eosinophil development (Lee *et al.*, 1997). Consistent with IL-33-induced eosinophilia, ST2-deficiency reduced eosinophil numbers in NJ.1638 mice (Johnston *et al.*, 2016).

Upon completion of haematopoiesis, eosinophils leave the BM and enter the bloodstream, circulating in the blood, before entering target tissues such as the lung, adipose tissue, spleen, and the lamina propria (Davoine and Lacy, 2014; Wen and Rothenberg, 2017). In essence, the increased eosinophil number in the BM subsequently caused eosinophilia in the blood. Interestingly, IL-33 treatment significantly increased eosinophil counts in CCL17- and/or CCL22- as well as CCR4-knockout mice, whereas the treatment did not affect eosinophil count in wt mice. Eosinophils enter the tissue when recruited through chemokines such as CCL11 and CCL24. The data in the present study indicates that the chemokines CCL17 and CCL22 as well as their receptor may be involved in tissue recruitment of eosinophils, indicating that the absence of CCL17, CCL22, or CCR4 retains eosinophils in the bloodstream. To date, the role of either chemokine in the recruitment of eosinophils has not been well established, and CCR4 is only moderately expressed in circulating eosinophils (Liu *et al.*, 2003; Zlotnik *et al.*, 2006; Yi *et al.*, 2018). However, in mice challenged with OVA aerosol, lung CCL17 and CCL22, expressed by cDC1, are required for eosinophil recruitment into the lung as inhibition of each chemokine via neutralising antibodies nullified eosinophil migration (Yi *et al.*, 2018). Taken together,

the present study also suggests a role for the CCL17/CCL22/CCR4-axis in the recruitment of IL-33-induced eosinophils into peripheral tissues. Which tissue, however, remains to be investigated. IL-33 itself does not induce eosinophil migration. While allergen-challenged wt mice showed significantly reduced numbers of eosinophils in the lung when they received ST2-deficient eosinophils through adoptive transfer, the loss of eosinophils was not due to impaired migration but rather impaired survival. The induction of GM-CSF by IL-33 promotes the expression of the anti-apoptotic protein Bcl-xL in eosinophils through an autocrine feedback loop (Holmes *et al.*, 2015).

It is possible that eosinophilia contributes to the observed IL-33-induced splenomegaly (Figure 4.8). While PreCFU-E, ProEry, and basophilic erythroblast counts were increased, as shown in this study, it is unlikely that they are the sole cause of the increased spleen size, because IL-33-induced splenomegaly was independent of the genotype but expansion of basophilic erythroblasts, for example, was strongly impacted by the absence of CCL22, showing increased numbers compared to wt, $CCL17^{E/E}$, and $CCR4^{-/-}$ mice. It is possible that the recruitment of circulating ILC2 or invariant NKT cells might also contribute to splenomegaly. Treatment of wt mice with IL-33 was shown to induce accumulations of $KLRG1^{+}$ ILC2 in the spleen, blood, and liver (Guillerey *et al.*, 2021). Furthermore, egress of ILC2 from the BM is induced by IL-33 (Stier *et al.*, 2018) and might contribute to accumulation of these cells in the spleen. ILC2 emigration from the BM could explain the overall reduction of lymphocytes in the BM after IL-33 treatment (Figure 4.19F, G), which was observed in the present study. Similarly to the increase of ILC2, IL-33 administration over seven days doubled invariant NKT cell counts in the spleen and liver (Bourgeois *et al.*, 2009)

Based on the present data, extramedullary haematopoises, in contrast, appears not to be involved in splenomegaly as progenitor cells (HSC, MPP, GMP, Pre MegE, and MkP) and counts of differentiated myeloid cells and B cells were unaffected by IL-33 treatment in all genotypes (Figure 4.14).

Taken together, IL-33 induced eosinophilia in the BM and subsequently enrichment of eosinophils in the blood. While eosinophilia in the BM was independent of CCL17, CCL22, and CCR4, the CCL17/CCL22/CCR4-axis appears to be important for eosinophil recruitment into the tissue as eosinphilia in the blood was only observed in the chemokine- or chemokine receptor-knockout mice but not wt mice, indicating retainment of the cells within the bloodstream. Eosinophils might contribute to splenomegaly but the participation of ILC2 and invariant NKT cells cannot be excluded as causes of increased spleen size. Further studies should be performed to clearly identify the contributing cell populations.

4.12.4 CCL17 and CCL22 have distinct roles in IL-33-dependent adipose tissue homeostasis, thermogenesis, and iWAT fibrosis

The adipose tissue regulates adipogenesis, adipokine secretion, and energy expenditure (Lee *et al.*, 2013). While these functions are mainly mediated by mature adipocytes, the adipose tissue holds numerous other cell types including adipocyte progenitor cells, endothelial cells, fibroblasts, and immune cells (Lee *et al.*, 2013; Garritson and Boudina, 2021). The WAT, divided into subcutaneous and visceral depots, is widely distributed throughout the organism (Kwok *et al.*, 2016) and serves to maintain energy homeostasis by storing excess lipids during positive energy balance and releasing them as energy source during an energy demand (Chudek and Więcek, 2006; Fiorenza *et al.*, 2011; Kwok *et al.*, 2016; El Hadi *et al.*, 2019). In contrast, the BAT is primarily found in rodents although BAT depots have also been found in human infants (Kwok *et al.*, 2016). It is involved in energy expenditure and heat production, which is largely dependent on UCP-1 (Kwok *et al.*, 2016). While the BAT is linked to weight loss and leanness based on its high metabolic activity, WAT lipid storage and expansion are rather associated with various health disorders, most importantly obesity (Griffin and Abbott, 2022). Additionally, the WAT can give rise to beige adipose tissue that adopts typical BAT-like features such as the expression of UCP-1, and contributes to thermogenesis (Harms and Seale, 2013; Kwok *et al.*, 2016).

Several studies have highlighted the essential role of IL-33 in lipid metabolism, especially in the context of obesity (Ashley M. Miller *et al.*, 2010; Brestoff *et al.*, 2015; Han *et al.*, 2015; Lee *et al.*, 2015). Overall, IL-33 and its receptor show protective function in obesity by reducing adiposity as well as regulating glucose and insulin tolerance. Adipose tissue homeostasis is maintained or restored by IL-33 through the activation of ILC2, M2 macrophage polarisation, and $ST2^+$ T_{reg} cell expansion (Weisberg *et al.*, 2003; Kurowska-Stolarska *et al.*, 2008; Kurowska-Stolarska *et al.*, 2009; Chawla *et al.*, 2011; Molofsky *et al.*, 2013).

The present study showed that administration of IL-33 caused immune cell infiltration and tissue fibrosis in the iWAT in all tested genotypes, except in $CCL22^{-/-}$ mice (Figure 4.21-Figure 4.24), indicating tissue damage and an uncontrolled and excessive ECM deposition.

Causes of tissue damage are diverse, ranging from infection and allergic responses to chemical or mechanical tissue injury (Wynn, 2008; Huang *et al.*, 2020). During wound healing, various immune cells are recruited into the tissue by cytokine and chemokine gradients, executing effector functions and secreting additional cytokines/chemokines to further recruit immune cells and support myofibroblast development. Myofibroblasts migrate into the wound, secrete collagen, and promote wound contraction, leading to wound closure (Wynn, 2008; Murray, 2016). IL-33 shows a dual function in the context of wound healing and tissue repair. While the cytokine is essential for the tissue repair process by promoting type 2 $ST2^+$ cells and conversion of macrophages from an inflammatory to a non-inflammatory state (Sandler *et al.*, 2003; Lee *et al.*, 2016; Kotsiou *et al.*, 2018; Dwyer *et al.*, 2022), it has often been observed to exacerbate tissue fibrosis like hepatic or pulmonary fibrosis (Marvie *et al.*, 2010; Mchedlidze *et al.*, 2013; Li *et al.*, 2014; Tan *et al.*, 2018).

IL-33 is constitutively expressed by various non-haematopoietic cell types including adipocytes. Indeed, pre-adipocytes and adipocytes produced ST2L and IL-33 *in vitro* (Wood *et al.*, 2009). Administration of exogenous IL-33 increases the steady state levels of IL-33 and may therefore promote inflammatory signals. Such inflammatory signals lead to the recruitment of immune cells like mast cells and IL-33 itself can

directly promote the production of IL-6, IL-13, and possibly TNFα by mast cells (Iikura *et al.*, 2007; Ho *et al.*, 2007). In turn, TNFα was shown to increase the expression of IL-33 by pre- and mature adipocytes *in vitro* (Wood *et al.*, 2009), which reveals an autocrine feedback loop increasing IL-33 levels in the adipose tissue. Moreover, mast cells might secrete serine proteases which can increase the bioactivity of IL-33 by cleaving the cytokine (Lefrançais *et al.*, 2012; Lefrançais and Cayrol, 2012; Lefrançais *et al.*, 2014). Therefore, the damaging effect of IL-33 on iWAT structure might not only be caused by increased levels but also a higher bioreactivity of the cytokine.

The initial trigger for the excessive iWAT fibrosis might be adipocyte cell death. Immunohistological stainings revealed the formation of crown-like structures (Figure 4.24C, D) which are known to be formed by macrophages surrounding apoptotic adipocytes where they take up the lipid droplets from the dying adipocytes (Cinti *et al.*, 2005; Cancello *et al.*, 2006; Giordano *et al.*, 2013; Haase *et al.*, 2014; Hill *et al.*, 2018). Additionally, areas of crown-like structures were observed to correlate with a disrupted basal membrane (Cinti *et al.*, 2005), paving the way for additional lymphocyte recruitment. Adipocyte cell death is positively linked with increased CCL2 levels (Strissel *et al.*, 2007), suggesting that dying adipocytes themselves release the chemokine and thereby recruit monocytes, which differentiate into macrophages within the tissue. Indeed, the absence of CCL2 or CCR2, the receptor for CCL2, reduced macrophage infiltration in the adipose tissue (Marcelin *et al.*, 2022).

Most of the immune infiltration after IL-33 treatment was observed at the sites of fibrosis within the collagen depositions. Which cell types were involved, however, remains to be investigated. For example, pro-inflammatory factors secreted by M1 macrophages, forming the crown-like structures around adipocytes, are responsible for in the recruitment of neutrophils (Nagareddy *et al.*, 2014; Bijnen *et al.*, 2018). Although M2 macrophages might also be involved in the formation of crown-like structures, it is thought that these structures are primarily comprised of M1 macrophages due to the pro-inflammatory environment (Springer *et al.*, 2019).

Infiltrating neutrophils can elicit a variety of functions. Neutrophils are producers of extracellular proteases like elastase and cathepsin G. Both proteases are known to cleave and increase the bioactivity of IL-33 (Lefrançais and Cayrol, 2012; Lefrançais et al., 2012; Lefrançais et al., 2014), which possibly drives the detrimental effects of IL-33 on iWAT fibrosis. Moreover, neutrophils induce macrophage recruitment (Elgazar-Carmon *et al.*, 2008) and cause IL-1β production by interaction with adipocytes together with macrophages (Watanabe *et al.*, 2019), further promoting immune cell infiltration into the iWAT. Additionally, circulating eosinophils likely contribute to the observed immune cell infiltration as IL-33 treatment caused eosinophilia in the BM and blood of CCL17 and/or CCL22- as well as CCR4-deficient mice. The fact that eosinophilia was not seen in IL-33-treated wt mice indicates that circulating eosinophil numbers were reduced due to the recruitment of eosinophils into the tissue (Figure 4.18D, E). Indeed, an accumulation of eosinophils was observed in the adipose tissue of IL-33-treated mice (Molofsky *et al.*, 2013; Lee *et al.*, 2015). This accumulation, however, was highly dependent on ILC2, which were also increased in the adipose tissue after IL-33 treatment, as a deficiency in ILC2 or ILC2-secreted IL-5 impaired IL-33-mediated eosinophilia (Molofsky *et al.*, 2013; Lee *et al.*, 2015; Wen and Rothenberg, 2017). However, eosinophils regulate the polarisation of alternatively activated M2 macrophages (Wu *et al.*, 2011) which together with T_{reg} cells, T_h2 cells, and ILC2 promote tissue repair and homeostasis (Odegaard *et al.*, 2008; Ricardo-Gonzalez *et al.*, 2010; Mathis, 2013; Rao *et al.*, 2014). Overall, a variety of immune cells might contribute to the observed immune cell infiltration and specific contributions need to be analysed to gain insight if IL-33-induced fibrosis is caused by an increasingly inflammatory environment due to the recruitment of neutrophils, mast cells, and M1 macrophages; or increased presence of tissue repair-mediating immune cells (M2 macrophages, T_{reg} cells, T_h2 cells, and ILC2) driving excessive ECM deposition; or a combination of both pathways.

Interestingly, IL-33-mediated fibrosis in iWAT was ameliorated in the absence of CCL22 (Figure 4.21). It should be noted, however, that iWAT morphology was already altered in the respective control mice, suggesting a role of CCL22 in adipose

tissue homeostasis. The absence of CCL17, however, did not change iWAT morphology and appears to be less important for tissue homeostasis, although the expression of CCL17 in the iWAT could be confirmed in the present study using $CCL17^{E/E}$ reporter mice (Figure 4.25). CCL22 shows dominance over CCL17 regarding receptor-binding affinity, receptor internalisation, and desensitisation (Viney *et al.*, 2014; Santulli-Marotto *et al.*, 2015). Thus, CCL22 induces desensitisation and internalisation of CCR4 more rapidly than CCL17 (Imai *et al.*, 1998; Mariani *et al.*, 2004a). In addition, both chemokines induce calcium flux and desensitise the cells to a second identical stimulus. In heterologous desensitisation, however, CCL22 desensitised CCR4 for a second CCL17 stimulus, whereas a second CCL22 stimulus, following a primary CCL17 stimulus, still induced calcium flux (Viney *et al.*, 2014). Furthermore, CCR4 can be expressed in two different conformations. While the major receptor population binds both chemokines, the second minor population is only activated by CCL22 (Viney *et al.*, 2014). In conclusion, biased agonism of both chemokines and the dominant role of CCL22 might explain the observed stronger impact of CCL22 on adipose tissue homeostasis. The cellular source for CCL17 and CCL22 in the iWAT could be M2 macrophages as they are known producers of these chemokines (Alferink *et al.*, 2003; Mantovani *et al.*, 2004; Orecchioni *et al.*, 2019; Erazo *et al.*, 2021). In addition, other cell types such as adipocytes themselves, may also be considered. CCL22 is especially associated with T_{reg} cells, which are crucial for maintaining adipose tissue homeostasis and mediating tissue repair (Shao *et al.*, 2021). In the absence of CCL22, tissue damage-induced repair mechanisms might be less tightly regulated in naïve mice due to impaired T_{reg} cell recruitment, leading to more excessive inflammatory responses and subsequently, the fibrotic-phenotype in the iWAT of PBS-treated CCL22-deficient mice observed in the present study. A dominant role of CCL22 in adipose tissue homeostasis was further supported by the morphologic changes and the reduced tissue weight of the BAT (Figure 4.21, Figure 4.27A). As CCL17 expression could not be detected in the BAT of naïve mice (Figure 4.26), an involvement of CCL17 in BAT homeostasis is unlikely. CCL22 and CCR4 were

shown to be expressed in the anterior hypothalamus/preoptic area, an area where pyrogens stimulate warm sensitive neurons, thereby affecting thermogenesis in the BAT as well as other thermogenically responsive tissues. Administration of CCL22 into the preoptic area induced PGE2 expression, which is a known pyrogen (Conti *et al.*, 2004), resulting in increased core temperature of C57BL/6 mice by increasing BAT activation and simultaneously decreasing respiratory exchange ratio (Osborn *et al.*, 2011). The findings of Osborn and colleagues support the involvement of CCL22 in controlling BAT activation. Whether this effect is regulated solely extrinsically or also intrinsically within the adipose tissue remains to be investigated. The dominance of CCL22 over CCL17 might also explain the differences in IL-33-induced iWAT fibrosis in the chemokine-deficient knockout mice. In $CCL17^{E/E}$ mice, iWAT fibrosis was observed after IL-33 treatment, whereas $CCL22^{-/-}$ mice showed no additional fibrosis through IL-33 treatment. Interestingly, CCL17 was described to drive peritoneal fibrosis by stimulating collagen production of submesothelial fibroblasts. Inhibition of CCL17 by neutralising antibodies improved the phenotype and reduced peritoneal fibrosis (Chen *et al.*, 2020). Similarly, inhibition of CCL17 decreased pulmonary fibrosis in bleomycin-treated mice (Belperio *et al.*, 2004). In contrast, the present study rather suggests a beneficial role of CCL17, protecting the iWAT in the absence of CCL22, and a detrimental role of CCL22, driving fibrosis in the absence of CCL17. In line, CCL22 levels were observed to be elevated in patients with idiopathic pulmonary fibrosis (Inoue *et al.*, 2004; Yogo *et al.*, 2009).

Due to the dominance of CCL22 over CCL17, however, the protective function of CCL17 is second and overshadowed by CCL22 as evidenced by the development of iWAT fibrosis in wt mice after IL-33 treatment. For future experiments, it would be interesting to know which cell type or types are mediating the detrimental effect of CCL22 regarding IL-33-induced iWAT fibrosis.

Several studies linked IL-33 to thermogenesis in the adipose tissue. Administration of IL-33 led to increased caloric expenditure (Brestoff *et al.*, 2015). Indeed, IL-33- or ST2-deficient mice gain weight and develop adiposity more rapidly than wt control mice. Moreover, in *in vitro* experiments using murine stromal vascular fraction cells,

IL-33 treatement reduced fat accumulation and adipogenic gene expression important for cell differentiation (Ashley M. Miller *et al.*, 2010; Brestoff *et al.*, 2015). The cytokine promotes white adipocytes browning by inducing ILC2-dependent upregulation of UCP-1. Deficiency in ILC2 abolishes browning in response to IL-33 treatment as ILC2-secreted IL-13 and IL-4 are crucial for the acquisition of a brown phenotype by pre-adipocytes (Lee *et al.*, 2015). Lack of IL-33 results in reduced UCP-1 expression and reduced numbers of beige adipocytes in the WAT (Brestoff *et al.*, 2015). While browning was only moderately observed in the present study, it should be noted that the investigation of WAT was limited to one fat depot, namely the iWAT. Subcutaneous depots, however, are manifold (Bagchi and MacDougald, 2019). To get a broader insight, additional fat depots should be analysed.

Among other things, increased energy expenditure after IL-33 treatment is due to browning and the presence of M2 macrophages, promoting lipolysis and thermogenic gene expression in WAT and BAT. The current study supports an IL-33-induced energy expenditure due to the observed weight loss. This could be due to increased browning of fat depots and subsequent increase of thermogenesis but further investigation is required. Additionally, immune cell infiltration in the BAT could promote lipolysis, explaining the reduction of TAG within the BAT (Figure 4.28M, Figure 4.29) and the observed densification of the brown adipocytes. Moreover, BAT weight was also decreased in wt mice after IL-33 treatment, supporting increased lipolysis. As the reduction of BAT weight and of TAG levels was only observed in IL-33-treated wt mice, the primary reason for weight loss might not be intrinsic to BAT but rather thermogenesis by IL-33-induced beige adipose tissue. Nevertheless, the data presented here support the role of CCL17 and CCL22 in the regulation of BAT functions as (i) BAT weight was already decreased in untreated knockout mice, (ii) IL-33 treatment did not reduce BAT weight any further, and (iii) lipid composition was only mildly affected by IL-33 treatment.

Overall the present study showed for the first time that the CCL17/CCL22/CCR4-axis is involved in adipose tissue homeostasis, indirectly and/or directly, and IL-33-promoted iWAT fibrosis with a dominant role of CCL22 over CCL17.

4.12.5 Differences between CCL17$^{E/E}$ CCL22$^{-/-}$ and CCR4$^{-/-}$ mice indicate a missing link in the CCL17/CCL22/CCR4-axis

The chemokine-chemokine-receptor network shows high complexity. So far, approximately 50 members of the chemokine family have been described (Griffith *et al.*, 2014). All chemokines signal through one or more of the 20 chemokine receptors (Viney *et al.*, 2014; Griffith *et al.*, 2014). Due to the disproportionate ratio of chemokines to chemokine receptors, chemokine receptors are promiscuous in their ligand interaction, meaning that one receptor can recognise many different chemokines and *vice versa* (Nibbs and Graham, 2013).

Interestingly, in the present study, CCR4$^{-/-}$ mice showed no significant weight loss after IL-33 treatment. It remains unclear, however, if the mice show full protection from weight loss or if the weight loss is only delayed. Nevertheless, this observation is significantly different from the behaviour phenotype of CCL17$^{E/E}$ CCL22$^{-/-}$ double knockout mice. One might expect that both knockouts should essentially be the same have a similar phenotype as CCR4 is the only described receptor for both chemokines so far, although CCR8 is discussed as a second receptor for CCL17 in humans (Panina-Bordignon *et al.*, 2001; Yoshie and Matsushima, 2015). However, subtle differences between CCL17$^{E/E}$ CCL22$^{-/-}$ and CCR4$^{-/-}$ mice could be observed throughout the IL-33 treatment. Next to the weight loss, IL-33-treated CCR4$^{-/-}$ mice showed higher KLRG1^{+} T_{reg} cell counts compared to IL-33-treated CCL17$^{E/E}$ CCL22$^{-/-}$ mice, although naïve levels were comparable, and administration of IL-33 increased the frequency of RORγt^{+} T_{reg} cells in CCL17$^{E/E}$ CCL22$^{-/-}$ mice but decreased it in CCR4$^{-/-}$ mice. Additionally, basophilic erythroblasts were significantly increased in CCL17$^{E/E}$ CCL22$^{-/-}$ mice but not in CCR4$^{-/-}$ mice after IL-33 treatment and cell counts of basophilic, polychromatic, and orthochromatic erythroblasts/ reticulocytes were significantly lower in CCR4$^{-/-}$ mice compared to CCL17$^{E/E}$ CCL22$^{-/-}$ mice in the blood of the IL-33-treated cohort. Together these findings indicate the existence of an additional player in the CCL17/CC22/CCR4-axis, either a second receptor for CCL17 and/or CCL22, or a third ligand for CCR4. Supporting the third player hypothesis, in a DNFB-induced CHS, comparing wt, CCL17$^{E/E}$,

$CCL17^{E/E}$ $CCL22^{-/-}$, and $CCR4^{-/-}$ mice, $CCR4^{-/-}$ mice showed greater ear swelling indicative of an exaggerated immune response, whereas $CCL17^{E/E}$ $CCL22^{-/-}$ mice were protected from CHS (Fülle, 2018).

The overall differences between $CCL17^{E/E}$ $CCL22^{-/-}$ and $CCR4^{-/-}$ mice indicate a missing link in the signaling pathway of CCL17, CCL22, and CCR4 – either a second receptor mediating signaling to the chemokines or a third ligand for CCR4.

Chapter 5: Identification of CCR4$^{-/-}$ primary cell populations binding to CCL17 and/or CCL22

Whereas CCL17$^{E/E}$ CCL22$^{-/-}$ and CCR4$^{-/-}$ mice did show similar survival after STM challenge, distinct differences after IL-33 treatment, regarding weight loss, KLRG1^{+} T_{reg} counts, and expansion of basophilic erythroblasts in the spleen, were visible between the two genotypes. Taken together with the previously mentioned CHS assay where CCR4$^{-/-}$ mice showed an exaggerated immune response, whereas CCL17$^{E/E}$ CCL22$^{-/-}$ mice were protected, this suggests the involvement of a second receptor for CCL17 and/or CCL22, mediating signals in the absence of CCR4, or alternatively the existence of a third ligand for CCR4.

Hence, this part of the thesis focuses on determining whether CCL17 and CCL22 are able to bind to the cell surface of primary T cells in the absence of CCR4. Such binding would support the theory of a yet undescribed second receptor that could potentially substitute or add to the functions of CCR4.

5.1 Establishing a chemokine-based receptor staining

Flow cytometry is a powerful technique for analysis of multiple cell populations within a cellular mixture based on cell-specific light scattering and fluorescent characteristics (McKinnon, 2018). Therefore, extracellular and intracellular markers are stained by fluorophore-coupled antigen-specific antibodies. In case of chemokine receptors this presents some limitations. Commercial availability of antibodies against chemokine receptors is sparse (Le Brocq *et al.*, 2014; Anselmo *et al.*, 2014), especially for atypical chemokine receptors, and often suffers from low sensitivity and specificity. As chemokine receptors also show posttranslational modifications, usage of monoclonal antibodies that are restricted to a specific epitope is limited (Anselmo *et al.*, 2014). An alternative approach is the use of fluorescently-labeled chemokines for staining. Chemokines show high specificity and sensitivity towards their receptors regardless of any posttranslational modification of the receptor (Le Brocq *et al.*, 2014; Anselmo *et al.*, 2014).

Furthermore, they are often conserved between species and can therefore be used for the analysis across multiple species (Ford *et al.*, 2013).
This part of the project aims to implement a staining approach for cell cultures and primary cells using the chemokines CCL17 and CCL22.

5.1.1 Staining with a Chemokine-Streptavidin-Tetramer

Although CCL17 and CCL22 both bind to CCR4, they induce different downstream signaling cascades (Lin *et al.*, 2018). Additionally, after binding of CCL22, CCR4 is rapidly internalised. CCL17, however, only partially leads to internalisation of CCR4 and only at much higher concentrations in comparison to CCL22 (Mariani *et al.*, 2004b; Ajram *et al.*, 2014). To exclude that biotinylated CCL22 is internalised prior to the addition of fluorophore-streptavidin, both biotinylated chemokine and fluorophore-streptavidin were pre-assembled according to a published protocol (Ford *et al.*, 2013) and prioir to the surface staining with antibodies (see 2.2.2.5.1.2). $CD4^+$ T cells were gated as described above (Figure 3.2) and incubated with either the CCL17- or CCL22-streptavidin-tetramer for 1 h at 37 °C or 4 °C. To assess specificity, a fluorophore-streptavidin control was included. For further purposes, the fluorophore-streptavidin control will be abbreviated as SA for streptavidin and the coupled fluorophore, meaning BV421-coupled streptavidin will be shortened to SABV while PE-coupled streptavidin will be designated as SAPE.
Unfortunately, the mean fluorescence intensity (MFI) of cells stained with bCCL17-tetramer was not different between samples stained at 37 °C or 4 °C and samples that were only stained with the respective streptavidin control (Figure 5.1A). The same could be observed for the staining with the bCCL22-tetramer (Figure 5.1B).

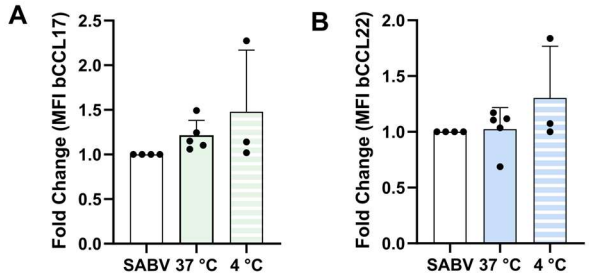

Figure 5.1: Fluorophore-streptavidin control shows high background staining
Thymus from naïve wt mice was harvested and stained with the respective fluorophore-streptavidin or the preformed chemokine-streptavidin-tetramer at 37 °C or 4 °C. MFI was analysed for (A) bCCL17 or (B) bCCL22. Symbols represent individual mice (n=3-4, pooled from three independent experiments). Statistical significance was tested using one-way ANOVA with Dunnett's test for multiple comparison. Data are presented as mean with SD.

This interference was observed for multiple tested cell lines. First, the T cell lymphoma cell line BW5147.3 was tested as the main target cell type for CCL17 and CCL22 *in vivo* are T cell subsets. The cell line was gated based on its FSC and SSC properties, doublet cells were excluded, alive CD44-expressing cells were selected and investigated for their tetramer-binding capacity (Figure 5.2A). BW5147.3 cells expressed the CCR4 receptor (Figure 5.2B) and should be able to bind to CCL17 and CCL22. However, MFI of the tetramer was as high as the SABV control (Figure 5.2C).

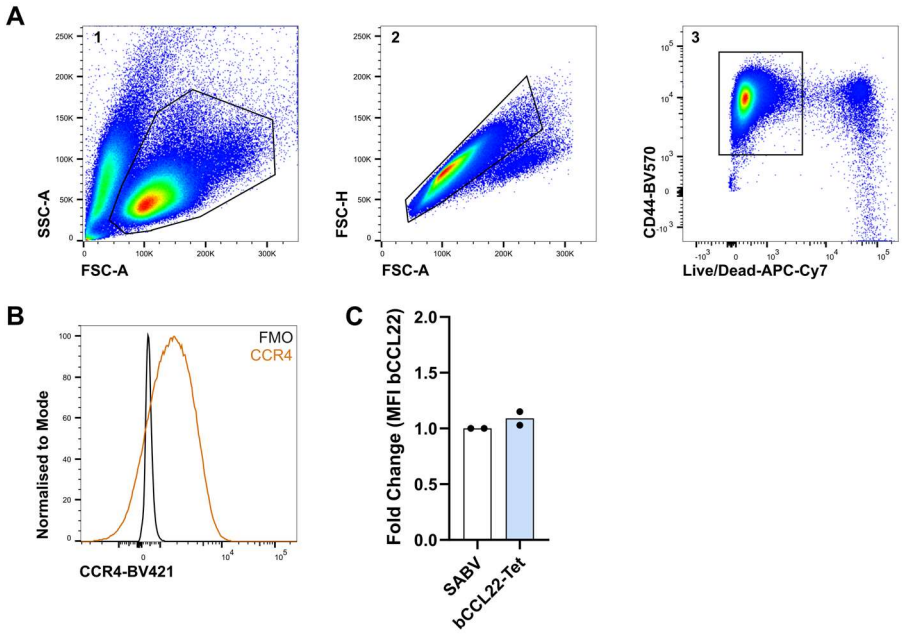

Figure 5.2: Fluorophore-streptavidin control shows high background staining in BW5147.3 T cell lymphoma cells
The T cell lymphoma cell line BW5147.3 was harvested and stained. (A) Gating strategy for BW5147.3 cells. Cells were selected for their FSC and SSC properties (A1). Doublet cells were excluded (A2) and viable CD44$^+$ cells were analysed (A3). (B) Representative histograms of FACS data generated after staining BW5147.3 cells with anti-CCR4-BV421 at 37 °C for 45 min. (C) MFI of bCCL22 after staining cells with the respective fluorophore-streptavidin or the preformed chemokine-streptavidin-tetramer at 4 °C. Symbols represent individual mice (n=2, pooled from two independent experiments). Data are presented as mean.

CCR4-transfected human embryonic kidney (HEK293T) cells, gated based on their FSC and SSC properties and selected for single cells and viability (Figure 5.3A), expressed the receptor (Figure 5.3B) but again showed no difference between the staining signals of samples stained with either of the chemokine-tetramers and the respective streptavidin control (Figure 5.3C). Moreover, HEK293T cells that did not express the receptor (HEK neo) also showed binding of the CCL17- and CCL22-tetramer (Figure 5.3D). Again, staining signals comparing chemokine-tetramers and the respective streptavidin control were similar. For both cell lines, however, the signal of the chemokine in stained conditions was higher than the fluorescence-minus-one (FMO) control, serving as an additional negative control (Figure 5.3E, F).

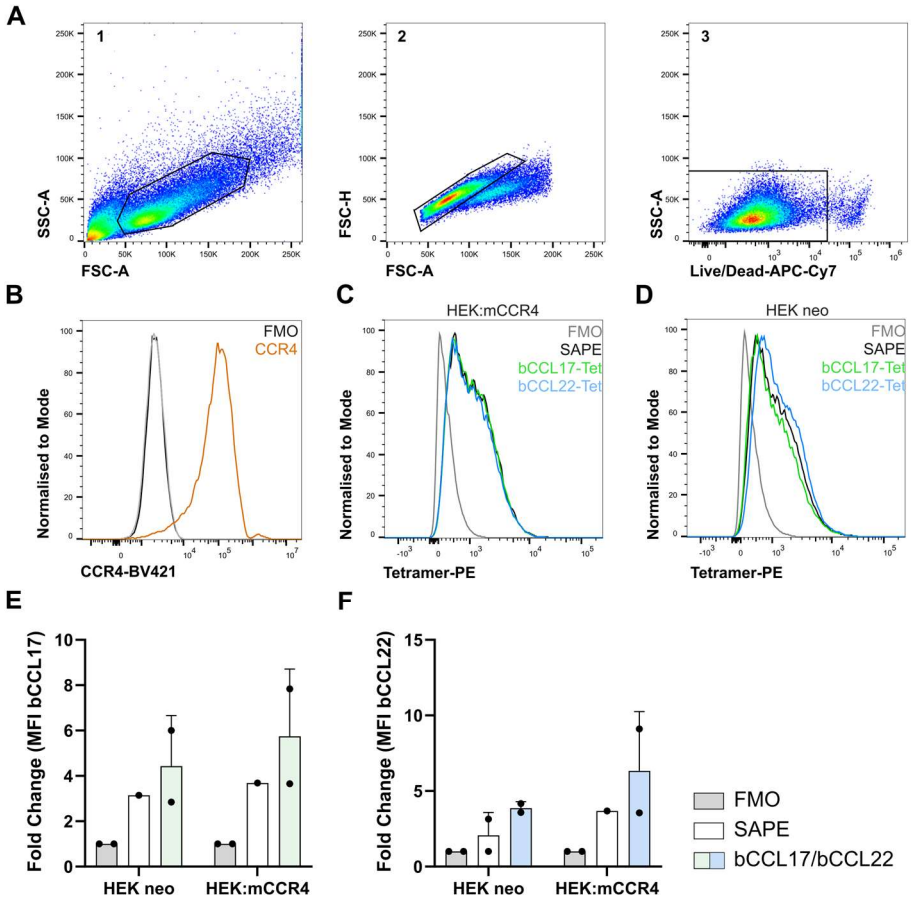

Figure 5.3: Fluorophore-streptavidin control shows high background staining in HEK293T cells

HEK293T cells carrying a neo cassette (HEK neo) or transfected with murine CCR4 (HEK:mCCR4) were harvested and stained. (A) Gating strategy for HEK neo or HEK:mCCR4 cells. Cells were selected for their FSC and SSC properties (A1). Doublet cells were excluded (A2) and viable cells were analysed (A3). (B) Representative histograms of FACS data generated after staining HEK:mCCR4 cells with anti-CCR4-BV421 at 37 °C for 45 min. Respective histograms of (C) HEK neo or (D) HEK:mCCR4 and the MFI of (E) bCCL17 and (F) bCCL22 of both cell lines after staining with the respective fluorophore-streptavidin or the preformed chemokine-streptavidin-tetramer (Tet) at 4 °C. (E, F) Symbols represent individual mice (n=1-2, pooled from two independent experiments). Data are presented as mean.

Lastly, the murine tumor dendritic cell lines (MutuDC) cDC1 and cDC2 were tested. Both were separately cultured and were identified by their CD11b expression. $CD11c^+$ $MHC\ II^+$ cDC1 showed intermediate CD11b expression while $CD11c^+$

MHC II$^+$ cDC2 expressed CD11b at high levels (Figure 5.4A, B). Both expressed CCR4, although this expression was very low in cDC1s (Figure 5.4C, D). But, as seen above for the other cell lines, tetramer staining was as high as the respective SABV control for both cDC1 and cDC2 (Figure 5.4E, F).

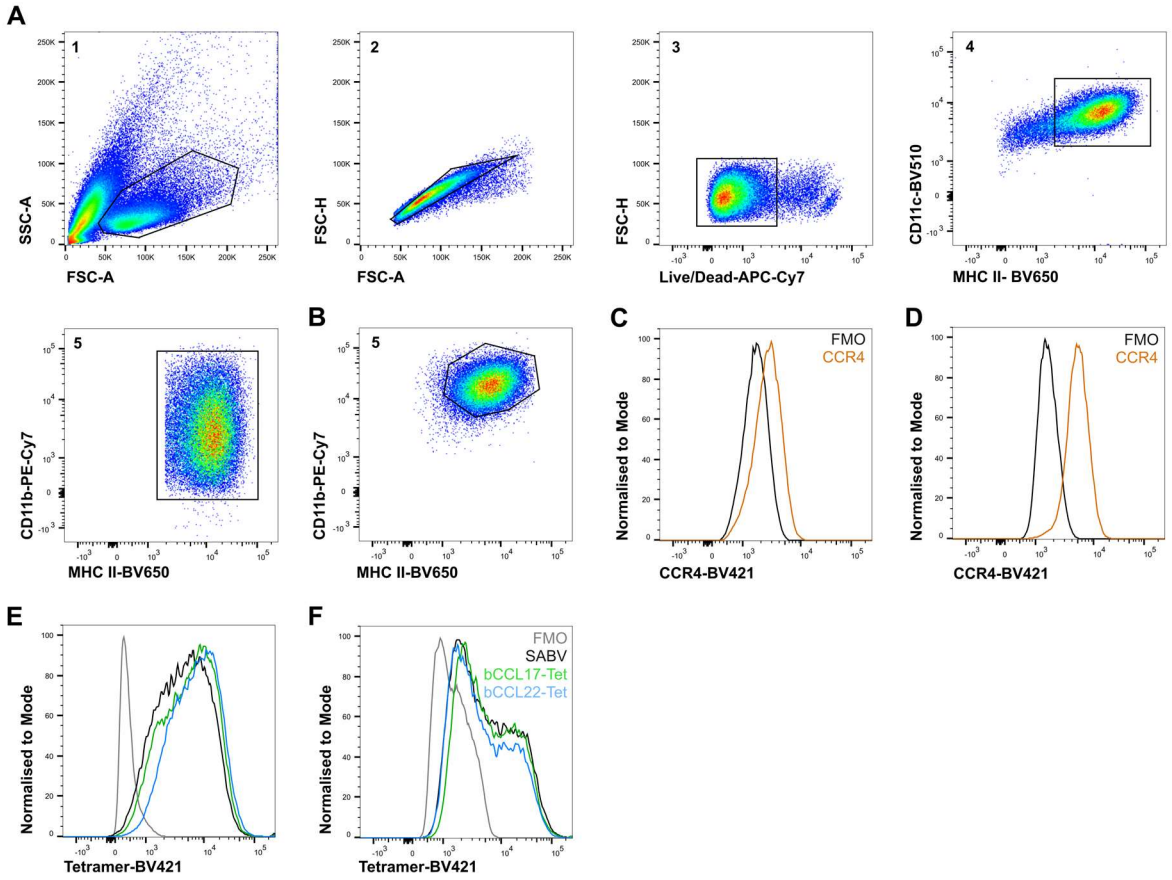

Figure 5.4: Fluorophore-streptavidin control shows high background staining in MutuDC cDC1 and cDC2 cell lines

MutuDC cDC1 and cDC2 cell lines were harvested and stained. (A) Gating strategy for HEK neo or HEK:mCCR4 cells. Cells were selected for their FSC and SSC properties (A1). Doublet cells were excluded (A2) and viable cells selected (A3). CD11c$^+$ MHC II$^+$ cells were selected (A4) and analysed for their CD11b expression. CD11b^{intermediate} cells were determined as MutuDC cDC1 cells (A5). (B) MutuDC cDC2 cells were stained separately and were identified through their high CD11b$^+$ expression. Representative histograms of FACS data generated after staining MutuDC (C) cDC1 or (D) cDC2 cells with anti-CCR4-BV421 at 37 °C for 45 min. Respective histrograms of MutuDC (E) cDC1 or (D) cDC2 cells after staining with the respective fluorophore-streptavidin or the preformed chemokine-streptavidin-tetramer (Tet) at 4 °C.

Testing different temperatures and incubation times also showed no difference between fluorophore-streptavidin control and the chemokine-tetramer (Figure 5.5A). Additionally, switching to another fluorophore-streptavidin combination (Figure **5.5**B), PE instead of BV421, or replacing the initial binding buffer with PBS (Figure 5.5C, D) resulted in the same outcome.

Taken together the data suggested that using a chemokine-tetramer is not suitable to stain for CCL17- or CCL22-binding cells due to high background of fluorophore-streptavidin or low binding of pre-assembled chemokine-tetramer through, for examples, steric hindrance.

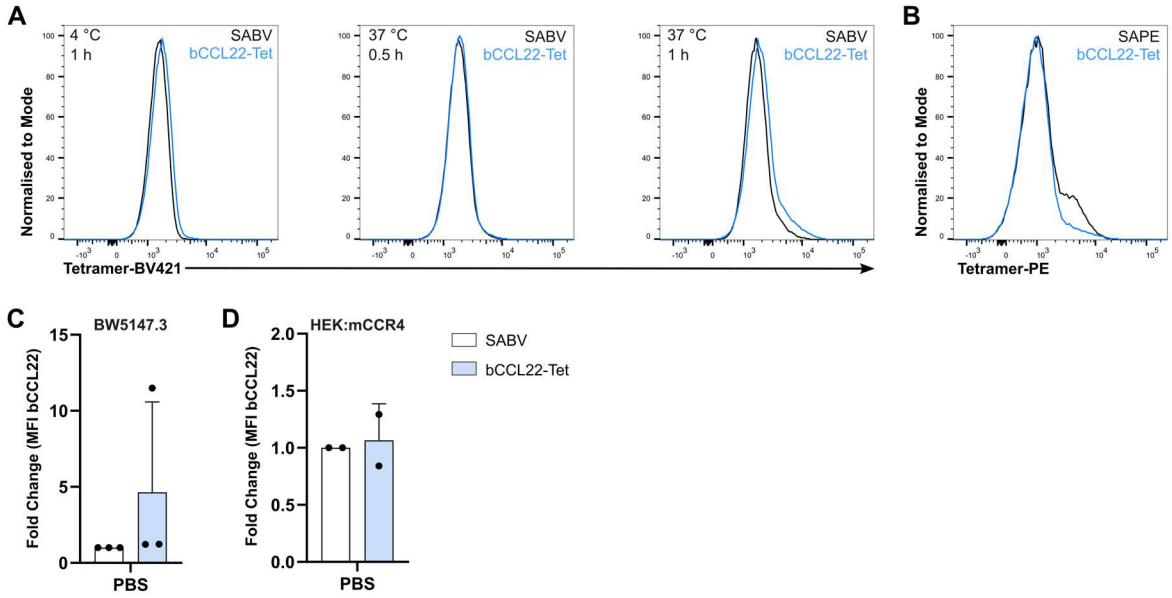

Figure 5.5: Change of incubation times, fluorophore-coupled streptavidin or incubation buffer for tetramer assembly does not reduce background of fluorophore-streptavidin

BW5147.3 or HEK:mCCR4 cells were harvested and stained with the respective fluorophore-streptavidin or the preformed chemokine-streptavidin-tetramer (Tet). (A) Representative histograms of FACS data generated after staining BW5147.3 cells (A) at different indicated temperatures and incubation times or (B) with bCCL22-SAPE instead of bCCL22-SABV. MFI of bCCL22 of stained (C) BW5147.3 cells or (D) HEK:mCCR4 cells after pre-forming tetramer in PBS instead of binding buffer. Symbols in (C) and (D) represent individual experiments (n=2-3, pooled from two or three independent experiments). Statistical significance was tested using unpaired t-test. Data are presented as mean with/without SD.

5.1.2 Staining with biotinylated chemokines

The pre-assembled tetramer did not show a specific staining signal. A possible explanation could be sterical hindrance as the chemokine-tetramer might block other tetramers from binding to the receptor or is too inflexible itself to properly engage in ligand-receptor-interaction. Therefore, the staining approach was used and optimised by adjusting the procedure to mimic common staining procedures of biotinylated antibodies, where biotinylated antibodies and fluorophore-streptavidin are used separately and consecutively.

The staining was established using BW5147.3 cells. Utilising the two-step procedure, biotinylated chemokines were effective in staining the cells without interference of the SABV control or the biotinylated chemokine only (Figure 5.6A, B). This was not only the case for the BW5147.3 cell line but also in CCR4-transfected HEK293T cells (Figure 5.6C).

Testing different staining conditions showed that staining with the biotinylated chemokine at 4 °C followed by staining with the fluorophore-coupled streptavidin at room temperature was optimal (Figure 5.6D). Performing both staining steps at 4 °C reduced the staining signal significantly. Reducing the staining time to 5 min per step also significantly decreased the signal. Additionally, to assess if parts of the biotinylated chemokines are internalised before adding streptavidin, cells were incubated with trypsin after the streptavidin staining step, thereby removing all surface receptors. Using trypsin reduced the signal significantly, indicating a surface staining (Figure 5.6D).

To evaluate the specificity of the staining, a competitive binding assay was performed. For this purpose, biotinylated and unlabeled chemokine were simultaneously added to BW5147.3 cells in a ratio of 1:10. Addition of unlabeled CCL17 significantly decreased the staining signal, while unlabled CCL22 increased the staining signal of bCCL17 significantly (Figure 5.6E). Similarly, unlabeled CCL22 was not able to outcompete biotinylated CCL22 signal but rather increased the signal (Figure 5.6F). Furthermore, addition of unlabeled CCL17 to bCCL22 showed a tendency to increase the bCCL22 staining signal, which was not significant.

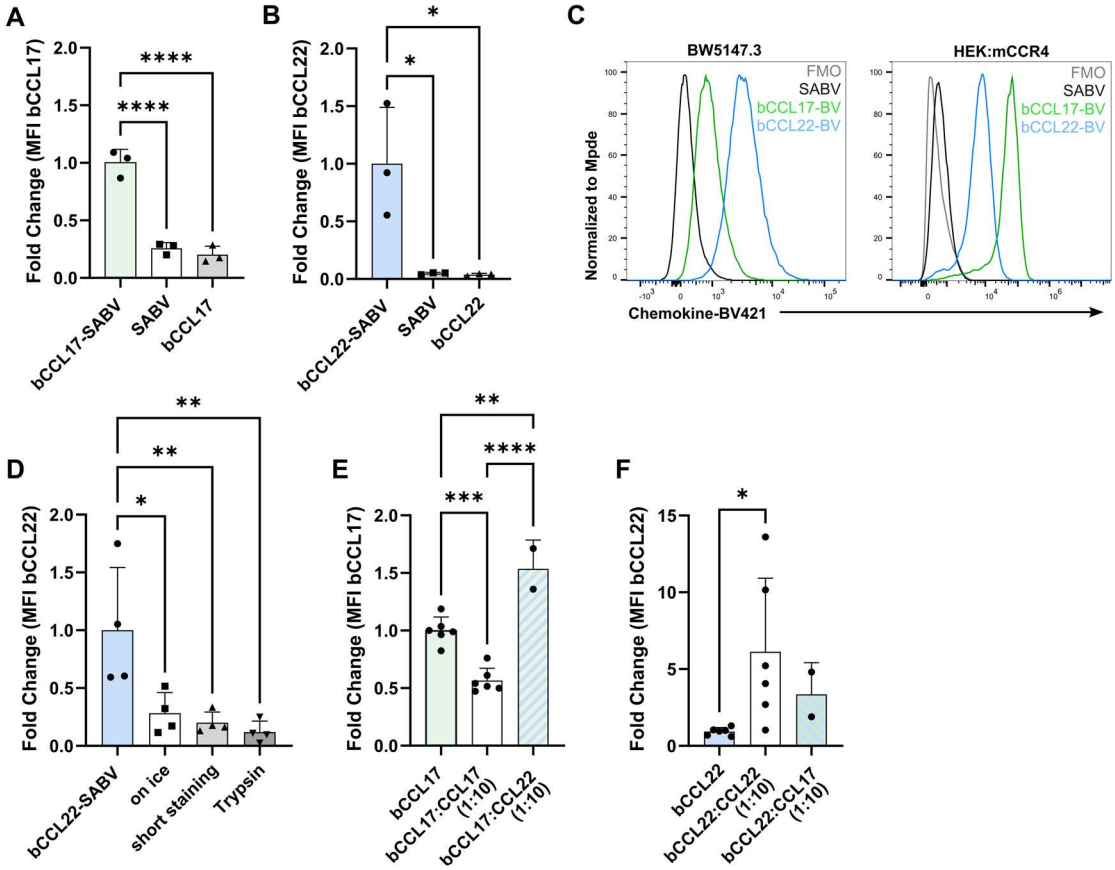

Figure 5.6: Surface staining using biotinylated chemokines shows low background and high specificity

BW5147.3 or HEK:mCCR4 cells were harvested and stained with either bCCL17 or bCCL22 for 30 min at 4 °C. In a second staining step, fluorophore-coupled streptavidin was added for 30 min at room temperature, followed by antibody surface staining. Fold change of the MFI of (A) bCCL17 or (B) bCCL22 of BW5147.3 cells. (C) Respective histograms of stained BW5147.3 or HEK:mCCR4 cells. (D) Fold change of bCCL22 of BW5147.3 cells after different staining temperatures or incubation times. Competitive binding assay for (E) bCCL17 and (F) bCCL22 with BW5174.3 cells, testing for specificity. (D-F) MFIs were normalised to respective SABV control. Symbols represent individual experiments (n=3-4, pooled from three to four independent experiments each). Statistical significance was tested using (A, B, D) one-way ANOVA with Dunnett's test for multiple comparison or (E, F) unpaired t-test. Data are presented as mean with SD.

5.2 CCL17 and CCL22 do not form dimers or oligomers

Unexpectedly, addition of unlabeled CCL22 lead to an increase in the staining signal of bCCL22-SABV. It is known that chemokines can form homo- or heterodimers, modifying their biological activity (Von Hundelshausen *et al.*, 2017). Therefore, it could be possible that CCL22 forms dimers/oligomers, leading to an enhanced affinity for the receptor. To address that question, a BN-PAGE with biotinylated chemokines, unlabeled chemokines and combinations thereof was performed. This method enables separation of proteins, multimers or protein complexes under native (non-denaturing) conditions.

Both proteins were found at their respective molecular weights of 7980 Da (CCL17) and 7800 Da (CCL22) (Figure 5.7). Also, combinations of CCL17 and CCL22, labeled and unlabeled, did not shift the molecular weight.

Taken together, both proteins did not form homodimers or heterodimers with each other. Hence, multimer formation is not able to explain the increase of the staining signal in the competitive binding assay.

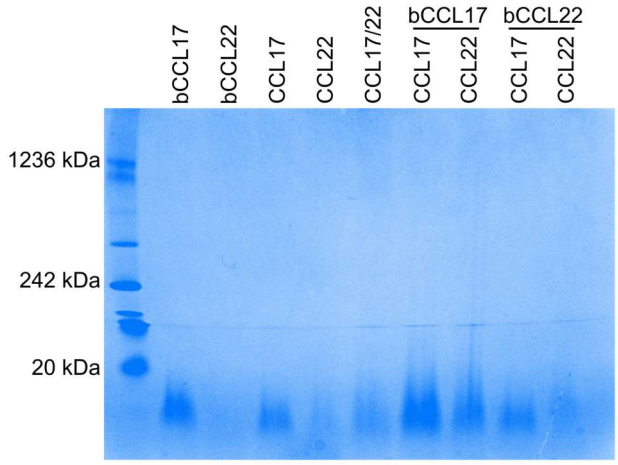

Figure 5.7: CCL17 and CCL22 do not form multimers with themselves or each other

Biotinylated or unlabeled chemokines only or in combinations were separated by BN-PAGE. A representative Coomassie-stained BN-PAGE gel is shown (n=3).

5.3 CCR4$^{-/-}$ T cells are still able to bind CCL17 and CCL22

CCR4 is expressed by a variety of T cell subsets and other cell types (Imai *et al.*, 1998; Imai *et al.*, 1999; Sebastiani *et al.*, 2001; Yoshie and Matsushima, 2015). To determine if CCL17 and CCL22 bind to other cell surface structures next to CCR4, thymus and spleen of wt (positive control) and CCR4$^{-/-}$ mice were stained with the biotinylated chemokines. Staining of the thymic cell suspension with bCCL17 showed a slight but not significant decrease of the MFI of different cell types in CCR4$^{-/-}$ compared to wt mice (Figure 5.8A). Staining with bCCL22, however, showed a significant reduction in the MFI for CD4^{+} T cells and GATA3^{+} T_h2 cells (Figure 5.8B) compared to wt mice. Both T cell populations also exhibited the highest expression of CCR4 compared to FoxP3^{+} T_{reg} cells and CD8^{+} T cells (Figure 5.8C). As expected, CCR4 expression was absent in CCR4$^{-/-}$ mice.

T cell subpopulations in the spleen showed comparable MFI levels for bCCL17 and bCCL22 between wt and CCR4$^{-/-}$ mice (Figure 5.8D, E). Notably, expression of CCR4 was nearly absent in T cell subpopulations of the spleen (Figure 5.8F).

Overall, T cells from CCR4$^{-/-}$ mice were still able to bind biotinylated CCL17 and CCL22 although CCR4 expression was not present. This suggested the possibility of a second receptor for both chemokines. Because the MFI for the staining of T cells with bCCL17 and bCCL22 from CCR4$^{-/-}$ mice was almost as high as the MFI obtained for T cells from wt mice, the postulated second receptor could also potentially compensate the loss of CCR4.

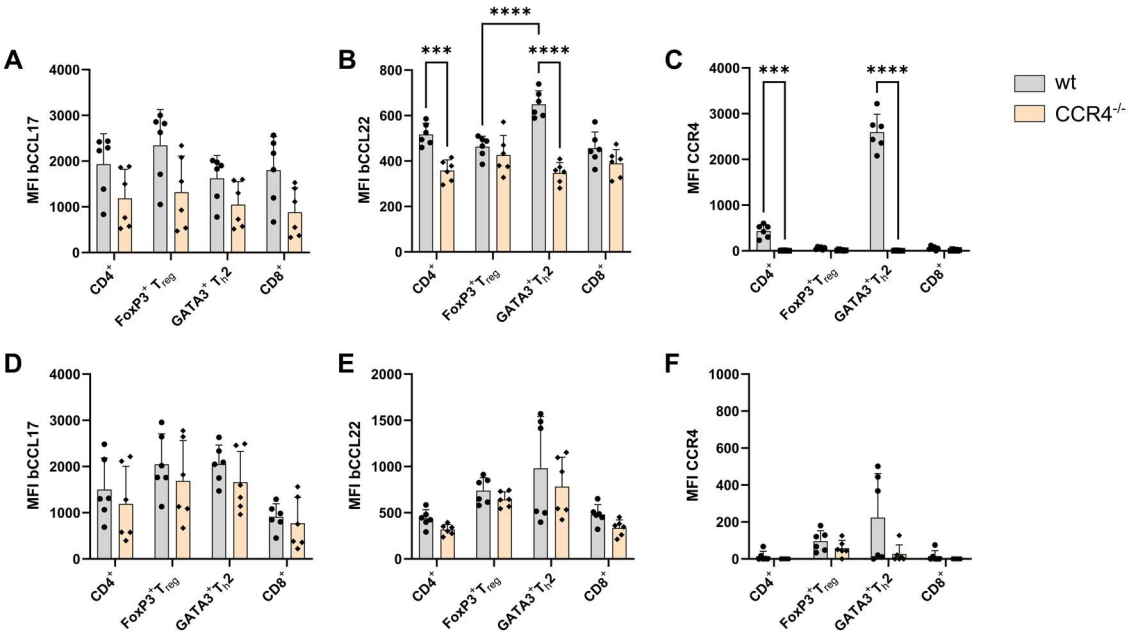

Figure 5.8: T cells bind bCCL17 and CCL22 even in the absence of CCR4
Thymus and spleen were harvested from naïve wt and CCR4$^{-/-}$ mice and stained with bCCL17, bCCL22 or against CCR4. Analysis of thymic T cell populations for MFI of (A) bCCL17, (B) bCCL22, or (C) CCR4. Analysis of splenic T cell populations for MFI of (D) bCCL17, (E) bCCL22, or (F) CCR4. MFIs were normalised to respective SABV control. Symbols represent individual mice (n=6, pooled from three independent experiments). Statistical significance was tested using two-way ANOVA with Tukey's test for multiple comparison. Data are presented as mean with SD.

5.4 CCR4-deficiency does not change CCL17 and CCL22 binding capacity of myeloid cells, B cells, and neutrophils

Next to T cell subsets, CCR4 is also expressed on DC and macrophages. Therefore, binding of CCL17 and CCL22 was also investigated on these cell types using the biotinylated chemokine staining. To separate myeloid cells, B cells, NK cells, and neutrophils the following gating strategy was used (Figure 5.9): cells were selected based on their FSC and SSC properties. Following exclusion of doublet cells, viable $CD45^+$ cells were analysed. Neutrophils were selected by their Ly6G expression. Remaining cells were selected first for $CD19^+$ $B220^+$ B cells, $F4/80^+$ macrophages, and MHC II^+ $CD11c^+$ DC. DC were further separated into $CD172\alpha^-$ cDC1 and $CD172\alpha^+$ cDC2. Remaining cells that were not yet selected for any of the previous markers were divided into $Ly6C^+$ and $Ly6C^-$ monocytes. Every cell population was analysed for their MFI regarding bCCL17- or bCCL22-SABV.

Within the thymus, wt and $CCR4^{-/-}$ mice showed comparable MFI levels of bCCL17 (Figure 5.10A) and bCCL22 staining (Figure 5.10B). The same observation was visible in the spleen (Figure 5.10C, D). $Ly6C^+$ monocytes showed the lowest MFI compared to other cell subsets in both organs and for both stainings.

Taken together, absence of CCR4 did not hinder binding of CCL17 and CCL22 in myeloid cells, B cells, and neutrophils. Moreover, MFI levels were comparable between wt and $CCR4^{-/-}$ mice. This again could suggest that the second receptor compensates the absence of CCR4 and might even be upregulated.

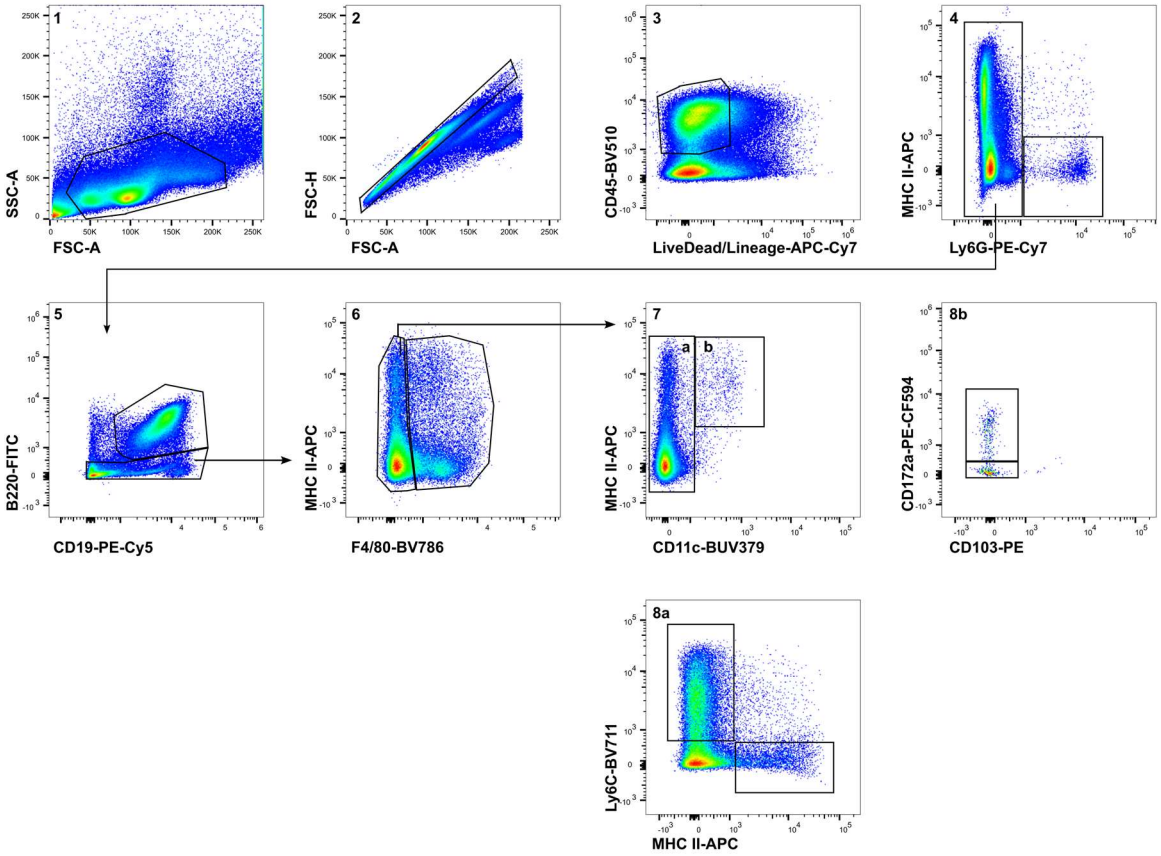

Figure 5.9: Gating strategy of myeloid cell, B cell, and neutrophil FACS analysis of naïve mice

Immune cells were selected based on their FSC and SSC properties (1). Doublet cells were excluded (2). Viable $CD45^+$ immune cells were selected (3). From the $CD45^+$ immune cell compartment neutrophils (4), B cells (5), macrophages (6), and DC (7b) were selected. Remaining cells, negative for all previous markers, were divided into $Ly6C^-$ and $Ly6C^+$ monocytes (8a). DC were further separated into $CD172\alpha^-$ cDC1 and $CD172\alpha^+$ cDC2 (8b).

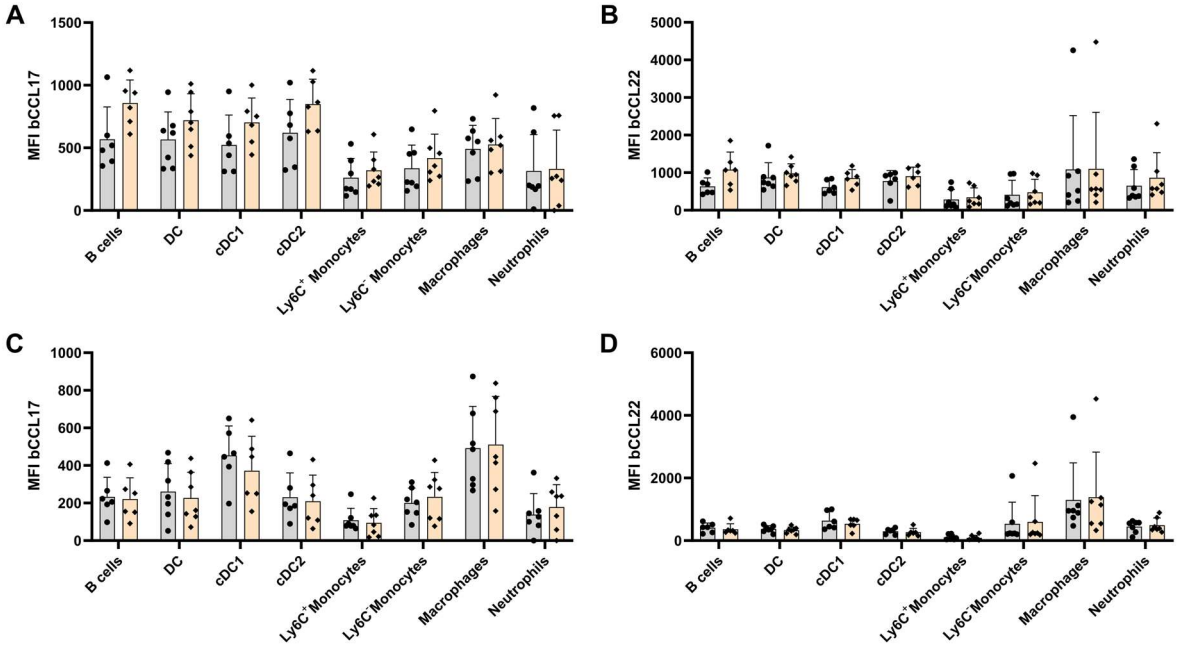

Figure 5.10: Absence of CCR4 does not change binding capacity of myeloid cells, B cells, and neutrophils for bCCL17 and bCCL22
Thymus and spleen were harvested from naïve wt and CCR4$^{-/-}$ mice and single cell suspension stained with bCCL17 or bCCL22. Analysis of thymic immune cell populations for MFI of (A) bCCL17 or (B) bCCL22. Analysis of splenic immune cell populations for MFI of (C) bCCL17 or (D) bCCL22. MFIs were normalised to the respective SABV control. Symbols represent individual mice (n=6, pooled from three independent experiments). Statistical significance was tested using two-way ANOVA with Tukey's test for multiple comparison. Data are presented as mean with SD.

5.5 Discussion

So far, the chemokine receptor CCR4 is the only described receptor for CCL17 and CCL22 (Santulli-Marotto, Fisher, *et al.*, 2013; Yoshie and Matsushima, 2015). Additionally, no other chemokines have been described to elicit signaling through CCR4 (Yoshie and Matsushima, 2015). The receptor is expressed on a variety of lymphocytes including NK cells, macrophages, DC, and CD4$^+$ T cells, especially T_h2 cells (Sells and Hwang, 2010; Poppensieker *et al.*, 2012; Solari and Pease, 2015; Ruland *et al.*, 2017). Due to its expression on T_h2 cells, CCR4 has a prominent role in allergic diseases. Several studies have demonstrated the involvement of the CCL17/CCL22/CCR4-axis in asthma and atopic dermatitis as well as contact

hypersensitivity in both humans and mice (Nakatani *et al.*, 2001; Kawasaki *et al.*, 2001; Okazaki *et al.*, 2002; Sebastiani *et al.*, 2002; Bochner *et al.*, 2003; Pilette *et al.*, 2004; Vijayanand *et al.*, 2010; Fülle *et al.*, 2018). Patients suffering from atopic dermatitis exhibit increased surface levels of CCR4 on peripheral blood $CD4^+$ T cells. Improvement of symptoms, however, decreases surface CCR4 expression (Wakugawa *et al.*, 2001). The involvement of CCL17, CCL22, and CCR4 in inflammatory and allergic diseases as well as cancer (Vestergaard *et al.*, 2000; Thompson *et al.*, 2001; Cronshaw *et al.*, 2004; Wiedemann *et al.*, 2016) promoted the extensive research on anti-CCR4 biologics and small molecule antagonists for therapeutic approaches (Solari and Pease, 2015; Ketcham *et al.*, 2018).

CCL17 and CCL22 interact with CCR4 through two distinct binding sites. Both binding sites are necessary to induce downstream signaling processes (Santulli-Marotto, Fisher, *et al.*, 2013; Santulli-Marotto, Boakye, *et al.*, 2013; Santulli-Marotto *et al.*, 2015). In addition, two receptor conformations for CCR4, termed major and minor, were described (Viney *et al.*, 2014). While the major conformation can interact with both chemokines, the minor conformation is exclusive for CCL22. Therefore, CCL22 can desensitise a cell to a second CCL17 stimulus, but can still elicit a signal following a primary CCL17 stimulus (Viney *et al.*, 2014). Furthermore, CCL22 is the dominant chemokine regarding receptor-binding affinity, receptor internalisation, and desensitisation (Santulli-Marotto, Fisher, *et al.*, 2013; Viney *et al.*, 2014). Similarly, the present study observed that CCL17 could not outcompete bCCL22 in a competitive binding assay. However, contradictory to previous studies CCL22 was not able to outcompete bCCL17 but rather increased the staining signals, as visualised by the MFI (Figure 5.6E, F). Moreover, the staining signal of bCCL22 was drastically increased in combination with unlabeled CCL22. Chemokines can form homo- and heterodimers as well as oligomers. The dimerisation is characterised as CC-type or CXC-type. In a CC-type dimerisation, flexible N termini of the chemokines interact with each other and form a two-stranded antiparallel β-sheet. In contrast, CXC-type dimerisation occurs through the antiparallel extension of preformed β-strands (Fernandez and Lolis, 2002). Interaction of CC chemokines preferentially

leads to CC-type dimerisation, whereas CXC chemokines favor the CXC-type (Nesmelova *et al.*, 2008). Interaction between both CC and CXC chemokines, however, can occur in both formations. Dimerisation of chemokines is linked to the modulation of the biological activity and receptor engagement of the respective chemokines. For example, dimerisation of some chemokines, either homo- or heteromerisation, allows for engagement with glycosaminoglycans (Crown *et al.*, 2006; Koenen *et al.*, 2009; Koenen and Weber, 2010). Mapping of the chemokine interactome revealed that CCL17 can engage with CCL5, CCL21, CCL25, CCL26, CCL28, CXCL4, and CXCL17 (Von Hundelshausen *et al.*, 2017). Interaction between CCL17 and CCL5 increased the potency regarding chemotaxis as the CCL17/CCL5-interaction induced migration of *in vitro* activated human T cells in a lower CCL17 concentration than CCL17 alone (Von Hundelshausen *et al.*, 2017). Like CCL17, CCL22 can interact with other chemokines including CCL14, CCL19, and CXCL4L1 modifying its activity (Von Hundelshausen *et al.*, 2017). In conclusion, CCL22 might form homodimers, thereby modifying its biological function. However, BN-PAGE revealed that neither CCL17 nor CCL22 form dimers or oligomers with themselves or each other (Figure 5.7). Therefore, the increase of the bCCL22 signal through the addition of unlabeled CCL22 is not due to homomerisation.

Receptors that possess multiple binding sites for their ligands can be subjected to positive or negative cooperativity (Sevlever *et al.*, 2020; Srinivasan, 2021). In the case of positive cooperativity, ligand binding to one binding site subsequently increases the affinity of remaining binding sites. In contrast, a decrease of ligand affinity following a ligand-receptor-interaction is noted as negative cooperativity. Cooperativity is not exclusive to ligand-receptor-interactions and can occur in multiple settings including the folding of proteins, enzyme-substrate interactions, and melting of phospholipid chains (Sevlever *et al.*, 2020). In the case of GPCRs, both positive and negative cooperativity were described (Notides *et al.*, 1981; Roed *et al.*, 2012). The secretin receptor primarily oligomerises on the cell surface and shows negative cooperativity upon binding to secretin which was absent, however, when the receptor was present as a monomer, mediated through mutations in the fourth

transmembrane domain (Harikumar *et al.*, 2007; Gao *et al.*, 2009). In contrast, positive cooperativity was observed for the estrogen receptor (Notides *et al.*, 1981). Taken together, positive cooperativity of the CCR4 receptor might explain the bCCL22-CCL22-signal increase phenomenon. Under normal circumstances, the staining signal is limited by the limited number of receptor molecules on the cell surface or open binding sites. Accessibility might be further limited due to the biotinylation. The NHS-LC-LC-Biotin used labels primary amino groups from the lysine side chain or the N-terminus through the N-hydroxysulfosuccinimide (NHS) ester. Although the ratio of biotin to chemokine was restricted to reduce the number of biotin per chemokine, excessive biotinylation cannot be excluded. The biotin-tag might hinder the binding of additional biotinylated chemokines to the same receptor through sterical hindrance. Unlabeled chemokines, however, are not affected by that and might open all available receptor binding sites through positive cooperativity.

T cell development occurs in the thymus. In the thymic cortex, immature thymocytes interact with cortical thymic epithelial cells providing survival cues and mediating differentiation (Shah and Zúñiga-Pflücker, 2014). $CD4^+$ $CD8^+$ double-positive thymocytes with a functional TCR recognising and moderately binding to antigens presented by MHC complexes (positive selection) are maintained and receive survival signals. Subsequently, they differentiate in either $CD4^+$ or $CD8^+$ single-positive thymocytes. Failure to signal through the TCR results in cell death of the thymocytes through absent survival signals (Klein *et al.*, 2014). Single-positive thymocytes migrate into the thymic medulla where they are further selected for central tolerance. Finally, mature naïve T cells leave the thymus and travel to secondary lymphoid organs (Takahama, 2006; Ehrlich *et al.*, 2009; Love and Bhandoola, 2011). Migration through the thymus as well as localisation in secondary lymphoid organs is mediated by chemokines and their receptors (Love and Bhandoola, 2011; Zlotnik and Yoshie, 2012; Hu *et al.*, 2015). CCR7, for example, mediates the migration of single-positive thymocytes into the thymic medulla (Ueno *et al.*, 2004; Ehrlich *et al.*, 2009). Similarly, CCR4 is expressed by $CD4^+$ $CD8^+$ double-positive and $CD4^+$ single-positive thymocytes and promotes their entry into

the thymic medulla. Absence of CCR4 decreases counts of $CD4^+$ $CD8^+$ double-positive and $CD4^+$ single-positive thymocytes in the medulla. Furthermore, CCR4-deficiency impairs interaction efficiency between those thymocytes and DC as well as the negative selection of the thymocytes via their TCR, resulting in an increased pool of autoreactive naïve $CD4^+$ T cells in secondary lymphoid organs (Hu *et al.*, 2015). CCR4 levels correlate with CD69 expression on $CD4^+$ single-positive thymocytes (Cowan *et al.*, 2014), a surface marker that is associated with TCR-mediated positive selection in the thymus and prevention of thymocyte egress during the maturation process (Yamashita *et al.*, 1993; Feng *et al.*, 2002). Indeed, CCR4 levels increase shortly after positive selection and are later replaced by high CCR7 expression (Cowan *et al.*, 2014). The present study confirmed CCR4 expression on T cells from the thymus (Figure 5.8C). Expression was especially high for $GATA3^+$ T_h2 T cells, in line with the literature. Therefore, thymic T cells were responsive to bCCL17 and bCCL22. Interestingly, the binding of both chemokines was reduced but not absent in CCR4-deficient mice, supporting the hypothesis of a second receptor for CCL17 and CCL22. The binding was most strongly reduced in T cell subsets with high CCR4 expression, meaning T_h2 cells and overall $CD4^+$ T cells. It should be noted, however, that the chemokine signal was still high in $CCR4^{-/-}$ mice, indicating that the second receptor might be upregulated in the absence of CCR4 to compensate for the loss of the signaling pathway. Differences in the spleen regarding the chemokine binding were not as prominent. Binding of both chemokines was similar in all T cell subsets tested comparing wt and $CCR4^{-/-}$ mice (Figure 5.8). However, CCR4 expression was also lower than in the thymus, suggesting an overall higher relevance for the second receptor in secondary lymphoid organs, although an upregulation of said second receptor in the absence of CCR4 cannot be excluded. A similar observation was made for myeloid cells and B cells, both in the thymus and spleen. DC and macrophages are known to express CCR4. Therefore, the comparably high chemokine binding was not surprising. In addition, CCR4 is expressed by naïve and memory B cells as well as moderately by germinal centre B cells of the human tonsil (Corcione *et al.*, 2002), indicating the possibility of CCR4

expression by splenic B cells. Indeed, B cells showed bCCL17 and bCCL22 binding in the present study. Again, the staining signal in CCR4$^{-/-}$ immune cell subsets was as high as in their wt counterparts, supporting a possible upregulation of the second receptor. However, the second receptor might also be more relevant in this context, meaning that the staining signal in wt cells does not result from binding of the biotinylated chemokine to CCR4 only but also to the additional receptor. To answer that question, expression levels of CCR4 on each of the subsets should be validated. Taken together, the present study showed that bCCL17 and bCCL22 are still bound by immune cells in the absence of CCR4, thereby giving evidence for a second receptor. This second receptor might be upregulated if CCR4 is lost to compensate for the missing protein. Additionally, CCR4 could display positive cooperativity in CCL22 binding.

Chapter 6: Identification of the second receptor for CCL17 and CCL22

Chemokines and chemokine receptors are often promiscuous in their interactions, meaning that some chemokines can bind to more than one receptor and *vice versa* (Hughes and Nibbs, 2018). In case of CCL17 and CCL22, CCR4 is the only receptor described so far. Nevertheless, CCR4-deficient T cells and other immune cell types were still able to bind both chemokines. Taken together with the functional differences observed between $CCL17^{E/E}$ $CCL22^{-/-}$ and $CCR4^{-/-}$ mice regarding weight loss and cellular composition of T_{reg} cell subsets and erythrocyte progenitors in IL-33-induced immune responses as well as immune responses in DNFB-induced CHS, the data suggested the possible presence of a second receptor.
The aim of this chapter was to identify potential receptor candidates by establishing a Pull Down Assay.

6.1 Generation of CCR4-deficient BW5147.3 cells

The T cell lymphoma cell line BW5147.3 was able to bind bCCL17 and bCCL22 and expresses CCR4. To perform the Pull Down Assay, BW5147.3 cells were intended to be used as positive control as at least CCR4 should be pulled down with the biotinylated chemokines. Additionally, CCR4-deficient cells that bind both chemokines were needed for comparison. As CCR4-deficient primary T cells are still able to bind bCCL17 and bCCL22, CCR4-deficient BW5147.3 cells could potentially show a similar binding behaviour. Therefore, CCR4-deficient BW5147.3 cells needed to be generated and validated for their actual loss of CCR4. Genome editing was performed using CRISPR/Cas9 technology and following the IDT genome editing protocol “Alt-R CRISPR-Cas9 System: Delivery of ribonucleoprotein complexes into Jurkat T cells using the Neon® Transfection System” as described in chapter 2.2.7.1.
Candidate CCR4-deficient clones were first validated using PCR. Successful knockout of CCR4 should result in a PCR product of 510 bp. Otherwise, the PCR

product would be visible at 2205 bp (Figure S.2). The PCR revealed that clones 7, 12, 18, 19, and 20 were knockouts for CCR4 (Figure 6.1A). Additionally, clones 2, 3, 5, 6, 8, 10, 14, and 17 showed both the 510 bp and 2205 bp PCR product, indicative of a heterogeneous cell population. Remaining cell clones were wt for CCR4 or showed no PCR product (clone 9, 15, and 16). To exclude that only primer binding sites were mutated or deleted, an additional PCR using a primer pair binding within the CCR4 gene sequence, was used. The PCR product should be absent in a full knockout, whereas a partial knockout would result in a 361 bp product. From all clones tested, clones 19 and 20 were a full knockout for CCR4 and were chosen for further experiments (Figure 6.1B, C). CCR4 expression of BW5147.3 clone 19 (BW#19) and clone 20 (BW#20) was tested for validation of the knockout using flow cytometry. As expected, untransfected BW5147.3 cells showed high signals for CCR4 (Figure 6.1D). In contrast, the CCR4 signal was absent in BW#19 and BW#20, confirming the knockout on protein level. Sequencing of both clones showed deletions at the cutting site as well as various point mutations (Figure S.3).

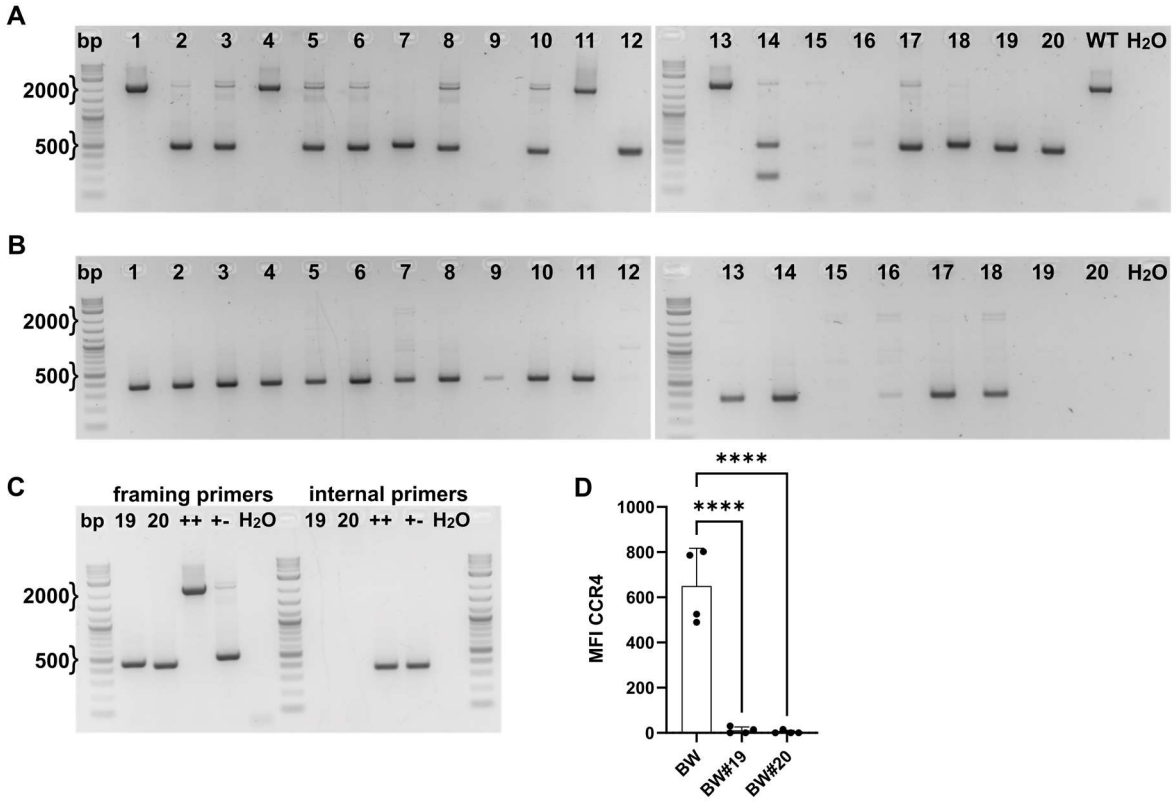

Figure 6.1: Validation of CCR4-deficient BW5147.3 cells
BW5147.3 cells were transfected using the Neon® Transfection System. Transfected cells were sorted into single cells. Single-cell clones were validated using PCR and CCR4 flow cytometry staining. Agarose gel of PCR products for (A) framing primers and (B) internal primers. (C) Confirming agarose gel of PCR products for BW5147.3 clones #19 and #20. (D) MFI of CCR4. MFIs were normalised to respective FMO control. Symbols represent individual experiments (n=4, pooled from four independent experiments). Statistical significance was tested using two-way ANOVA with Tukey's test for multiple comparison. Data are presented as mean with SD.

6.2 CCR4-deficient BW5147.3 still bind CCL17 and CCL22 but fail to migrate

After confirming CCR4-deficiency, the two BW5147.3 clones were tested for bCCL17 and bCCL22 binding. Based on the previously positive bCCL17 or bCCL22 binding results using CCR4-deficient primary T cells, CCR4-deficient BW5147.3 cells were predicted to potentially show a similar binding behaviour.

Interestingly, BW#19 showed significantly better binding of bCCL17 compared to wt BW5147.3 cells (Figure 6.2A). In BW#20 cells, however, binding of bCCL17 was slightly reduced but not significantly compared to wt BW5147.3 cells. In contrast, binding of bCCL22 was unchanged between wt BW and BW#19 but slightly reduced in BW#20 (Figure 6.2B). As previously seen, the addition of unlabeled CCL17 reduced the bCCL17 signal significantly, while unlabeled CCL22 increased the bCCL22 signal (Figure 6.2C). The same was observed in a competitive binding assay with BW#19 cells (Figure 6.2D). In contrast, unlabeled CCL17 only slightly decreased bCCL17 signal in BW#20 cells (Figure 6.2E). The signal of bCCL22 was again increased after the addition of unlabeled CCL22.

One major function of the CCL17/CCL22-CCR4-interaction is the induction of immune cell migration. Therefore, BW#19 and BW#20 were also tested for migration towards both chemokines. As expected, wt BW5147.3 cells migrated towards CCL17 and CCL22 with the latter being more potent in inducing migration (Figure 6.2F). In the absence of CCR4, cells failed to migrate. Both BW#19 and BW#20 showed no migration towards CCL17 or CCL22.

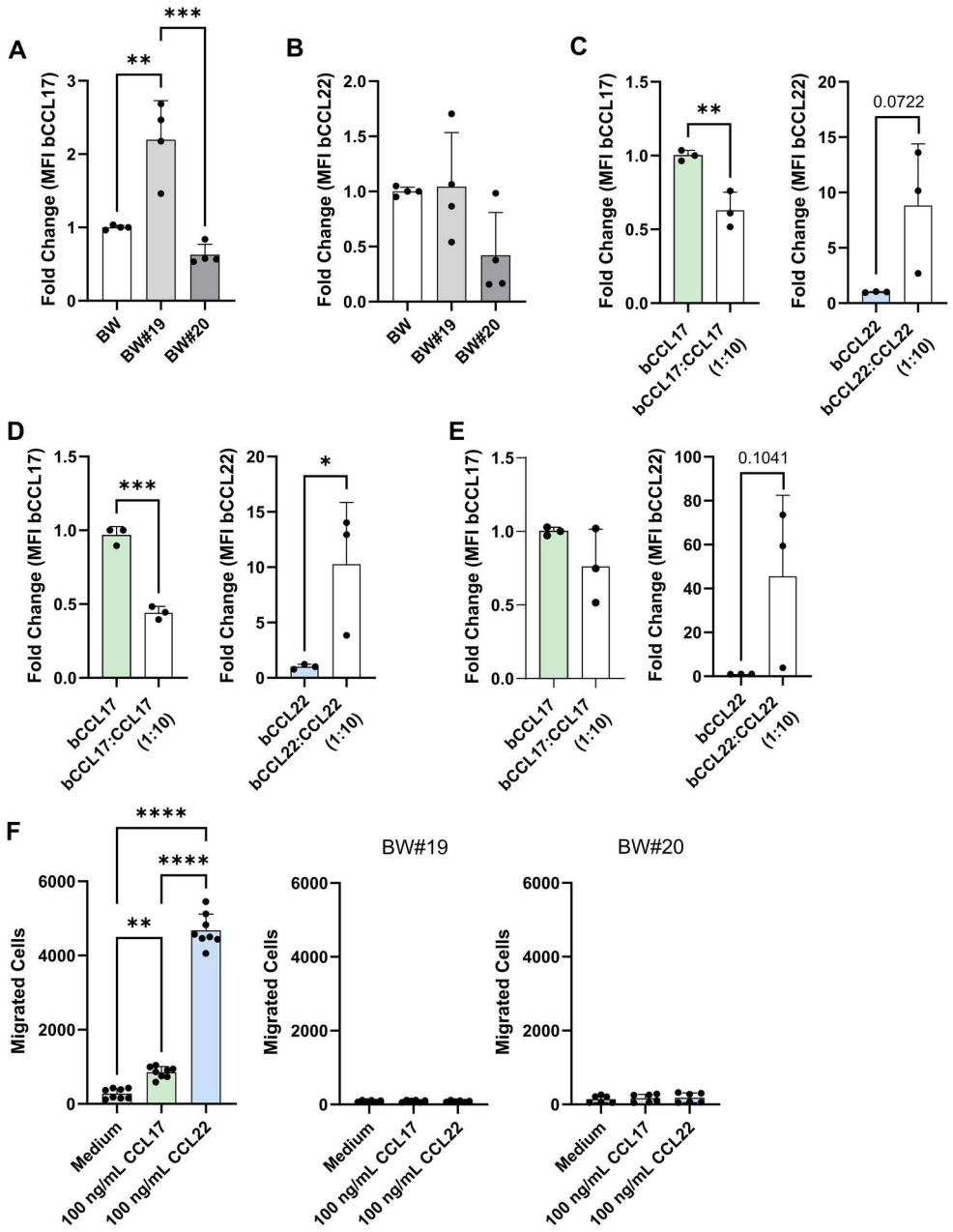

Figure 6.2: CCR4-deficient BW5147.3 cells show binding of bCCL17 and bCCL22 but fail to migrate towards both chemokines

BW5147.3 cells (wt, BW#19, BW#20) were harvested and stained with either bCCL17 or bCCL22 for 30 min at 4 °C. In a second staining step, fluorophore-coupled streptavidin was added for 30 min at room temperature, followed by antibody surface staining. Fold change of the MFI of (A) bCCL17 or (B) bCCL22. Competitive binding assay for bCCL17 (green) or bCCL22 (blue) with (C) wt BW5147.3, (D) BW#19, or (E) BW#20. (F) Transwell assay of starved BW5147.3 cells to assess migration towards 100 ng/mL CCL17 or CCL22. Depiction of total

migrated cells per condition. (A-E) MFI were normalised to the respective SABV control. Symbols represent individual experiments (n=3-4, pooled from three different experiments). (F) Symbols represent individual values (n=6-8, pooled from two independent experiments). Statistical significance was tested using one-way ANOVA with Dunnett's test for multiple comparison or (C-E) unpaired t-test. Data are presented as mean with SD.

These results were comparable to the migration of primary thymocytes. Thymic T cells were sorted into three populations defined as mature $CD4^+$ $CD69^-$ T cells, immature $CD4^+$ $CD69^+$ T cells, and $CD8^+$ T cells. The marker CD69 was chosen because it is a marker of positive selection and prevents thymocyte egress from the thymus (Nakayama *et al.*, 2002; Feng *et al.*, 2002). Additionally, CCR4 may play a role in cell migration during the development of T cells. Receptor upregulation is found in thymocytes during migration from the cortex to the medulla but downregulation is observed when cells leave the thymus for the periphery (J J Campbell *et al.*, 1999). Therefore, we presumed a low or no CCR4 expression in $CD4^+$ $CD69^-$ cells, whereas it can be assumed that $CD4^+$ $CD69^+$ have a higher CCR4 expression.

Immature $CD4^+$ $CD69^+$ T cells showed migration towards CCL22 (Figure 6.3A). Mature $CD4^+$ $CD69^-$ and $CD8^+$ T cells, however, failed to migrate. In the absence of CCR4, migration of immature $CD4^+$ $CD69^+$ T cells was abolished (Figure 6.3B).

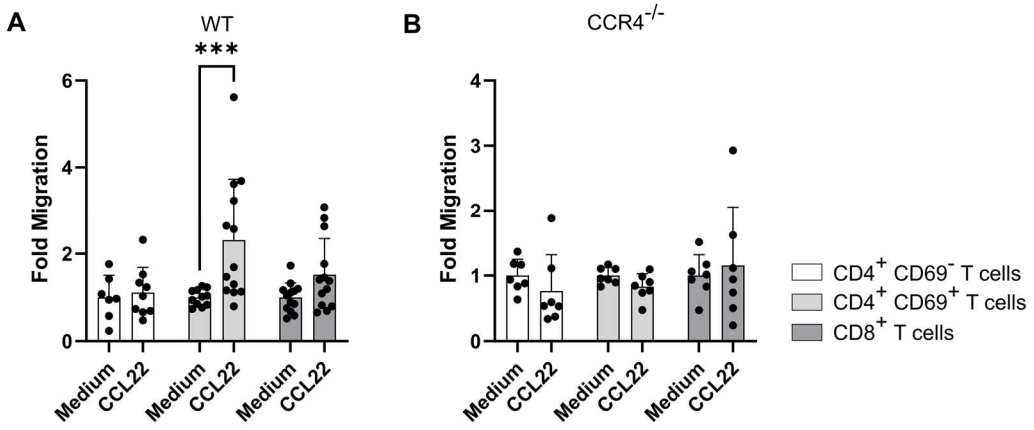

Figure 6.3: **Absence of CCR4 prevents migration of immature CD4⁺ T cells toward CCL22**
Thymic T cells were sorted into mature CD4⁺ CD69⁻ T cells, immature CD4⁺ CD69⁺ T cells, and CD8⁺ T cells. All subsets were starved in FCS-free media for 1 h before starting the transwell migration assay with 100 ng/mL CCL22 for 2 h at 37 °C. Fold migration of (A) wt or (B) CCR4-deficient thymocytes. Values of migrated cells were normalised to respective medium control. Symbols represent individual values (n=7-13, pooled from two to four independent experiments). Statistical significance was tested using two-way ANOVA with Šidák's test for multiple comparison. Data are presented as mean with SD.

Taken together, the data suggests that the potential second receptor is able to bind both chemokines but is not involved in the induction of cell migration. Therefore, the function is unclear and may resemble the role of an ACKR (see discussion).

6.3 SK113AE-4 hybridoma cells do not bind CCL17 and CCL22

To validate the results of the Pull Down Assay and select potential candidates, various controls are needed among them a cell line that does not bind the chemokines. Although B cells are able to secrete CCL17 and CCL22 upon CD40 stimulation, they do not express CCR4 (Liu *et al.*, 2021). Therefore, B cells could be a potential negative control. For that purpose, the B cell hybridoma cell line SK113AE-4 (αIL18) was selected and analysed for their bCCL17 and bCCL22 binding capacity. The cells were gated based on their FSC and SSC properties and selected for single cells and viability (Figure 6.4A), and showed no expression of CCR4 (Figure 6.4B). Indeed, SK113AE-4 cells showed significantly less binding of bCCL17 (Figure 6.4C) and bCCL22 (Figure 6.4D) compared to BW5147.3 cells. Overall, SK113AE-4 cells appeared suitable as a negative control for the Pull Down Assay.

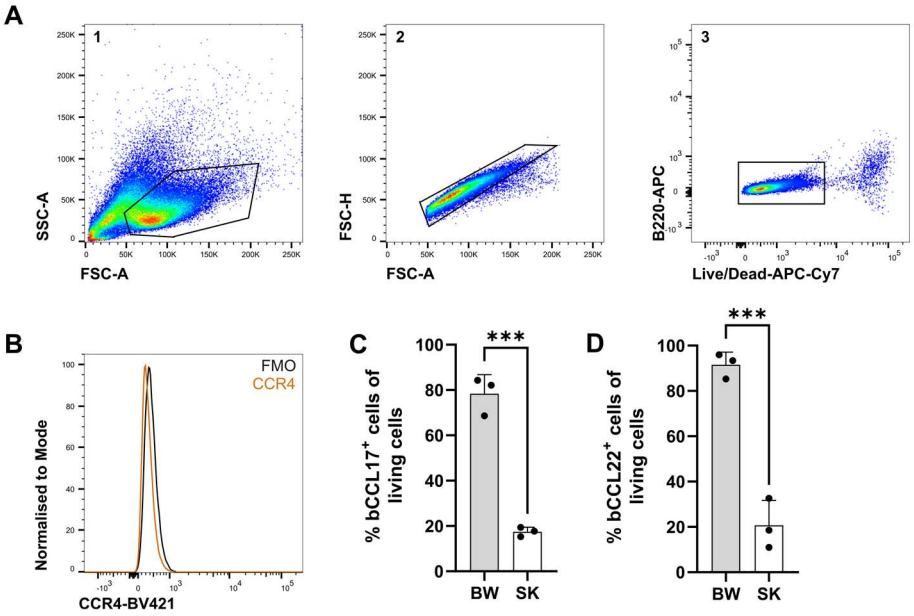

Figure 6.4: SK11AEαIL18 hybridoma cell line shows low binding of bCCL17 and bCCL22

Gating strategy for SK113AE-4 cells. Cells were selected for their FSC and SSC properties (A1). Doublet cells were excluded (A2) and viable cells were analysed (A3). (B) Representative histograms of FACS data generated after staining SK113AE-4 cells with anti-CCR4-BV421 at 37 °C for 45 min. Frequency of (C) bCCL17$^+$ or (D) bCCL22$^+$ BW5147.3 or SK113AE-4 cells after staining with the respective fluorophore-streptavidin at 4 °C. Values were normalised to respective streptavidin control. Symbols represent individual experiments (n=3, pooled from three independent experiments). Statistical significance was tested using unpaired t-test. Data are presented as mean with SD.

6.4 CXCL1 as negative chemokine control

As a second negative control a chemokine not binding to the target cells was needed to assess background or unspecific binding. CXCL1, a ligand for CXCR2, was chosen as T cells are not known to bind this ligand. While CC-chemokines mainly attract monocytes and T cells, CXC chemokines primarily attract neutrophils (Sawant *et al.*, 2016; Singhal and Baune, 2018). Indeed, CXCR2-deficient mice show severely impaired neutrophil recruitment in response to pneumococcal pneumonia (Herbold *et al.*, 2010).

To evaluate the capability of CXCL1 as a non-binding chemokine, BW5147.3 cells were stained with biotinylated CXCL1 (bCXCL1) and the staining signal was

compared to the bCCL17 and bCCL22 signal. Staining of BW5147.3 and CCR4-deficient BW#19 cells with bCXCL1 showed reduced binding compared to bCCL17 and bCCL22 (same concentration) (Figure 6.5). However, some overlap between the staining signals was visible, most strongly in BW5147.3 cells for both bCCL17 and bCCL22 or regarding bCCL22 in BW#19 cells. As CXCL1 does not bind to T cells, remaining overlap of staining signal is potentially due to unspecific staining. Therefore, bCXCL1 is needed to determine unspecific interaction partners in the Pull Down Assay.

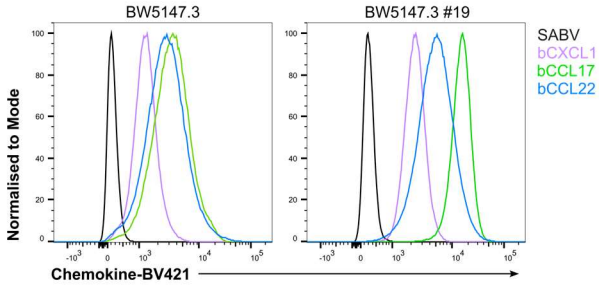

Figure 6.5: bCXCL1 is suitable to assess background binding of biotinylated chemokines
BW5147.3 and BW#19 cells were harvested and stained with either bCXCL1, bCCL17, or bCCL22. Histograms of FACS data generated after staining. (n=1, one experiment)

6.5 Pull Down Assay to identify the second receptor for CCL17 and/or CCL22

To perform the Pull Down Assay and identify potential second receptor candidates, cell culture cells were incubated with the biotinylated chemokines followed by an incubation with streptavidin-coated magnetic beads. Cells binding the biotinylated chemokines are captured by the magnetic beads through biotin-streptavidin-interaction. Using a magnet, bead-bound cells were retained during multiple washing steps while unbound cells were removed. Afterwards, cells were lysed. In theory, chemokine-interaction structures and indirect interaction partners through the receptor should remain bound to the magnetic beads while non-interacting proteins should be removed. For the assay, untransfected BW5147.3 cells were used as

positive control due to their expression of CCR4 which should be captured in the assay. SK113AE-4 cells as well as bCXCL1 were used as negative cell line and chemokine, respectively, to assess unspecific or background binding. CCR4-deficient BW5147.3 cell clones BW#19 and BW#20 were needed to screen for the second receptor as they bound CCL17 and CCL22 without expression of CCR4.

Remaining proteins were digested into peptides using trypsin, measured with MS and analysed using Peaks 11 software. To identify the proteins at least one unique peptide was needed, which was set as an identification criterion.

The analysis determined 76 proteins that showed differential abundance (color code) within the samples compared to the set negative control SK113AE-4 cells incubated with bCCL17 (Figure 6.6). However, the peptides detected mainly aligned to nuclear proteins like histones and ribosomal proteins (Figure 6.7). CCR4 was not found in the positive control of untransfected BW5147.3 cells.

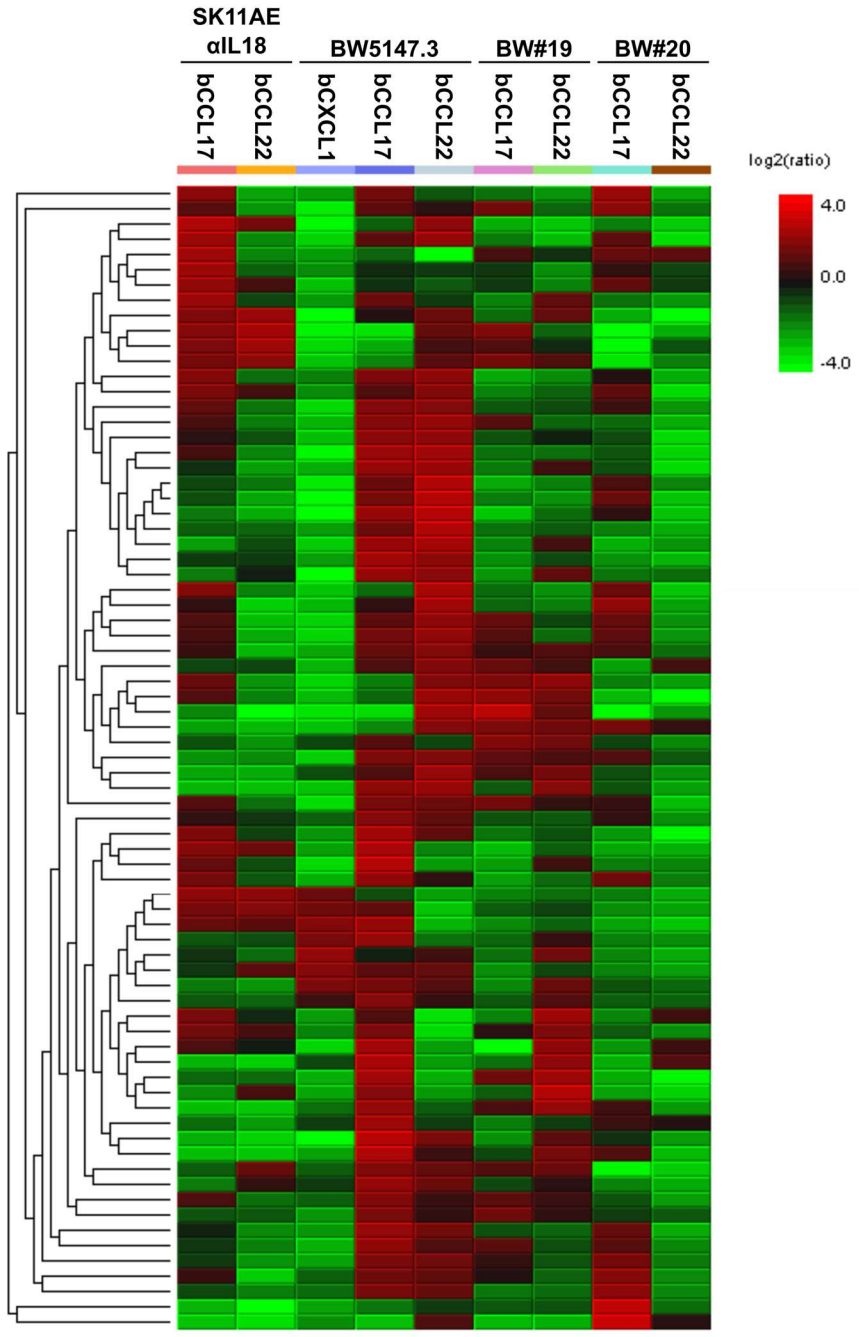

Figure 6.6: Protein profile heatmap
Pull Down Assay was performed with SK11AEαIL18, BW5147.3, and CCR4-deficient BW#19 and BW#20 using bCCL17, bCCL22, and bCXCL1. Chemokine-bound cells were isolated using streptavidin-coated magnetic beads and lysed. Potential interaction partners were digested using trypsin and measured through MS. Cell colour represents log2 (ratio) to the average abundance across different samples. SK113AE-4 cells incubated with bCCL17 were set as control. (n=1)

Protein Group	Protein ID	Accession	Significance	Coverage (%)	#Peptides	#Unique	PTM	Avg. Mass	Sample Profile	Group Profile	Description
2	23	Q8BTI8	200.00	1	2	2	N	294841			Serine/arginine repetitive matrix protein 2 OS=Mus musculus OX=10090 GN=Srrm2 PE=1 SV=3
3	8	P63038	200.00	10	3	3	N	60956			60 kDa heat shock protein, mitochondrial OS=Mus musculus OX=10090 GN=Hspd1 PE=1 SV=1
4	18	P03975	200.00	11	4	4	N	62747			IgE-binding protein OS=Mus musculus OX=10090 GN=Iap PE=2 SV=1
6	6	P09405	200.00	3	1	1	N	76723			Nucleolin OS=Mus musculus OX=10090 GN=Ncl PE=1 SV=2
7	3	P43277	200.00	20	5	3	Y	22100			Histone H1.3 OS=Mus musculus OX=10090 GN=H1-3 PE=1 SV=2
9	1	P15864	200.00	20	3	1	Y	21267			Histone H1.2 OS=Mus musculus OX=10090 GN=H1-2 PE=1 SV=2
11	44	Q64525	200.00	58	9	1	Y	13920			Histone H2B type 2-B OS=Mus musculus OX=10090 GN=Hist2h2bb PE=1 SV=3
14	2	P43274	200.00	20	4	3	Y	21977			Histone H1.4 OS=Mus musculus OX=10090 GN=H1-4 PE=1 SV=2
15	10	Q9D0E1	200.00	3	1	1	N	77649			Heterogeneous nuclear ribonucleoprotein M OS=Mus musculus OX=10090 GN=Hnrnpm PE=1 SV=3
18	7	P20152	200.00	5	1	1	N	53688			Vimentin OS=Mus musculus OX=10090 GN=Vim PE=1 SV=3
20	4	P43276	200.00	21	3	3	Y	22576			Histone H1.5 OS=Mus musculus OX=10090 GN=H1-5 PE=1 SV=2
21	26	Q7TPV4	200.00	1	1	1	N	152036			Myb-binding protein 1A OS=Mus musculus OX=10090 GN=Mybbp1a PE=1 SV=2
28	37	P43275	200.00	10	2	2	Y	21785			Histone H1.1 OS=Mus musculus OX=10090 GN=H1-1 PE=1 SV=2
29	11	Q03265	200.00	7	3	3	N	59753			ATP synthase subunit alpha, mitochondrial OS=Mus musculus OX=10090 GN=Atp5f1a PE=1 SV=1
30	5	Q91VM5	200.00	14	4	1	N	42162			RNA binding motif protein, X-linked-like-1 OS=Mus musculus OX=10090 GN=Rbmxl1 PE=2 SV=1
36	121	P62960	200.00	11	1	1	N	35730			Y-box-binding protein 1 OS=Mus musculus OX=10090 GN=Ybx1 PE=1 SV=3
39	32	P10126	200.00	2	1	1	N	50114			Elongation factor 1-alpha 1 OS=Mus musculus OX=10090 GN=Eef1a1 PE=1 SV=3
43	57	Q9D6Z1	200.00	2	1	1	N	64464			Nucleolar protein 56 OS=Mus musculus OX=10090 GN=Nop56 PE=1 SV=2
44	77	Q61937	200.00	5	1	1	N	32560			Nucleophosmin OS=Mus musculus OX=10090 GN=Npm1 PE=1 SV=1
45	9	P56480	200.00	4	1	1	N	56301			ATP synthase subunit beta, mitochondrial OS=Mus musculus OX=10090 GN=Atp5f1b PE=1 SV=2
52	19	P20029	200.00	3	1	1	N	72422			Endoplasmic reticulum chaperone BiP OS=Mus musculus OX=10090 GN=Hspa5 PE=1 SV=3
53	21	P63017	200.00	2	1	1	N	70871			Heat shock cognate 71 kDa protein OS=Mus musculus OX=10090 GN=Hspa8 PE=1 SV=1
55	131	P62806	200.00	47	6	6	Y	11367			Histone H4 OS=Mus musculus OX=10090 GN=H4f16 PE=1 SV=2
60	76	Q8C2Q3	200.00	1	1	1	N	69449			RNA-binding protein 14 OS=Mus musculus OX=10090 GN=Rbm14 PE=1 SV=1
61	56	Q925I1	200.00	3	1	1	N	66742			ATPase family AAA domain-containing protein 3 OS=Mus musculus OX=10090 GN=Atad3 PE=1 SV=1
63	33	Q99JF8	200.00	4	1	1	N	59697			PC4 and SFRS1-interacting protein OS=Mus musculus OX=10090 GN=Psip1 PE=1 SV=1
67	34	P38647	200.00	2	1	1	N	73461			Stress-70 protein, mitochondrial OS=Mus musculus OX=10090 GN=Hspa9 PE=1 SV=3
68	99	Q8VEK3	200.00	2	1	1	N	87918			Heterogeneous nuclear ribonucleoprotein U OS=Mus musculus OX=10090 GN=Hnrnpu PE=1 SV=1
71	162	Q91VE6	200.00	6	1	1	N	36265			MKI67 FHA domain-interacting nucleolar phosphoprotein OS=Mus musculus OX=10090 GN=Nifk PE=1 SV=1
77	170	P62918	200.00	6	1	1	N	28025			60S ribosomal protein L8 OS=Mus musculus OX=10090 GN=Rpl8 PE=1 SV=2
80	105	Q9QZQ8	200.00	5	1	1	N	39735			Core histone macro-H2A.1 OS=Mus musculus OX=10090 GN=Macroh2a1 PE=1 SV=3
81	38	P12970	200.00	3	1	1	N	29977			60S ribosomal protein L7a OS=Mus musculus OX=10090 GN=Rpl7a PE=1 SV=2
84	143	Q9Z204	200.00	9	2	2	Y	34385			Heterogeneous nuclear ribonucleoproteins C1/C2 OS=Mus musculus OX=10090 GN=Hnrnpc PE=1 SV=1
85	169	Q88569	200.00	11	2	2	N	37403			Heterogeneous nuclear ribonucleoproteins A2/B1 OS=Mus musculus OX=10090 GN=Hnrnpa2b1 PE=1 SV=2
86	152	P62754	200.00	5	1	1	N	28681			40S ribosomal protein S6 OS=Mus musculus OX=10090 GN=Rps6 PE=1 SV=1
91	104	Q6PDM2	200.00	14	2	2	N	27745			Serine/arginine-rich splicing factor 1 OS=Mus musculus OX=10090 GN=Srsf1 PE=1 SV=3
94	257	Q99JB2	200.00	4	1	1	N	38385			Stomatin-like protein 2, mitochondrial OS=Mus musculus OX=10090 GN=Stoml2 PE=1 SV=1
101	110	Q8VIJ6	200.00	2	1	1	N	75442			Splicing factor, proline- and glutamine-rich OS=Mus musculus OX=10090 GN=Sfpq PE=1 SV=1

Protein Group	Protein ID	Accession	Significance	Coverage (%)	#Peptides	#Unique	PTM	Avg. Mass	Sample Profile	Group Profile	Description
108	200	P62242	200.00	13	2	2	N	24205			40S ribosomal protein S8 OS=Mus musculus OX=10090 GN=Rps8 PE=1 SV=2
110	95	P97351	200.00	9	1	1	N	29885			40S ribosomal protein S3a OS=Mus musculus OX=10090 GN=Rps3a PE=1 SV=3
111	283	P51881	200.00	7	1	1	Y	32931			ADP/ATP translocase 2 OS=Mus musculus OX=10090 GN=Slc25a5 PE=1 SV=3
113	411	P62264	200.00	30	3	3	N	16273			40S ribosomal protein S14 OS=Mus musculus OX=10090 GN=Rps14 PE=1 SV=3
116	247	P35979	200.00	10	1	1	N	17805			60S ribosomal protein L12 OS=Mus musculus OX=10090 GN=Rpl12 PE=1 SV=2
118	203	P62270	200.00	6	1	1	N	17719			40S ribosomal protein S18 OS=Mus musculus OX=10090 GN=Rps18 PE=1 SV=3
119	90	P14148	200.00	4	1	1	N	31420			60S ribosomal protein L7 OS=Mus musculus OX=10090 GN=Rpl7 PE=1 SV=2
127	107	P47963	200.00	10	2	2	N	24305			60S ribosomal protein L13 OS=Mus musculus OX=10090 GN=Rpl13 PE=1 SV=3
128	292	P84104	200.00	13	1	1	N	19330			Serine/arginine-rich splicing factor 3 OS=Mus musculus OX=10090 GN=Srsf3 PE=1 SV=1
141	326	Q9D8B3	200.00	13	2	2	N	24936			Charged multivesicular body protein 4b OS=Mus musculus OX=10090 GN=Chmp4b PE=1 SV=2
146	444	Q62093	200.00	10	1	1	Y	25476			Serine/arginine-rich splicing factor 2 OS=Mus musculus OX=10090 GN=Srsf2 PE=1 SV=4
151	146	P25444	200.00	4	1	1	N	31231			40S ribosomal protein S2 OS=Mus musculus OX=10090 GN=Rps2 PE=1 SV=3
154	725	P22629	200.00	10	1	1	N	18834			Streptavidin OS=Streptomyces avidinii OX=1895 PE=1 SV=1
156	175	P61358	200.00	6	1	1	N	15798			60S ribosomal protein L27 OS=Mus musculus OX=10090 GN=Rpl27 PE=1 SV=2
167	159	P35980	200.00	7	1	1	N	21645			60S ribosomal protein L18 OS=Mus musculus OX=10090 GN=Rpl18 PE=1 SV=3
168	130	Q6ZQ58	200.00	2	1	1	Y	121125			La-related protein 1 OS=Mus musculus OX=10090 GN=Larp1 PE=1 SV=3
175	264	P62849	200.00	9	1	1	N	15423			40S ribosomal protein S24 OS=Mus musculus OX=10090 GN=Rps24 PE=1 SV=1
189	245	Q61686	200.00	4	1	1	N	22186			Chromobox protein homolog 5 OS=Mus musculus OX=10090 GN=Cbx5 PE=1 SV=1
230	548	P62843	200.00	15	1	1	N	17040			40S ribosomal protein S15 OS=Mus musculus OX=10090 GN=Rps15 PE=1 SV=2
235	183	Q99K48	200.00	3	1	1	N	54541			Non-POU domain-containing octamer-binding protein OS=Mus musculus OX=10090 GN=Nono PE=1 SV=3
303	367	Q9CY66	200.00	8	1	1	N	23474			H/ACA ribonucleoprotein complex subunit 1 OS=Mus musculus OX=10090 GN=Gar1 PE=1 SV=1
333	265	Q9JJ80	200.00	4	1	1	N	35364			Ribosome production factor 2 homolog OS=Mus musculus OX=10090 GN=Rpf2 PE=2 SV=2
469	525	P47964	200.00	10	1	1	N	12216			60S ribosomal protein L36 OS=Mus musculus OX=10090 GN=Rpl36 PE=1 SV=2
480	284	Q9CQF0	200.00	9	1	1	N	20680			39S ribosomal protein L11, mitochondrial OS=Mus musculus OX=10090 GN=Mrpl11 PE=1 SV=1
124	173	P47915	135.20	7	1	1	N	17587			60S ribosomal protein L29 OS=Mus musculus OX=10090 GN=Rpl29 PE=1 SV=2
100	136	P41105	132.88	8	1	1	N	15733			60S ribosomal protein L28 OS=Mus musculus OX=10090 GN=Rpl28 PE=1 SV=2
274	620	P47955	123.90	14	1	1	N	11475			60S acidic ribosomal protein P1 OS=Mus musculus OX=10090 GN=Rplp1 PE=1 SV=1
114	149	P62751	110.40	11	2	2	N	17695			60S ribosomal protein L23a OS=Mus musculus OX=10090 GN=Rpl23a PE=1 SV=1
350	233	Q80WJ7	109.07	2	1	1	N	63846			Protein LYRIC OS=Mus musculus OX=10090 GN=Mtdh PE=1 SV=1
284	281	Q60875	63.31	2	1	1	N	111974			Rho guanine nucleotide exchange factor 2 OS=Mus musculus OX=10090 GN=Arhgef2 PE=1 SV=4
253	441	Q8BG05	59.73	6	1	1	N	39652			Heterogeneous nuclear ribonucleoprotein A3 OS=Mus musculus OX=10090 GN=Hnrnpa3 PE=1 SV=1
162	181	Q9D903	44.00	4	1	1	N	34703			Probable rRNA-processing protein EBP2 OS=Mus musculus OX=10090 GN=Ebna1bp2 PE=2 SV=1
93	207	Q08288	40.11	4	1	1	N	43736			Cell growth-regulating nucleolar protein OS=Mus musculus OX=10090 GN=Lyar PE=1 SV=2
51	336	P0C0S6	39.22	30	2	1	N	13553			Histone H2A.Z OS=Mus musculus OX=10090 GN=H2az1 PE=1 SV=2
51	337	Q3THW5	39.22	30	2	1	N	13509			Histone H2A.V OS=Mus musculus OX=10090 GN=H2az2 PE=1 SV=3
41	79	P84228	29.71	34	3	1	N	15388			Histone H3.2 OS=Mus musculus OX=10090 GN=H3c15 PE=1 SV=2
493	678	P62862	27.69	17	1	1	N	6648			40S ribosomal protein S30 OS=Mus musculus OX=10090 GN=Fau PE=1 SV=1
165	219	Q8BMF4	26.84	2	1	1	N	67942			Dihydrolipoyllysine-residue acetyltransferase component of pyruvate dehydrogenase complex, mitochondrial OS=Mus musculus OX=10090 GN=Dlat PE=1 SV=2

Figure 6.7: Detected proteins isolated through the Pull Down Assay
Pull Down Assay was performed with SK113AE-4, BW5147.3, and CCR4-deficient BW#19 and BW#20 using bCCL17, bCCL22, and bCXCL1. Chemokine-bound cells were isolated using streptavidin-coated magnetic beads and lysed. Potential interaction partners were digested using trypsin and measured through MS. (n=1)

6.6 Discussion

The present study revealed subtle phenotypic differences between CCL17$^{E/E}$ CCL22$^{-/-}$ and CCR4$^{-/-}$ mice in a mouse model of IL-33 treatment. CCR4$^{-/-}$ but not CCL17$^{E/E}$ CCL22$^{-/-}$ mice were protected from IL-33 weight loss and basophilic erythroblast counts were only significantly increased in CCL17$^{E/E}$ CCL22$^{-/-}$ (and CCL22$^{-/-}$). Additionally, there were differences between the two genotypes in KLRG1^{+} T_{reg} cell and RORγt^{+} T_{reg} cell composition as well as some erythroid progenitors in the spleen. In subsequent analysis, the binding of bCCL17 and bCCL22 by thymic and splenic T cells as well as myeloid and B cells even in the absence of CCR4 indicated and supported the presence of a second receptor for both chemokines. Hence, a Pull Down Assay was established to identify this second receptor. BW5147.3 cells were used for establishing the Pull Down Assay as this cell line originates from the thymus, where binding of bCCL17 and bCCL22 in the absence of CCL22 was observed. The BW5147.3 cell line originated from a thymic lymphoma in an AKR/J mouse (Köhler *et al.*, 1977), which was immortalised and primarily used to study TCRs (White *et al.*, 2020).

Chemokines are potent chemoattractants orchestrating immune cell migration into sites of inflammation and the tumor microenvironment. Atypical chemokine receptors (ACKR), while structurally similar to conventional chemokine receptors, fail to elicit downstream signaling (Hansell *et al.*, 2011). So far, four ACKR, showing differential ligand-specificity and distribution, have been identified (Gardner *et al.*, 2004; Savino *et al.*, 2009; Novitzky-Basso and Rot, 2012; Nibbs and Graham, 2013; Bonecchi and Graham, 2016). In the context of CCL17 and CCL22, ACKR1 and ACKR2 are most relevant. ACKR3 and ACKR4 show high ligand-specificity, each binding only 2-3 chemokines, neither CCL17 nor CCL22 (Nibbs and Graham, 2013). ACKR1 also known as Duffy antigen receptor for chemokines (DARC) is expressed on erythrocytes and endothelial cells of the blood vessel (Gardner *et al.*, 2004). Experiments with ACKR1-deficient mice uncovered that the receptor functions as a blood-borne buffer of inflammatory chemokines, regulating their bioavailability (Mangalmurti *et al.*, 2009; Schnabel *et al.*, 2010). Indeed, due to the lack of ACKR1

expression on erythrocytes, African people demonstrate higher levels of circulating chemokines (Howes *et al.*, 2011). *In vitro* ACKR1-transfected and polarised cells revealed that the receptor internalises after binding to a ligand and transports the chemokine across the cell where it is again presented to leukocytes, thereby promoting transcytosis. This ability is exclusive for ACKR1 (Pruenster *et al.*, 2009). In contrast, ACKR2, also called D6, is predominantly expressed on innate-like-B cells in mice (Bordon *et al.*, 2009). Additionally, low level transcripts of the receptor could be found in T cells, neutrophils, *in vitro*-derived DC, and mast cells. It functions as a chemokine scavenger removing excessive chemokines from the extracellular space, thereby inhibiting leukocyte recruitment and promoting the resolution of inflammation. Upon ligand engagement, the receptor is rapidly internalised. While the receptor is later recycled and transported back to the surface, the chemokine is degraded in the lysosome (Weber *et al.*, 2004). Concomitant with the literature, untransfected BW5147.3 cells migrated towards CCL17 or CCL22 with CCL22 being the more potent inducer of migration (Figure 6.2F) (Fülle *et al.*, 2018). Loss of CCR4, however, abolished cell migration towards CCL17 or CCL22, although both CCR4-deficient cell clones were observed to still bind bCCL17 and bCCL22 (Figure 6.2F). A similar finding was also obtained using primary thymocytes (Figure 6.3). This indicates a non-migratory function of the second receptor, consistent with the functions of ACKR. ACKR1 is not expressed on lymphocytes and only shows ligand-specificity for CCL17 (Gardner *et al.*, 2004), leaving no explanation for bCCL22 binding in the absence of CCR4. ACKR2 regulates the activity of both chemokines, although it preferentially binds to CCL22 (Santulli-Marotto, Boakye, *et al.*, 2013). Low levels of ACKR2 transcription were found in T cells from the lymph node and spleen (Mckimmie *et al.*, 2008). On protein level, approximately 40 % of naïve $CD4^+$ T cells and 30 % of $CD8^+$ T cells of the blood showed ACKR2 expression. The expression is reduced in memory or transition T cells. In addition, ACKR2 expression is not only found on the surface of these cells but also intracellularly, suggesting pre-formed receptor molecules that are transported to the cell surface upon a stimulus (Pacheco *et al.*, 2022). In conclusion, ACKR2 expression in T cell subsets tested in this study

and in BW5147.3 cells might explain binding of the biotinylated chemokines. Whereas ACKR expression on lymphocytes might explain binding of bCCL17 and bCCL22 without inducing migration, it would not explain the differences observed between $CCL17^{E/E}$ $CCL22^{-/-}$ and $CCR4^{-/-}$ mice in the IL-33 model nor the differential function of both chemokines in a DNFB-induced CHS model (Fülle *et al.*, 2018).

Initially, GPCR were thought to function as monomers. For example, the monomeric rhodopsin receptor is sufficient to couple to a G protein, phosphorylate the rhodopsin kinase and bind arrestin-1 (Whorton *et al.*, 2007; Whorton *et al.*, 2008; Bayburt *et al.*, 2011). Since then, however, many GPCR, including chemokine receptors, were shown to form homo- and heteromers. Such receptor clusters are thought to be crucial for the assembly of large signaling hubs. In many cell types, clusters of CD4, CCR5 and CXCR4 have been observed. These clusters were primarily found on microvilli and intracellularly in trans golgi vesicles (Singer *et al.*, 2001). The function of chemokine receptor clusters has yet to be investigated but it is suggested that they are involved in sensing the environment during cell migration. Receptor oligomerisation can be dependent or independent of the ligand (Vila-Coro *et al.*, 1999; Vila-Coro *et al.*, 2000). Several studies, investigating chemokine receptor complexes, highlighted that (i) ligand-binding by one of the receptors within the complex inhibits ligand binding of the other receptors, (ii) receptor heterodimers can only engage with one single chemokine, and (iii) interaction occurs between receptor homo- and heterodimers, forming larger allosteric clusters of chemokine receptors (Springael *et al.*, 2006; Sohy *et al.*, 2007; Sohy *et al.*, 2009). Another example of chemokine receptor clusters are CCR2 and CCR5 that can form heterodimers with each other (El-Asmar *et al.*, 2005). Interestingly, interaction between CCL2 and monomeric CCR2 was unaffected by the presence of CCR5 ligands (CCL4 and CCL5) and *vice versa* for CCR5 and its ligand by the presence of CCL2. Dimerisation of both receptors, however, caused the inhibition of one receptor by ligand-receptor-engagement of the second receptor (Percherancier *et al.*, 2005). In the context of CXCR7-CXCR4-oligomerisation, receptor complexes showed an increased response to CXCL12, measured by calcium flux, and decreased inhibition cAMP

(Percherancier *et al.*, 2005; Levoye *et al.*, 2009; Decaillot *et al.*, 2011). Oligomerisation is not exclusive between chemokine receptor pairs. Moreover, chemokine receptors can form oligomers with receptors not belonging to the chemokine receptor family, mostly the opioid family of GPCR (Suzuki *et al.*, 2002; Chen *et al.*, 2004; Pello *et al.*, 2008; Parenty *et al.*, 2008). In conclusion, the second receptor might be expressed in a complex with CCR4 on the cell surface but fails to initiate signaling in the absence of CCR4. Therefore, it is more likely that the second receptor within this complex does not belong to the chemokine receptor family.

The Pull Down Assay performed with cell culture cells to identify possible second receptor candidates, primarily yielded nuclear proteins instead of surface receptors, indicating the necessity for protocol optimisation. Pull Down Assays or co-immunoprecipitation (Co-IP) are the primary method used for purification and identification of protein-protein or protein-nucleic acid interactions (Nilsson *et al.*, 2010). Most commonly, a specific antibody is immobilised and used for enrichment of the target protein and its direct as well as indirect interaction partners. Downstream processing often includes western blotting or MS (Meyer and Selbach, 2015). In the present study, the Pull Down Assay was performed using the respective chemokines and intact target cells were enriched via biotin-streptavidin interaction. The protocol used resembles a two-step Co-IP, which unites two consecutive Co-IPs and was developed to achieve higher purity and better enrichment. The first Co-IP employs a biotinylated antibody against the bait protein. Afterwards, the protein complex is eluted using an anti-biotin substrate. Finally, the complex is re-precipitated with protein A/G beads (Sciuto *et al.*, 2018).

However, the protocol used in this study relied on multiple washing steps to remove proteins unspecifically bound to the biotinylated chemokine. Multiple washing steps with repeated centrifugation, aspiration and resuspension, causes a continuous if small loss of target protein, which is especially concerning if the target protein is expressed in low abundance. Reduction of washing steps, however, might decrease specificity.

An additional factor to consider is the lysis of the cells to exclusively enrich for target protein interaction complexes. As typical for GPCR, chemokine receptors consist of seven transmembrane domains connected through extramembranous loops (Allen *et al.*, 2007). The N-terminus is located outside the cell, while the C-terminus is located within the cytoplasma. The N-terminus is especially important for ligand binding (Mayer and Stone, 2000; Booth *et al.*, 2002), although additional extracellular loops are involved in interaction with the ligand (Skelton *et al.*, 1999; Blanspain *et al.*, 2003). Therefore, the chemokine receptor structure is essential for ligand binding. A too long or aggressive lysis might result in the loss of the chemokine receptor structure and subsequent disengagement of the ligand. However, gentle lysis conditions might maintain chemokine receptor integrity but could cause the enrichment of unspecific binders. This is especially problematic for the identification of protein complex members in low abundancy, which are overshadowed by the myriad of non-specific proteins (Selbach and Mann, 2006).

To increase purity and enrichment, several approaches could be employed. Tandem Affinity Purification uses two separate tags fused to one single bait protein for affinity purification. Enrichment of the protein via sequential usage of the tags yields higher purity, which is beneficial for MS (Rigaut *et al.*, 1999; Bürckstümmer *et al.*, 2006; Li, 2010; Bigenzahn *et al.*, 2016). This method is limited, however, as artificial fusion of the tags to the bait protein might interfere with protein functions, such as binding to their interaction partners. In the case of low abundance of the targeted receptor, rapid immunoprecipitation MS of endogenous protein (RIME) could be employed. RIME, combined with MS, is a sensitive method for identification of protein complexes with low-abundance proteins (Mohammed *et al.*, 2016). To stabilise the complex, formaldehyde is used as a cross-linking reagent. Formaldehyde is small and can penetrate the cell membrane, cross-linking proteins intracellularly and in close proximity. In addition, its fast reaction can conserve even transient protein-protein interactions (Vasilescu *et al.*, 2004; Sutherland *et al.*, 2008; Srinivasa *et al.*, 2015).

In conclusion, to improve the Pull Down Assay, cross-linking of the chemokine-chemokine receptor-complex, higher target cell concentration, and lysis optimisation should be considered.

Chapter 7: Concluding remarks

7.1 CCL17 and CCL22 in *Salmonella* infection

The role of CCL17 and CCL22 on the adaptive immune response against *Salmonella* infections was investigated in this study by comparing the survival and T cell composition of vaccinated and challenged CCL17$^{E/E}$ CCL22$^{-/-}$, CCR4$^{-/-}$, and wt mice. Chemokine- or chemokine receptor-deficient mice were more susceptible to *Salmonella* challenge, probably due to impaired immune cell recruitment, especially T cells, and altered T cell activation. As chemoattractants, both CCL17 and CCL22 are well described in T cell recruitment (Sebastiani *et al.*, 2001; Curiel *et al.*, 2004; Weber *et al.*, 2011; Eby *et al.*, 2015; Wiedemann *et al.*, 2016; Fülle *et al.*, 2018; Ketcham *et al.*, 2018) and activation through facilitation of the DC-T cell interaction (Semmling *et al.*, 2010; Rapp *et al.*, 2019). Impairments in both of these processes might reduce the number of activated CD4$^+$ T cells, which are essential for the clearance of *Salmonella* infection (Weintraub *et al.*, 1998; Ravindran *et al.*, 2005; Kupz *et al.*, 2014). In addition, KLRG1$^+$ T_{reg} cells were shown to be reduced in naïve CCL17$^{E/E}$ CCL22$^{-/-}$ and CCR4$^{-/-}$ mice compared to naïve wt mice, suggesting a possible impact during the vaccination phase in generating long-lasting immunity.

The present study gave insights into the involvement of the CCL17/CCL22/CCR4-axis in the context of infection, a field that has not been extensively researched in the literature. Future investigations should focus on determining the contributing factor(s) for vaccine efficiency. Therefore, it is necessary to analyse the immune cell composition in PP, mLN, and spleen during the vaccination phase and at earlier time points of the STM challenge (approximately 5 days post challenge). In this context, it should also be determined if CCL17, CCL22, or both in combination are promoting survival of animals after STM challenge. Hence, chemokine single-deficient mice should be employed for further investigations. Additionally, it would be interesting to analyse the impact of the gut microbiome on the chemokine levels, both in steady state and during infection. The differential outcomes in the infection experiments in

Melbourne and Bonn, highlighted a prominent role of the gut microbiota beyond the direct interference with the pathogen (Lv *et al.*, 2019).

7.2 CCL17 and CCL22 in IL-33-mediated immune responses

The interplay between IL-33-mediated immune responses and the CCL17/CCL22/CCR4-axis was investigated by administering IL-33 to wt and single- or double-knockouts of the receptor and the respective chemokines.

KLRG1^{+} T_{reg} cells, although expressing ST2 in lower levels than previously investigated adipose tissue T_{reg} cells (Vasanthakumar *et al.*, 2015), expanded in response to the IL-33 treatment. This expansion was independent of the genotype or organ (PP, mLN, and spleen). Overall, the results were in line with the literature (Schiering *et al.*, 2014; Vasanthakumar *et al.*, 2015; Matta *et al.*, 2016) and proved the functionality of the model in our lab.

IL-33 impaired terminal erythroid differentiation in the BM, visualised through the reduction of erythroid progenitor counts, except for the last erythroblastic stage (orthochromatic erythroblasts). This process was independent of CCL17, CCL22, and CCR4. Meanwhile, CFU-E, ProEry, and basophilic erythroblast were increased in the spleen, especially in the IL-33-treated CCL22$^{-/-}$ and CCL17$^{E/E}$ CCL22$^{-/-}$ mice. Subsequent studies should focus on determining if IL-33 directly induces extramedullary erythropoiesis in the spleen or if this is induced indirectly by the impairment of BM erythropoiesis as described (Millot *et al.*, 2010; Jackson *et al.*, 2010; Greenwald *et al.*, 2019; Jing *et al.*, 2021). In this context, the kinetics of the erythropoiesis in BM and spleen after IL-33 treatment should be assessed. Additionally, prolongated IL-33 administration should be considered to assess (i) whether similar counts of orthochromatic erythroblasts in the BM are due to unresponsiveness to a direct IL-33 stimulus and depletion of the progenitor pool to uphold erythropoiesis; and (ii) whether polychromatic and orthochromatic erythroblasts in the spleen are expanded in the long run.

The present study showed a novel role for CCL17 and CCL22 in adipose tissue homeostasis, which has not been well described so far (Conti *et al.*, 2004;

Macdougall *et al.*, 2018). Key observations from the present study included the expression of CCL17 in the iWAT of naïve mice, visualised through use of the reporter line CCL17$^{E/E}$, and the BAT morphology change in the absence of CCL22. Additionally, an IL-33-induced increase in fibrosis of iWAT was not observed in CCL22$^{-/-}$ mice, implicating a detrimental role of CCL22 in fibrosis development. In contrast, CCL17$^{E/E}$ CCL22$^{-/-}$ mice were not protected from IL-33-induced iWAT fibrosis, suggesting a supplementary and beneficial role of CCL17 counteracting the dominant CCL22 stimulus. The iWAT fibrosis was accompanied by massive immune cell infiltration, potentially increasing the CCL17 and CCL22 levels further. Future studies should consider the following: Which cell types express CCL17 in the steady state? Next to M2 macrophages (Mantovani *et al.*, 2004; Orecchioni *et al.*, 2019), present in the steady state and maintaining adipose tissue homeostasis (Weisberg *et al.*, 2003; Kurowska-Stolarska *et al.*, 2009; Chawla *et al.*, 2011), might pre- and mature adipocytes also have a potential to secrete CCL17 and/or CCL22? Is CCL22 also expressed in the iWAT? Do the chemokine levels increase after IL-33 treatment in the adipose tissue? How does the cell composition between steady state and inflammatory state change? Which cell types are driving the IL-33-induced iWAT fibrosis? For the last question, eosinophils might be a likely candidate, as they are already present in the adipose tissue during steady state and IL-33 treatment significantly increased eosinophils in the BM. Absence of the chemokines or their receptor, however, potentially impaired eosinophil migration into the tissue as eosinophilia in the blood was only observed in knockout mice. As the increase in eosinophils was substantial, they are likely to contribute to both the iWAT fibrosis and the splenomegaly observed after IL-33 treatment. In follow-up studies, eosinophil localisation throughout the organism and their contribution to iWAT fibrosis after IL-33 treatment should be investigated.

During the experimental procedure, weight loss of IL-33-treated animals, except CCR4$^{-/-}$ mice, was observed. Morphologic changes, suggestive of lipid loss, were obvious in mice treated with IL-33. CCL22$^{-/-}$ mice were the only exception from this finding, again supporting a role for the chemokine in adipose tissue homeostasis.

Lipid loss and weight reduction of the BAT, however, was only observed in wt mice, supporting the relevance of both chemokines in adipose tissue homeostasis. To uncover the reason for the IL-33-induced weight loss, UCP-1 expression should be analysed in the iWAT, BAT, and other adipose tissue depots. UCP-1 upregulation is linked to browning in the WAT, indicative of a higher thermogenesis (Brestoff *et al.*, 2015; Thyagarajan and Foster, 2017; Lee *et al.*, 2021). Concomitantly, IL-33 is also known to increase energy expenditure (Brestoff *et al.*, 2015).

Overall, IL-33 treatment has been shown to elicit a variety of immune responses, correlating with its pleiotropic functional spectrum. Most strikingly, however, was the effect of the CCL17/CCL22/CCR4-axis regarding adipose tissue homeostasis and fibrosis as well as eosinophilia. Uncovering both protective and detrimental functions of CCL17 and CCL22 in the adipose tissue, might reveal new key players in adipose tissue diseases such as obesity, an increasing problem worldwide (Budnik and Henneberg, 2017).

7.3 Additional receptor for CCL17 and CCL22

The present study also demonstrated that CCL17 and CCL22 can bind to primary T cells (overall $CD4^+$ T cell, $GATA3^+$ T cells, T_{reg} cells, and $CD8^+$ T cells), primary myeloid cells and the T cell lymphoma cell line BW5147.3 even in the absence of the chemokine receptor CCR4. The postulated second receptor, however, does not appear to induce cell migration as CCR4-deficiency abolished migration towards CCL17 and CCL22. Possible candidates as second receptor are ACKR, although this would not explain the functional differences between $CCL17^{E/E}$ $CCL22^{-/-}$ and $CCR4^{-/-}$ mice in IL-33-mediated immune responses (observed in this study) and DNFB-induced CHS (Fülle *et al.*, 2018); or a receptor not belonging to the chemokine receptor family. Additionally, the second receptor might cluster with CCR4 and requires this interaction to elicit signaling. A first attempt to uncover the second receptor was performed but requires further optimisation. Next to increasing target cell input, decreasing washing steps, and adjusting lysis conditions, cross-linking of the interaction partners is probably the best approach to secure the identification of

interaction partners in low abundance forming transient interactions only (Vasilescu *et al.*, 2004; Sutherland *et al.*, 2008; Srinivasa *et al.*, 2015; Mohammed *et al.*, 2016). Furthermore, additional functional studies, such as calcium flux measurements could be employed to narrow potential receptor candidates. In parallel, the possibility of a third ligand for CCR4 should be acknowledged and analysed using bioinformatics to predict candidates in combination with experimental approaches such as ligand screening.

As part of this project, a chemokine-based receptor staining using biotinylated chemokines has been established and validated. Determination of the staining specificity through competitive binding assays revealed that unlabeled CCL22 enhanced the staining signal, meaning the binding efficiency, of bCCL22. Homo- or heterodimerisation of CCL17 and CCL22 with themselves or each other could be excluded using BN-PAGE. To explain this binding phenomenon, future studies, should focus on determining the potential positive cooperativity of the chemokine receptor CCR4. Cooperativity is a well described process in ligand-receptor-interactions, including GPCR, protein folding, and enzyme-substrate reactions (Notides *et al.*, 1981; Harikumar *et al.*, 2007; Gao *et al.*, 2009; Roed *et al.*, 2012; Sevlever *et al.*, 2020).

Determining additional players in the CCL17/CCL22/CCR4-axis would add additional complexity to the chemokine network and be an important aspect to consider in future applications, disease studies and even therapeutic approaches.

Chapter 8: References

Abbas, A.K. *et al.* (2013) 'Regulatory T Cells: Recommendations to Simplify the Nomenclature'. *Nature Immunology*, 14(4), pp. 307–308. DOI: 10.1038/ni.2554.

Achtman, M. *et al.* (2020) 'Genomic Diversity of Salmonella Enterica -The UoWUCC 10K Genomes Project'. *Wellcome Open Research*, 5, p. 223. DOI: 10.12688/wellcomeopenres.16291.1.

Achuthan, A. *et al.* (2016) 'Granulocyte Macrophage Colony-Stimuating Factor Induces CCL17 Production via IRF4 to Mediate Inflammation'. *The Journal of Clinical Investigation*, 126(9), pp. 3453–3466. DOI: 10.1172/JCI87828DS1.

Ahluwalia, B., Magnusson, M.K. and Öhman, L. (2017) 'Mucosal Immune System of the Gastrointestinal Tract: Maintaining Balance between the Good and the Bad'. *Scandinavian Journal of Gastroenterology*, 52(11), pp. 1185–1193. DOI: 10.1080/00365521.2017.1349173.

Ajram, L. *et al.* (2014) 'Internalization of the Chemokine Receptor CCR4 Can Be Evoked by Orthosteric and Allosteric Receptor Antagonists'. *European Journal of Pharmacology*, 729(1), pp. 75–85. DOI: 10.1016/j.ejphar.2014.02.007.

Akimova, T. *et al.* (2011) 'Helios Expression Is a Marker of T Cell Activation and Proliferation'. *PLoS ONE*, 6(8). DOI: 10.1371/journal.pone.0024226.

Al-Haidari, A.A. *et al.* (2013) 'CCR4 Mediates CCL17 (TARC)-Induced Migration of Human Colon Cancer Cells via RhoA/Rho-Kinase Signaling'. *International Journal of Colorectal Disease*, 28(11), pp. 1479–1487. DOI: 10.1007/s00384-013-1712-y.

Alexander, M.P. *et al.* (2015) 'Renal Extramedullary Hematopoiesis: Interstitial and Glomerular Pathology'. *Modern Pathology*, 28(12), pp. 1574–1583. DOI: 10.1038/modpathol.2015.117.

Alferink, J. *et al.* (2003) 'Compartmentalized Production of CCL17 In Vivo: Strong Inducibility in Peripheral Dendritic Cells Contrasts Selective Absence from the Spleen'. *The Journal of Experimental Medicine*, 197(5), pp. 585–599. DOI: 10.1084/jem.20021859.

Ali, S. *et al.* (2011) ‘The Dual Function Cytokine IL-33 Interacts with the Transcription Factor NF-KB To Dampen NF-KB–Stimulated Gene Transcription’. *The Journal of Immunology*, 187(4), pp. 1609–1616. DOI: 10.4049/jimmunol.1003080.

Allen, S.J., Crown, S.E. and Handel, T.M. (2007) ‘Chemokine: Receptor Structure, Interactions, and Antagonism’. *Annual Review of Immunology*, 25, pp. 787–820. DOI: 10.1146/annurev.immunol.24.021605.090529.

Anand, G. *et al.* (2014) ‘Increased IL-12 and Decreased IL-33 Serum Levels Are Associated with Increased Th1 and Suppressed Th2 Cytokine Profile in Patients with Diabetic Nephropathy (CURES-134)’. *International Journal of Clinical and Experimental Pathology*, 7(11), pp. 8008–8015.

Anderson, C.A., Solari, R. and Pease, J.E. (2016) ‘Biased Agonism at Chemokine Receptors: Obstacles or Opportunities for Drug Discovery?’ *Journal of Leukocyte Biology*, 99(6), pp. 901–909. DOI: 10.1189/jlb.2mr0815-392r.

Andrade, M. V. *et al.* (2011) ‘Amplification of Cytokine Production through Synergistic Activation of NFAT and AP-1 Following Stimulation of Mast Cells with Antigen and IL-33’. *European Journal of Immunology*, 41(3), pp. 760–772. DOI: 10.1002/eji.201040718.

Anselmo, A. *et al.* (2014) ‘Flow Cytometry Applications for the Analysis of Chemokine Receptor Expression and Function’. *Cytometry Part A*, 85(4), pp. 292–301. DOI: 10.1002/cyto.a.22439.

Arimont, M. *et al.* (2017) ‘Structural Analysis of Chemokine Receptor-Ligand Interactions’. *Journal of Medicinal Chemistry*, 60(12), pp. 4735–4779. DOI: 10.1021/acs.jmedchem.6b01309.

Arner, P. *et al.* (2011) ‘Dynamics of Human Adipose Lipid Turnover in Health and Metabolic Disease’. *Nature*, 478(7367), pp. 110–113. DOI: 10.1038/nature10426.

Awad, K. *et al.* (2023) ‘Impaired Intestinal Permeability of Tricellular Tight Junctions in Patients with Irritable Bowel Syndrome with Mixed Bowel Habits (IBS-M)’. *Cells*, 12(2). DOI: 10.3390/cells12020236.

Baekkevold, E.S. *et al.* (2003) ‘Molecular Characterization of NF-HEV, a Nuclear Factor Preferentially Expressed in Human High Endothelial Venules’. *American Journal of Pathology*, 163(1), pp. 69–79. DOI: 10.1016/S0002-9440(10)63631-0.

Bagchi, D.P. and MacDougald, O.A. (2019) ‘Identification and Dissection of Diverse Mouse Adipose Depots’. *Journal of Visualized Experiments*. DOI: 10.3791/59499.

Bakowski, M.A. *et al.* (2007) ‘SopD Acts Cooperatively with SopB during Salmonella Enterica Serovar Typhimurium Invasion’. *Cellular Microbiology*, 9(12), pp. 2839–2855. DOI: 10.1111/j.1462-5822.2007.01000.x.

Bakowski, M.A. *et al.* (2010) ‘The Phosphoinositide Phosphatase SopB Manipulates Membrane Surface Charge and Trafficking of the Salmonella-Containing Vacuole’. *Cell Host and Microbe*, 7(6), pp. 453–462. DOI: 10.1016/j.chom.2010.05.011.

Balabanian, K. *et al.* (2005) ‘The Chemokine SDF-1/CXCL12 Binds to and Signals through the Orphan Receptor RDC1 in T Lymphocytes’. *Journal of Biological Chemistry*, 280(42), pp. 35760–35766. DOI: 10.1074/jbc.M508234200.

Baliban, S.M. *et al.* (2018) ‘Immunogenicity and Efficacy Following Sequential Parenterally-Administered Doses of Salmonella Enteritidis COPS:FliC Glycoconjugates in Infant and Adult Mice’. *PLoS Neglected Tropical Diseases*, 12(5), pp. 1–20. DOI: 10.1371/journal.pntd.0006522.

Baliban, S.M., Lu, Y.J. and Malley, R. (2020) ‘Overview of the Nontyphoidal and Paratyphoidal Salmonella Vaccine Pipeline: Current Status and Future Prospects’. *Clinical Infectious Diseases*, 71(day 28), pp. S151–S154. DOI: 10.1093/cid/ciaa514.

Bao, Y. *et al.* (2018) ‘Extramedullary Hematopoiesis Secondary to Malignant Solid Tumors: A Case Report and Literature Review’. *Cancer Management and Research*, 10, pp. 1461–1470. DOI: 10.2147/CMAR.S161746.

Bargut, T.C.L. *et al.* (2017) ‘Browning of White Adipose Tissue: Lessons from Experimental Models’. *Hormone Molecular Biology and Clinical Investigation*, 31(1), pp. 1–13. DOI: 10.1515/hmbci-2016-0051.

Barlow, J.L. *et al.* (2013) ‘IL-33 Is More Potent than IL-25 in Provoking IL-13-

Producing Nuocytes (Type 2 Innate Lymphoid Cells) and Airway Contraction'. *Journal of Allergy and Clinical Immunology*, 132(4), pp. 933–941. DOI: 10.1016/j.jaci.2013.05.012.

Bayburt, T.H. *et al.* (2011) 'Monomeric Rhodopsin Is Sufficient for Normal Rhodopsin Kinase (GRK1) Phosphorylation and Arrestin-1 Binding'. *Journal of Biological Chemistry*, 286(2), pp. 1420–1428. DOI: 10.1074/jbc.M110.151043.

Beck, T.C. *et al.* (2014) 'CXCR4 and a Cell-Extrinsic Mechanism Control Immature B Lymphocyte Egress from Bone Marrow'. *Journal of Experimental Medicine*, 211(13), pp. 2567–2581. DOI: 10.1084/jem.20140457.

Bel, S. *et al.* (2017) 'Paneth Cells Secrete Lysozyme via Secretory Autophagy during Bacterial Infection of the Intestine'. *Science*, 357(6355), pp. 1047–1052.

Belperio, J.A. *et al.* (2004) 'The Role of the Th2 CC Chemokine Ligand CCL17 in Pulmonary Fibrosis'. *The Journal of Immunology*, 173(7), pp. 4692–4698. DOI: 10.4049/jimmunol.173.7.4692.

Beltrán, C.J. *et al.* (2010) 'Characterization of the Novel ST2/IL-33 System in Patients with Inflammatory Bowel Disease'. *Inflammatory Bowel Diseases*, 16(7), pp. 1097–1107. DOI: 10.1002/ibd.21175.

Benoun, J.M. *et al.* (2018) 'Optimal Protection against Salmonella Infection Requires Noncirculating Memory'. *Proceedings of the National Academy of Sciences*, p. 201808339. DOI: 10.1073/pnas.1808339115.

Bergers, G. *et al.* (1994) 'Alternative Promoter Usage of the Fos-Responsive Gene Fit-1 Generates MRNA Isoforms Coding for Either Secreted or Membrane-Bound Proteins Related to the IL-1 Receptor'. *EMBO Journal*, 13(5), pp. 1176–1188. DOI: 10.1002/j.1460-2075.1994.tb06367.x.

Bergsbaken, T., Fink, S.L. and Cookson, B.T. (2009) 'Pyroptosis: Host Cell Death and Inflammation'. *Nature Reviews Microbiology*, 7(2), pp. 99–109. DOI: 10.1038/nrmicro2070.

Besnard, A.G. *et al.* (2011) 'IL-33-Activated Dendritic Cells Are Critical for Allergic

Airway Inflammation'. *European Journal of Immunology*, 41(6), pp. 1675–1686. DOI: 10.1002/eji.201041033.

Bessa, J. *et al.* (2014) 'Altered Subcellular Localization of IL-33 Leads to Non-Resolving Lethal Inflammation'. *Journal of Autoimmunity*, 55(1), pp. 33–41. DOI: 10.1016/j.jaut.2014.02.012.

Bessis, M. (1958) 'L'îlot Érythroblastique, Unité Fonctionnelle de La Moelle Osseuse [Erythroblastic Island, Functional Unity of Bone Marrow]'. *Review Hematology*, 13(1), pp. 8–11. DOI: 13555228.

Bessis, M. and Breton-Gorius, J. (1957) 'Granules Ferrugineux Dans Les Cellules Macrophages et Les Érythrocytes Au Cours Du Saturnisme Expérimental. Examen Au Microscope Électronique. [Ferruginous Granules in Macrophage Cells and Erythrocytes in Experimental Saturnism; E'. *Comptes Rendus Des Séances de La Société de Biologie et de Ses Filiales*, 151(2), pp. 275–276.

Bessis, M.C. and Breton-Gorius, J. (1962) 'Iron Metabolism in the Bone Marrow as Seen by Electron Microscopy: A Critical Review'. *Blood*, 19, pp. 635–63.

Bevins, C.L. and Salzman, N.H. (2011) 'Paneth Cells, Antimicrobial Peptides and Maintenance of Intestinal Homeostasis'. *Nature Reviews Microbiology*, 9(5), pp. 356–368. DOI: 10.1038/nrmicro2546.

Bigenzahn, J.W. *et al.* (2016) 'An Inducible Retroviral Expression System for Tandem Affinity Purification Mass- Spectrometry-Based Proteomics Identifies Mixed Lineage Kinase Domain-like Protein (MLKL) as an Heat Shock Protein 90 (HSP90) Client'. *Molecular and Cellular Proteomics*, 15, pp. 1139–1150. DOI: 10.1074/mcp.O115.055350.

Bijnen, M. *et al.* (2018) 'Adipose Tissue Macrophages Induce Hepatic Neutrophil Recruitment and Macrophage Accumulation in Mice'. *Gut*, 67, pp. 1317–1327.

Billett, H.H. (1990) 'Hemoglobin and Hematocrit'. In Walter, H.Hall, W.and Hurst, J. (eds.) *Clinical Methods: The History, Physical, and Laboratory Examinations*. Boston: Butterworths.

Bischoff, L. *et al.* (2015) ‘Cellular Mechanisms of CCL22-Mediated Attenuation of Autoimmune Diabetes’. *The Journal of Immunology*, 194(7), pp. 3054–3064. DOI: 10.4049/jimmunol.1400567.

Bischoff, S.C. *et al.* (2014) ‘Intestinal Permeability - a New Target for Disease Prevention and Therapy’. *BMC Gastroenterology*, 14(1), pp. 1–25. DOI: 10.1186/s12876-014-0189-7.

Blanc, L. *et al.* (2005) ‘Exosome Release by Reticulocytes - An Integral Part of the Red Blood Cell Differentiation System’. *Blood Cells, Molecules, and Diseases*, 35(1), pp. 21–26. DOI: 10.1016/j.bcmd.2005.04.008.

Blanspain, C. *et al.* (2003) ‘The Core Domain of Chemokines Binds CCR5 Extracellular Domains While Their Amino Terminus Interacts with the Transmembrane Helix Bundle’. *Journal of Biological Chemistry*, 278(7), pp. 5179–5187. DOI: 10.1074/jbc.M205684200.

Bochner, B.S. *et al.* (2003) ‘Release of Both CCR4-Active and CXCR3-Active Chemokines during Human Allergic Pulmonary Late-Phase Reactions’. *Journal of Allergy and Clinical Immunology*, 112(5), pp. 930–934. DOI: 10.1016/j.jaci.2003.08.012.

De Boer, O.J. *et al.* (1999) ‘Cytokine Secretion Profiles of Cloned T Cells from Human Aortic Atherosclerotic Plaques’. *Journal of Pathology*, 188(2), pp. 174–179. DOI: 10.1002/(SICI)1096-9896(199906)188:2<174::AID-PATH333>3.0.CO;2-3.

Bonaud, A. *et al.* (2021) ‘Hematopoietic Multipotent Progenitors and Plasma Cells: Neighbors or Roommates in the Mouse Bone Marrow Ecosystem?’ *Frontiers in Immunology*, 12(April), pp. 1–13. DOI: 10.3389/fimmu.2021.658535.

Bonecchi, R. *et al.* (1998) ‘Differential Expression of Chemokine Receptors and Chemotactic Responsiveness of Type 1 T Helper Cells (Th1s) and Th2s’. *Journal of Experimental Medicine*, 187(1), pp. 129–134. DOI: 10.1084/jem.187.1.129.

Bonecchi, R. *et al.* (2004) ‘Differential Recognition and Scavenging of Native and Truncated Macrophage-Derived Chemokine (Macrophage-Derived Chemokine/CC

Chemokine Ligand 22) by the D6 Decoy Receptor'. *The Journal of Immunology*, 172(8), pp. 4972–4976. DOI: 10.4049/jimmunol.172.8.4972.

Bonecchi, R. and Graham, G.J. (2016) 'Atypical Chemokine Receptors and Their Roles in the Resolution of the Inflammatory Response'. *Frontiers in Immunology*, 7(JUN), pp. 1–7. DOI: 10.3389/fimmu.2016.00224.

Booth, V. *et al.* (2002) 'The CXCR3 Binding Chemokine IP-10 / CXCL10 : Structure and Receptor'. *Biochemistry*, 41, pp. 10418–10425. DOI: 10.1021/bi026020q.

Bordon, Y. *et al.* (2009) 'The Atypical Chemokine Receptor D6 Contributes to the Development of Experimental Colitis'. *Journal of Immunology*, 182(8), pp. 5032–5040. DOI: 10.4049/jimmunol.0802802.

Bourgeois, E. *et al.* (2009) 'The Pro-Th2 Cytokine IL-33 Directly Interacts with Invariant NKT and NK Cells to Induce IFN-γ Production'. *European Journal of Immunology*, 39(4), pp. 1046–1055. DOI: 10.1002/eji.200838575.

Bozzini, C.E. *et al.* (1970) 'Studies on Medullary and Extramedullary Erythropoiesis in the Adult Mouse.' *The American Journal of Physiology*, 219(3), pp. 724–728. DOI: 10.1152/ajplegacy.1970.219.3.724.

Brandtzaeg, P. *et al.* (2008) 'Terminology: Nomenclature of Mucosa-Associated Lymphoid Tissue'. *Mucosal Immunology*, 1(1), pp. 31–37. DOI: 10.1038/mi.2007.9.

Bravo-Blas, A. *et al.* (2019) ' Salmonella Enterica Serovar Typhimurium Travels to Mesenteric Lymph Nodes Both with Host Cells and Autonomously '. *The Journal of Immunology*, 202(1), pp. 260–267. DOI: 10.4049/jimmunol.1701254.

Brenner, F.W. *et al.* (2000) 'Guest Commentary: Salmonella Nomenclature'. *Journal of Clinical Microbiology*, 38(7), pp. 2465–2467.

Brestoff, J.R. *et al.* (2015) 'Group 2 Innate Lymphoid Cells Promote Beiging of White Adipose Tissue and Limit Obesity'. *Nature*, 519(7542), pp. 242–246. DOI: 10.1038/nature14115.

Le Brocq, M.L. *et al.* (2014) 'Chemokines as Novel and Versatile Reagents for Flow Cytometry and Cell Sorting'. *The Journal of Immunology*, 192(12), pp. 6120–6130.

DOI: 10.4049/jimmunol.1303371.

Brosset Ugas, M. *et al.* (2016) 'Salmonella Typhi-Induced Septic Shock and Acute Respiratory Distress Syndrome in a Previously Healthy Teenage Patient Treated with High-Dose Dexamethasone'. *Journal of Investigative Medicine High Impact Case Reports*, 4(2), pp. 0–4. DOI: 10.1177/2324709616652642.

Browne, R.K. (1868) 'On Our True and False "Knowledge" of the Physiological Character and Action of the Red-Blood Corpuscles'. *American Journal of Dentist Science*, 1(9), pp. 431–440.

Broz, P. and Monack, D.M. (2011) 'Molecular Mechanisms of Inflammasome Activation during Microbial Infections'. *Immunological Reviews*, 243(1), pp. 174–190. DOI: 10.1111/j.1600-065X.2011.01041.x.

Broz, P., Ohlson, M.B. and Monack, D.M. (2012) 'Innate Immune Response to Salmonella Typhimurium, a Model Enteric Pathogen'. *Gut Microbes*, 3(2), pp. 62–70. DOI: 10.4161/gmic.19141.

Brunkow, M.E. *et al.* (2001) 'Disruption of a New Forkhead / Winged-Helix Protein , Scurfin , Results in the Fatal Lymphoproliferative Disorder of the Scurfy Mouse'. *Nature Genetics*, 27(January), pp. 68–73.

Brunner, S.M. *et al.* (2011) 'Interleukin-33 Prolongs Allograft Survival during Chronic Cardiac Rejection'. *Transplant International*, 24(10), pp. 1027–1039. DOI: 10.1111/j.1432-2277.2011.01306.x.

Buchmeier, N.A. and Heffron, F. (1991) 'Inhibition of Macrophage Phagosome-Lysosome Fusion by Salmonella Typhimurium'. *Infection and Immunity*, 59(7), pp. 2232–2238. DOI: 10.1128/iai.59.7.2232-2238.1991.

Budnik, A. and Henneberg, M. (2017) 'Worldwide Increase of Obesity Is Related to the Reduced Opportunity for Natural Selection'. *PLoS ONE*, 12(1), pp. 1–11. DOI: 10.1371/journal.pone.0170098.

Bumann, D. (2001) 'In Vivo Visualization of Bacterial Colonization, Antigen Expression, and Speci c T-Cell Induction Following Oral Administration of Live

Recombinant'. *Society*, 69(7), pp. 4618–4626. DOI: 10.1128/IAI.69.7.4618.

Bürckstümmer, T. *et al.* (2006) 'An Efficient Tandem Affinity Purification Procedure for Interaction Proteomics in Mammalian Cells'. *Nature Methods*, 3(12). DOI: 10.1038/NMETH968.

Busch, K. *et al.* (2015) 'Fundamental Properties of Unperturbed Haematopoiesis from Stem Cells in Vivo'. *Nature*, 518(7540), pp. 542–546. DOI: 10.1038/nature14242.

Butler, T. *et al.* (1990) 'Patterns of Morbidity and Mortality in Typhoid Fever Dependent on Age and Gender: Review of 552 Hopitalized Patients with Diarrhea'. *Reviews of Infectious Diseases*, 13(1), pp. 85–90. DOI: 10.1093/clinids/13.1.85.

Byers, D.E. *et al.* (2013) 'Long-Term IL-33-Producing Epithelial Progenitor Cells in Chronic Obstructive Lung Disease'. *Journal of Clinical Investigation*, 123(9), pp. 3967–3982. DOI: 10.1172/JCI65570.

Cabezas-Wallscheid, N. *et al.* (2014) 'Identification of Regulatory Networks in HSCs and Their Immediate Progeny via Integrated Proteome, Transcriptome, and DNA Methylome Analysis'. *Cell Stem Cell*, 15(4), pp. 507–522. DOI: 10.1016/j.stem.2014.07.005.

Campbell, J. J. *et al.* (1999) 'The Chemokine Receptor CCR4 in Vascular Recognition by Cutaneous but Not Intestinal Memory T Cells'. *Nature*, 400(August), pp. 776–780.

Campbell, J J., Pan, J. and Butcher, E.C. (1999) 'Cutting Edge: Developmental Switches in Chemokine Responses during T Cell Maturation.' *Journal of Immunology (Baltimore, Md. : 1950)*, 163(5), pp. 2353–7. DOI: 10.4049/jimmunol.163.5.2353.

Cancello, R. *et al.* (2006) 'Increased Infiltration of Macrophages in Omental Adipose Tissue Is Associated with Marked Hepatic Lesions in Morbid Human Obesity'. *Diabetes*, 55(6), pp. 1554–1561. DOI: 10.2337/db06-0133.

Cani, P.D. *et al.* (2009) 'Changes in Gut Microbiota Control Inflammation in Obese Mice through a Mechanism Involving GLP-2-Driven Improvement of Gut

Permeability'. *Gut*, 58(8), pp. 1091–1103. DOI: 10.1136/gut.2008.165886.

Cao, X. *et al.* (2007) 'Granzyme B and Perforin Are Important for Regulatory T Cell-Mediated Suppression of Tumor Clearance'. *Immunity*, 27(4), pp. 635–646. DOI: 10.1016/j.immuni.2007.08.014.

Cardilo-Reis, L. *et al.* (2012) 'Interleukin-13 Protects from Atherosclerosis and Modulates Plaque Composition by Skewing the Macrophage Phenotype'. *EMBO Molecular Medicine*, 4(10), pp. 1072–1086. DOI: 10.1002/emmm.201201374.

Carey, M.E., McCann, N.S. and Gibani, M.M. (2022) 'Typhoid Fever Control in the 21st Century: Where Are We Now?' *Current Opinion in Infectious Diseases*, 35(5), pp. 424–430. DOI: 10.1097/QCO.0000000000000879.

Carlock, C.I. *et al.* (2014) 'Unique Temporal and Spatial Expression Patterns of IL-33 in Ovaries during Ovulation and Estrous Cycle Are Associated with Ovarian Tissue Homeostasis'. *The Journal of Immunology*, 193(1), pp. 161–169. DOI: 10.4049/jimmunol.1400381.

Carriere, V. *et al.* (2007) 'IL-33, the IL-1-like Cytokine Ligand for ST2 Receptor, Is a Chromatin-Associated Nuclear Factor in Vivo'. *Proceedings of the National Academy of Sciences of the United States of America*, 104(1), pp. 282–287. DOI: 10.1073/pnas.0606854104.

Caruso, R. *et al.* (2019) 'Dynamic and Asymmetric Changes of the Microbial Communities after Cohousing in Laboratory Mice'. *Cell Reports*, 27(11), pp. 3401–3412. DOI: 10.1016/j.celrep.2019.05.042.Dynamic.

Casaccia, M. *et al.* (2017) 'Peritoneal Carcinomatosis-like Implants of Extramedullary Hematopoiesis. An Insolite Occurrence during Splenectomy for Myelofibrosis'. *International Journal of Surgery Case Reports*, 41, pp. 9–11. DOI: 10.1016/j.ijscr.2017.09.030.

Cayrol, C. and Girard, J.P. (2014) 'IL-33: An Alarmin Cytokine with Crucial Roles in Innate Immunity, Inflammation and Allergy'. *Current Opinion in Immunology*, 31, pp. 31–37. DOI: 10.1016/j.coi.2014.09.004.

Cederbom, L., Hall, H. and Ivars, F. (2000) ‘CD4 + CD25 + Regulatory T Cells Down-Regulate Co- Stimulatory Molecules on Antigen-Presenting Cells’. *European Journal of Immunology*, 30(6), pp. 1538–1543.

Celik, M. *et al.* (2020) ‘IL-4 Induces M2 Macrophages to Produce Sustained Analgesia via Opioids’. *JCI Insight*, 5(4), pp. 1–16. DOI: 10.1172/jci.insight.133093.

Cenariu, D. *et al.* (2021) ‘Extramedullary Hematopoiesis of the Liver and Spleen’. *Journal of Clinical Medicine*, 10(24), pp. 1–12. DOI: 10.3390/jcm10245831.

Chakravortty, D. *et al.* (2005) ‘Formation of a Novel Surface Structure Encoded by Salmonella Pathogenicity Island 2’. *EMBO Journal*, 24(11), pp. 2043–2052. DOI: 10.1038/sj.emboj.7600676.

Chang, D.K. *et al.* (2016) ‘Anti-CCR4 Monoclonal Antibody Enhances Antitumor Immunity by Modulating Tumor-Infiltrating Tregs in an Ovarian Cancer Xenograft Humanized Mouse Model’. *OncoImmunology*, 5(3), pp. 1–14. DOI: 10.1080/2162402X.2015.1090075.

Chang, Y.J. *et al.* (2011) ‘Innate Lymphoid Cells Mediate Influenza-Induced Airway Hyper-Reactivity Independently of Adaptive Immunity’. *Nature Immunology*, 12(7), pp. 631–638. DOI: 10.1038/ni.2045.

Chao, G. *et al.* (2017) ‘MicroRNA-29a Increased the Intestinal Membrane Permeability of Colonic Epithelial Cells in Irritable Bowel Syndrome Rats’. *Oncotarget*, 8(49), pp. 85828–85837. DOI: 10.18632/oncotarget.20687.

Chapes, S.K. *et al.* (2001) ‘ MHCII, Tlr4 and Nramp1 Genes Control Host Pulmonary Resistance against the Opportunistic Bacterium Pasteurella Pneumotropica ’. *Journal of Leukocyte Biology*, 69(3), pp. 381–386. DOI: 10.1189/jlb.69.3.381.

Chasis, J.A. *et al.* (1989) ‘Membrane Assembly and Remodeling during Reticulocyte Maturation’. *Blood*, 74(3), pp. 1112–1120. DOI: 10.1182/blood.v74.3.1112.1112.

Chasis, J.A. and Mohandas, N. (2008) ‘Erythroblastic Islands: Niches for Erythropoiesis’. *Blood*, 112(3), pp. 470–478. DOI: 10.1182/blood-2008-03-077883.

Chattaway, M.A., Langridge, G.C. and Wain, J. (2021) ‘Salmonella Nomenclature in

the Genomic Era: A Time for Change'. *Scientific Reports*, 11(1), pp. 1–8. DOI: 10.1038/s41598-021-86243-w.

Chawla, A., Nguyen, K.D. and Goh, Y.P.S. (2011) 'Macrophage-Mediated Inflammation in Metabolic Disease'. *Nature Reviews Immunology*, 11(11), pp. 738–749. DOI: 10.1038/nri3071.

Chelakkot, C., Ghim, J. and Ryu, S.H. (2018) 'Mechanisms Regulating Intestinal Barrier Integrity and Its Pathological Implications'. *Experimental and Molecular Medicine*, 50(8). DOI: 10.1038/s12276-018-0126-x.

Chen, C. *et al.* (2004) 'Heterodimerization and Cross-Desensitization between the A -Opioid Receptor and the Chemokine CCR5 Receptor'. *European Journal of Pharmacology*, 483, pp. 175–186. DOI: 10.1016/j.ejphar.2003.10.033.

Chen, W.J. *et al.* (2003) 'Conversion of Peripheral CD4+CD25- Naive T Cells to CD4+CD25+ Regulatory T Cells by TGF-β Induction of Transcription Factor Foxp3'. *Journal of Experimental Medicine*, 198(12), pp. 1875–1886. DOI: 10.1084/jem.20030152.

Chen, Y.T. *et al.* (2020) 'Inflammatory Macrophages Switch to CCL17-Expressing Phenotype and Promote Peritoneal Fibrosis'. *Journal of Pathology*, 250(1), pp. 55–66. DOI: 10.1002/path.5350.

Cheng, G. *et al.* (2012) 'Interleukin-2 Receptor Signaling Is Essential for the Development of Klrg1+ Terminally Differentiated T Regulatory Cells'. *Journal of Immunology*, 189(4), pp. 1780–1791. DOI: 10.4049/jimmunol.1103768.

Chiaramonte, M.G. *et al.* (1999) 'An IL-13 Inhibitor Blocks the Development of Hepatic Fibrosis during a T-Helper Type 2-Dominated Inflammatory Response'. *Journal of Clinical Investigation*, 104(6), pp. 777–785. DOI: 10.1172/JCI7325.

Choi, S.-I. *et al.* (2023) 'N-Acetylglucosamine and Its Dimer Ameliorate Inflammation in Murine Colitis by Strengthening the Gut Barrier Function'. *Food & Function*. DOI: 10.1039/d3fo00282a.

Chou, D.B. *et al.* (2012) 'Stromal-Derived IL-6 Alters the Balance of Myeloerythroid

Progenitors during Toxoplasma Gondii Infection'. *Journal of Leukocyte Biology*, 92(1), pp. 123–131. DOI: 10.1189/jlb.1011527.

Chow, W.L. and Lee, Y.K. (2008) 'Free Fucose Is a Danger Signal to Human Intestinal Epithelial Cells'. *British Journal of Nutrition*, 99(3), pp. 449–454. DOI: 10.1017/S0007114507812062.

Christ, A. *et al.* (2018) 'Western Diet Triggers NLRP3-Dependent Innate Immune Reprogramming'. *Cell*, 172(1–2), pp. 162–175. DOI: 10.1016/j.cell.2017.12.013.

Chudek, J. and Więcek, A. (2006) 'Adipose Tissue, Inflammation and Endothelial Dysfunction'. *Pharmacological Reports*, 58(SUPPL.), pp. 81–88. DOI: 10.111/J.1734-1140.

Chvatchko, Y. *et al.* (2000) 'A Key Role for Cc Chemokine Receptor 4 in Lipopolysaccharide-Induced Endotoxic Shock'. *The Journal of Experimental Medicine*, 191(10), pp. 1755–1764. DOI: 10.1084/jem.191.10.1755.

Cinti, S. *et al.* (2005) 'Adipocyte Death Defines Macrophage Localization and Function in Adipose Tissue of Obese Mice and Humans'. *Journal of Lipid Research*, 46(11), pp. 2347–2355. DOI: 10.1194/jlr.M500294-JLR200.

Clark, L.B. *et al.* (1999) 'Cellular and Molecular Characterization of the Scurfy Mouse Mutant'. *The Journal of Immunology*, 162(5), pp. 2546–2554. DOI: 10.4049/jimmunol.162.5.2546.

Clore, G.M. *et al.* (1990) 'Three-Dimensional Structure of Interleukin 8 in Solution'. *Biochemistry*, 29(7), pp. 1689–1696.

Cobbold, S. and Waldmann, H. (1998) 'Infectious Tolerance'. *Current Opinion in Immunology*, 10(5), pp. 518–524. DOI: 10.1016/S0952-7915(98)80217-3.

Conlan, J.W. (1996) 'Neutrophils Prevent Extracellular Colonization of the Liver Microvasculature by Salmonella Typhimurium'. *Infection and Immunity*, 64(3), pp. 1043–1047. DOI: 10.1128/iai.64.3.1043-1047.1996.

Conti, B. *et al.* (2004) 'Cytokines and Fever'. *Frontiers in Biosciences*, 9, pp. 1433–49. DOI: 10.2741/1341.

Copperi, F. *et al.* (2022) ‘EBI2 Is a Negative Modulator of Brown Adipose Tissue Energy Expenditure in Mice and Human Brown Adipocytes’. *Communications Biology*, 5(1), pp. 1–9. DOI: 10.1038/s42003-022-03201-6.

Corcione, A. *et al.* (2002) ‘Chemotaxis of Human Tonsil B Lymphocytes to CC Chemokine Receptor (CCR) 1, CCR2 and CCR4 Ligands Is Restricted to Non-Germinal Center Cells’. *International Immunology*, 14(8), pp. 883–892. DOI: 10.1093/intimm/dxf054.

Cosovanu, C. and Neumann, C. (2020) ‘The Many Functions of Foxp3+ Regulatory T Cells in the Intestine’. *Frontiers in Immunology*, 11(October), pp. 1–9. DOI: 10.3389/fimmu.2020.600973.

Da Costa, L. *et al.* (2001) ‘Temporal Differences in Membrane Loss Lead to Distinct Reticulocyte Features in Hereditary Spherocytosis and in Immune Hemolytic Anemia’. *Blood*, 98(10), pp. 2894–2899.

Cousin, B. *et al.* (1992) ‘Occurrence of Brown Adipocytes in Rat White Adipose Tissue: Molecular and Morphological Characterization’. *Journal of Cell Science*, 103(4), pp. 931–942. DOI: 10.1242/jcs.103.4.931.

Cowan, J.E. *et al.* (2014) ‘Differential Requirement for CCR4 and CCR7 during the Development of Innate and Adaptive T Cells in the Adult Thymus’. *The Journal of Immunology*, 193(3), pp. 1204–1212. DOI: 10.4049/jimmunol.1400993.

Cronshaw, D.G. *et al.* (2004) ‘Activation of Phosphoinositide 3-Kinases by the CCR4 Ligand Macrophage-Derived Chemokine Is a Dispensable Signal for T Lymphocyte Chemotaxis’. *The Journal of Immunology*, 172(12), pp. 7761–7770. DOI: 10.4049/jimmunol.172.12.7761.

Crown, S.E. *et al.* (2006) ‘Heterodimerization of CCR2 Chemokines and Regulation by Glycosaminoglycan Binding’. *Journal of Biological Chemistry*, 281(35), pp. 25438–25446. DOI: 10.1074/jbc.M601518200.

Curiel, T.J. *et al.* (2004) ‘Specific Recruitment of Regulatory T Cells in Ovarian Carcinoma Fosters Immune Privilege and Predicts Reduced Survival’. *Nature*

Medicine, 10(9), pp. 942–949. DOI: 10.1038/nm1093.

Davoine, F. and Lacy, P. (2014) 'Eosinophil Cytokines, Chemokines, and Growth Factors: Emerging Roles in Immunity'. *Frontiers in Immunology*, 5(NOV), pp. 1–17. DOI: 10.3389/fimmu.2014.00570.

Dayer, C. and Stamenkovic, I. (2015) 'Recruitment of Matrix Metalloproteinase-9 (MMP-9) to the Fibroblast Cell Surface by Lysyl Hydroxylase 3 (LH3) Triggers Transforming Growth Factor-β (TGF-β) Activation and Fibroblast Differentiation'. *Journal of Biological Chemistry*, 290(22), pp. 13763–13778. DOI: 10.1074/jbc.M114.622274.

Decaillot, F.M. *et al.* (2011) 'CXCR7 / CXCR4 Heterodimer Constitutively Recruits ß-Arrestin to Enhance Cell Migration'. *Journal of Biological Chemistry*, 286(37), pp. 32188–32197. DOI: 10.1074/jbc.M111.277038.

Decman, V. *et al.* (2012) 'Defective CD8 T Cell Responses in Aged Mice Are Due to Quantitative and Qualitative Changes in Virus-Specific Precursors'. *The Journal of Immunology*, 188(4), pp. 1933–1941. DOI: 10.4049/jimmunol.1101098.

DeFea, K. (2018) 'Arresting CCR4: A New Look at an Old Approach to Combating Asthma'. *American Journal of Respiratory Cell and Molecular Biology*, 58(6), pp. 673–675. DOI: 10.1165/rcmb.2017-0396ED.

Deloris Alexander, A. *et al.* (2006) 'Quantitative PCR Assays for Mouse Enteric Flora Reveal Strain-Dependent Differences in Composition That Are Influenced by the Microenvironment'. *Mammalian Genome*, 17(11), pp. 1093–1104. DOI: 10.1007/s00335-006-0063-1.

Denning, T.L. *et al.* (2007) 'Mouse TCRαβ+ CD8αα Intraepithelial Lymphocytes Express Genes That Down-Regulate Their Antigen Reactivity and Suppress Immune Responses'. *Journal of Immunology*, 178(7), pp. 4230–4239.

Deshpande, N.R., Parrish, H.L. and Kuhns, M.S. (2015) 'Self-Recognition Drives the Preferential Accumulation of Promiscuous CD4+ t-Cells in Aged Mice'. *ELife*, 4(JULY 2015), pp. 1–12. DOI: 10.7554/eLife.05949.

Dias, S. *et al.* (2017) ‘Effector Regulatory T Cell Differentiation and Immune Homeostasis Depend on the Transcription Factor Myb’. *Immunity*, 46(1), pp. 78–91. DOI: 10.1016/j.immuni.2016.12.017.

Díaz-Jiménez, D. *et al.* (2011) ‘Soluble ST2: A New and Promising Activity Marker in Ulcerative Colitis’. *World Journal of Gastroenterology*, 17(17), pp. 2181–2190. DOI: 10.3748/wjg.v17.i17.2181.

Díaz-Jiménez, D. *et al.* (2016) ‘Soluble ST2 Is a Sensitive Clinical Marker of Ulcerative Colitis Evolution’. *BMC Gastroenterology*, 16(1), pp. 1–10. DOI: 10.1186/s12876-016-0520-6.

Dieleman, L.A. *et al.* (2000) ‘Helicobacter Hepaticus Does Not Induce or Potentiate Colitis in Interleukin-10-Deficient Mice’. *Infection and Immunity*, 68(9), pp. 5107–5113. DOI: 10.1128/IAI.68.9.5107-5113.2000.

Dougan, G. *et al.* (2011) ‘Immunity to Salmonellosis’. *Immunological Reviews*, 240(1), pp. 196–210. DOI: 10.1111/j.1600-065X.2010.00999.x.

Dowling, M.R. *et al.* (2018) ‘Regulatory T Cells Suppress Effector T Cell Proliferation by Limiting Division Destiny’. *Frontiers in Immunology*, 9(October), pp. 1–10. DOI: 10.3389/fimmu.2018.02461.

Drake, L.Y. and Kita, H. (2017) ‘IL-33: Biological Properties, Functions, and Roles in Airway Disease’. *Immunological Reviews*, 278(1), pp. 173–184. DOI: 10.1111/imr.12552.

Dubiel, W. and Rapoport, S.M. (1989) ‘ATP-Dependent Proteolysis of Mitochondria of Reticulocytes’. *Revisiones Sobre Biologica Celular: RBC*, 21, pp. 505–521.

Ducarmon, Q.R. *et al.* (2019) ‘Gut Microbiota and Colonization Resistance against Bacterial Enteric Infection’. *Microbiology and Molecular Biology Reviews*, 83(3). DOI: 10.1128/mmbr.00007-19.

Durham, H.E. (1898) ‘On an Epidemic of Gastro-Enteritits Associated with the Pressence of a Variety of the Bacillus Enteritidis (Gaertner), and with Positive Sero-Diagnostic Evidence (In Vivo and In Vitro)’. *British Medical Journal*, 2, pp. 600–601.

Dwyer, G.K., D'Cruz, L.M. and Turnquist, H.R. (2022) 'Emerging Functions of IL-33 in Homeostasis and Immunity'. *Annual Review of Immunology*, 40, pp. 15–43. DOI: 10.1146/annurev-immunol-101320-124243.

Dzierzak, E. and Philipsen, S. (2013) 'Erythropoiesis: Development and Differentiation'. *Cold Spring Harbor Perspectives in Medicine*, 3(4), pp. 1–16. DOI: 10.1101/cshperspect.a011601.

Eberth, C.J. (1880) 'Die Organismen in Den Organen Bei Typhus Abdominalis'. *Archiv Für Pathologische Anatomie Und Physiologie Und Für Klinische Medicin*, 81(1), pp. 58–74. DOI: 10.1007/BF01995472.

Eby, J.M. *et al.* (2015) 'CCL22 to Activate Treg Migration and Suppress Depigmentation in Vitiligo'. *Journal of Investigative Dermatology*, 135(6), pp. 1574–1580. DOI: 10.1038/jid.2015.26.

Edwards, R.A., Schifferli, D.M. and Maloy, S.R. (2000) 'A Role for Salmonella Fimbriae in Intraperitoneal Infections'. *Proceedings of the National Academy of Sciences of the United States of America*, 97(3), pp. 1258–1262. DOI: 10.1073/pnas.97.3.1258.

Ehrlich, L.I.R. *et al.* (2009) 'Differential Contribution of Chemotaxis and Substrate Restriction to Segregation of Immature and Mature Thymocytes'. *Immunity*, 31(6), pp. 986–998. DOI: 10.1016/j.immuni.2009.09.020.

El-Asmar, L. *et al.* (2005) 'Evidence for Negative Binding Cooperativity within CCR5-CCR2b Heterodimers'. *Molecular Pharmacology*, 67(2), pp. 460–469. DOI: 10.1124/mol.104.003624.to.

Elgazar-Carmon, V. *et al.* (2008) 'Neutrophils Transiently Infiltrate Intra-Abdominal Fat Early in the Course of High-Fat Feeding'. *Journal of Lipid Research*, 49(9), pp. 1894–1903. DOI: 10.1194/jlr.M800132-JLR200.

Emont, M.P. *et al.* (2022) 'A Single-Cell Atlas of Human and Mouse White Adipose Tissue'. *Nature*, 603(7903), pp. 926–933. DOI: 10.1038/s41586-022-04518-2.

Erazo, A.B. *et al.* (2021) 'CCL17-Expressing Dendritic Cells in the Intestine Are

Preferentially Infected by Salmonella but CCL17 Plays a Redundant Role in Systemic Dissemination'. *Immunity, Inflammation and Disease*, 9(3), pp. 891–904. DOI: 10.1002/iid3.445.

Erazo, A.B. (2020) *Role of the Chemokines CCL17 and CCL22 in the Immune Defence against Salmonella Infection*. Rheinische Friedrich-Wilhelms-Universität Bonn, The University of Melbourne.

Eto, H. *et al.* (2009) 'Characterization of Structure and Cellular Components of Aspirated and Excised Adipose Tissue'. *Plastic and Reconstructive Surgery*, 124(4), pp. 1087–1097. DOI: 10.1097/PRS.0b013e3181b5a3f1.

Fàbrega, A. and Vila, J. (2013) 'Salmonella Enterica Serovar Typhimurium Skills to Succeed in the Host: Virulence and Regulation'. *Clinical Microbiology Reviews*, 26(2), pp. 308–341. DOI: 10.1128/CMR.00066-12.

Faustino, L. *et al.* (2012) 'Regulatory T Cells Accumulate in the Lung Allergic Inflammation and Efficiently Suppress T-Cell Proliferation but Not Th2 Cytokine Production'. *Clinical and Developmental Immunology*, 2012, pp. 13–15. DOI: 10.1155/2012/721817.

Feng, C. *et al.* (2002) 'A Potential Role for CD69 in Thymocyte Emigration'. *International Immunology*, 14(6), pp. 535–544. DOI: 10.1093/intimm/dxf020.

Fernández-García, V. *et al.* (2020) 'Contribution of Extramedullary Hematopoiesis to Atherosclerosis. The Spleen as a Neglected Hub of Inflammatory Cells'. *Frontiers in Immunology*, 11(October), pp. 1–12. DOI: 10.3389/fimmu.2020.586527.

Fernandez, E.J. and Lolis, E. (2002) 'Structure, Function, and Inhibition of Chemokines'. *Annual Review of Pharmacology and Toxicology*, 42(February), pp. 469–499. DOI: 10.1146/annurev.pharmtox.42.091901.115838.

Ferreira, R.B.R. *et al.* (2011) 'The Intestinal Microbiota Plays a Role in Salmonella-Induced Colitis Independent of Pathogen Colonization'. *PLoS ONE*, 6(5). DOI: 10.1371/journal.pone.0020338.

Fettrelet, T. *et al.* (2021) 'The Enigma of Eosinophil Degranulation'. *International*

Journal of Molecular Sciences, 22(13), pp. 1–19. DOI: 10.3390/ijms22137091.

Feuerer, M. *et al.* (2009) 'Lean, but Not Obese, Fat Is Enriched for a Unique Population of Regulatory T Cells That Affect Metabolic Parameters'. *Nature Medicine*, 15(8), pp. 930–939. DOI: 10.1038/nm.2002.

Fields, J.K., Günther, S. and Sundberg, E.J. (2019) 'Structural Basis of IL-1 Family Cytokine Signaling'. *Frontiers in Immunology*, 10(JUN), pp. 1–20. DOI: 10.3389/fimmu.2019.01412.

Fiorenza, C.G., Chou, S.H. and Mantzoros, C.S. (2011) 'Lipodystrophy: Pathophysiology and Advances in Treatment'. *Nature Reviews Endocrinology*, 7(3), pp. 137–150. DOI: 10.1038/nrendo.2010.199.

Fistonich, C. *et al.* (2018) 'Cell Circuits between B Cell Progenitors and IL-7+mesenchymal Progenitor Cells Control B Cell Development'. *Journal of Experimental Medicine*, 215(10), pp. 2586–2599. DOI: 10.1084/JEM.20180778.

Fontenot, J.D., Gavin, M.A. and Rudensky, A.Y. (2017) 'Foxp3 Programs the Development and Function of CD4+CD25+ Regulatory T Cells'. *Journal of Immunology*, 198(3), pp. 986–992. DOI: 10.1038/ni904.

Ford, L.B., Hansell, C.A.H. and Nibbs, R.J.B. (2013) 'Using Fluorescent Chemokine Uptake to Detect Chemokine Receptors by Fluorescent Activated Cell Sorting'. In Cardona, A.E. and Ubogu, E.E. (eds.) *Chemokines : Methods and Protocols*. New York: Humana Totowa, NJ, pp. 203–214. DOI: 10.1007/978-1-62703-426-5.

Forthal, D.N. (2008) 'Functions of Antibodies'. *Microbiology Spectrum*, 2(4), pp. 1–17.

Foster, J.W. and Hall, H.K. (1990) 'Adaptive Acidification Tolerance Response of Salmonella Typhimurium'. *Journal of Bacteriology*, 172(2), pp. 771–778. DOI: 10.1128/jb.172.2.771-778.1990.

Francis, C.L., Starnbach, M.N. and Falkow, S. (1992) 'Morphological and Cytoskeletal Changes in Epithelial Cells Occur Immediately upon Interaction with Salmonella Typhimurium Grown under Low□oxygen Conditions'. *Molecular*

Microbiology, 6(21), pp. 3077–3087. DOI: 10.1111/j.1365-2958.1992.tb01765.x.

Franklin, C.L. and Ericsson, A.C. (2017) 'Microbiota and Reproducibility of Rodent Models'. *Lab Animal*, 46(4), pp. 114–122. DOI: 10.1038/laban.1222.

Fraser, J. *et al.* (2018) 'A Shared Signaling Network That Maintains Erythroid Homeostasis By Activating Stress Erythropoiesis Regulates Inflammation: Implications for the Anemia of Chronic Inflammation'. *Blood*, 132(Supplement 1), pp. 629–629. DOI: 10.1182/blood-2018-99-113448.

Friess, M.C. *et al.* (2022) 'Mechanosensitive ACKR4 Scavenges CCR7 Chemokines to Facilitate T Cell De-Adhesion and Passive Transport by Flow in Inflamed Afferent Lymphatics'. *Cell Reports*, 38(5), p. 110334. DOI: 10.1016/j.celrep.2022.110334.

Frimpong-Boateng, K., van Rooijen, N. and Geiben-Lynn, R. (2010) 'Regulatory T Cells Suppress Natural Killer Cells during Plasmid DNA Vaccination in Mice, Blunting the CD8+ T Cell Immune Response by the Cytokine TGFβ'. *PLoS ONE*, 5(8), pp. 1–8. DOI: 10.1371/journal.pone.0012281.

Fuertes Marraco, S.A. *et al.* (2012) 'Novel Murine Dendritic Cell Lines: A Powerful Auxiliary Tool for Dendritic Cell Research'. *Frontiers in Immunology*, 3(November). DOI: 10.3389/fimmu.2012.00331.

Fujimoto, S. *et al.* (2008) 'CCR4 and CCR10 Are Expressed on Epidermal Keratinocytes and Are Involved in Cutaneous Immune Reaction'. *Cytokine*, 44(1), pp. 172–178. DOI: 10.1016/j.cyto.2008.07.472.

Fukuda, K. *et al.* (2003) 'Differential Expression of Thymus- and Activation-Regulated Chemokine (CCL17) and Macrophage-Derived Chemokine (CCL22) by Human Fibroblasts from Cornea, Skin, and Lung'. *Journal of Allergy and Clinical Immunology*, 111(3), pp. 520–526. DOI: 10.1067/mai.2003.59.

Fukuma, N. *et al.* (2003) 'A Role of the Duffy Antigen for the Maintenance of Plasma Chemokine Concentrations'. *Biochemical and Biophysical Research Communications*, 303(1), pp. 137–139. DOI: 10.1016/S0006-291X(03)00293-6.

Fülle, L. (2018) *Functional Roles of the Chemokine CCL17 in Skin and Brain*

Immunity. Rheinische Friedrich-Wilhelms-Universität Bonn.

Fülle, L. *et al.* (2018) 'RNA Aptamers Recognizing Murine CCL17 Inhibit T Cell Chemotaxis and Reduce Contact Hypersensitivity In Vivo'. *Molecular Therapy*, 26(1), pp. 95–104. DOI: 10.1016/j.ymthe.2017.10.005.

Gajardo, T. *et al.* (2015) 'Exogenous Interleukin-33 Targets Myeloid-Derived Suppressor Cells and Generates Periphery-Induced Foxp3+ Regulatory T Cells in Skin-Transplanted Mice'. *Immunology*, 146(1), pp. 81–88. DOI: 10.1111/imm.12483.

Gallo, R.L. and Hooper, L. V. (2012) 'Epithelial Antimicrobial Defence of the Skin and Intestine'. *Nature Reviews Immunology*, 12(7), pp. 503–516. DOI: 10.1038/nri3228.

Gao, F. *et al.* (2009) 'Functional Importance of a Structurally Distinct Homodimeric Complex of the Family B G Protein-Coupled Secretin Receptor'. *Molecular Pharmacology*, 76(2), pp. 264–274. DOI: 10.1124/mol.109.055756.

Gao, Q. *et al.* (2016) 'Lentivirus Expressing Soluble ST2 Alleviates Bleomycin-Induced Pulmonary Fibrosis in Mice'. *International Immunopharmacology*, 30, pp. 188–193. DOI: 10.1016/j.intimp.2015.11.015.

Gao, Y. *et al.* (2018) 'Acute and Chronic Cold Exposure Differentially Affects the Browning of Porcine White Adipose Tissue'. *Animal*, 12(7), pp. 1435–1441. DOI: 10.1017/S1751731117002981.

Gao, Y. *et al.* (2016) 'IL-33 Treatment Attenuated Diet-Induced Hepatic Steatosis but Aggravated Hepatic Fibrosis'. *Oncotarget*, 7(23), pp. 33649–33661. DOI: 10.18632/oncotarget.9259.

García-de-Alba, C. *et al.* (2010) 'Expression of Matrix Metalloproteases by Fibrocytes: Possible Role in Migration and Homing'. *American Journal of Respiratory and Critical Care Medicine*, 182(9), pp. 1144–1152. DOI: 10.1164/rccm.201001-0028OC.

Gardner, L. *et al.* (2004) 'The Human Duffy Antigen Binds Selected Inflammatory but Not Homeostatic Chemokines'. *Biochemical and Biophysical Research*

Communications, 321(2), pp. 306–312. DOI: 10.1016/j.bbrc.2004.06.146.

Garlanda, C., Dinarello, C.A. and Mantovani, A. (2013) 'The Interleukin-1 Family: Back to the Future'. *Immunity*, 39(6), pp. 1003–1018. DOI: 10.1016/j.immuni.2013.11.010.

Garrett, D.O. *et al.* (2022) 'Incidence of Typhoid and Paratyphoid Fever in Bangladesh, Nepal, and Pakistan: Results of the Surveillance for Enteric Fever in Asia Project'. *The Lancet Global Health*, 10(7), pp. e978–e988. DOI: 10.1016/S2214-109X(22)00119-X.

Garritson, J.D. and Boudina, S. (2021) 'The Effects of Exercise on White and Brown Adipose Tissue Cellularity, Metabolic Activity and Remodeling'. *Frontiers in Physiology*, 12(November), pp. 1–7. DOI: 10.3389/fphys.2021.772894.

Garro, A.P. *et al.* (2011) 'Eosinophils Elicit Proliferation of Naive and Fungal-Specific Cells in Vivo so Enhancing a T Helper Type 1 Cytokine Profile in Favour of a Protective Immune Response against Cryptococcus Neoformans Infection'. *Immunology*, 134(2), pp. 198–213. DOI: 10.1111/j.1365-2567.2011.03479.x.

Gershon, R.K. and Kondo, K. (1970) 'Cell Interactions in the Induction of Tolerance: The Role of Thymic Lymphocytes.' *Immunology*, 18(5), pp. 723–37. Available at: http://www.ncbi.nlm.nih.gov/pubmed/4911896%0Ahttp://www.pubmedcentral.nih.gov/articlerender.fcgi?artid=PMC1455602.

Gershon, R.K. and Kondo, K. (1971) 'Infectious Immunological Tolerance.' *Immunology*, 21(6), pp. 903–14. Available at: http://www.ncbi.nlm.nih.gov/pubmed/4943147%0Ahttp://www.pubmedcentral.nih.gov/articlerender.fcgi?artid=PMC1408252.

Ghorbani, M., Claus, T.H. and Himms-Hagen, J. (1997) 'Hypertrophy of Brown Adipocytes in Brown and White Adipose Tissues and Reversal of Diet-Induced Obesity in Rats Treated with a B3-Adrenoceptor Agonist'. *Biochemical Pharmacology*, 54(1), pp. 121–131. DOI: 10.1016/S0006-2952(97)00162-7.

Giordano, A. *et al.* (2013) 'Obese Adipocytes Show Ultrastructural Features of

Stressed Cells and Die of Pyroptosis'. *Journal of Lipid Research*, 54(9), pp. 2423–2436. DOI: 10.1194/jlr.M038638.

Glineur, C., Leleu, I. and Pied, S. (2022) 'The IL-33/ST2 Pathway in Cerebral Malaria'. *International Journal of Molecular Sciences*, 23(21), p. 13457. DOI: 10.3390/ijms232113457.

Godin, I. and Cumano, A. (2005) 'Of Birds and Mice: Hematopoietic Stem Cell Development'. *International Journal of Developmental Biology*, 49(2-3 SPEC. ISS.), pp. 251–257. DOI: 10.1387/ijdb.041945ig.

Golozoubova, V. *et al.* (2001) 'Only UCP1 Can Mediate Adaptive Nonshivering Thermogenesis in the Cold'. *The FASEB Journal*, 15(11), pp. 2048–2050. DOI: 10.1096/fj.00-0536fje.

Gómez-López, S., Lerner, R.G. and Petritsch, C. (2014) 'Asymmetric Cell Division of Stem and Progenitor Cells during Homeostasis and Cancer'. *Cellular and Molecular Life Sciences*, 71(4), pp. 575–597. DOI: 10.1007/s00018-013-1386-1.

Gondek, D.C. *et al.* (2005) 'Cutting Edge: Contact-Mediated Suppression by CD4+CD25+ Regulatory Cells Involves a Granzyme B-Dependent, Perforin-Independent Mechanism'. *The Journal of Immunology*, 174(4), pp. 1783–1786. DOI: 10.4049/jimmunol.174.4.1783.

Gordon, M.A. (2008) 'Salmonella Infections in Immunocompromised Adults'. *Journal of Infection*, 56(6), pp. 413–422. DOI: 10.1016/j.jinf.2008.03.012.

Goswami, T. *et al.* (2001) 'Natural-Resistance-Associated Macrophage Protein 1 Is an H+/Bivalent Cation Antiporter'. *Biochemical Journal*, 354(3), pp. 511–519. DOI: 10.1042/0264-6021:3540511.

Gottschalk, R.A., Corse, E. and Allison, J.P. (2012) 'Expression of Helios in Peripherally Induced Foxp3+ Regulatory T Cells'. *The Journal of Immunology*, 188(3), pp. 976–980. DOI: 10.4049/jimmunol.1102964.

Govoni, G. *et al.* (1996) 'The Bcg/Ity/Lsh Locus: Genetic Transfer of Resistance to Infections in C57BL/6J Mice Transgenic for the Nramp1(Gly169) Allele'. *Infection*

and Immunity, 64(8), pp. 2923–2929. DOI: 10.1128/iai.64.8.2923-2929.1996.

Greaves, D.R. *et al.* (2001) 'Linked Chromosome 16q13 Chemokines, Macrophage-Derived Chemokine, Fractalkine, and Thymus- and Activation-Regulated Chemokine, Are Expressed in Human Atherosclerotic Lesions'. *Arteriosclerosis, Thrombosis, and Vascular Biology*, 21(6), pp. 923–929. DOI: 10.1161/01.ATV.21.6.923.

Greenwald, A.C. *et al.* (2019) 'VEGF Expands Erythropoiesis via Hypoxia-Independent Induction of Erythropoietin in Noncanonical Perivascular Stromal Cells'. *Journal of Experimental Medicine*, 216(1), pp. 215–230. DOI: 10.1084/jem.20180752.

Griesenauer, B. and Paczesny, S. (2017) 'The ST2/IL-33 Axis in Immune Cells during Inflammatory Diseases'. *Frontiers in Immunology*, 8(APR), pp. 1–17. DOI: 10.3389/fimmu.2017.00475.

Griffin, A.J. and McSorley, S.J. (2011) 'Development of Protective Immunity to Salmonella, a Mucosal Pathogen with a Systemic Agenda'. *Mucosal Immunology*, 4(4), pp. 371–382. DOI: 10.1038/mi.2011.2.

Griffin, M.D. and Abbott, R.D. (2022) 'Bioreactors and Microphysiological Systems for Adipose-Based Pharmacologic Screening'. In Kokai, L.Marra, K.and Rubin, J.P. (eds.) *Scientific Principles of Adipose Stem Cells*. Academic Press, pp. 121–146. DOI: https://doi.org/10.1016/B978-0-12-819376-1.00011-1.

Griffith, J.W., Sokol, C.L. and Luster, A.D. (2014) 'Chemokines and Chemokine Receptors: Positioning Cells for Host Defense and Immunity'. *Annual Review of Immunology*, 32, pp. 659–702. DOI: 10.1146/annurev-immunol-032713-120145.

Grimont, P.A.D. and Weil, F.-X. (2007) *Antigenic Formulae of the Salmonella Serovars. 9th Edition*. Paris Available at: https://www.pasteur.fr/ip/portal/action/WebdriveActionEvent/oid/01s-000036-089.

Gronowicz, G., Swift, H. and Steck, T.L. (1984) 'Maturation on the Reticulocyte in Vitro'. *Journal of Cell Science*, VOL. 71, pp. 177–197. DOI: 10.1242/jcs.71.1.177.

Groschwitz, K.R. and Hogan, S.P. (2009) ‘Intestinal Barrier Function: Molecular Regulation and Disease Pathogenesis’. *Journal of Allergy and Clinical Immunology*, 124(1), pp. 3–20. DOI: 10.1016/j.jaci.2009.05.038.

Grossman, W.J. *et al.* (2004) ‘Human T Regulatory Cells Can Use the Perforin Pathway to Cause Autologous Target Cell Death’. *Immunity*, 21(4), pp. 589–601. DOI: 10.1016/j.immuni.2004.09.002.

Grzymajlo, K. (2022) ‘The Game for Three: Salmonella–Host–Microbiota Interaction Models’. *Frontiers in Microbiology*, 13(April), pp. 1–18. DOI: 10.3389/fmicb.2022.854112.

Guerra, C. *et al.* (1998) ‘Emergence of Brown Adipocytes in White Fat in Mice Is under Genetic Control Effects on Body Weight and Adiposity’. *Journal of Clinical Investigation*, 102(2), pp. 412–420. DOI: 10.1172/JCI3155.

Guillerey, C. *et al.* (2021) ‘Systemic Administration of IL-33 Induces a Population of Circulating KLRG1hi Type 2 Innate Lymphoid Cells and Inhibits Type 1 Innate Immunity against Multiple Myeloma’. *Immunology and Cell Biology*, 99(1), pp. 65–83. DOI: 10.1111/imcb.12390.

Guina, T. *et al.* (2000) ‘A PhoP-Regulated Outer Membrane Protease of Salmonella Enterica Serovar Typhimurium Promotes Resistance to Alpha-Helical Antimicrobial Peptides’. *Journal of Bacteriology*, 182(14), pp. 4077–4086. DOI: 10.1128/JB.182.14.4077-4086.2000.

Gupta, S. *et al.* (1997) ‘IFN-γ, Potentiates Atherosclerosis in ApoE Knock-out Mice’. *Journal of Clinical Investigation*, 99(11), pp. 2752–2761. DOI: 10.1172/JCI119465.

Haase, J. *et al.* (2014) ‘Local Proliferation of Macrophages in Adipose Tissue during Obesity-Induced Inflammation’. *Diabetologia*, 57(3), pp. 562–571. DOI: 10.1007/s00125-013-3139-y.

El Hadi, H. *et al.* (2019) ‘Food Ingredients Involved in White-to-Brown Adipose Tissue Conversion and in Calorie Burning’. *Frontiers in Physiology*, 10(JAN), pp. 1–8. DOI: 10.3389/fphys.2018.01954.

Hallstrom, K. and McCormick, B.A. (2011) ‘Salmonella Interaction with and Passage through the Intestinal Mucosa: Through the Lens of the Organism’. *Frontiers in Microbiology*, 2(APR), pp. 1–10. DOI: 10.3389/fmicb.2011.00088.

Hamada, H. *et al.* (2002) ‘Identifcation of Multiple Isolated Lymphoid Follicles on the Antimesenteric Wall of the Mouse Small Intestine’. *The Journal of Immunology*, 168(1), pp. 57–64. DOI: 10.4049/jimmunol.168.1.57.

Han, J.M. *et al.* (2015) ‘IL-33 Reverses an Obesity-Induced Deficit in Visceral Adipose Tissue ST2+ T Regulatory Cells and Ameliorates Adipose Tissue Inflammation and Insulin Resistance’. *The Journal of Immunology*, 194(10), pp. 4777–4783. DOI: 10.4049/jimmunol.1500020.

Handel, T.M. and Domaille, P.J. (1996) ‘Heteronuclear (1H, 13C, 15N) NMR Assignments and Solution Structure of the Monocyte Chemoattractant Protein-1 (MCP-1) Dimer’. *Biochemistry*, 35(21), pp. 6569–6584. DOI: 10.1021/bi9602270.

Hansell, C.A.H., Hurson, C.E. and Nibbs, R.J.B. (2011) ‘DARC and D6 : Silent Partners in Chemokine Regulation ?’ *Immunol Cell Biology*, 89(2), pp. 197–206. DOI: 10.1038/icb.2010.147.DARC.

Hardman, C.S., Panova, V. and Mckenzie, A.N.J. (2013) ‘IL-33 Citrine Reporter Mice Reveal the Temporal and Spatial Expression of IL-33 during Allergic Lung Inflammation’. *European Journal of Immunology*, 43(2), pp. 488–498. DOI: 10.1002/eji.201242863.

Harikumar, K.G., Pinon, D.I. and Miller, L.J. (2007) ‘Transmembrane Segment IV Contributes a Functionally Important Interface for Oligomerization of the Class II G Protein-Coupled Secretin Receptor’. *Journal of Biological Chemistry*, 282(42), pp. 30363–30372. DOI: 10.1074/jbc.M702325200.

Harms, M. and Seale, P. (2013) ‘Brown and Beige Fat: Development, Function and Therapeutic Potential’. *Nature Medicine*, 19(10), pp. 1252–1263. DOI: 10.1038/nm.3361.

Harris, J.B. and Brooks, W.A. (2012) *Typhoid and Paratyphoid (Enteric) Fever*. ninth

edit. Elsevier Inc. DOI: 10.1016/B978-1-4160-4390-4.00069-2.

Harrison, O.J. *et al.* (2018) 'Commensal-Specific T Cell Plasticity Promotes Rapid Tissue Adaptation to Injury'. *Science*, 363(6422). DOI: DOI: 10.1126/science.aat6280.

Hase, K. *et al.* (2009) 'Uptake through Glycoprotein 2 of FimH + Bacteria by M Cells Initiates Mucosal Immune Response'. *Nature*, 462(7270), pp. 226–230. DOI: 10.1038/nature08529.

Hashim, S. *et al.* (2000) 'Live Salmonella Modulate Expression of Rab Proteins to Persist in a Specialized Compartment and Escape Transport to Lysosomes'. *Journal of Biological Chemistry*, 275(21), pp. 16281–16288. DOI: 10.1074/jbc.275.21.16281.

Hatai, S. (1902) 'On the Presence in Human Embryos of an Interscapular Gland Corresponding to the So-Called Hibernating Gland of Lower Mammals'. *Annals of Anatomy*, 21, pp. 369–373.

Hayakawa, H. *et al.* (2007) 'Soluble ST2 Blocks Interleukin-33 Signaling in Allergic Airway Inflammation'. *Journal of Biological Chemistry*, 282(36), pp. 26369–26380. DOI: 10.1074/jbc.M704916200.

He, Y. *et al.* (2020) 'IL-4 Switches Microglia/Macrophage M1/M2 Polarization and Alleviates Neurological Damage by Modulating the JAK1/STAT6 Pathway Following ICH'. *Neuroscience*, 437, pp. 161–171. DOI: 10.1016/j.neuroscience.2020.03.008.

Heiseke, A.F. *et al.* (2012) 'CCL17 Promotes Intestinal Inflammation in Mice and Counteracts Regulatory T Cellmediated Protection from Colitis'. *Gastroenterology*, 142(2), pp. 335–345. DOI: 10.1053/j.gastro.2011.10.027.

Hellwig, S.M.M. *et al.* (2001) 'Targeting to Fcγ Receptors, but Not CR3 (CD11b/CD18), Increases Clearance of Bordetella Pertussis'. *Journal of Infectious Diseases*, 183(6), pp. 871–879. DOI: 10.1086/319266.

Herbold, W. *et al.* (2010) 'Importance of CXC Chemokine Receptor 2 in Alveolar Neutrophil and Exudate Macrophage Recruitment in Response to Pneumococcal Lung Infection'. *Infection and Immunity*, 78(6), pp. 2620–2630. DOI:

10.1128/IAI.01169-09.

Hernandez, L.D. *et al.* (2004) ‘Salmonella Modulates Vesicular Traffic by Altering Phosphoinositide Metabolism’. *Science*, 304(5678), pp. 1805–1807. DOI: 10.1126/science.1098188.

Hess, J. *et al.* (1996) ‘Salmonella Typhimurium AroA- Infection in Gene-Targeted Immunodeficient Mice: Major Role of CD4+ TCR-Alpha Beta Cells and IFN-Gamma in Bacterial Clearance Independent of Intracellular Location’. *Journal of Immunology*, 156(9), pp. 3321–3326.

Hessell, A.J. *et al.* (2007) ‘Fc Receptor but Not Complement Binding Is Important in Antibody Protection against HIV’. *Nature*, 449(7158), pp. 101–104. DOI: 10.1038/nature06106.

Higginson, E.E., Simon, R. and Tennant, S.M. (2016) ‘Animal Models for Salmonellosis: Applications in Vaccine Research’. *Clinical and Vaccine Immunology*, 23(9), pp. 746–756. DOI: 10.1128/CVI.00258-16.

Hill, D.A. *et al.* (2018) ‘Distinct Macrophage Populations Direct Inflammatory versus Physiological Changes in Adipose Tissue’. *Proceedings of the National Academy of Sciences of the United States of America*, 115(22), pp. E5096–E5105. DOI: 10.1073/pnas.1802611115.

Ho, L.H. *et al.* (2007) ‘IL-33 Induces IL-13 Production by Mouse Mast Cells Independently of IgE-Fc RI Signals’. *Journal of Leukocyte Biology*, 82(6), pp. 1481–1490. DOI: 10.1189/jlb.0407200.

Holden, C., Hennessy, O. and Lee, W.K. (2006) ‘Diffuse Mesenteric Extramedullary Hematopoiesis with Ascites: Sonography, CT, MRI Findings’. *American Journal of Roentgenology*, 186(2), pp. 507–509. DOI: 10.2214/AJR.04.1788.

Holmes, D.A. *et al.* (2015) ‘ Dusp5 Negatively Regulates IL -33-mediated Eosinophil Survival and Function ’. *The EMBO Journal*, 34(2), pp. 218–235. DOI: 10.15252/embj.201489456.

Hori, S., Nomura, T. and Sakaguchi, S. (2003) ‘Control of Regulatory T Cell

Development by the Transcription Factor Foxp3'. *Science*, 299(5609), pp. 1057–1061.

Howes, R.E. *et al.* (2011) 'The Global Distribution of the Duffy Blood Group'. *Nature Communications*, 2(266). DOI: 10.1038/ncomms1265.

Hsieh, C.S. *et al.* (2004) 'Recognition of the Peripheral Self by Naturally Arising CD25+ CD4+ T Cell Receptors'. *Immunity*, 21(2), pp. 267–277. DOI: 10.1016/j.immuni.2004.07.009.

Hsu, C.-L. and Bryce, P.J. (2012) 'Inducible IL-33 Expression by Mast Cells Is Regulated by a Calcium-Dependent Pathway'. *The Journal of Immunology*, 189(7), pp. 3421–3429. DOI: 10.4049/jimmunol.1201224.

Hsu, C.L., Neilsen, C. V. and Bryce, P.J. (2010) 'IL-33 Is Produced by Mast Cells and Regulates IgE-Dependent Inflammation'. *PLoS ONE*, 5(8). DOI: 10.1371/journal.pone.0011944.

Hu, Z. *et al.* (2015) 'CCR4 Promotes Medullary Entry and Thymocyte–Dendritic Cell Interactions Required for Central Tolerance'. *The Journal of Experimental Medicine*, 212(11), pp. 1947–1965. DOI: 10.1084/jem.20150178.

Huang, E. *et al.* (2020) 'The Roles of Immune Cells in the Pathogenesis of Fibrosis'. *International Journal of Molecular Sciences*, 21(15), pp. 1–27. DOI: 10.3390/ijms21155203.

Hufeldt, M.R. *et al.* (2010) 'Family Relationship of Female Breeders Reduce the Systematic Inter-Individual Variation in the Gut Microbiota of Inbred Laboratory Mice'. *Laboratory Animals*, 44(4), pp. 283–289. DOI: 10.1258/la.2010.010058.

Hughes, C.E. and Nibbs, R.J.B. (2018) 'A Guide to Chemokines and Their Receptors'. *FEBS Journal*, 285(16), pp. 2944–2971. DOI: 10.1111/febs.14466.

Von Hundelshausen, P. *et al.* (2017) 'Chemokine Interactome Mapping Enables Tailored Intervention in Acute and Chronic Inflammation'. *Science Translational Medicine*, 9(384), pp. 1–15. DOI: 10.1126/scitranslmed.aah6650.

Hung, L.Y. *et al.* (2020) 'Cellular Context of IL-33 Expression Dictates Impact on

Anti-Helminth Immunity'. *Science Immunology*, 5(53). DOI: 10.1126/sciimmunol.abc6259.

Hung, L.Y. *et al.* (2013) 'IL-33 Drives Biphasic IL-13 Production for Noncanonical Type 2 Immunity against Hookworms'. *Proceedings of the National Academy of Sciences of the United States of America*, 110(1), pp. 282–287. DOI: 10.1073/pnas.1206587110.

Huttenhower, C. *et al.* (2012) 'Structure, Function and Diversity of the Healthy Human Microbiome'. *Nature*, 486(7402), pp. 207–214. DOI: 10.1038/nature11234.

Iikura, M. *et al.* (2007) 'IL-33 Can Promote Survival, Adhesion and Cytokine Production in Human Mast Cells'. *Laboratory Investigation*, 87(10), pp. 971–978. DOI: 10.1038/labinvest.3700663.

Imai, T. *et al.* (1998) 'Macrophage-Derived Chemokine Is a Functional Ligand for the CC Chemokine Receptor 4'. *Journal of Biological Chemistry*, 273(3), pp. 1764–1768. DOI: 10.1074/jbc.273.3.1764.

Imai, T. *et al.* (1999) 'Selective Recruitment of CCR4-Bearing T(h)2 Cells toward Antigen-Presenting Cells by the CC Chemokines Thymus and Activation-Regulated Chemokine and Macrophage-Derived Chemokine'. *International Immunology*, 11(1), pp. 81–88. DOI: 10.1093/intimm/11.1.81.

Imai, Y. *et al.* (2013) 'Skin-Specific Expression of IL-33 Activates Group 2 Innate Lymphoid Cells and Elicits Atopic Dermatitis-like Inflammation in Mice'. *Proceedings of the National Academy of Sciences of the United States of America*, 110(34), pp. 13921–13926. DOI: 10.1073/pnas.1307321110.

Ingram, J.P., Brodsky, I.E. and Balachandran, S. (2017) 'Interferon-γ in Salmonella Pathogenesis: New Tricks for an Old Dog'. *Cytokine*, 98, pp. 27–32. DOI: 10.1016/j.cyto.2016.10.009.

Inoue, T. *et al.* (2004) 'CCL22 and CCL17 in Rat Radiation Pneumonitis and in Human Idiopathic Pulmonary Fibrosis'. *European Respiratory Journal*, 24(1), pp. 49–56. DOI: 10.1183/09031936.04.00110203.

Iwahana, H. *et al.* (1999) ‘Different Promoter Usage and Multiple Transcription Initiation Sites of the Interleukin-1 Receptor-Related Human ST2 Gene in UT-7 and TM12 Cells’. *European Journal of Biochemistry*, 264(2), pp. 397–406. DOI: 10.1046/j.1432-1327.1999.00615.x.

Iwahana, H. *et al.* (2004) ‘Molecular Cloning of the Chicken ST2 Gene and a Novel Variant Form of the ST2 Gene Product, ST2LV’. *Biochimica et Biophysica Acta - Gene Structure and Expression*, 1681(1), pp. 1–14. DOI: 10.1016/j.bbaexp.2004.08.013.

Jackson, A. *et al.* (2010) ‘Innate Immune Activation during Salmonella Infection Initiates Extramedullary Erythropoiesis and Splenomegaly’. *The Journal of Immunology*, 185(10), pp. 6198–6204. DOI: 10.4049/jimmunol.1001198.

Jacobs, I. *et al.* (2021) ‘Role of Eosinophils in Intestinal Inflammation and Fibrosis in Inflammatory Bowel Disease: An Overlooked Villain?’ *Frontiers in Immunology*, 12(October), pp. 1–17. DOI: 10.3389/fimmu.2021.754413.

Jacobsen, E.A. *et al.* (2008) ‘Allergic Pulmonary Inflammation in Mice Is Dependent on Eosinophil-Induced Recruitment of Effector T Cells’. *Journal of Experimental Medicine*, 205(3), pp. 699–710. DOI: 10.1084/jem.20071840.

Jensen, K.D.C. *et al.* (2008) ‘Thymic Selection Determines Γδ T Cell Effector Fate: Antigen-Naive Cells Make Interleukin-17 and Antigen-Experienced Cells Make Interferon γ’. *Immunity*, 29(1), pp. 90–100. DOI: 10.1016/j.immuni.2008.04.022.

Ji, Y.Q. *et al.* (2011) ‘EPO Improves the Proliferation and Inhibits Apoptosis of Trophoblast and Decidual Stromal Cells through Activating STAT-5 and Inactivating P38 Signal in Human Early Pregnancy’. *International Journal of Clinical and Experimental Pathology*, 4(8), pp. 765–774.

Jing, W. *et al.* (2021) ‘G-CSF Shifts Erythropoiesis from Bone Marrow into Spleen in the Setting of Systemic Inflammation’. *Life Science Alliance*, 4(1), pp. 1–18. DOI: 10.26508/LSA.202000737.

Jinnohara, T. *et al.* (2017) ‘IL-22BP Dictates Characteristics of Peyer’s Patch

Follicleassociated Epithelium for Antigen Uptake'. *Journal of Experimental Medicine*, 214(6), pp. 1607–1618. DOI: 10.1084/jem.20160770.

Johanns, T.M. *et al.* (2010) 'Regulatory t Cell Suppressive Potency Dictates the Balance between Bacterial Proliferation and Clearance during Persistent Salmonella Infection'. *PLoS Pathogens*, 6(8), pp. 31–32. DOI: 10.1371/journal.ppat.1001043.

Johansson, M.E.V. *et al.* (2008) 'The Inner of the Two Muc2 Mucin-Dependent Mucus Layers in Colon Is Devoid of Bacteria'. *Proceedings of the National Academy of Sciences of the United States of America*, 105(39), pp. 15064–15069. DOI: 10.1073/pnas.0803124105.

John, A.E. *et al.* (2016) 'Loss of Epithelial Gq and G11 Signaling Inhibits TGFβ Production but Promotes IL-33-Mediated Macrophage Polarization and Emphysema'. *Science Signaling*, 9(451). DOI: 10.1126/scisignal.aad5568.

Johnson, G.R. and Jones, R.O. (1973) 'Differentiation of the Mammalian Hepatic Primordium in Vitro. I. Morphogenesis and the Onset of Haematopoiesis'. *Journal of Embryology and Experimental Morphology*, 30(1), pp. 83–96. DOI: 10.1242/dev.30.1.83.

Johnson, G.R. and Moore, M.A.S. (1975) 'Role of Stem Cell Migration in Initiation of Mouse Foetal Liver Haemopoiesis'. *Nature*, 258(5537), pp. 726–728. DOI: 10.1038/258726a0.

Johnston, L.K. *et al.* (2016) 'IL-33 Precedes IL-5 in Regulating Eosinophil Commitment and Is Required for Eosinophil Homeostasis'. *The Journal of Immunology*, 197(9), pp. 3445–3453. DOI: 10.4049/jimmunol.1600611.

Johnston, L.K. and Bryce, P.J. (2017) 'Understanding Interleukin 33 and Its Roles in Eosinophil Development'. *Frontiers in Medicine*, 4(MAY), pp. 1–7. DOI: 10.3389/fmed.2017.00051.

Jones, B.D., Ghori, N. and Falkow, S. (1994) 'Salmonella Typhlrnurium Initiates Murine Infection by Penetrating and Destroying the Specialized Epithelial M Cells of the Peyer's Patches'. *Journal of Experimental Medicine*, 180(1), pp. 15–23. DOI:

10.1084/jem.180.1.15.

Jones, J.E.C. *et al.* (2020) ‘The Adipocyte Acquires a Fibroblast-Like Transcriptional Signature in Response to a High Fat Diet’. *Scientific Reports*, 10(1), pp. 1–15. DOI: 10.1038/s41598-020-59284-w.

de Jong, H.K. *et al.* (2012) ‘Host-Pathogen Interaction in Invasive Salmonellosis’. *PLoS Pathogens*, 8(10), pp. 1–9. DOI: 10.1371/journal.ppat.1002933.

Josefowicz, S.Z. *et al.* (2012) ‘Extrathymically Generated Regulatory T Cells Control Mucosal Th2 Inflammation’. *Nature*, 482(7385), pp. 395–399. DOI: 10.1038/nature10772.

Kaczmarek, A., Vandenabeele, P. and Krysko, D. V. (2013) ‘Necroptosis: The Release of Damage-Associated Molecular Patterns and Its Physiological Relevance’. *Immunity*, 38(2), pp. 209–223. DOI: 10.1016/j.immuni.2013.02.003.

Kai, Y. *et al.* (2021) ‘Effects of IL-33 on 3T3-L1 Cells and Obese Mice Models Induced by a High-Fat Diet’. *International Immunopharmacology*, 101(PA), p. 108209. DOI: 10.1016/j.intimp.2021.108209.

Kakkar, R. *et al.* (2012) ‘Interleukin 33 as a Mechanically Responsive Cytokine Secreted by Living Cells’. *Journal of Biological Chemistry*, 287(9), pp. 6941–6948. DOI: 10.1074/jbc.M111.298703.

Kamsteeg, M. *et al.* (2010) ‘Molecular Diagnostics of Psoriasis, Atopic Dermatitis, Allergic Contact Dermatitis and Irritant Contact Dermatitis’. *British Journal of Dermatology*, 162(3), pp. 568–578. DOI: 10.1111/j.1365-2133.2009.09547.x.

Karamitros, D. *et al.* (2018) ‘Single-Cell Analysis Reveals the Continuum of Human Lympho-Myeloid Progenitor Cells Article’. *Nature Immunology*, 19(1), pp. 85–97. DOI: 10.1038/s41590-017-0001-2.

Katakura, T. *et al.* (2004) ‘CCL17 and IL-10 as Effectors That Enable Alternatively Activated Macrophages to Inhibit the Generation of Classically Activated Macrophages’. *The Journal of Immunology*, 172(3), pp. 1407–1413. DOI: 10.4049/jimmunol.172.3.1407.

Kato, M. *et al.* (1998) ‘Eosinophil Infiltration and Degranulation in Normal Human Tissue’. *Anatomical Record*, 252(3), pp. 418–425. DOI: 10.1002/(SICI)1097-0185(199811)252:3<418::AID-AR10>3.0.CO;2-1.

Kaviratne, M. *et al.* (2004) ‘IL-13 Activates a Mechanism of Tissue Fibrosis That Is Completely TGF-β Independent’. *The Journal of Immunology*, 173(6), pp. 4020–4029. DOI: 10.4049/jimmunol.173.6.4020.

Kawasaki, S. *et al.* (2001) ‘Intervention of Thymus and Activation-Regulated Chemokine Attenuates the Development of Allergic Airway Inflammation and Hyperresponsiveness in Mice’. *The Journal of Immunology*, 166(3), pp. 2055–2062. DOI: 10.4049/jimmunol.166.3.2055.

Kay, M.M.B. (1975) ‘Mechanism of Removal of Senescent Cells by Human Macrophages in Situ’. *Proceedings of the National Academy of Sciences of the United States of America*, 72(9), pp. 3521–3525. DOI: 10.1073/pnas.72.9.3521.

Kelly, E. *et al.* (2007) ‘IL-2 and Related Cytokines Can Promote T Cell Survival by Activating AKT’. *The Journal of Immunology*, 179(12), pp. 8569.1-8569. DOI: 10.4049/jimmunol.179.12.8569.

Ketcham, J.M., Marshall, L.A. and Talay, O. (2018) ‘CCR4 Antagonists Inhibit Treg Trafficking into the Tumor Microenvironment’. *ACS Medicinal Chemistry Letters*, 9(10), pp. 953–955. DOI: 10.1021/acsmedchemlett.8b00351.

Khan, M.I. *et al.* (2012) ‘Effectiveness of Vi Capsular Polysaccharide Typhoid Vaccine among Children: A Cluster Randomized Trial in Karachi, Pakistan’. *Vaccine*, 30(36), pp. 5389–5395. DOI: 10.1016/j.vaccine.2012.06.015.

Kim, B.-S. *et al.* (2017) ‘Generation of RORγt+ Antigen-Specific T Regulatory 17 (Tr17) Cells from Foxp3+ Precursors in Autoimmunity’. *Cell Reports*, 21(1), pp. 195–207. DOI: doi:10.1016/j.celrep.2017.09.021.

Kim, C. (2010) ‘Homeostatic and Pathogenic Extramedullary Hematopoiesis’. *Journal of Blood Medicine*, p. 13. DOI: 10.2147/jbm.s7224.

Kim, K.S. *et al.* (2016) ‘Dietary Antigens Limit Mucosal Immunity by Inducing

Regulatory T Cells in the Small Intestine'. *Science*, 351(6275), pp. 858–863. DOI: 10.1126/science.aac5560.

Kinjo, Y. *et al.* (2005) 'Recognition of Bacterial Glycosphingolipids by Natural Killer T Cells'. *Nature*, 434(7032), pp. 520–525. DOI: 10.1038/nature03407.

Kitaura, M. *et al.* (1996) 'Molecular Cloning of Human Eotaxin, an Eosinophil-Selective CC Chemokine, and Identification of a Specific Eosinophil Eotaxin Receptor, CC Chemokine Receptor 3'. *Journal of Biological Chemistry*, 271(13), pp. 7725–7730. DOI: 10.1074/jbc.271.13.7725.

De Kleer, I. *et al.* (2014) 'Ontogeny of Myeloid Cells'. *Frontiers in Immunology*, 5(AUG), pp. 1–11. DOI: 10.3389/fimmu.2014.00423.

Klei, T.R.L. *et al.* (2017) 'From the Cradle to the Grave: The Role of Macrophages in Erythropoiesis and Erythrophagocytosis'. *Frontiers in Immunology*, 8(FEB). DOI: 10.3389/fimmu.2017.00073.

Klein, L. *et al.* (2014) 'Positive and Negative Selection of the T Cell Repertoire: What Thymocytes See (and Don't See)'. *Nature Reviews Immunology*, 14(6), pp. 377–391. DOI: 10.1038/nri3667.

Klein, L., Robey, E.A. and Hsieh, C.S. (2019) 'Central CD4 + T Cell Tolerance: Deletion versus Regulatory T Cell Differentiation'. *Nature Reviews Immunology*, 19(1), pp. 7–18. DOI: 10.1038/s41577-018-0083-6.

Klemm, E.J. *et al.* (2018) 'Emergence of an Extensively Drug-Resistant Salmonella Enterica Serovar Typhi Clone Harboring a Promiscuous Plasmid Encoding Resistance to Fluoroquinolones and Third-Generation Cephalosporins'. *MBio*, 9(1). DOI: 10.1128/mBio.00105-18.

Koch, A.E. *et al.* (1992) 'Enhanced Production of Monocyte Chemoattractant Protein-1 in Rheumatoid Arthritis'. *Journal of Clinical Investigation*, 90(3), pp. 772–779. DOI: 10.1172/JCI115950.

Koch, A.E. *et al.* (1994) 'Macrophage Inflammatory Protein-1a'. *The Journal of Clinical Investigation*, 93(March), pp. 921–928.

Koch, M.A. *et al.* (2009) ‘The Transcription Factor T-Bet Controls Regulatory T Cell Homeostasis and Function during Type 1 Inflammation’. *Nature Immunology*, 10(6), pp. 595–602. DOI: 10.1038/ni.1731.

Koenen, R.R. *et al.* (2009) ‘Disrupting Functional Interactions between Platelet Chemokines Inhibits Atherosclerosis in Hyperlipidemic Mice’. *Nature Medicine*, 15(1), pp. 97–103. DOI: 10.1038/nm.1898.

Koenen, R.R. and Weber, C. (2010) ‘Therapeutic Targeting of Chemokine Interactions in Atherosclerosis’. *Nature Reviews Drug Discovery*, 9(2), pp. 141–153. DOI: 10.1038/nrd3048.

Köhler, G. *et al.* (1977) ‘Derivation of Hybrids between a Thymoma Line and Spleen Cells Activated in a Mixed Leukocyte Reation’. *European Journal of Immunology*, 7, pp. 758–761.

Koizumi, S. and Ishikawa, H. (2019) ‘Transcriptional Regulation of Differentiation and Functions of Effector T Regulatory Cells’. *Cells*, 8(8), p. 939. DOI: 10.3390/cells8080939.

Kolodin, D. *et al.* (2015) ‘Antigen- and Cytokine-Driven Accumulation of Regulatory t Cells in Visceral Adipose Tissue of Lean Mice’. *Cell Metabolism*, 21(4), pp. 543–557. DOI: 10.1016/j.cmet.2015.03.005.

Kotsiou, O.S., Gourgoulianis, K.I. and Zarogiannis, S.G. (2018) ‘IL-33/ST2 Axis in Organ Fibrosis’. *Frontiers in Immunology*, 9(OCT), pp. 1–15. DOI: 10.3389/fimmu.2018.02432.

Koulnis, M. *et al.* (2012) ‘Contrasting Dynamic Responses in Vivo of the Bcl-XL and Bim Erythropoietic Survival Pathways’. *Blood*, 119(5), pp. 1228–1239. DOI: 10.1182/blood-2011-07-365346.

Koulnis, M. *et al.* (2011) ‘Identification and Analysis of Mouse Erythroid Progenitors Using the CD71/TER119 Flow-Cytometric Assay’. *Journal of Visualized Experiments*, i(54), pp. 6–11. DOI: 10.3791/2809.

Koury, M.J. *et al.* (2005) ‘In Vitro Maturation of Nascent Reticulocytes to

Erythrocytes'. *Blood*, 105(5), pp. 2168–2174. DOI: 10.1182/blood-2004-02-0616.

Kouzaki, H. *et al.* (2011) 'The Danger Signal, Extracellular ATP, Is a Sensor for an Airborne Allergen and Triggers IL-33 Release and Innate Th2-Type Responses'. *The Journal of Immunology*, 186(7), pp. 4375–4387. DOI: 10.4049/jimmunol.1003020.

Krishnarajah, S. *et al.* (2022) 'Single-Cell Profiling of Immune System Alterations in Lymphoid, Barrier and Solid Tissues in Aged Mice'. *Nature Aging*, 2(1), pp. 74–89. DOI: 10.1038/s43587-021-00148-x.

Kufareva, I., Salanga, C.L. and Handel, T.M. (2015) 'Chemokine and Chemokine Receptor Structure and Interactions: Implications for Therapeutic Strategies'. *Immunology and Cell Biology*, 93(4), pp. 372–383. DOI: 10.1038/icb.2015.15.

Kühn, R. *et al.* (1993) 'Interleukin-10-Deficient Mice Develop Chronic Enterocolitis'. *Cell*, 75(2), pp. 263–274. DOI: 10.1016/0092-8674(93)80068-P.

Kuhn, V. *et al.* (2017) 'Red Blood Cell Function and Dysfunction: Redox Regulation, Nitric Oxide Metabolism, Anemia'. *Antioxidants and Redox Signaling*, 26(13), pp. 718–742. DOI: 10.1089/ars.2016.6954.

Kumaravelu, P. *et al.* (2002) 'Quantitative Developmental Anatomy of Definite Haematopoietic Stem Cells/Long-Term Repopulating Units (HSC/RUs): Role of the Aorta-Gonad-Mesonephros (AGM) Region and the Yolk Sac in Colonisation of the Mouse Embryonic Liver'. *Development*, 129(21), pp. 4891–4899. DOI: 10.1242/dev.129.21.4891.

Kupz, A. *et al.* (2013) 'Contribution of Thy1+ NK Cells to Protective IFN- Production during Salmonella Typhimurium Infections'. *Proceedings of the National Academy of Sciences*, 110(6), pp. 2252–2257. DOI: 10.1073/pnas.1222047110.

Kupz, A., Bedoui, S. and Strugnell, R.A. (2014) 'Cellular Requirements for Systemic Control of Salmonella Enterica Serovar Typhimurium Infections in Mice'. *Infection and Immunity*, 82(12), pp. 4997–5004. DOI: 10.1128/IAI.02192-14.

Kurokawa, M. *et al.* (2013) 'Interleukin-33-Activated Dendritic Cells Induce the Production of Thymus and Activation-Regulated Chemokine and Macrophage-

Derived Chemokine'. *International Archives of Allergy and Immunology*, 161(suppl 2), pp. 52–57. DOI: 10.1159/000350363.

Kurowska-Stolarska, M. *et al.* (2009) 'IL-33 Amplifies the Polarization of Alternatively Activated Macrophages That Contribute to Airway Inflammation'. *The Journal of Immunology*, 183(10), pp. 6469–6477. DOI: 10.4049/jimmunol.0901575.

Kurowska-Stolarska, M. *et al.* (2008) 'IL-33 Induces Antigen-Specific IL-5+ T Cells and Promotes Allergic-Induced Airway Inflammation Independent of IL-4'. *The Journal of Immunology*, 181(7), pp. 4780–4790.

Kurtz, J.R., Goggins, J.A. and McLachlan, J.B. (2017) 'Salmonella Infection: Interplay between the Bacteria and Host Immune System'. *Immunology Letters*, 190, pp. 42–50. DOI: 10.1016/j.imlet.2017.07.006.

Kwok, K.H.M., Lam, K.S.L. and Xu, A. (2016) 'Heterogeneity of White Adipose Tissue: Molecular Basis and Clinical Implications'. *Experimental and Molecular Medicine*, 48(3). DOI: 10.1038/emm.2016.5.

Lara-Tejero, M. *et al.* (2006) 'Role of the Caspase-1 Inflammasome in Salmonella Typhimurium Pathogenesis'. *Journal of Experimental Medicine*, 203(6), pp. 1407–1412. DOI: 10.1084/jem.20060206.

Lassen, P.B. *et al.* (2017) 'The Fat Score, a Fibrosis Score of Adipose Tissue: Predicting Weight-Loss Outcome after Gastric Bypass'. *Journal of Clinical Endocrinology and Metabolism*, 102(7), pp. 2443–2453. DOI: 10.1210/jc.2017-00138.

Lécuyer, E. *et al.* (2014) 'Segmented Filamentous Bacterium Uses Secondary and Tertiary Lymphoid Tissues to Induce Gut IgA and Specific T Helper 17 Cell Responses'. *Immunity*, 40(4), pp. 608–620. DOI: 10.1016/j.immuni.2014.03.009.

Lee, J.H., Wang, C. and Kim, C.H. (2009) 'FoxP3+ Regulatory T Cells Restrain Splenic Extramedullary Myelopoiesis via Suppression of Hematopoietic Cytokine-Producing T Cells'. *Journal of Immunology*, 183(10), pp. 6377–6386. DOI: 10.4049/jimmunol.0901268.

Lee, J.S. *et al.* (2016) ‘ST2 Receptor Invalidation Maintains Wound Inflammation, Delays Healing and Increases Fibrosis’. *Experimental Dermatology*, 25(1), pp. 71–74. DOI: 10.1111/exd.12833.

Lee, M.J., Wu, Y. and Fried, S.K. (2013) ‘Adipose Tissue Heterogeneity: Implication of Depot Differences in Adipose Tissue for Obesity Complications’. *Molecular Aspects of Medicine*, 34(1), pp. 1–11. DOI: 10.1016/j.mam.2012.10.001.

Lee, M.K., Lee, B. and Kim, C.Y. (2021) ‘Natural Extracts That Stimulate Adipocyte Browning and Their Underlying Mechanisms’. *Antioxidants*, 10(2), pp. 1–17. DOI: 10.3390/antiox10020308.

Lee, M.W. *et al.* (2015) ‘Activated Type 2 Innate Lymphoid Cells Regulate Beige Fat Biogenesis’. *Cell*, 160(1–2), pp. 74–87. DOI: 10.1016/j.cell.2014.12.011.

Lee, N.A. *et al.* (1997) ‘Expression of IL-5 in Thymocytes/T Cells Leads to the Development of a Massive Eosinophilia, Extramedullary Eosinophilopoiesis, and Unique Histopathologies’. *Journal of Immunology*, 158(3), pp. 1332–1344. DOI: https://doi.org/10.4049/jimmunol.158.3.1332.

Lee, S.J., Dunmire, S. and McSorley, S.J. (2012) ‘MHC Class-I-Restricted CD8 T Cells Play a Protective Role during Primary Salmonella Infection’. *Immunology Letters*, 148(2), pp. 138–143. DOI: 10.1016/j.imlet.2012.10.009.

Lefrançais, E. *et al.* (2012) ‘IL-33 Is Processed into Mature Bioactive Forms by Neutrophil Elastase and Cathepsin G’. *Proceedings of the National Academy of Sciences of the United States of America*, 109(5), pp. 1673–1678. DOI: 10.1073/pnas.1115884109.

Lefrançais, E. and Cayrol, C. (2012) ‘Mechanisms of IL-33 Processing and Secretion: Differences and Similarities between IL-1 Family Members’. *European Cytokine Network*, 23(4), pp. 120–127. DOI: 10.1684/ecn.2012.0320.

Lefrançais, E. *et al.* (2014) ‘Central Domain of IL-33 Is Cleaved by Mast Cell Proteases for Potent Activation of Group-2 Innate Lymphoid Cells’. *Proceedings of the National Academy of Sciences of the United States of America*, 111(43), pp.

15502–15507. DOI: 10.1073/pnas.1410700111.

Lelouard, H. *et al.* (2012) ‘Peyer’s Patch Dendritic Cells Sample Antigens by Extending Dendrites through M Cell-Specific Transcellular Pores’. *Gastroenterology*, 142(3), pp. 592-601.e3. DOI: 10.1053/j.gastro.2011.11.039.

Levine, A.G. *et al.* (2014) ‘Continuous Requirement for the TCR in Regulatory T Cell Function’. *Nature Immunology*, 15(11), pp. 1070–1078. DOI: 10.1038/ni.3004.

Levine, A.G. *et al.* (2017) ‘Stability and Function of Regulatory T Cells Expressing the Transcription Factor T-Bet’. *Nature*, 546(7658), pp. 421–425. DOI: 10.1038/nature22360.Stability.

Levine, M.M. *et al.* (1999) ‘Duration of Efficacy of Ty21a, Attenuated Salmonella Typhi Live Oral Vaccine’. *Vaccine*, 17(SUPPL. 2), pp. 22–27. DOI: 10.1016/S0264-410X(99)00231-5.

Levoye, A. *et al.* (2009) ‘CXCR7 Heterodimerizes with CXCR4 and Regulates CXCL12-Mediated G Protein Signaling’. *Blood*, 113(24), pp. 6085–6093. DOI: 10.1182/blood-2008-12-196618.The.

Ley, R.E. *et al.* (2005) ‘Obesity Alters Gut Microbial Ecology’. *Proceedings of the National Academy of Sciences of the United States of America*, 102(31), pp. 11070–11075. DOI: 10.1073/pnas.0504978102.

Leystra, A.A. and Clapper, M.L. (2019) ‘Gut Microbiota Influences Experimental Outcomes in Mouse Models of Colorectal Cancer’. *Genes*, 10(11). DOI: 10.3390/genes10110900.

Li, C. *et al.* (2018) ‘TCR Transgenic Mice Reveal Stepwise, Multi-Site Acquisition of the Distinctive Fat-Treg Phenotype’. *Cell*, 174(2), pp. 285-299.e12. DOI: 10.1016/j.cell.2018.05.004.

Li, D. *et al.* (2014) ‘IL-33 Promotes ST2-Dependent Lung Fibrosis by the Induction of Alternatively Activated Macrophages and Innate Lymphoid Cells in Mice’. *Journal of Allergy and Clinical Immunology*, 134(6), pp. 1422-1432.e11. DOI: 10.1016/j.jaci.2014.05.011.

Li, Y. (2010) ‘Commonly Used Tag Combinations for Tandem Affinity Purification’. *Biotechnology Applied Biochemistry*, 55, pp. 73–83. DOI: 10.1042/BA20090273.

Li, Y.Q. *et al.* (2013) ‘Tumor Secretion of CCL22 Activates Intratumoral Treg Infiltration and Is Independent Prognostic Predictor of Breast Cancer’. *PLoS ONE*, 8(10), pp. 1–9. DOI: 10.1371/journal.pone.0076379.

Liang, S.C. *et al.* (2006) ‘Interleukin (IL)-22 and IL-17 Are Coexpressed by Th17 Cells and Cooperatively Enhance Expression of Antimicrobial Peptides’. *Journal of Experimental Medicine*, 203(10), pp. 2271–2279. DOI: 10.1084/jem.20061308.

Liang, Y. *et al.* (2013) ‘IL-33 Induces Nuocytes and Modulates Liver Injury in Viral Hepatitis’. *The Journal of Immunology*, 190(11), pp. 5666–5675. DOI: 10.4049/jimmunol.1300117.

Lieberam, I. and Förster, I. (1999) ‘The Murine β-Chemokine TARC Is Expressed by Subsets of Dendritic Cells and Attracts Primed CD4+ T Cells’. *European Journal of Immunology*, 29(9), pp. 2684–2694. DOI: 10.1002/(SICI)1521-4141(199909)29:09<2684::AID-IMMU2684>3.0.CO;2-Y.

Liew, F.Y., Pitman, N.I. and McInnes, I.B. (2010) ‘Disease-Associated Functions of IL-33: The New Kid in the IL-1 Family’. *Nature Reviews Immunology*, 10(2), pp. 103–110. DOI: 10.1038/nri2692.

Lin, R. *et al.* (2018) ‘β-Arrestin-2-Dependent Signaling Promotes CCR4-Mediated Chemotaxis of Murine T-Helper Type 2 Cells’. *American Journal of Respiratory Cell and Molecular Biology*, 58(6), pp. 745–755. DOI: 10.1165/rcmb.2017-0240OC.

Lin, Y.H. *et al.* (2016) ‘Distribution and Clinical Association of Plasma Soluble ST2 during the Development of Type 2 Diabetes’. *Diabetes Research and Clinical Practice*, 118, pp. 140–145. DOI: 10.1016/j.diabres.2016.06.006.

Liu, B. *et al.* (2021) ‘Affinity-Coupled CCL22 Promotes Positive Selection in Germinal Centres’. *Nature*, (June 2020), pp. 1–5. DOI: 10.1038/s41586-021-03239-2.

Liu, L.Y. *et al.* (2003) ‘Chemokine Receptor Expression on Human Eosinophils from Peripheral Blood and Bronchoalveolar Lavage Fluid after Segmental Antigen

Challenge'. *Journal of Allergy and Clinical Immunology*, 112(3), pp. 556–562. DOI: 10.1016/S0091-6749(03)01798-6.

Liu, X. *et al.* (2013) 'Structural Insights into the Interaction of IL-33 with Its Receptors'. *Proceedings of the National Academy of Sciences of the United States of America*, 110(37), pp. 14918–14923. DOI: 10.1073/pnas.1308651110.

Llewellyn, S.R. *et al.* (2018) 'Interactions Between Diet and the Intestinal Microbiota Alter Intestinal Permeability and Colitis Severity in Mice'. *Gastroenterology*, 154(4), pp. 1037-1046.e2. DOI: 10.1053/j.gastro.2017.11.030.

Lo, W.F. *et al.* (1999) 'T Cell Responses to Gram-Negative Intracellular Bacterial Pathogens: A Role for CD8+ T Cells in Immunity to Salmonella Infection and the Involvement of MHC Class Ib Molecules'. *Journal of Immunology*, 162(9), pp. 5398–5406.

Lochner, M. *et al.* (2002) 'Generation of Neutralizing Mouse Anti-Mouse IL-18 Antibodies for Inhibition of Inflammatory Responses in Vivo'. *Journal of Immunological Methods*, 259(1–2), pp. 149–157. DOI: 10.1016/S0022-1759(01)00505-1.

Lodi, P.J. *et al.* (1994) 'High-Resolution Solution Structure of the β Chemokine HMIP-1β by Multidimensional NMR'. *Science*, 263(5154), pp. 1762–1767. DOI: 10.1126/science.8134838.

Löhning, M. *et al.* (1998) 'T1/ST2 Is Preferentially Expressed on Murine Th2 Cells, Independent of Interleukin 4, Interleukin 5, and Interleukin 10, and Important for Th2 Effector Function'. *Proceedings of the National Academy of Sciences of the United States of America*, 95(12), pp. 6930–6935. DOI: 10.1073/pnas.95.12.6930.

Lorenz, R.G. and Newberry, R.D. (2004) 'Isolated Lymphoid Follicles Can Function as Sites for Induction of Mucosal Immune Responses'. *Annals of the New York Academy of Sciences*, 1029, pp. 44–57. DOI: 10.1196/annals.1309.006.

Love, P.E. and Bhandoola, A. (2011) 'Signal Integration and Crosstalk during Thymocyte Migration and Emigration'. *Nature Reviews Immunology*, 11(7), pp. 469–

477. DOI: 10.1038/nri2989.

Lowell, B.B. *et al.* (1993) 'Development of Obesity in Transgenic Mice after Genetic Ablation of Brown Adipose Tissue'. *Nature*, 366(6457), pp. 740–742. DOI: 10.1038/366740a0.

Lu, Y. *et al.* (2020) 'Interleukin-33 Signaling Controls the Development of Iron-Recycling Macrophages'. *Immunity*, 52(5), pp. 782-793.e5. DOI: 10.1016/j.immuni.2020.03.006.

Vander Lugt, M.T. *et al.* (2013) 'ST2 as a Marker for Risk of Therapy-Resistant Graft-versus-Host Disease and Death'. *New England Journal of Medicine*, 369(6), pp. 529–539. DOI: 10.1056/nejmoa1213299.

Lundberg, R. *et al.* (2017) 'Microbiota Composition of Simultaneously Colonized Mice Housed under Either a Gnotobiotic Isolator or Individually Ventilated Cage Regime'. *Scientific Reports*, 7(November 2016), pp. 1–11. DOI: 10.1038/srep42245.

Luster, A.D. (1998) 'Chemokines - Chemotactic Cytokines That Mediate Inflammation'. *The New England Journal of Medicine*, 338, pp. 436–45. DOI: 10.1056/NEJM199802123380706.

Lüthi, A.U. *et al.* (2009) 'Suppression of Interleukin-33 Bioactivity through Proteolysis by Apoptotic Caspases'. *Immunity*, 31(1), pp. 84–98. DOI: 10.1016/j.immuni.2009.05.007.

Luzina, I.G. *et al.* (2013) 'Interleukin-33 Potentiates Bleomycin-Induced Lung Injury'. *American Journal of Respiratory Cell and Molecular Biology*, 49(6), pp. 999–1008. DOI: 10.1165/rcmb.2013-0093OC.

Lv, L.-X. *et al.* (2019) 'Interactions Between Gut Microbiota and Hosts and Their Role in Infectious Diseases'. *Infectious Microbes & Diseases*, 1(1), pp. 3–9. DOI: 10.1097/IM9.0000000000000001.

Mabbott, N.A. *et al.* (2013) 'Microfold (M) Cells: Important Immunosurveillance Posts in the Intestinal Epithelium'. *Mucosal Immunology*, 6(4), pp. 666–677. DOI: 10.1038/mi.2013.30.

Macdougall, C.E. *et al.* (2018) 'Visceral Adipose Tissue Immune Homeostasis Is Regulated by the Crosstalk between Adipocytes and Dendritic Cell Subsets'. *Cell Metabolism*, 27(3), pp. 588-601.e4. DOI: 10.1016/j.cmet.2018.02.007.

MacMicking, J.D. (2012) 'Interferon-Inducible Effector Mechanisms in Cell-Autonomous Immunity'. *Nature Reviews Immunology*, 12(5), pp. 367–382. DOI: 10.1038/nri3210.

Magne, F. *et al.* (2020) 'The Firmicutes/Bacteroidetes Ratio: A Relevant Marker of Gut Dysbiosis in Obese Patients?' *Nutrients*, 12(5). DOI: 10.3390/nu12051474.

Mahapatro, M. *et al.* (2016) 'Programming of Intestinal Epithelial Differentiation by IL-33 Derived from Pericryptal Fibroblasts in Response to Systemic Infection'. *Cell Reports*, 15(8), pp. 1743–1756. DOI: 10.1016/j.celrep.2016.04.049.

Maharjan, B.R. *et al.* (2021) 'The Effect of a Sustained High-Fat Diet on the Metabolism of White and Brown Adipose Tissue and Its Impact on Insulin Resistance: A Selected Time Point Cross-Sectional Study'. *International Journal of Molecular Sciences*, 22(24). DOI: 10.3390/ijms222413639.

Malleret, B. *et al.* (2013) 'Significant Biochemical, Biophysical and Metabolic Diversity in Circulating Human Cord Blood Reticulocytes'. *PLoS ONE*, 8(10). DOI: 10.1371/journal.pone.0076062.

Maloy, K.J. and Powrie, F. (2001) 'Regulatory T Cells in the Control of Immune Pathology'. *Nature Immunology*, 2(9), pp. 816–822. DOI: 10.1038/ni0901-816.

Mangalmurti, N.S. *et al.* (2009) 'Loss of Red Cell Chemokine Scavenging Promotes Transfusion-Related Lung Inflammation'. *Blood*, 113(5), pp. 1158–1166. DOI: 10.1182/blood-2008-07-166264.

Mantis, N.J. *et al.* (2002) 'Selective Adherence of IgA to Murine Peyer's Patch M Cells: Evidence for a Novel IgA Receptor'. *The Journal of Immunology*, 169(4), pp. 1844–1851. DOI: 10.4049/jimmunol.169.4.1844.

Mantovani, A. *et al.* (2004) 'The Chemokine System in Diverse Forms of Macrophage Activation and Polarization'. *Trends in Immunology*, 25(12), pp. 677–

686. DOI: 10.1016/j.it.2004.09.015.

Manwani, D. and Bieker, J.J. (2008) 'The Erythroblastic Island'. *Current Topics in Developmental Biology*, 82(07), pp. 23–53. DOI: 10.1016/S0070-2153(07)00002-6.

Marcelin, G., Gautier, E.L. and Clement, K. (2022) 'Adipose Tissue Fibrosis in Obesity: Etiology and Challenges'. *Annual Review of Physiology*, 84, pp. 135–155. DOI: 10.1146/annurev-physiol-060721-092930.

Marchello, C.S., Hong, C.Y. and Crump, J.A. (2019) 'Global Typhoid Fever Incidence: A Systematic Review and Meta-Analysis'. *Clinical Infectious Diseases*, 68(Suppl 2), pp. S105–S116. DOI: 10.1093/cid/ciy1094.

Marchi, L.F. *et al.* (2014) 'In Vitro Activation of Mouse Neutrophils by Recombinant Human Interferon-Gamma: Increased Phagocytosis and Release of Reactive Oxygen Species and pro-Inflammatory Cytokines'. *International Immunopharmacology*, 18(2), pp. 228–235. DOI: 10.1016/j.intimp.2013.12.010.

Mariani, M. *et al.* (2004a) 'Dominance of CCL22 over CCL17 in Induction of Chemokine Receptor CCR4 Desensitization and Internalization on Human Th2 Cells'. *European Journal of Immunology*, 34(1), pp. 231–240. DOI: 10.1002/eji.200324429.

Mariani, M. *et al.* (2004b) 'Dominance of CCL22 over CCL17 in Induction of Chemokine Receptor CCR4 Desensitization and Internalization on Human Th2 Cells'. *European Journal of Immunology*, 34(1), pp. 231–240. DOI: 10.1002/eji.200324429.

Marvie, P. *et al.* (2010) 'Interleukin-33 Overexpression Is Associated with Liver Fibrosis in Mice and Humans'. *Journal of Cellular and Molecular Medicine*, 14(6 B), pp. 1726–1739. DOI: 10.1111/j.1582-4934.2009.00801.x.

Maskey, A.P. *et al.* (2006) 'Salmonella Enterica Serovar Paratyphi A and S. Enterica Serovar Typhi Cause Indistinguishable Clinical Syndromes in Kathmandu, Nepal'. *Clinical Infectious Diseases*, 42(9), pp. 1247–1253. DOI: 10.1086/503033.

Mason, K.L. *et al.* (2008) 'Overview of Gut Immunolog'. In Huffnagle, G.B. and

Noverr, M.C. (eds.) *GI Microbiota and Regulation of the Immune System.* New York: Springer New York, pp. 1–15.

Masopust, D. *et al.* (2010) 'Dynamic T Cell Migration Program Provides Resident Memory within Intestinal Epithelium'. *Journal of Experimental Medicine*, 207(3), pp. 553–564. DOI: 10.1084/jem.20090858.

Mastroeni, P., Vazquez-Torres, A., *et al.* (2000) 'Antimicrobial Actions of the NADPH Phagocyte Oxidase and Inducible Nitric Oxide Synthase in Experimental Salmonellosis. II. Effects on Microbial Proliferation and Host Survival In Vivo'. *Journal of Experimental Medicine*, 192(2), pp. 237–248. DOI: 10.1084/jem.192.2.237.

Mastroeni, P., Simmons, C., *et al.* (2000) 'Igh-6(-/-) (B-Cell-Deficient) Mice Fail to Mount Solid Acquired Resistance to Oral Challenge with Virulent Salmonella Enterica Serovar Typhimurium and Show Impaired Th1 T-Cell Responses to Salmonella Antigens'. *Infection and Immunity*, 68(1), pp. 46–53. DOI: 10.1128/IAI.68.1.46-53.2000.

Mastroeni, P. and Rossi, O. (2020) 'Antibodies and Protection in Systemic Salmonella Infections: Do We Still Have More Questions than Answers?' *Infection and Immunity*, 88(10), pp. 1–15. DOI: 10.1128/IAI.00219-20.

Mathis, D. (2013) 'Immunological Goings-On in Visceral Adipose Tissue'. *Cell Metabolism*, 17(6), pp. 851–859. DOI: 10.1016/j.cmet.2013.05.008.

Matta, B.M. *et al.* (2014) 'IL-33 Is an Unconventional Alarmin That Stimulates IL-2 Secretion by Dendritic Cells To Selectively Expand IL-33R/ST2+ Regulatory T Cells'. *The Journal of Immunology*, 193(8), pp. 4010–4020. DOI: 10.4049/jimmunol.1400481.

Matta, B.M. *et al.* (2016) 'Peri-AlloHCT IL-33 Administration Expands Recipient T-Regulatory Cells That Protect Mice against Acute GVHD'. *Blood*, 128(3), pp. 427–439. DOI: 10.1182/blood-2015-12-684142.

Matta, B.M. and Turnquist, H.R. (2016) 'Expansion of Regulatory T Cells in Vitro and

in Vivo by IL-33'. *Methods in Molecular Biology*, 1371, pp. 29–41. DOI: 10.1007/978-1-4939-3139-2_3.

Mayer, K.L. and Stone, M.J. (2000) 'NMR Solution Structure and Receptor Peptide Binding of the CC Chemokine'. *Biochemistry*, 39(29), pp. 8382–8395. DOI: 10.1021/bi000523j.

McBrien, C.N. and Menzies-Gow, A. (2017) 'The Biology of Eosinophils and Their Role in Asthma'. *Frontiers in Medicine*, 4(JUN). DOI: 10.3389/fmed.2017.00093.

Mchedlidze, T. *et al.* (2013) 'Interleukin-33-Dependent Innate Lymphoid Cells Mediate Hepatic Fibrosis'. *Immunity*, 39(2), pp. 357–371. DOI: 10.1016/j.immuni.2013.07.018.

Mckimmie, C.S. *et al.* (2008) 'Hemopoietic Cell Expression of the Chemokine Decoy Recepotr D6 Is Dynamic and Regulated by GATA1'. *Journal of Immunology*, 181(5), pp. 3353–3363. DOI: https://doi.org/10.4049/jimmunol.181.5.3353.

McKinnon, K.M. (2018) 'Flow Cytometry: An Overview.' *Current Protocols in Immunology*, 120, pp. 5.1.1-5.1.11. DOI: 10.1002/cpim.40.

McSorley, S.J. *et al.* (2002) 'Bacterial Flagellin Is an Effective Adjuvant for CD4+ T Cells In Vivo'. *The Journal of Immunology*, 169(7), pp. 3914–3919. DOI: 10.4049/jimmunol.169.7.3914.

McSorley, S.J. and Jenkins, M.K. (2000) 'Antibody Is Required for Protection against Virulent but Not Attenuated Salmonella Enterica Serovar Typhimurium'. *Infection and Immunity*, 68(6), pp. 3344–3348. DOI: 10.1128/IAI.68.6.3344-3348.2000.

Medvinsky, A.L. *et al.* (1996) 'Development of Day-8 Colony-Forming Unit-Spleen Hematopoietic Progenitors during Early Murine Embryogenesis: Spatial and Temporal Mapping'. *Blood*, 87(2), pp. 557–566. DOI: 10.1182/blood.v87.2.557.bloodjournal872557.

Medzhitov, R. (2001) 'Toll-like Receptors and Innate Immunity'. *Nature Reviews Immunology*, 1(2), pp. 135–145. Available at: https://doi.org/10.1038/35100529%0Ahttps://www.nature.com/articles/nri35100529.

pdf.

Meiring, J.E. *et al.* (2021) ‘Burden of Enteric Fever at Three Urban Sites in Africa and Asia: A Multicentre Population-Based Study’. *The Lancet Global Health*, 9(12), pp. e1688–e1696. DOI: 10.1016/S2214-109X(21)00370-3.

Mel, H., Prenant, M. and Mohandas, N. (1977) ‘Reticulocyte Motility and Form: Studies on Maturation and Classification’. *Blood*, 49(6), pp. 1001–1009. DOI: 10.1182/blood.v49.6.1001.1001.

Meyer, K. and Selbach, M. (2015) ‘Quantitative Affinity Purification Mass Spectrometry : A Versatile Technology to Study Protein – Protein Interactions’. *Frontiers in Genetics*, 6(237), pp. 1–7. DOI: 10.3389/fgene.2015.00237.

Mian, M.F. *et al.* (2011) ‘Humanized Mice Are Susceptible to Salmonella Typhi Infection’. *Cellular and Molecular Immunology*, 8(1), pp. 83–87. DOI: 10.1038/cmi.2010.52.

Miao, E.A. *et al.* (2010) ‘Caspase-1-Induced Pyroptosis Is an Innate Immune Effector Mechanism against Intracellular Bacteria’. *Nature Immunology*, 11(12), pp. 1136–1142. DOI: 10.1038/ni.1960.

Miao, R. *et al.* (2020) ‘Hematopoietic Stem Cell Niches and Signals Controlling Immune Cell Development and Maintenance of Immunological Memory’. *Frontiers in Immunology*, 11(November), pp. 1–13. DOI: 10.3389/fimmu.2020.600127.

Miller, Ashley M. *et al.* (2010) ‘IL-33 Induces Protective Effects in Adipose Tissue Inflammation during Obesity in Mice’. *Circ Res*, 107(5), pp. 650–658. DOI: 10.1161/CIRCRESAHA.110.218867.IL-33.

Miller, A.M. *et al.* (2008) ‘IL-33 Reduces the Development of Atherosclerosis’. *Journal of Experimental Medicine*, 205(2), pp. 339–346. DOI: 10.1084/jem.20071868.

Miller, Ashley M. *et al.* (2010) ‘Interleukin-33 Induces Protective Effects in Adipose Tissue Inflammation during Obesity in Mice’. *Circulation Research*, 107(5), pp. 650–658. DOI: 10.1161/CIRCRESAHA.110.218867.

Miller, A.M. *et al.* (2012) ‘Soluble ST2 Associates with Diabetes but Not Established Cardiovascular Risk Factors: A New Inflammatory Pathway of Relevance to Diabetes?’ *PLoS ONE*, 7(10), pp. 1–7. DOI: 10.1371/journal.pone.0047830.

Miller, S.I., Kukral, A.M. and Mekalanos, J.J. (1989) ‘A Two-Component Regulatory System (PhoP PhoQ) Controls Salmonella Typhimurium Virulence’. *Proceedings of the National Academy of Sciences of the United States of America*, 86(13), pp. 5054–5058. DOI: 10.1073/pnas.86.13.5054.

Millot, S. *et al.* (2010) ‘Erythropoietin Stimulates Spleen BMP4-Dependent Stress Erythropoiesis and Partially Corrects Anemia in a Mouse Model of Generalized Inflammation’. *Blood*, 116(26), pp. 6072–6081. DOI: 10.1182/blood-2010-04-281840.

Minokoshi, Y., Saito, M. and Shimazu, T. (1986) ‘Metabolic and Morphological Alterations of Brown Adipose Tissue after Sympathetic Denervation in Rats’. *Journal of the Autonomic Nervous System*, 15(3), pp. 197–204. DOI: 10.1016/0165-1838(86)90063-9.

Le Minor, L. and Popoff, M.Y. (1987) ‘Designation of Salmonella Enterica Sp. Nov., Norn. Rev., as the Type and Only Species of the Genus Salmonella’. *International Journal of Systematic Bacteriology*, 37(4), pp. 465–468. Available at: http://ijs.sgmjournals.org/content/37/4/465.full.pdf#page=1&view=FitH%5Cnpapers2://publication/uuid/7B2C0D30-82DA-46B0-A33F-6C1EB1B7B19E.

Mirkovich, A.M. *et al.* (1986) ‘Increased Myelopoiesis during Leishmania Major Infection in Mice: Generation of “Safe Targets”, a Possible Way to Evade the Immune Mechanism’. *Clinical and Experimental Immunology*, 64(1), pp. 1–7.

Mittrücker, H.-W. *et al.* (2000) ‘ Cutting Edge: Role of B Lymphocytes in Protective Immunity Against Salmonella Typhimurium Infection ’. *The Journal of Immunology*, 164(4), pp. 1648–1652. DOI: 10.4049/jimmunol.164.4.1648.

Mizukami, Y. *et al.* (2008) ‘CCL17 and CCL22 Chemokines within Tumor Microenvironment Are Related to Accumulation of Foxp3+ Regulatory T Cells in Gastric Cancer’. *International Journal of Cancer*, 122(10), pp. 2286–2293. DOI:

10.1002/ijc.23392.

Modigliani, Y. *et al.* (1996) ‘Establishment of Tissue-Specific Tolerance Is Driven by Regulatory T Cells Selected by Thymic Epithelium’. *European Journal of Immunology*, 26, pp. 1807–1815.

Moe, H. (1953) ‘Mucus-Producing Goblet Cells of the Small Intestine’. *Nature*, 172(4372), p. 309. DOI: 10.1038/172309a0.

Mohamed, O.Y.E. *et al.* (2016) ‘Local Elevation of CCL22: A New Trend in Immunotherapy (Skin Model)’. *Journal of Cellular Immunotherapy*, 2(2), pp. 79–84. DOI: 10.1016/j.jocit.2015.12.001.

Mohammed, H. *et al.* (2016) ‘Rapid Immunoprecipitation Mass Spectrometry of Endogenous Proteins (RIME) for Analysis of Chromatin Complexes’. *Nature Protocols*, 11(2), pp. 316–326. DOI: 10.1038/nprot.2016.020.

Molofsky, A.B. *et al.* (2013) ‘Innate Lymphoid Type 2 Cells Sustain Visceral Adipose Tissue Eosinophils and Alternatively Activated Macrophages’. *Journal of Experimental Medicine*, 210(3), pp. 535–549. DOI: 10.1084/jem.20121964.

Molofsky, A.B., Savage, A. and Locksley, R.M. (2015) ‘Interleukin-33 in Tissue Homeostasis, Injury and Inflammation’. *Immunity*, 42(6), pp. 1005–1019. DOI: 10.1016/j.immuni.2015.06.006.Interleukin-33.

Monack, D.M., Bouley, D.M. and Falkow, S. (2004) ‘Salmonella Typhimurium Persists within Macrophages in the Mesenteric Lymph Nodes of Chronically Infected Nramp1+/+ Mice and Can Be Reactivated by IFNγ Neutralization’. *Journal of Experimental Medicine*, 199(2), pp. 231–241. DOI: 10.1084/jem.20031319.

Monticelli, L.A. *et al.* (2011) ‘Innate Lymphoid Cells Promote Lung-Tissue Homeostasis after Infection with Influenza Virus’. *Nature Immunology*, 12(11), pp. 1045–1054. DOI: 10.1038/ni.2131.

Montpas, N. *et al.* (2018) ‘Ligand-Specific Conformational Transitions and Intracellular Transport Are Required for Atypical Chemokine Receptor 3–Mediated Chemokine Scavenging’. *Journal of Biological Chemistry*, 293(3), pp. 893–905. DOI:

10.1074/jbc.M117.814947.

Moras, M., Lefevre, S.D. and Ostuni, M.A. (2017) 'From Erythroblasts to Mature Red Blood Cells: Organelle Clearance in Mammals'. *Frontiers in Physiology*, 8(DEC), pp. 1–9. DOI: 10.3389/fphys.2017.01076.

Morgan, M.J. and Liu, Z.G. (2011) 'Crosstalk of Reactive Oxygen Species and NF-KB Signaling'. *Cell Research*, 21(1), pp. 103–115. DOI: 10.1038/cr.2010.178.

Moro, K. *et al.* (2010) 'Innate Production of TH 2 Cytokines by Adipose Tissue-Associated c-Kit+ Sca-1+ Lymphoid Cells'. *Nature*, 463(7280), pp. 540–544. DOI: 10.1038/nature08636.

Moussion, C., Ortega, N. and Girard, J.P. (2008) 'The IL-1-like Cytokine IL-33 Is Constitutively Expressed in the Nucleus of Endothelial Cells and Epithelial Cells in Vivo: A Novel "Alarmin"?' *PLoS ONE*, 3(10), pp. 1–8. DOI: 10.1371/journal.pone.0003331.

Mowat, A.M. and Agace, W.W. (2014) 'Regional Specialization within the Intestinal Immune System'. *Nature Reviews Immunology*, 14(10), pp. 667–685. DOI: 10.1038/nri3738.

Mowat, A.M.I. (2003) 'Anatomical Basis of Tolerance and Immunity to Intestinal Antigens'. *Nature Reviews Immunology*, 3(4), pp. 331–341. DOI: 10.1038/nri1057.

Mowat, A.M.I. and Viney, J.L. (1997) 'The Anatomical Basis of Intestinal Immunity'. *Immunological Reviews*, 156, pp. 145–166. DOI: 10.1111/j.1600-065X.1997.tb00966.x.

Muller, C. *et al.* (2009) 'Acid Stress Activation of the ΣE Stress Response in Salmonella Enterica Serovar Typhimurium'. *Molecular Microbiology*, 71(5), pp. 1128–1238. DOI: 10.1111/j.1365-2958.2009.06597.x.Acid.

Mungyer, G. *et al.* (1983) 'Plasmodium Berghei: Influence on Granulopoiesis and Macrophage Production in BALB/c Mice'. *Experimental Parasitology*, 56(2), pp. 266–276. DOI: 10.1016/0014-4894(83)90072-3.

Muotiala, A. and Mäkelä, P.H. (1990) 'The Role of IFN-γ in Murine Salmonella

Typhimurium Infection'. *Microbial Pathogenesis*, 8(2), pp. 135–141. DOI: 10.1016/0882-4010(90)90077-4.

Murphy, K. and Weaver, C. (2017) *Janeway's Immunobiology*. 9th Edition. New York: Garland Science: New York.

Murray, L.A. (2016) 'Editorial: The Cell Types of Fibrosis'. *Frontiers in Pharmacology*, 6(JAN), pp. 2015–2016. DOI: 10.3389/fphar.2015.00311.

Nagai, Y. *et al.* (2006) 'Toll-like Receptors on Hematopoietic Progenitor Cells Stimulate Innate Immune System Replenishment'. *Immunity*, 24(6), pp. 801–812. DOI: 10.1016/j.immuni.2006.04.008.

Nagareddy, P.R. *et al.* (2014) 'Adipose Tissue Macrophages Promote Myelopoiesis and Monocytosis in Obesity'. *Cell Metabolism*, 19(5), pp. 821–835. DOI: 10.1016/j.cmet.2014.03.029.

Naik, S. *et al.* (2017) 'Inflammatory Memory Sensitizes Skin Epithelial Stem Cells to Tissue Damage'. *Nature*, 550(7677), pp. 475–480. DOI: 10.1038/nature24271.

Nakatani, T. *et al.* (2001) 'CCR4+ Memory CD4+ T Lymphocytes Are Increased in Peripheral Blood and Lesional Skin from Patients with Atopic Dermatitis'. *Journal of Allergy and Clinical Immunology*, 107(2), pp. 353–358. DOI: 10.1067/mai.2001.112601.

Nakayama, T. *et al.* (2002) 'The Generation of Mature, Single-Positive Thymocytes In Vivo Is Dysregulated by CD69 Blockade or Overexpression'. *The Journal of Immunology*, 168(1), pp. 87–94. DOI: 10.4049/jimmunol.168.1.87.

Nakorn, T.N., Miyamoto, T. and Weissman, I.L. (2003) 'Characterization of Mouse Clonogenic Megakaryocyte Progenitors'. *Proceedings of the National Academy of Sciences of the United States of America*, 100(1), pp. 205–210. DOI: 10.1073/pnas.262655099.

Nanton, M.R. *et al.* (2012) ' Cutting Edge: B Cells Are Essential for Protective Immunity against Salmonella Independent of Antibody Secretion '. *The Journal of Immunology*, 189(12), pp. 5503–5507. DOI: 10.4049/jimmunol.1201413.

Nauciel, C. (1990) ‘Role of CD4+ T Cells and T-Independent Mechanisms in Acquired Resistance to Salmonella Typhimurium Infection.’ *The Journal of Immunology*, 145(4), pp. 1265–1269. DOI: 10.4049/jimmunol.145.4.1265.

Nesmelova, I. V. *et al.* (2008) ‘CXC and CC Chemokines Form Mixed Heterodimers: Association Free Energies from Molecular Dynamics Simulations and Experimental Correlations’. *Journal of Biological Chemistry*, 283(35), pp. 24155–24166. DOI: 10.1074/jbc.M803308200.

Netea, M.G. *et al.* (2020) ‘Defining Trained Immunity and Its Role in Health and Disease’. *Nature Reviews Immunology*, 20(6), pp. 375–388. DOI: 10.1038/s41577-020-0285-6.

Neuman, H. *et al.* (2015) ‘Microbial Endocrinology: The Interplay between the Microbiota and the Endocrine System’. *FEMS Microbiology Reviews*, 39(4), pp. 509–521. DOI: 10.1093/femsre/fuu010.

Ney, P.A. (2011) ‘Normal and Disordered Reticulocyte Maturation’. *Current Opinion in Hematology*, 18(3), pp. 152–157. DOI: 10.1097/MOH.0b013e328345213e.

Ng, K.M. *et al.* (2013) ‘Microbiota-Liberated Host Sugars Facilitate Post-Antibiotic Expansion of Enteric Pathogens’. *Nature*, 502(7469), pp. 96–99. DOI: 10.1038/nature12503.

Nibbs, R.J.B. and Graham, G.J. (2013) ‘Immune Regulation by Atypical Chemokine Receptors’. *Nature Reviews Immunology*, 13(11), pp. 815–829. DOI: 10.1038/nri3544.

Niess, J.H. *et al.* (2005) ‘CX3CR1-Mediated Dendritic Cell Access to the Intestinal Lumen and Bacterial Clearance’. *Science*, 307(5707), pp. 254–258. DOI: 10.1126/science.1102901.

Nikaido, E. *et al.* (2012) ‘Effects of Indole on Drug Resistance and Virulence of Salmonella Enterica Serovar Typhimurium Revealed by Genome-Wide Analyses’. *Gut Pathogens*, 4(1), pp. 1–13. DOI: 10.1186/1757-4749-4-5.

Nilsson, T. *et al.* (2010) ‘Mass Spectrometry in High-Throughput Proteomics : Ready

for the Big Time'. *Nature Publishing Group*, 7(9), pp. 681–685. DOI: 10.1038/nmeth0910-681.

Noel, G. *et al.* (2016) 'Ablation of Interaction between IL-33 and ST2+regulatory t Cells Increases Immune Cell-Mediated Hepatitis and Activated NK Cell Liver Infiltration'. *American Journal of Physiology - Gastrointestinal and Liver Physiology*, 311(2), pp. G313–G323. DOI: 10.1152/ajpgi.00097.2016.

Noetzli, L.J., French, S.L. and Machlus, K.R. (2019) 'New Insights into the Differentiation of Megakaryocytes from Hematopoietic Progenitors'. *Arteriosclerosis, Thrombosis, and Vascular Biology*, 39(7), pp. 1288–1300. DOI: 10.1161/ATVBAHA.119.312129.

Norreen-Thorsen, M. *et al.* (2022) 'A Human Adipose Tissue Cell-Type Transcriptome Atlas'. *Cell Reports*, 40(2). DOI: 10.1016/j.celrep.2022.111046.

Notides, A.C., Lerner, N. and Hamilton, D.E. (1981) 'Positive Cooperativity of the Estrogen Receptor'. *Proceedings of the National Academy of Sciences of the United States of America*, 78(8 I), pp. 4926–4930. DOI: 10.1073/pnas.78.8.4926.

Novitzky-Basso, I. and Rot, A. (2012) 'Duffy Antigen Receptor for Chemokines and Its Involvement in Patterning and Control of Inflammatory Chemokines'. *Frontiers in Immunology*, 3(AUG), pp. 1–6. DOI: 10.3389/fimmu.2012.00266.

Nurnaningsih. *et al.* (2022) 'Sepsis and Disseminated Intravascular Coagulation Are Rare Complications of Typhoid Fever: A Case Report'. *Annals of Medicine and Surgery*, 73(November 2021), p. 103226. DOI: 10.1016/j.amsu.2021.103226.

Nussbaum, J.C. *et al.* (2013) 'Type 2 Innate Lymphoid Cells Control Eosinophil Homeostasis'. *Nature*, 502(7470), pp. 245–248. DOI: 10.1038/nature12526.

Oberle, N. *et al.* (2007) 'Rapid Suppression of Cytokine Transcription in Human CD4+ CD25- T Cells by CD4+ Foxp3+ Regulatory T Cells: Independence of IL-2 Consumption, TGF-ß, and Various Inhibitors of TCR Signaling'. *The Journal of Immunology*, 179, pp. 3578–3587.

Ochando, J. *et al.* (2023) 'Trained Immunity — Basic Concepts and Contributions to

Immunopathology'. *Nature Reviews Nephrology*, 19(1), pp. 23–37. DOI: 10.1038/s41581-022-00633-5.

Odegaard, J.I. *et al.* (2008) 'Alternative M2 Activation of Kupffer Cells by PPARδ Ameliorates Obesity-Induced Insulin Resistance'. *Cell Metabolism*, 7(6), pp. 496–507. DOI: 10.1016/j.cmet.2008.04.003.

Oderup, C. *et al.* (2006) 'Cytotoxic T Lymphocyte Antigen-4-Dependent down-Modulation of Costimulatory Molecules on Dendritic Cells in CD4+ CD25+ Regulatory T-Cell-Mediated Suppression'. *Immunology*, 118(2), pp. 240–249. DOI: 10.1111/j.1365-2567.2006.02362.x.

Ogawa, M. *et al.* (1988) 'B Cell Ontogeny in Murine Embryo Studied by a Culture System with the Monolayer of a Stromal Cell Clone, ST2: B Cell Progenitor Develops First in the Embryonal Body Rather than in the Yolk Sac.' *The EMBO Journal*, 7(5), pp. 1337–1343. DOI: 10.1002/j.1460-2075.1988.tb02949.x.

Öhman, L., Törnblom, H. and Simrén, M. (2015) 'Crosstalk at the Mucosal Border: Importance of the Gut Microenvironment in IBS'. *Nature Reviews Gastroenterology and Hepatology*, 12(1), pp. 36–49. DOI: 10.1038/nrgastro.2014.200.

Ohnmacht, C. *et al.* (2015) 'The Microbiota Regulates Type 2 Immunity through RORγt+ T Cells'. *Science*, 349(6251), pp. 989–993. DOI: 10.1126/science.aac4263.

Okazaki, H. *et al.* (2002) 'Characterization of Chemokine Receptor Expression and Cytokine Production in Circulating CD4+ T Cells from Patients with Atopic Dermatitis: Up-Regulation of C-C Chemokine Receptor 4 in Atopic Dermatitis'. *Clinical and Experimental Allergy*, 32(8), pp. 1236–1242. DOI: 10.1046/j.1365-2745.2002.01383.x.

Onishi, Y. *et al.* (2008) 'Foxp3+ Natural Regulatory T Cells Preferentially Form Aggregates on Dendritic Cells in Vitro and Actively Inhibit Their Maturation'. *Proceedings of the National Academy of Sciences of the United States of America*, 105(29), pp. 10113–10118. DOI: 10.1073/pnas.0711106105.

Orecchioni, M. *et al.* (2019) 'Macrophage Polarization: Different Gene Signatures in

M1(Lps+) vs. Classically and M2(LPS-) vs. Alternatively Activated Macrophages'. *Frontiers in Immunology*, 10(MAY), pp. 1–14. DOI: 10.3389/fimmu.2019.01084.

Osborn, O. *et al.* (2011) 'Ccl22/MDC, Is a Prostaglandin Dependent Pyrogen, Acting in the Anterior Hypothalamus to Induce Hyperthermia via Activation of Brown Adipose Tissue'. *Cytokine*, 53(3), pp. 311–319. DOI: 10.1016/j.cyto.2010.11.017.

Oshikawa, K. *et al.* (2002) 'Expression and Function of the ST2 Gene in a Murine Model of Allergic Airway Inflammation'. *Clinical and Experimental Allergy*, 32(10), pp. 1520–1526. DOI: 10.1046/j.1365-2745.2002.01494.x.

Ovchynnikova, E. *et al.* (2017) 'DARC Extracellular Domain Remodeling in Maturating Reticulocytes Explains Plasmodium Vivax Tropism'. *Blood*, 130(12), pp. 1441–1444. DOI: 10.1182/blood-2017-03-774364.

Owen, D.L., Sjaastad, L.E. and Farrar, M.A. (2019) 'Regulatory T Cell Development in the Thymus'. *The Journal of Immunology*, 203(8), pp. 2031–2041. DOI: 10.4049/jimmunol.1900662.

Owen, R.L. and Jones, A.L. (1974) 'Epithelial Cell Specialization within Human Peyer's Patches: An Ultrastructural Study of Intestinal Lymphoid Follicles'. *Gastroenterology*, 66(2), pp. 189–203.

Owens, B.M.J. *et al.* (2013) 'CD90+ Stromal Cells Are Non-Professional Innate Immune Effectors of the Human Colonic Mucosa'. *Frontiers in Immunology*, 4(SEP). DOI: 10.3389/fimmu.2013.00307.

Pacheco, A.R. *et al.* (2012) 'Fucose Sensing Regulates Bacterial Intestinal Colonization'. *Nature*, 492(7427), pp. 113–117. DOI: 10.1038/nature11623.

Pacheco, M.O. *et al.* (2022) 'Evaluation of Atypical Chemokine Receptor Expression in T Cell Subsets'. *Cells*, 11(24). DOI: 10.3390/cells11244099.

Pacholczyk, R. *et al.* (2006) 'Origin and T Cell Receptor Diversity of Foxp3+CD4+CD25+ T Cells'. *Immunity*, 25(2), pp. 249–259. DOI: 10.1016/j.immuni.2006.05.016.

Padigel, U.M. *et al.* (2007) 'Eosinophils Act as Antigen-Presenting Cells to Induce

Immunity to Strongyloides Stercoralis in Mice'. *Journal of Infectious Diseases*, 196(12), pp. 1844–1851. DOI: 10.1086/522968.

Palis, J. (2014) 'Primitive and Definitive Erythropoiesis in Mammals'. *Frontiers in Physiology*, 5 JAN(January), pp. 1–9. DOI: 10.3389/fphys.2014.00003.

Palmer, A.D. and Slauch, J.M. (2017) 'Mechanisms of Salmonella Pathogenesis in Animal Models'. *Human and Ecological Risk Assessment*, 23(8), pp. 1877–1892. DOI: 10.1080/10807039.2017.1353903.

Panina-Bordignon, P. *et al.* (2001) 'The C-C Chemokine Receptors CCR4 and CCR8 Identify Airway T Cells of Allergen-Challenged Atopic Asthmatics'. *Journal of Clinical Investigation*, 107(11), pp. 1357–1364. DOI: 10.1172/JCI12655.

Parenty, G., Appelbe, S. and Milligan, G. (2008) 'CXCR2 Chemokine Receptor Antagonism Enhances DOP Opioid Receptor Function via Allosteric Regulation of the CXCR2 – DOP Receptor Heterodimer'. *Biochemical Journal*, 412, pp. 245–256. DOI: 10.1042/BJ20071689.

Park, D. *et al.* (2018) 'Visualization of the Type III Secretion Mediated Salmonella - Host Cell Interface Using Cryo-Electron Tomography'. *ELife*, 7(e359166).

Parry, C.M. *et al.* (2002) 'Typhoid Fever'. *The New England Journal of Medicine*, 347(22), pp. 1770–1782.

Pasman, L. and Kasper, D.L. (2017) 'Building Conventions for Unconventional Lymphocytes'. *Immunological Reviews*, 279(1), pp. 52–62. DOI: 10.1111/imr.12576.

Pastille, E. *et al.* (2019) 'The IL-33/ST2 Pathway Shapes the Regulatory T Cell Phenotype to Promote Intestinal Cancer'. *Mucosal Immunology*, 12(4), pp. 990–1003. DOI: 10.1038/s41385-019-0176-y.

Pastorelli, L. *et al.* (2010) 'Epithelial-Derived IL-33 and Its Receptor ST2 Are Dysregulated in Ulcerative Colitis and in Experimental Th1/Th2 Driven Enteritis'. *Proceedings of the National Academy of Sciences of the United States of America*, 107(17), pp. 8017–8022. DOI: 10.1073/pnas.0912678107.

Patel, J.C. and Galán, J.E. (2006) 'Differential Activation and Function of Rho

GTPases during Salmonella-Host Cell Interactions'. *Journal of Cell Biology*, 175(3), pp. 453–463. DOI: 10.1083/jcb.200605144.

Paulson, R.F., Hariharan, S. and Little, J.A. (2020) 'Stress Erythropoiesis: Definitions and Models for Its Study'. *Experimental Hematology*, 89, pp. 43-54.e2. DOI: 10.1016/j.exphem.2020.07.011.

Pello, O.M. *et al.* (2008) 'Ligand Stabilization of CXCR4 / d -Opioid Receptor Heterodimers Reveals a Mechanism for Immune Response Regulation'. *European Journal of Immunology*, 38, pp. 537–549. DOI: 10.1002/eji.200737630.

Peng, G. *et al.* (2007) 'Tumor-Infiltrating Γδ T Cells Suppress T and Dendritic Cell Function via Mechanisms Controlled by a Unique Toll-like Receptor Signaling Pathway'. *Immunity*, 27(2), pp. 334–348. DOI: 10.1016/j.immuni.2007.05.020.

Peng, M. *et al.* (2018) 'Linoleic Acids Overproducing Lactobacillus Casei Limits Growth, Survival, and Virulence of Salmonella Typhimurium and Enterohaemorrhagic Escherichia Coli'. *Frontiers in Microbiology*, 9(NOV), pp. 1–14. DOI: 10.3389/fmicb.2018.02663.

Percherancier, Y. *et al.* (2005) 'Bioluminescence Resonance Energy Transfer Reveals Ligand-Induced Conformational Changes in CXCR4 Homo- and Heterodimers *'. *Journal of Biological Chemistry*, 280(11), pp. 9895–9903. DOI: 10.1074/jbc.M411151200.

Pereira, A. *et al.* (1990) 'Bone Marrow Histopathology in Primary Myelofibrosis: Clinical and Haematologic Correlations and Prognostic Evaluation'. *European Journal of Haematology*, 44(2), pp. 95–99. DOI: 10.1111/j.1600-0609.1990.tb00357.x.

Pesce, J. *et al.* (2006) 'The IL-21 Receptor Augments Th2 Effector Function and Alternative Macrophage Activation'. *Journal of Clinical Investigation*, 116(7), pp. 2044–2055. DOI: 10.1172/JCI27727.

Peterson, L.W. and Artis, D. (2014) 'Intestinal Epithelial Cells: Regulators of Barrier Function and Immune Homeostasis'. *Nature Reviews Immunology*, 14(3), pp. 141–

153. DOI: 10.1038/nri3608.

Pham, O.H. *et al.* (2017) ‘T Cell Expression of IL-18R and DR3 Is Essential for Non-Cognate Stimulation of Th1 Cells and Optimal Clearance of Intracellular Bacteria’. *PLoS Pathogens*, 13(8), pp. 1–22. DOI: 10.1371/journal.ppat.1006566.

Pham, O.H. and McSorley, S.J. (2015) ‘Protective Host Immune Responses to Salmonella Infection’. *Future Microbiology*, 10(1), pp. 101–110. DOI: 10.2217/fmb.14.98.

Piao, W.H. *et al.* (2008) ‘IL-21 Modulates CD4+ CD25+ Regulatory T-Cell Homeostasis in Experimental Autoimmune Encephalomyelitis’. *Scandinavian Journal of Immunology*, 67(1), pp. 37–46. DOI: 10.1111/j.1365-3083.2007.02035.x.

Pichery, M. *et al.* (2012) ‘Endogenous IL-33 Is Highly Expressed in Mouse Epithelial Barrier Tissues, Lymphoid Organs, Brain, Embryos, and Inflamed Tissues: In Situ Analysis Using a Novel Il-33–LacZ Gene Trap Reporter Strain’. *The Journal of Immunology*, 188(7), pp. 3488–3495. DOI: 10.4049/jimmunol.1101977.

Piehler, D. *et al.* (2016) ‘The IL-33 Receptor (ST2) Regulates Early IL-13 Production in Fungus-Induced Allergic Airway Inflammation’. *Mucosal Immunology*, 9(4), pp. 937–949. DOI: 10.1038/mi.2015.106.

Pietras, E.M. *et al.* (2015) ‘Functionally Distinct Subsets of Lineage-Biased Multipotent Progenitors Control Blood Production in Normal and Regenerative Conditions’. *Cell Stem Cell*, 17(1), pp. 35–46. DOI: 10.1016/j.stem.2015.05.003.

Pilette, C. *et al.* (2004) ‘CCR4 Ligands Are Up-Regulated in the Airways of Atopic Asthmatics after Segmental Allergen Challenge’. *European Respiratory Journal*, 23(6), pp. 876–884. DOI: 10.1183/09031936.04.00102504.

Plant, J. and Glynn, A.A. (1979) ‘Locating Salmonella Resistance Gene on Mouse Chromosome 1.’ *Clinical and Experimental Immunology*, 37(1), pp. 1–6.

Polumuri, S.K. *et al.* (2012) ‘Transcriptional Regulation of Murine IL-33 by TLR and Non-TLR Agonists’. *The Journal of Immunology*, 189(1), pp. 50–60. DOI: 10.4049/jimmunol.1003554.

Ponce, D.M. *et al.* (2015) 'High Day 28 ST2 Levels Predict for Acute Graft-versus-Host Disease and Transplant-Related Mortality after Cord Blood Transplantation'. *Blood*, 125(1), pp. 199–205. DOI: 10.1182/blood-2014-06-584789.

Poppensieker, K. *et al.* (2012) 'CC Chemokine Receptor 4 Is Required for Experimental Autoimmune Encephalomyelitis by Regulating GM-CSF and IL-23 Production in Dendritic Cells'. *Proceedings of the National Academy of Sciences*, 109(10), pp. 3897–3902. DOI: 10.1073/pnas.1114153109.

Pozo, V. Del. *et al.* (1992) 'Eosinophil as Antigen-presenting Cell: Activation of T Cell Clones and T Cell Hybridoma by Eosinophils after Antigen Processing'. *European Journal of Immunology*, 22(7), pp. 1919–1925. DOI: 10.1002/eji.1830220736.

Préfontaine, D. *et al.* (2010) 'Increased IL-33 Expression by Epithelial Cells in Bronchial Asthma'. *Journal of Allergy and Clinical Immunology*, 125(3), pp. 752–754. DOI: 10.1016/j.jaci.2009.12.935.

Price-Carter, M. *et al.* (2001) 'The Alternative Electron Acceptor Tetrathionate Supports B12-Dependent Anaerobic Growth of Salmonella Enterica Serovar Typhimurium on Ethanolamine or 1,2-Propanediol'. *Journal of Bacteriology*, 183(8), pp. 2463–2475. DOI: 10.1128/JB.183.8.2463-2475.2001.

Price, A.E. *et al.* (2010) 'Systemically Dispersed Innate IL-13-Expressing Cells in Type 2 Immunity'. *Proceedings of the National Academy of Sciences of the United States of America*, 107(25), pp. 11489–11494. DOI: 10.1073/pnas.1003988107.

Pronk, C.J.H. *et al.* (2007) 'Elucidation of the Phenotypic, Functional, and Molecular Topography of a Myeloerythroid Progenitor Cell Hierarchy'. *Cell Stem Cell*, 1(4), pp. 428–442. DOI: 10.1016/j.stem.2007.07.005.

Pruenster, M. *et al.* (2009) 'The Duffy Antigen Receptor for Chemokines Transports Chemokines and Supports Their Promigratory Activity'. *Nature Immunology*, 10(1), pp. 101–108. DOI: 10.1038/ni.1675.

Raciti, G.A. *et al.* (2017) 'Specific CpG Hyper-Methylation Leads to Ankrd26 Gene down-Regulation in White Adipose Tissue of a Mouse Model of Diet-Induced

Obesity'. *Scientific Reports*, 7(August 2016), pp. 1–13. DOI: 10.1038/srep43526.

Raffatellu, M., Wilson, R.P., *et al.* (2008) 'Clinical Pathogenesis of Typhoid Fever.' *Journal of Infection in Developing Countries*, 2(4), pp. 260–266. DOI: 10.3855/jidc.219.

Raffatellu, M. *et al.* (2009) 'Lipocalin-2 Resistance Confers an Advantage to Salmonella Enterica Serotype Typhimurium for Growth and Survival in the Inflamed Intestine'. *Cell Host and Microbe*, 5(5), pp. 476–486. DOI: 10.1016/j.chom.2009.03.011.

Raffatellu, M., Santos, R.L., *et al.* (2008) 'Simian Immunodeficiency Virus–Induced Mucosal Interleukin-17 Deficiency Promotes Salmonella Dissemination from the Gut'. *Nature Medicine*, 14(4), pp. 421–428. DOI: 10.1038/nm1743.Simian.

Rajagopal, S. *et al.* (2013) 'Biased Agonism as a Mechanism for Differential Signaling by Chemokine Receptors'. *Journal of Biological Chemistry*, 288(49), pp. 35039–35048. DOI: 10.1074/jbc.M113.479113.

Rao, R.R. *et al.* (2014) 'Meteorin-like Is a Hormone That Regulates Immune-Adipose Interactions to Increase Beige Fat Thermogenesis'. *Cell*, 157(6), pp. 1279–1291. DOI: 10.1016/j.cell.2014.03.065.

Rapp, M. *et al.* (2019) 'CCL22 Controls Immunity by Promoting Regulatory T Cell Communication with Dendritic Cells in Lymph Nodes'. *The Journal of Experimental Medicine*, p. jem.20170277. DOI: 10.1084/jem.20170277.

Rathanaswami, P. *et al.* (1993) 'Expression of the Cytokine RANTES in Human Rheumatoid Synovial Fibroblasts'. *Journal of Biological Chemistry*, 268(8), pp. 5834–5839. DOI: 10.1016/s0021-9258(18)53395-0.

Rathman, M., Barker, L.P. and Falkow, S. (1997) 'The Unique Trafficking Pattern of Salmonella Typhimurium-Containing Phagosomes in Murine Macrophages Is Independent of the Mechanism of Bacterial Entry'. *Infection and Immunity*, 65(4), pp. 1475–1485. DOI: 10.1128/iai.65.4.1475-1485.1997.

Raupach, B. *et al.* (2006) 'Caspase-1-Mediated Activation of Interleukin-1β (IL-1β)

and IL-18 Contributes to Innate Immune Defenses against Salmonella Enterica Serovar Typhimurium Infection'. *Infection and Immunity*, 74(8), pp. 4922–4926. DOI: 10.1128/IAI.00417-06.

Rausch, P. *et al.* (2016) 'Analysis of Factors Contributing to Variation in the C57BL/6J Fecal Microbiota across German Animal Facilities'. *International Journal of Medical Microbiology*, 306(5), pp. 343–355. DOI: 10.1016/j.ijmm.2016.03.004.

Ravindran, R. *et al.* (2005) 'Expression of T-Bet by CD4 T Cells Is Essential for Resistance to Salmonella Infection'. *Journal of Immunology*, 175(7), pp. 4603–4610. DOI: https://doi.org/10.4049/jimmunol.175.7.4603.

Reddy, E.A., Shaw, A. V. and Crump, J.A. (2010) 'Community-Acquired Bloodstream Infections in Africa: A Systematic Review and Meta-Analysis'. *The Lancet Infectious Diseases*, 10(6), pp. 417–432. DOI: 10.1016/S1473-3099(10)70072-4.

Reeves, M.W. *et al.* (1989) 'Clonal Nature of Salmonella Typhi and Its Genetic Relatedness to Other Salmonellae as Shown by Multilocus Enzyme Electrophoresis, and Proposal of Salmonella Bongori Comb. Nov.' *Journal of Clinical Microbiology*, 27(2), pp. 313–320.

Reiman, R.M. *et al.* (2006) 'Interleukin-5 (IL-5) Augments the Progression of Liver Fibrosis by Regulating IL-13 Activity'. *Infection and Immunity*, 74(3), pp. 1471–1479. DOI: 10.1128/IAI.74.3.1471-1479.2006.

Rescigno, M. *et al.* (2001) 'Dendritic Cells Express Tight Junction Proteins and Penetrate Gut Epithelial Monolayers to Sample Bacteria'. *Nature Immunology*, 2(4), pp. 361–367. DOI: 10.1038/86373.

Rhodes, M.M. *et al.* (2008) 'Adherence to Macrophages in Erythroblastic Islands Enhances Erythroblast Proliferation and Increases Erythrocyte Production by a Different Mechanism than Erythropoietin'. *Blood*, 111(3), pp. 1700–1708. DOI: 10.1182/blood-2007-06-098178.

Rhyu, M.S., Jan, L.Y. and Jan, Y.N. (1994) 'Asymmetric Distribution of Numb Protein during Division of the Sensory Organ Precursor Cell Confers Distinct Fates to

Daughter Cells'. *Cell*, 76(3), pp. 477–491. DOI: 10.1016/0092-8674(94)90112-0.

Ricardo-Gonzalez, R.R. *et al.* (2010) 'IL-4/STAT6 Immune Axis Regulates Peripheral Nutrient Metabolism and Insulin Sensitivity'. *Proceedings of the National Academy of Sciences of the United States of America*, 107(52), pp. 22617–22622. DOI: 10.1073/pnas.1009152108.

Ricquier, D. and Kader, J.C. (1976) 'Mitochondrial Protein Alteration in Active Brown Fat: A Sodium Dodecyl Sulfate-Polyacrylamide Gel Electrophoretic Study'. *Biochemical and Biophysical Research Communications*, 73(3), pp. 577–583. DOI: 10.1016/0006-291X(76)90849-4.

Rigaut, G., Ingelheim, B. and Shevchenko, A. (1999) 'IN THE LABORATORY A Generic Protein Purification Method for Protein Complex Characterization and Proteome Exploration'. *Nature Biotechnology*, (17), pp. 1030–1032. DOI: 10.1038/13732.

Rodriguez-Fraticelli, A.E. *et al.* (2018) 'Clonal Analysis of Lineage Fate in Native Haematopoiesis'. *Nature*, 553(7687), pp. 212–216. DOI: 10.1038/nature25168.

Roed, S.N. *et al.* (2012) 'Receptor Oligomerization in Family B1 of G-Protein-Coupled Receptors: Focus on BRET Investigations and the Link between GPCR Oligomerization and Binding Cooperativity'. *Frontiers in Endocrinology*, 3(MAY), pp. 1–13. DOI: 10.3389/fendo.2012.00062.

Romagnoli, P., Hudrisier, D. and van Meerwijk, J.P.M. (2002) 'Preferential Recognition of Self Antigens Despite Normal Thymic Deletion of CD4+CD25+ Regulatory T Cells'. *The Journal of Immunology*, 168(4), pp. 1644–1648. DOI: 10.4049/jimmunol.168.4.1644.

Roussel, L. *et al.* (2008) 'Molecular Mimicry between IL-33 and KSHV for Attachment to Chromatin through the H2A-H2B Acidic Pocket'. *EMBO Reports*, 9(10), pp. 1006–1012. DOI: 10.1038/embor.2008.145.

Rowland, I. *et al.* (2018) 'Gut Microbiota Functions: Metabolism of Nutrients and Other Food Components'. *European Journal of Nutrition*, 57(1), pp. 1–24. DOI:

10.1007/s00394-017-1445-8.

Ruland, C. *et al.* (2017) ‘Chemokine CCL17 Is Expressed by Dendritic Cells in the CNS during Experimental Autoimmune Encephalomyelitis and Promotes Pathogenesis of Disease’. *Brain, Behavior, and Immunity*, 66, pp. 382–393. DOI: 10.1016/j.bbi.2017.06.010.

Sait, L. *et al.* (2003) ‘Secretory Antibodies Do Not Affect the Composition of the Bacterial Microbiota in the Terminal Ileum of 10-Week-Old Mice’. *Applied and Environmental Microbiology*, 69(4), pp. 2100–2109. DOI: 10.1128/AEM.69.4.2100-2109.2003.

Sakaguchi, S. *et al.* (1995) ‘Immunologic Self-Tolerance Maintained by Activated T Cells Expressing IL-2 Receptor a-Chains (CD25)’. *Journal of Immunology*, 155(3), pp. 1151–54.

Sakaguchi, S. (2004) ‘Naturally Arising CD4+ Regulatory T Cells for Immunologic Self-Tolerance and Negative Control of Immune Responses’. *Annual Review of Immunology*, 22, pp. 531–562. DOI: 10.1146/annurev.immunol.21.120601.141122.

Sakaguchi, S. *et al.* (2006) ‘SKG Mice, a Monogenic Model of Autoimmune Arthritis Due to Altered Signal Transduction in T-Cells’. *The Hereditary Basis of Rheumatic Diseases*, pp. 147–159. DOI: 10.1007/3-7643-7419-5_11.

Sakhony, O.S. *et al.* (2015) ‘M Cell-Derived Vesicles Suggest a Unique Pathway for Trans-Epithelial Antigen Delivery’. *Tissue Barriers*, 3(1). DOI: 10.1080/21688370.2015.1004975.

Sakurai, T. *et al.* (2020) ‘GITR Controls Intestinal Inflammation by Suppressing IL-15-Dependent NK Cell Activity’. *FASEB Journal*, 34(11), pp. 14820–14831. DOI: 10.1096/fj.202001675R.

Salazar-Gonzalez, R.-M. *et al.* (2007) ‘ Salmonella Flagellin Induces Bystander Activation of Splenic Dendritic Cells and Hinders Bacterial Replication In Vivo ’. *The Journal of Immunology*, 179(9), pp. 6169–6175. DOI: 10.4049/jimmunol.179.9.6169.

Salazar-Gonzalez, R.M. *et al.* (2006) ‘CCR6-Mediated Dendritic Cell Activation of

Pathogen-Specific T Cells in Peyer's Patches'. *Immunity*, 24(5), pp. 623–632. DOI: 10.1016/j.immuni.2006.02.015.

Salimi, M. *et al.* (2013) 'A Role for IL-25 and IL-33-Driven Type-2 Innate Lymphoid Cells in Atopic Dermatitis'. *Journal of Experimental Medicine*, 210(13), pp. 2939–2950. DOI: 10.1084/jem.20130351.

Salmonella Subcommittee of the Nomenclature Committee of the International Society for Microbiology. (1934) 'The Genus Salmonella Lignières, 1900.' *The Journal of Hygiene*, 34(3), pp. 333–350. DOI: 10.1017/s0022172400034677.

Sanada, S. *et al.* (2007) 'IL-33 and ST2 Comprise a Critical Biomechanically Induced and Cardioprotective Signaling System'. *Journal of Clinical Investigation*, 117(6), pp. 1538–1549. DOI: 10.1172/JCI30634.

Sandler, N.G. *et al.* (2003) 'Global Gene Expression Profiles During Acute Pathogen-Induced Pulmonary Inflammation Reveal Divergent Roles for Th1 and Th2 Responses in Tissue Repair 1'. *The Journal of Immunology*, 171(7), pp. 3655–3667.

Santamaria, J.C., Borelli, A. and Irla, M. (2021) 'Regulatory T Cell Heterogeneity in the Thymus: Impact on Their Functional Activities'. *Frontiers in Immunology*, 12(February), pp. 1–8. DOI: 10.3389/fimmu.2021.643153.

Santos, R.L. *et al.* (2009) 'Life in the Inflamed Intestine, Salmonella Style'. *Trends in Microbiology*, 17(11), pp. 498–506. DOI: 10.1016/j.tim.2009.08.008.

Santulli-Marotto, S. *et al.* (2015) 'CCL22-Specific Antibodies Reveal That Engagement of Two Distinct Binding Domains on CCL22 Is Required for CCR4-Mediated Function'. *Monoclonal Antibodies in Immunodiagnosis and Immunotherapy*, 34(6), pp. 373–380. DOI: 10.1089/mab.2015.0039.

Santulli-Marotto, S., Boakye, K., *et al.* (2013) 'Engagement of Two Distinct Binding Domains on CCL17 Is Required for Signaling through CCR4 and Establishment of Localized Inflammatory Conditions in the Lung'. *PLoS ONE*, 8(12). DOI: 10.1371/journal.pone.0081465.

Santulli-Marotto, S., Fisher, J., *et al.* (2013) 'Surrogate Antibodies That Specifically

Bind and Neutralize CCL17 But Not CCL22'. *Monoclonal Antibodies in Immunodiagnosis and Immunotherapy*, 32(3), pp. 162–171. DOI: 10.1089/mab.2012.0112.

Sarma, P. (1990) 'Red Cell Indices'. In Walker, H.Hall, W.and Hurst, J. (eds.) *Clinical Methods: The History, Physical, and Laboratory Examinations*. Boston: Butterworths.

Savino, B. *et al.* (2009) 'Recognition versus Adaptive Up-Regulation and Degradation of CC Chemokines by the Chemokine Decoy Receptor D6 Are Determined by Their N-Terminal Sequence'. *Journal of Biological Chemistry*, 284(38), pp. 26207–26215. DOI: 10.1074/jbc.M109.029249.

Sawant, K. V. *et al.* (2016) 'Chemokine CXCL1 Mediated Neutrophil Recruitment: Role of Glycosaminoglycan Interactions'. *Scientific Reports*, 6, pp. 4–11. DOI: 10.1038/srep33123.

Scaldaferri, F. *et al.* (2012) 'The Gut Barrier: New Acquisitions and Therapeutic Approaches'. *Journal of Clinical Gastroenterology*, 46(SUPPL. 1), pp. 12–17. DOI: 10.1097/MCG.0b013e31826ae849.

Schaniel, C. *et al.* (1998) 'Activated Murine B Lymphocytes and Dendritic Cells Produce a Novel CC Chemokine Which Acts Selectively on Activated T Cells'. *Journal of Experimental Medicine*, 188(3), pp. 451–463. DOI: 10.1084/jem.188.3.451.

Schiering, C. *et al.* (2014) 'The Alarmin IL-33 Promotes Regulatory T-Cell Function in the Intestine'. *Nature*, 513(7519), pp. 564–568. DOI: 10.1038/nature13577.

Schlageter, A.M. and Kozel, T.R. (1990) 'Opsonization of Cryptococcus Neoformans by a Family of Isotype-Switch Variant Antibodies Specific for the Capsular Polysaccharide'. *Infection and Immunity*, 58(6), pp. 1914–1918. DOI: 10.1128/iai.58.6.1914-1918.1990.

Schmidt, A., Oberle, N. and Krammer, P.H. (2012) 'Molecular Mechanisms of Treg-Mediated T Cell Suppression'. *Frontiers in Immunology*, 3(MAR), pp. 1–20. DOI:

10.3389/fimmu.2012.00051.

Schmitz, J. *et al.* (2005) 'IL-33, an Interleukin-1-like Cytokine That Signals via the IL-1 Receptor-Related Protein ST2 and Induces T Helper Type 2-Associated Cytokines'. *Immunity*, 23(5), pp. 479–490. DOI: 10.1016/j.immuni.2005.09.015.

Schmitz, J. *et al.* (2016) 'Obesogenic Memory Can Confer Long-Term Increases in Adipose Tissue but Not Liver Inflammation and Insulin Resistance after Weight Loss'. *Molecular Metabolism*, 5(5), pp. 328–339. DOI: 10.1016/j.molmet.2015.12.001.

Schnabel, R.B. *et al.* (2010) 'Duffy Antigen Receptor for Chemokines (Darc) Polymorphism Regulates Circulating Concentrations of Monocyte Chemoattractant Protein-1 and Other Inflammatory Mediators'. *Blood*, 115(26), pp. 5289–5299. DOI: 10.1182/blood-2009-05-221382.

Schoenborn, J.R. and Wilson, C.B. (2007) 'Regulation of Interferon-γ During Innate and Adaptive Immune Responses'. *Advances in Immunology*, 96(07), pp. 41–101. DOI: 10.1016/S0065-2776(07)96002-2.

Schroeder, B.O. *et al.* (2015) 'Paneth Cell α-Defensin 6 (HD-6) Is an Antimicrobial Peptide'. *Mucosal Immunology*, 8(3), pp. 661–671. DOI: 10.1038/mi.2014.100.

Schulz, S.M. *et al.* (2008) 'IL-17A Is Produced by Th17, Γδ T Cells and Other CD4- Lymphocytes during Infection with Salmonella Enterica Serovar Enteritidis and Has a Mild Effect in Bacterial Clearance'. *International Immunology*, 20(9), pp. 1129–1138. DOI: 10.1093/intimm/dxn069.

Sciuto, M.R. *et al.* (2018) 'Two-Step Coimmunoprecipitation (TIP) Enables Efficient and Highly Selective Isolation of Native Protein Complexes'. *Molecular and Cellular Proteomics*, 17(5), pp. 993–1009. DOI: 10.1074/mcp.O116.065920.

Sebastiani, S. *et al.* (2001) 'Chemokine Receptor Expression and Function in CD4+ T Lymphocytes with Regulatory Activity'. *The Journal of Immunology*, 166(2), pp. 996–1002.

Sebastiani, S. *et al.* (2002) 'Nickel-Specific CD4+ and CD8+ T Cells Display Distinct

Migratory Responses to Chemokines Produced during Allergic Contact Dermatitis'. *Journal of Investigative Dermatology*, 118(6), pp. 1052–1058. DOI: 10.1046/j.1523-1747.2002.01771.x.

Sefik, E. *et al.* (2015) 'Individual Intestinal Symbionts Induce a Distinct Population of RORg+ Regulatory T Cells'. *Science*, 349(6251), pp. 993–997.

Seki, K. *et al.* (2009) 'Interleukin-33 Prevents Apoptosis and Improves Survival after Experimental Myocardial Infarction through ST2 Signaling'. *Circulation: Heart Failure*, 2(6), pp. 684–691. DOI: 10.1161/CIRCHEARTFAILURE.109.873240.

Sekirov, I. *et al.* (2008) 'Antibiotic-Induced Perturbations of the Intestinal Microbiota Alter Host Susceptibility to Enteric Infection'. *Infection and Immunity*, 76(10), pp. 4726–4736. DOI: 10.1128/IAI.00319-08.

Selbach, M. and Mann, M. (2006) 'Protein Interaction Screening by Quantitative Immunoprecipitation Combined With'. *Nature Methods*, 3(12), pp. 981–983. DOI: 10.1038/NMETH972.

Sells, R.E. and Hwang, S.T. (2010) 'Paradoxical Increase in Skin Inflammation in the Absence of CCR4'. *Journal of Investigative Dermatology*, 130(12), pp. 2697–2699. DOI: 10.1038/jid.2010.292.

Semmling, V. *et al.* (2010) 'Alternative Cross-Priming through CCL17-CCR4-Mediated Attraction of CTLs toward NKT Cell-Licensed DCs'. *Nature Immunology*, 11(4), pp. 313–320. DOI: 10.1038/ni.1848.

Seu, K.G. *et al.* (2017) 'Unraveling Macrophage Heterogeneity in Erythroblastic Islands'. *Frontiers in Immunology*, 8(SEP). DOI: 10.3389/fimmu.2017.01140.

Sevlever, F., Di Bella, J.P. and Ventura, A.C. (2020) 'Discriminating between Negative Cooperativity and Ligand Binding to Independent Sites Using Pre-Equilibrium Properties of Binding Curves'. *PLoS Computational Biology*, 16(6), pp. 1–21. DOI: 10.1371/journal.pcbi.1007929.

Sfeir, M., Youssef, P. and Mokhbat, J.E. (2013) 'Salmonella Typhi Sternal Wound Infection'. *American Journal of Infection Control*, 41(12), pp. e123–e124. DOI:

10.1016/j.ajic.2013.04.012.

Shah, D.K. and Zúñiga-Pflücker, J.C. (2014) 'An Overview of the Intrathymic Intricacies of T Cell Development'. *The Journal of Immunology*, 192(9), pp. 4017–4023. DOI: 10.4049/jimmunol.1302259.

Shao, Q. *et al.* (2021) 'Tissue Tregs and Maintenance of Tissue Homeostasis'. *Frontiers in Cell and Developmental Biology*, 9(August), pp. 1–11. DOI: 10.3389/fcell.2021.717903.

Shi, Y. *et al.* (2004) 'PhoP-Regulated Salmonella Resistance to the Antimicrobial Peptides Magainin 2 and Polymyxin B'. *Molecular Microbiology*, 53(1), pp. 229–241. DOI: 10.1111/j.1365-2958.2004.04107.x.

Shimada, Y. *et al.* (2013) 'Commensal Bacteria-Dependent Indole Production Enhances Epithelial Barrier Function in the Colon'. *PLoS ONE*, 8(11), pp. 1–10. DOI: 10.1371/journal.pone.0080604.

Shimpo, M. *et al.* (2004) 'Serum Levels of the Interleukin-1 Receptor Family Member ST2 Predict Mortality and Clinical Outcome in Acute Myocardial Infarction'. *Circulation*, 109(18), pp. 2186–2190. DOI: 10.1161/01.CIR.0000127958.21003.5A.

Shin, S. *et al.* (2005) 'Antigen Recognition Determinants of Γδ T Cell Receptors'. *Science*, 308(5719), pp. 252–255. DOI: 10.1126/science.1106480.

Shinde, A. V., Humeres, C. and Frangogiannis, N.G. (2017) 'The Role of α-Smooth Muscle Actin in Fibroblast-Mediated Matrix Contraction and Remodeling'. *Biochimica et Biophysica Acta - Molecular Basis of Disease*, 1863(1), pp. 298–309. DOI: 10.1016/j.bbadis.2016.11.006.

Siede, J. *et al.* (2016) 'IL-33 Receptor-Expressing Regulatory t Cells Are Highly Activated, Th2 Biased and Suppress CD4 T Cell Proliferation through IL-10 and TGFβ Release'. *PLoS ONE*, 11(8), pp. 1–15. DOI: 10.1371/journal.pone.0161507.

Singer, I.I. *et al.* (2001) 'CCR5 , CXCR4 , and CD4 Are Clustered and Closely Apposed on Microvilli of Human Macrophages and T Cells'. 75(8), pp. 3779–3790. DOI: 10.1128/JVI.75.8.3779.

Singh, I. *et al.* (2017) ‘Pulmonary Extra-Medullary Hematopoiesis and Pulmonary Hypertension from Underlying Polycythemia Vera: A Case Series’. *Pulmonary Circulation*, 7(1), pp. 261–267. DOI: 10.1177/2045893217702064.

Singhal, G. and Baune, B.T. (2018) *Do Chemokines Have a Role in the Pathophysiology of Depression?* Elsevier Inc. DOI: 10.1016/B978-0-12-811073-7.00008-8.

Skelton, N.J. *et al.* (1995) ‘Proton NMR Assignments and Solution Conformation of RANTES, a Chemokine of the C-C Type’. *Biochemistry*, 34(16), pp. 5329–5342.

Skelton, N.J. *et al.* (1999) ‘Structure of a CXC Chemokine-Receptor Fragment in Complex with Interleukin-8’. *Structure*, 7, pp. 157–168.

Skrypnik, K. and Suliburska, J. (2018) ‘Association between the Gut Microbiota and Mineral Metabolism’. *Journal of the Science of Food and Agriculture*, 98(7), pp. 2449–2460. DOI: 10.1002/jsfa.8724.

Small, P.L.C., Isberg, R.R. and Falkow, S. (1987) ‘Comparison of the Ability of Enteroinvasive Escherichia Coli, Salmonella Typhimurium, Yersinia Pseudotuberculosis, and Yersinia Enterocolitica to Enter and Replicate within HEp-2 Cells’. *Infection and Immunity*, 55(7), pp. 1674–1679. DOI: 10.1128/iai.55.7.1674-1679.1987.

Smigiel, K.S. *et al.* (2014) ‘CCR7 Provides Localized Access to IL-2 and Defines Homeostatically Distinct Regulatory T Cell Subsets’. *Journal of Experimental Medicine*, 211(1), pp. 121–136. DOI: 10.1084/jem.20131142.

Sohy, D. *et al.* (2009) ‘Hetero-Oligomerization of CCR2 , CCR5 , and CXCR4 and the Protean Effects of “ Selective ” Antagonists’. *Journal of Biological Chemistry*, 284(45), pp. 31270–31279. DOI: 10.1074/jbc.M109.054809.

Sohy, D., Parmentier, M. and Springael, J. (2007) ‘Allosteric Transinhibition by Specific Antagonists In’. *Journal of Biological Chemistry*, 282(41), pp. 30062–30069. DOI: 10.1074/jbc.M705302200.

Sojka, D.K. and Fowell, D.J. (2011) ‘Regulatory T Cells Inhibit Acute IFN-γ Synthesis

without Blocking T-Helper Cell Type 1 (Th1) Differentiation via a Compartmentalized Requirement for IL-10'. *Proceedings of the National Academy of Sciences of the United States of America*, 108(45), pp. 18336–18341. DOI: 10.1073/pnas.1110566108.

Solari, R. and Pease, J.E. (2015) 'Targeting Chemokine Receptors in Disease - A Case Study of CCR4'. *European Journal of Pharmacology*, 763, pp. 169–177. DOI: 10.1016/j.ejphar.2015.05.018.

Soni, S. *et al.* (2006) 'Absence of Erythroblast Macrophage Protein (Emp) Leads to Failure of Erythroblast Nuclear Extrusion'. *Journal of Biological Chemistry*, 281(29), pp. 20181–20189. DOI: 10.1074/jbc.M603226200.

Spath, S. *et al.* (2022) 'Profiling of Tregs across Tissues Reveals Plasticity in ST2 Expression and Hierarchies in Tissue-Specific Phenotypes'. *IScience*, 25(9). DOI: 10.1016/j.isci.2022.104998.

Spencer, L.A. *et al.* (2009) 'Human Eosinophils Constitutively Express Multiple Th1, Th2, and Immunoregulatory Cytokines That Are Secreted Rapidly and Differentially'. *Journal of Leukocyte Biology*, 85(1), pp. 117–123. DOI: 10.1189/jlb.0108058.

Springael, J. *et al.* (2006) 'Allosteric Modulation of Binding Properties between Units of Chemokine Receptor Homo- and Hetero-Oligomers'. *Molecular Pharmacology*, 69(5), pp. 1652–1661. DOI: 10.1124/mol.105.019414.kine-1.

Springer, N.L. *et al.* (2019) 'Obesity-Associated Extracellular Matrix Remodeling Promotes a Macrophage Phenotype Similar to Tumor-Associated Macrophages'. *American Journal of Pathology*, 189(10), pp. 2019–2035. DOI: 10.1016/j.ajpath.2019.06.005.

Srinivasa, S., Ding, X. and Kast, J. (2015) 'Formaldehyde Cross-Linking and Structural Proteomics : Bridging the Gap'. *Methods*, 89, pp. 91–98. DOI: 10.1016/j.ymeth.2015.05.006.

Srinivasan, B. (2021) 'Explicit Treatment of Non-Michaelis-Menten and Atypical Kinetics in Early Drug Discovery**'. *ChemMedChem*, 16(6), pp. 899–918. DOI:

10.1002/cmdc.202000791.

Stanaway, J.D. *et al.* (2019) 'The Global Burden of Typhoid and Paratyphoid Fevers: A Systematic Analysis for the Global Burden of Disease Study 2017'. *The Lancet Infectious Diseases*, 19(4), pp. 369–381. DOI: 10.1016/S1473-3099(18)30685-6.

Stanchina, M. *et al.* (2019) 'Extramedullary Hematopoiesis of the Renal Pelvis in a Patient with Myelofibrosis'. *Journal of Oncology Practice*, 15(8), pp. 458–459. DOI: 10.1200/JOP.19.00041.

Stecher, B. *et al.* (2005) 'Comparison of Salmonella Enterica Serovar Typhimurium Colitis in Germfree Mice and Mice Pretreated with Streptomycin'. *Infection and Immunity*, 73(6), pp. 3228–3241. DOI: 10.1128/IAI.73.6.3228-3241.2005.

Stecher, B. *et al.* (2010) 'Like Will to like: Abundances of Closely Related Species Can Predict Susceptibility to Intestinal Colonization by Pathogenic and Commensal Bacteria'. *PLoS Pathogens*, 6(1). DOI: 10.1371/journal.ppat.1000711.

Stier, M.T. *et al.* (2018) 'IL-33 Promotes the Egress of Group 2 Innate Lymphoid Cells from the Bone Marrow'. *Journal of Experimental Medicine*, 215(1), pp. 263–281. DOI: 10.1084/jem.20170449.

Stijlemans, B. *et al.* (2015) 'Development of a PHrodo-Based Assay for the Assessment of In Vitro and In Vivo Erythrophagocytosis during Experimental Trypanosomosis'. *PLoS Neglected Tropical Diseases*, 9(3), pp. 1–21. DOI: 10.1371/journal.pntd.0003561.

Strissel, K.J. *et al.* (2007) 'Adipocyte Death, Adipose Tissue Remodeling, and Obesity Complications'. *Diabetes*, 56(12), pp. 2910–2918. DOI: 10.2337/db07-0767.

Strugnell, R.A. *et al.* (2014) 'Salmonella Vaccines: Lessons from the Mouse Model or Bad Teaching?' *Current Opinion in Microbiology*, 17(1), pp. 99–105. DOI: 10.1016/j.mib.2013.12.004.

Strugnell, R.A. and Wijburg, O.L.C. (2010) 'The Role of Secretory Antibodies in Infection Immunity'. *Nature Reviews Microbiology*, 8(9), pp. 656–667. DOI: 10.1038/nrmicro2384.

Stutte, S. *et al.* (2010) ‘Requirement of CCL17 for CCR7- and CXCR4-Dependent Migration of Cutaneous Dendritic Cells’. *Proceedings of the National Academy of Sciences*, 107(19), pp. 8736–8741. DOI: 10.1073/pnas.0906126107.

Sun, J. *et al.* (2014) ‘Clonal Dynamics of Native Haematopoiesis’. *Nature*, 514(7522), pp. 322–327. DOI: 10.1038/nature13824.

Sutherland, B.W., Toews, J. and Kast, J. (2008) ‘Utility of Formaldehyde Cross-Linking and Mass Spectrometry in the Study of Protein – Protein Interactions’. *Journal of Mass Spectrometry*, 43, pp. 699–715. DOI: 10.1002/jms.1415.

Suwandi, A. *et al.* (2019) ‘Std Fimbriae-Fucose Interaction Increases Salmonella-Induced Intestinal Inflammation and Prolongs Colonization’. *PLoS Pathogens*, 15(7), pp. 1–22. DOI: 10.1371/journal.ppat.1007915.

Suzuki, S. *et al.* (2002) ‘Interactions of Opioid and Chemokine Receptors : Oligomerization of Mu , Kappa , and Delta with CCR5 on Immune Cells’. *Experimental Cell Research*, 280, pp. 192–200. DOI: 10.1006/excr.2002.5638.

Swann, J.W. *et al.* (2020) ‘IL-33 Promotes Anemia during Chronic Inflammation by Inhibiting Differentiation of Erythroid Progenitors’. *Journal of Experimental Medicine*, 217(9). DOI: 10.1084/jem.20200164.

Tago, K. *et al.* (2001) ‘Tissue Distribution and Subcellular Localization of a Variant Form of the Human ST2 Gene Product, ST2V’. *Biochemical and Biophysical Research Communications*, 285(5), pp. 1377–1383. DOI: 10.1006/bbrc.2001.5306.

Takahama, Y. (2006) ‘Journey through the Thymus: Stromal Guides for T-Cell Development and Selection’. *Nature Reviews Immunology*, 6(2), pp. 127–135. DOI: 10.1038/nri1781.

Takahashi, T. *et al.* (2000) ‘Immunologic Self-Tolerance Maintained by CD25+ CD4+ Regulatory T Cells Constitutively Expressing Cytotoxic T Lymphocyte-Associated Antigen 4’. *Journal of Experimental Medicine*, 192(2), pp. 303–309.

Takahashi, T. *et al.* (1998) ‘Immunologic Self-Tolerance Maintained by CD25+CD4+ Naturally Anergic and Suppressive T Cells: Induction of Autoimmune Disease by

Breaking Their Anergic/Suppressive State'. *International Immunology*, 10(12), pp. 1969–1980. DOI: 10.1093/intimm/10.12.1969.

Talabot-Ayer, D. *et al.* (2009) 'Interleukin-33 Is Biologically Active Independently of Caspase-1 Cleavage'. *Journal of Biological Chemistry*, 284(29), pp. 19420–19426. DOI: 10.1074/jbc.M901744200.

Talabot-Ayer, D. *et al.* (2015) 'Severe Neutrophil-Dominated Inflammation and Enhanced Myelopoiesis in IL-33–Overexpressing CMV/IL33 Mice'. *The Journal of Immunology*, 194(2), pp. 750–760. DOI: 10.4049/jimmunol.1402057.

Talmon, G.A. (2010) 'Pure Erythropoiesis in Clear Cell Renal Cell Carcinoma'. *International Journal of Surgical Pathology*, 18(6), pp. 544–546. DOI: 10.1177/1066896910376769.

Tan, Z. *et al.* (2018) 'Interleukin-33 Drives Hepatic Fibrosis through Activation of Hepatic Stellate Cells'. *Cellular and Molecular Immunology*, 15(4), pp. 388–398. DOI: 10.1038/cmi.2016.63.

Tanabe, H. *et al.* (2021) 'Association of the Maternal Gut Microbiota/Metabolome with Cord Blood CCL17.' *Nutrients*, 13(8), p. 2837.

Tashiro, H. *et al.* (2016) 'Interleukin-33 from Monocytes Recruited to the Lung Contributes to House Dust Mite-Induced Airway Inflammation in a Mouse Model'. *PLoS ONE*, 11(6), pp. 1–16. DOI: 10.1371/journal.pone.0157571.

Tauro, S. *et al.* (2013) 'Diversification and Senescence of Foxp3+ Regulatory T Cells during Experimental Autoimmune Encephalomyelitis'. *European Journal of Immunology*, 43(5), pp. 1195–1207. DOI: 10.1002/eji.201242881.

Theurl, I. *et al.* (2016) 'On-Demand Erythrocyte Disposal and Iron Recycling Requires Transient Macrophages in the Liver'. *Nature Medicine*, 22(8), pp. 945–951. DOI: 10.1038/nm.4146.

Thiele, J. *et al.* (1992) 'Vascular Architecture and Collagen Type IV in Primary Myelofibrosis and Polycythaemia Vera: An Immunomorphometric Study on Trephine Biopsies of the Bone Marrow'. *British Journal of Haematology*, 80(2), pp. 227–234.

DOI: 10.1111/j.1365-2141.1992.tb08905.x.

Thiennimitr, P. *et al.* (2011) 'Intestinal Inflammation Allows Salmonella to Use Ethanolamine to Compete with the Microbiota'. *Proceedings of the National Academy of Sciences of the United States of America*, 108(42), pp. 17480–17485. DOI: 10.1073/pnas.1107857108.

Thompson, S.D. *et al.* (2001) 'Chemokine Receptor CCR4 on CD4 + T Cells in Juvenile Rheumatoid Arthritis Synovial Fluid Defines a Subset of Cells with Increased IL-4:IFN-γ MRNA Ratios'. *The Journal of Immunology*, 166(11), pp. 6899–6906. DOI: 10.4049/jimmunol.166.11.6899.

Thornton, A.M. *et al.* (2010) 'Expression of Helios, an Ikaros Transcription Factor Family Member, Differentiates Thymic-Derived from Peripherally Induced Foxp3 + T Regulatory Cells'. *The Journal of Immunology*, 184(7), pp. 3433–3441. DOI: 10.4049/jimmunol.0904028.

Thornton, A.M. and Shevach, E.M. (1998a) 'CD4+CD25+ Immunoregulatory T Cells Suppress Polyclonal T Cell Activation in Vitro by Inhibiting Interleukin 2 Production'. *Journal of Experimental Medicine*, 188(2), pp. 287–296. DOI: 10.1084/jem.188.2.287.

Thornton, A.M. and Shevach, E.M. (1998b) 'Interleukin 2 Production'. *The Journal of Experiment*, 188(2), pp. 287–296.

Thyagarajan, B. and Foster, M.T. (2017) 'Beiging of White Adipose Tissue as a Therapeutic Strategy for Weight Loss in Humans'. *Hormone Molecular Biology and Clinical Investigation*, 31(2), pp. 1–13. DOI: 10.1515/hmbci-2017-0016.

Tjota, M.Y. *et al.* (2013) 'IL-33 – Dependent Induction of Allergic Lung Inflammation by Fc γ RIII Signaling'. *Journal of Clinical Investigation*, 123(5), pp. 2287–2297. DOI: 10.1172/JCI63802.body-dependent.

Tjota, M.Y. *et al.* (2014) 'Signaling through FcRγ-Associated Receptors on Dendritic Cells Drives IL-33-Dependent TH2-Type Responses'. *The Journal of Allergy and Clinical Immunology*, 134(3), pp. 706-713.e8. DOI: 10.1016/j.jaci.2014.06.013.

Tominaga, S. ichi. (1989) ‘A Putative Protein of a Growth Specific CDNA from BALB/C-3T3 Cells Is Highly Similar to the Extracellular Portion of Mouse Interleukin 1 Receptor’. *FEBS Letters*, 258(2), pp. 301–304. DOI: 10.1016/0014-5793(89)81679-5.

Tran, C.P. *et al.* (2022) ‘IL-33 Promotes Gastric Tumour Growth in Concert with Activation and Recruitment of Inflammatory Myeloid Cells’. *Oncotarget*, 13(1), pp. 785–799. DOI: 10.18632/oncotarget.28238.

Trier, J.S. (1963) ‘Studies on Small Intestinal Crypt Epithelium’. *Journal of Cell Biology*, 18(3), pp. 599–620. DOI: 10.1083/jcb.18.3.599.

Trum, N.A. *et al.* (2022) ‘Mogamulizumab Efficacy Is Underscored by Its Associated Rash That Mimics Cutaneous T-Cell Lymphoma: A Retrospective Single-Centre Case Series*’. *British Journal of Dermatology*, 186(1), pp. 153–166. DOI: 10.1111/bjd.20708.

Tu, L. and Yang, L. (2019) ‘IL-33 at the Crossroads of Metabolic Disorders and Immunity’. *Frontiers in Endocrinology*, 10(JAN), pp. 1–5. DOI: 10.3389/fendo.2019.00026.

Turnquist, H.R. *et al.* (2011) ‘ IL-33 Expands Suppressive CD11b + Gr-1 Int and Regulatory T Cells, Including ST2L + Foxp3 + Cells, and Mediates Regulatory T Cell-Dependent Promotion of Cardiac Allograft Survival ’. *The Journal of Immunology*, 187(9), pp. 4598–4610. DOI: 10.4049/jimmunol.1100519.

Tusi, B.K. *et al.* (2018) ‘Population Snapshots Predict Early Haematopoietic and Erythroid Hierarchies’. *Nature*, 555(7694), pp. 54–60. DOI: 10.1038/nature25741.

Ueno, T. *et al.* (2004) ‘CCR7 Signals Are Essential for Cortex-Medulla Migration of Developing Thymocytes’. *Journal of Experimental Medicine*, 200(4), pp. 493–505. DOI: 10.1084/jem.20040643.

Urisarri, A. *et al.* (2021) ‘BMP8 and Activated Brown Adipose Tissue in Human Newborns’. *Nature Communications*, 12(1), pp. 1–13. DOI: 10.1038/s41467-021-25456-z.

Vadrevu, K.M. *et al.* (2021) ‘Persisting Antibody Responses to Vi Polysaccharide–Tetanus Toxoid Conjugate (Typbar TCV®) Vaccine up to 7 years Following Primary Vaccination of Children < 2 years of Age with, or without, a Booster Vaccination’. *Vaccine*, 39(45), pp. 6682–6690. DOI: 10.1016/j.vaccine.2021.07.073.

Vanker, N. and Ipp, H. (2014) ‘Large Unstained Cells: A Potentially Valuable Parameter in the Assessment of Immune Activation Levels in HIV Infection’. *Acta Haematologica*, 131(4), pp. 208–212. DOI: 10.1159/000355184.

Vasanthakumar, A. *et al.* (2015) ‘The Transcriptional Regulators IRF4, BATF and IL-33 Orchestrate Development and Maintenance of Adipose Tissue-Resident Regulatory T Cells’. *Nature Immunology*, 16(3), pp. 276–285. DOI: 10.1038/ni.3085.

Vasilescu, J., Guo, X. and Kast, J. (2004) ‘Identification of Protein-Protein Interactions Using in Vivo Cross-Linking and Mass Spectrometry’. *Proteomics*, 4, pp. 3845–3854. DOI: 10.1002/pmic.200400856.

Vasquez, K.S., Shiver, A.L. and Huang, K.C. (2018) ‘Cutting the Gordian Knot of the Microbiota’. *Molecular Cell*, 70(5), pp. 765–767. DOI: 10.1016/j.molcel.2018.05.034.

Vassiliou, V. *et al.* (2012) ‘Presacral Extramedullary Hematopoiesis in a Patient with Rectal Adenocarcinoma: Report of a Case and Literature Review’. *Journal of Gastrointestinal Cancer*, 43(SUPPL. 1). DOI: 10.1007/s12029-012-9370-9.

Vassiloyanakopoulos, A.P., Okamoto, S. and Fierer, J. (1998) ‘The Crucial Role of Polymorphonuclear Leukocytes in Resistance to Salmonella Dublin Infections in Genetically Susceptible and Resistant Mice’. *Proceedings of the National Academy of Sciences of the United States of America*, 95(13), pp. 7676–7681. DOI: 10.1073/pnas.95.13.7676.

Vazquez-Torres, A., Jones-Carson, J., *et al.* (2000) ‘Antimicrobial Actions of the Nadph Phagocyte Oxidase and Inducible Nitric Oxide Synthase in Experimental Salmonellosis. II. Effects on Microbial Proliferation and Host Survival in Vivo’. *Journal of Experimental Medicine*, 192(2), pp. 227–236. DOI: 10.1084/jem.192.2.237.

Vazquez-Torres, A., Xu, Y., *et al.* (2000) ‘Salmonella Pathogenicity Island 2-Dependent Evasion of the Phagocyte NADPH Oxidase’. *Science*, 287(5458), pp. 1655–1658. DOI: 10.1126/science.287.5458.1655.

Veeraveedu, P.T. *et al.* (2017) ‘Ablation of IL-33 Gene Exacerbate Myocardial Remodeling in Mice with Heart Failure Induced by Mechanical Stress’. *Biochemical Pharmacology*, 138, pp. 73–80. DOI: 10.1016/j.bcp.2017.04.022.

Velazquez, E.M. *et al.* (2019) ‘Endogenous Enterobacteriaceae Underlie Variation in Susceptibility to Salmonella Infection’. *Nature Microbiology*, 4(6), pp. 1057–1064. DOI: 10.1038/s41564-019-0407-8.

Vestergaard, C. *et al.* (2000) ‘A Th2 Chemokine, TARC, Produced by Keratinocytes May Recruit CLA+CCR4+ Lymphocytes into Lesional Atopic Dermatitis Skin’. *Journal of Investigative Dermatology*, 115(4), pp. 640–646. DOI: 10.1046/j.1523-1747.2000.00115.x.

Vidal, S. *et al.* (1995) ‘The Ity/Lsh/Bcg Locus: Natural Resistance to Infection with Intracellular Parasites Is Abrogated by Disruption of the Nrampl Gene’. *Journal of Experimental Medicine*, 182(3), pp. 655–666. DOI: 10.1084/jem.182.3.655.

Vijayanand, P. *et al.* (2010) ‘Chemokine Receptor 4 Plays a Key Role in T Cell Recruitment into the Airways of Asthmatic Patients’. *The Journal of Immunology*, 184(8), pp. 4568–4574. DOI: 10.4049/jimmunol.0901342.

Vila-Coro, A.J. *et al.* (2000) ‘HIV-1 Infection through the CCR5 Receptor Is Blocked by Receptor Dimerization’. *Proceedings of the National Academy of Sciences*, 97(7), pp. 3388–3393.

Vila-Coro, A.J. *et al.* (1999) ‘The Chemokine SDF-1alpha Triggers CXCR4 Receptor Dimerization and Activates the JAK/STAT Pathway’. *FASEB Journal*, 13(13), pp. 1699–710.

Viney, J.M. *et al.* (2014) ‘Distinct Conformations of the Chemokine Receptor CCR4 with Implications for Its Targeting in Allergy’. *The Journal of Immunology*, 192(7), pp. 3419–3427. DOI: 10.4049/jimmunol.1300232.

Voedisch, S. *et al.* (2009) ‘Mesenteric Lymph Nodes Confine Dendritic Cell-Mediated Dissemination of Salmonella Enterica Serovar Typhimurium and Limit Systemic Disease in Mice’. *Infection and Immunity*, 77(8), pp. 3170–3180. DOI: 10.1128/IAI.00272-09.

Vogel, B. *et al.* (2015) ‘Determination of Collagen Content within Picrosirius Red Stained Paraffin-Embedded Tissue Sections Using Fluorescence Microscopy’. *MethodsX*, 2, pp. 124–134. DOI: 10.1016/j.mex.2015.02.007.

Vulcano, M. *et al.* (2001) ‘Dendritic Cells as a Major Source of Macrophage-Derived Chemokine/CCL22 in Vitro and in Vivo’. *European Journal of Immunology*, 31(3), pp. 812–822. DOI: 10.1002/1521-4141(200103)31:3<812::AID-IMMU812>3.0.CO;2-L.

Wagner, C. and Hensel, M. (2011) ‘Adhesive Mechanisms of Salmonella Enterica’. In Linke, D. and Goldman, A. (eds.) *Bacterial Adhesion*. Springer, Dordrecht, pp. 17–34. DOI: 10.1007/978-94-007-0940-9.

Wakugawa, M. *et al.* (2001) ‘CC Chemokine Receptor 4 Expression on Peripheral Blood CD4+ T Cells Reflects Disease Activity of Atopic Dermatitis’. *Journal of Investigative Dermatology*, 117(2), pp. 188–196. DOI: 10.1046/j.0022-202x.2001.01430.x.

Wang, R. *et al.* (2007) ‘Mechanisms of Regulatory T-Cell Induction by Antigen-IgG-Transduced Splenocytes’. *Scandinavian Journal of Immunology*, 66(5), pp. 515–522. DOI: 10.1111/j.1365-3083.2007.02004.x.

Wang, Y., Su, M.A. and Wan, Y.Y. (2011) ‘An Essential Role of the Transcription Factor GATA-3 for the Function of Regulatory T Cells’. *Immunity*, 35(3), pp. 337–348. DOI: 10.1016/j.immuni.2011.08.012.

Wang, Z. *et al.* (2020) ‘Chronic Cold Exposure Enhances Glucose Oxidation in Brown Adipose Tissue’. *EMBO Reports*, 21(11), pp. 1–13. DOI: 10.15252/embr.202050085.

Ward, J.M., Cherian, S. and Linden, M.A. (2018) ‘Hematopoietic and Lymphoid Tissues’. In Treuting, P.M.Dintzis, S.M.and Montine, K.S. (eds.) *Comparative*

Anatomy and Histology. Academic Press, pp. 365–401. DOI: https://doi.org/10.1016/B978-0-12-802900-8.00019-1.

Warren, K.J. *et al.* (2021) 'Neutralization of IL-33 Modifies the Type 2 and Type 3 Inflammatory Signature of Viral Induced Asthma Exacerbation'. *Respiratory Research*, 22(1), pp. 1–14. DOI: 10.1186/s12931-021-01799-5.

Watanabe, Y. *et al.* (2019) 'Bidirectional Crosstalk between Neutrophils and Adipocytes Promotes Adipose Tissue Inflammation'. *FASEB Journal*, 33(11), pp. 11821–11835. DOI: 10.1096/fj.201900477RR.

Waugh, R.E. *et al.* (2001) 'Membrane Instability in Late-Stage Erythropoiesis'. *Blood*, 97(6), pp. 1869–1875. DOI: 10.1182/blood.V97.6.1869.

Waugh, R.E. *et al.* (1997) 'Surface Area and Volume Changes during Maturation of Reticulocytes in the Circulation of the Baboon'. *Journal of Laboratory and Clinical Medicine*, 129(5), pp. 527–535. DOI: 10.1016/S0022-2143(97)90007-X.

Weber, C. *et al.* (2011) 'CCL17-Expressing Dendritic Cells Drive Atherosclerosis by Restraining Regulatory T Cell Homeostasis in Mice'. *Journal of Clinical Investigation*, 121(7), pp. 2898–2910. DOI: 10.1172/JCI44925.

Weber, M. *et al.* (2004) 'The Chemokine Receptor D6 Constitutively Traffics to and from the Cell Surface to Internalize and Degrade Chemokines'. *Molecular Biology of the Cell*, 15(May), pp. 2492–2508. DOI: 10.1091/mbc.E03.

Wei, J. *et al.* (2015) 'Red Blood Cells Store and Release Interleukin-33'. *Journal of Investigative Medicine*, 63(6), pp. 806–810. DOI: 10.1097/JIM.0000000000000213.Red.

Weinberg, E.O. *et al.* (2002) 'Expression and Regulation of ST2, an Interleukin-1 Receptor Family Member, in Cardiomyocytes and Myocardial Infarction'. *Circulation*, 106(23), pp. 2961–2966. DOI: 10.1161/01.CIR.0000038705.69871.D9.

Weinberg, E.O. *et al.* (2003) 'Identification of Serum Soluble ST2 Receptor as a Novel Heart Failure Biomarker'. *Circulation*, 107(5), pp. 721–726. DOI: 10.1161/01.CIR.0000047274.66749.FE.

Weinstein, P.D. and Cebra, J.J. (1991) 'The Preference for Switching to IgA Expression by Peyer's Patch Germinal Center B Cells Is Likely Due to the Intrinsic Influence of Their Microenvironment'. *Journal of Immunology*, 147(12), pp. 4126–4135.

Weintraub, B.C. *et al.* (1998) 'Erratum: Role of Aβ and Γδ T Cells in the Host Response to Salmonella Infection as Demonstrated in T-Cell-Receptor-Deficient Mice of Defined Ity Genotypes (Infection and Immunity 65:6 (2307))'. *Infection and Immunity*, 66(2), p. 882. DOI: 10.1128/iai.66.2.882-882.1998.

Weisberg, S.P. *et al.* (2003) 'Obesity Is Associated with Macrophage Accumulation in Adipose Tissue'. *Journal of Clinical Investigation*, 112(12), pp. 1796–1808. DOI: 10.1172/JCI200319246.

Weiskirchen, R. and Tacke, F. (2017) 'Interleukin-33 in the Pathogenesis of Liver Fibrosis: Alarming ILC2 and Hepatic Stellate Cells'. *Cellular and Molecular Immunology*, 14(2), pp. 143–145. DOI: 10.1038/cmi.2016.62.

Weiss, J.M. *et al.* (2012) 'Neuropilin 1 Is Expressed on Thymus-Derived Natural Regulatory T Cells, but Not Mucosagenerated Induced Foxp3+ T Reg Cells'. *Journal of Experimental Medicine*, 209(10), pp. 1723–1742. DOI: 10.1084/jem.20120914.

Wen, T. and Rothenberg, M.E. (2017) 'The Regulatory Function of Eosinophils'. *Myeloid Cells in Health and Disease: A Synthesis*, 4(5), pp. 257–269. DOI: 10.1128/9781555819194.ch14.

Wershil, B.K. and Furuta, G.T. (2008) '4. Gastrointestinal Mucosal Immunity'. *Journal of Allergy and Clinical Immunology*, 121(2 SUPPL. 2), pp. 380–383. DOI: 10.1016/j.jaci.2007.10.023.

White, J., O'Brien, R.L. and Born, W.K. (2020) 'BW5147 and Derivatives for the Study of T Cells and Their Antigen Receptors'. *Archivum Immunologiae et Therapiae Experimentalis*, 68(3), pp. 1–7. DOI: 10.1007/s00005-020-00579-1.

Whorton, M.R. *et al.* (2007) 'A Monomeric G Protein-Coupled Receptor Isolated in a High-Density Lipoprotein Particle Efficiently Activates Its G Protein'. *Proceedings of*

the National Academy of Sciences, 104(18), pp. 7682–7687. DOI: 10.1073/pnas.0611448104.

Whorton, M.R. *et al.* (2008) 'Efficient Coupling of Transducin to Monomeric Rhodopsin in a Phospholipid Bilayer'. *Journal of Biological Chemistry*, 283(7), pp. 4387–4394. DOI: 10.1074/jbc.M703346200.

Wiedemann, A. *et al.* (2014) 'Interactions of Salmonella with Animals and Plants'. *Frontiers in Microbiology*, 5(DEC), pp. 1–18. DOI: 10.3389/fmicb.2014.00791.

Wiedemann, G.M. *et al.* (2016) 'Cancer Cell-Derived IL-1α Induces CCL22 and the Recruitment of Regulatory T Cells'. *OncoImmunology*, 5(9), pp. 1–11. DOI: 10.1080/2162402X.2016.1175794.

Wijburg, O.L.C. *et al.* (2006) 'Innate Secretory Antibodies Protect against Natural Salmonella Typhimurium Infection'. *Journal of Experimental Medicine*, 203(1), pp. 21–26. DOI: 10.1084/jem.20052093.

Wildin, R.S. *et al.* (2001) 'X-Linked Neonatal Diabetes Mellitus, Enteropathy and Endocrinopathy Syndrome Is the Human Equivalent of Mouse Scurfy'. *Nature Genetics*, 27, pp. 18–20.

Wills-Karp, M. *et al.* (2012) 'Trefoil Factor 2 Rapidly Induces Interleukin 33 to Promote Type 2 Immunity during Allergic Asthma and Hookworm Infection'. *Journal of Experimental Medicine*, 209(3), pp. 607–622. DOI: 10.1084/jem.20110079.

Wilmes-Riesenberg, M.R. *et al.* (1996) 'Role of the Acid Tolerance Response in Virulence of Salmonella Typhimurium'. *Infection and Immunity*, 64(4), pp. 1085–1092. DOI: 10.1128/iai.64.4.1085-1092.1996.

Wilson, A. *et al.* (2008) 'Hematopoietic Stem Cells Reversibly Switch from Dormancy to Self-Renewal during Homeostasis and Repair'. *Cell*, 135(6), pp. 1118–1129. DOI: 10.1016/j.cell.2008.10.048.

Wilson, C.L. *et al.* (1999) 'Regulation of Intestinal α-Defensin Activation by the Metalloproteinase Matrilysin in Innate Host Defense'. *Science*, 286(5437), pp. 113–117. DOI: 10.1126/science.286.5437.113.

Winter, S.E. *et al.* (2010) ‘Gut Inflammation Provides a Respiratory Election Acceptor for Salmonella’. *Nature*, 467(7314), pp. 426–429. DOI: 10.1038/nature09415.Gut.

Wohlfert, E.A. *et al.* (2011) ‘GATA3 Controls Foxp3+ Regulatory T Cell Fate during Inflammation in Mice’. *Journal of Clinical Investigation*, 121(11), pp. 4503–4515. DOI: 10.1172/JCI57456.

Wood, I.S., Wang, B. and Trayhurn, P. (2009) ‘IL-33, a Recently Identified Interleukin-1 Gene Family Member, Is Expressed in Human Adipocytes’. *Biochemical and Biophysical Research Communications*, 384(1), pp. 105–109. DOI: 10.1016/j.bbrc.2009.04.081.

World Health Organization. (2023) *Nontyphoidal Salmonella Disease*. *Immunization, Vaccines and Biologicals*. Available at: https://www.who.int/teams/immunization-vaccines-and-biologicals/diseases/nontyphoidal-salmonella-disease (Accessed: 28 March 2023).

World Health Organization. (2019) ‘Typhoid Vaccines: WHO Position Paper, March 2018 – Recommendations’. *Vaccine*, 37(2), pp. 214–216. DOI: 10.1016/j.vaccine.2018.04.022.

Wray, C. and Sojka, W.J. (1978) ‘Experimental Salmonella Typhimurium Infection in Calves’. *Research in Veterinary Science*, 25(2), pp. 139–43. DOI: https://doi.org/10.1016/S0034-5288(18)32968-0.

Wu, D. *et al.* (2011) ‘Eosinophils Sustain Adipose Alternatively Activated Macrophages Associated with Glucose Homeostasis’. *Science*, 332(6026), pp. 243–247. DOI: 10.1126/science.1201475.

Wu, X. *et al.* (2015) ‘TNF-a Mediated Inflammatory Macrophage Polarization Contributes to the Pathogenesis of Steroid-Induced Osteonecrosis in Mice’. *International Journal of Immunopathology and Pharmacology*, 28(3), pp. 351–361. DOI: 10.1177/0394632015593228.

Wunderling, K. *et al.* (2021) ‘Hepatic Synthesis of Triacylglycerols Containing Medium-Chain Fatty Acids Is Dominated by Diacylglycerol Acyltransferase 1 and

Efficiently Inhibited by Etomoxir'. *Molecular Metabolism*, 45(December 2020), p. 101150. DOI: 10.1016/j.molmet.2020.101150.

Wunderling, K. *et al.* (2023) 'Triglyceride Cycling Enables Modification of Stored Fatty Acids'. *Nature Metabolism*, 5(4), pp. 699–709. DOI: 10.1038/s42255-023-00769-z.

Wynn, T.A. *et al.* (1995) 'An IL-12-Based Vaccination Method for Preventing Fibrosis Induced by Schistosome Infection'. *Nature*, 376(6541), pp. 594–596.

Wynn, T.A. (2008) 'Cellular and Molecular Mechanisms in Fibrosis'. *Journal of Pathology*, 2014(2), pp. 199–210. DOI: 10.1002/path.227.

Xu, D. *et al.* (1998) 'Selective Expression of a Stable Cell Surface Molecule on Type 2 but Not Type 1 Helper T Cells'. *Journal of Experimental Medicine*, 187(5), pp. 787–794. DOI: 10.1084/jem.187.5.787.

Xu, H. *et al.* (2003) 'Chronic Inflammation in Fat Plays a Crucial Role in the Development of Obesity-Related Insulin Resistance'. *Journal of Clinical Investigation*, 112(12), pp. 1821–1830. DOI: 10.1172/JCI200319451.Introduction.

Xu, J. *et al.* (2016) 'IL-33/ST2 Pathway in a Bleomycin-Induced Pulmonary Fibrosis Model'. *Molecular Medicine Reports*, 14(2), pp. 1704–1708. DOI: 10.3892/mmr.2016.5446.

Xu, M. *et al.* (2018) 'C-MAF-Dependent Regulatory T Cells Mediate Immunological Tolerance to a Gut Pathobiont'. *Nature*, 554(7692), pp. 373–377. DOI: 10.1038/nature25500.

Xu, T. *et al.* (2017) 'Metabolic Control of TH17 and Induced Treg Cell Balance by an Epigenetic Mechanism'. *Nature*, 548(7666), pp. 228–233. DOI: 10.1038/nature23475.

Yadav, M. *et al.* (2012) 'Neuropilin-1 Distinguishes Natural and Inducible Regulatory T Cells among Regulatory T Cell Subsets in Vivo'. *Journal of Experimental Medicine*, 209(10), pp. 1713–1722. DOI: 10.1084/jem.20120822.

Yadav, M., Stephan, S. and Bluestone, J.A. (2013) 'Peripherally Induced Tregs-Role

in Immune Homeostasis and Autoimmunity'. *Frontiers in Immunology*, 4(AUG), pp. 1–12. DOI: 10.3389/fimmu.2013.00232.

Yamashita, I. *et al.* (1993) 'CD69 Cell Surface Expression Identifies Developing Thymocytes Which Audition for T Cell Antigen Receptor-Mediated Positive Selection'. *International Immunology*, 5(9), p. 1139.1150. DOI: https://doi.org/10.1093/intimm/5.9.1139.

Yanaba, K. *et al.* (2011) 'Serum IL-33 Levels Are Raised in Patients with Systemic Sclerosis: Association with Extent of Skin Sclerosis and Severity of Pulmonary Fibrosis'. *Clinical Rheumatology*, 30(6), pp. 825–830. DOI: 10.1007/s10067-011-1686-5.

Yanagisawa, K. *et al.* (1993) 'Presence of a Novel Primary Response Gene ST2L, Encoding a Product Highly Similar to the Interleukin 1 Receptor Type 1 ProbeAB'. *Federation of European Biochemical Societies*, 318(1), pp. 83–87.

Yang, B.H. *et al.* (2016) 'Foxp3+ T Cells Expressing RORγt Represent a Stable Regulatory T-Cell Effector Lineage with Enhanced Suppressive Capacity during Intestinal Inflammation'. *Mucosal Immunology*, 9(2), pp. 444–457. DOI: 10.1038/mi.2015.74.

Yang, I. *et al.* (2013) 'Intestinal Microbiota Composition of Interleukin-10 Deficient C57BL/6J Mice and Susceptibility to Helicobacter Hepaticus-Induced Colitis'. *PLoS ONE*, 8(8). DOI: 10.1371/journal.pone.0070783.

Yasuda, K. *et al.* (2012) 'Contribution of IL-33-Activated Type II Innate Lymphoid Cells to Pulmonary Eosinophilia in Intestinal Nematode-Infected Mice'. *Proceedings of the National Academy of Sciences of the United States of America*, 109(9), pp. 3451–3456. DOI: 10.1073/pnas.1201042109.

Yates, K. *et al.* (2018) 'Comparative Transcriptome Analysis Reveals Distinct Genetic Modules Associated with Helios Expression in Intratumoral Regulatory T Cells'. *Proceedings of the National Academy of Sciences of the United States of America*, 115(9), pp. 2162–2167. DOI: 10.1073/pnas.1720447115.

Yeo, J.H., Lam, Y.W. and Fraser, S.T. (2019) ‘Cellular Dynamics of Mammalian Red Blood Cell Production in the Erythroblastic Island Niche’. *Biophysical Reviews*, 11(6), pp. 873–894. DOI: 10.1007/s12551-019-00579-2.

Yi, S. *et al.* (2018) ‘Eosinophil Recruitment Is Dynamically Regulated by Interplay among Lung Dendritic Cell Subsets after Allergen Challenge’. *Nature Communications*, 9(1). DOI: 10.1038/s41467-018-06316-9.

Yin, H. *et al.* (2013) ‘IL-33 Accelerates Cutaneous Wound Healing Involved in Upregulation of Alternatively Activated Macrophages’. *Molecular Immunology*, 56(4), pp. 347–353. DOI: 10.1016/j.molimm.2013.05.225.

Yin, H. *et al.* (2010) ‘IL-33 Prolongs Murine Cardiac Allograft Survival through Induction of TH2-Type Immune Deviation’. *Transplantation*, 89(10), pp. 1189–1197. DOI: 10.1097/TP.0b013e3181d720af.

Yogo, Y. *et al.* (2009) ‘Macrophage Derived Chemokine (CCL22), Thymus and Activation-Regulated Chemokine (CCL17), and CCR4 in Idiopathic Pulmonary Fibrosis’. *Respiratory Research*, 10, pp. 1–11. DOI: 10.1186/1465-9921-10-80.

Yordanova, I.A. *et al.* (2019) ‘RORγt+ Treg to Th17 Ratios Correlate with Susceptibility to Giardia Infection’. *Scientific Reports*, 9(1), pp. 1–16. DOI: 10.1038/s41598-019-56416-9.

Yoshida, H. *et al.* (2005) ‘Phosphatidylserine-Dependent Engulfment by Macrophages of Nuclei from Erythroid Precursor Cells’. *Nature*, 437(7059), pp. 754–758. DOI: 10.1038/nature03964.

Yoshie, O. and Matsushima, K. (2015) ‘CCR4 and Its Ligands: From Bench to Bedside’. *International Immunology*, 27(1), pp. 11–20. DOI: 10.1093/intimm/dxu079.

Zeyda, M. *et al.* (2013) ‘Severe Obesity Increases Adipose Tissue Expression of Interleukin-33 and Its Receptor ST2, Both Predominantly Detectable in Endothelial Cells of Human Adipose Tissue’. *International Journal of Obesity*, 37(5), pp. 658–665. DOI: 10.1038/ijo.2012.118.

Zhang, L. *et al.* (2015) ‘Dermal Adipocytes Protect against Invasive Staphylococcus

Aureus Skin Infection'. *Science*, 347(6217), pp. 67–72.

Zhang, M.-Z. *et al.* (2017) 'IL-4/IL-13–Mediated Polarization of Renal Macrophages/Dendritic Cells to an M2a Phenotype Is Essential for Recovery from Acute Kidney Injury'. *Kidney International*, 91(2), pp. 375–386. DOI: 10.1016/j.kint.2016.08.020.IL-4/IL-13.

Zhang, N., Ju, Z. and Zuo, T. (2018) 'Time for Food: The Impact of Diet on Gut Microbiota and Human Health'. *Nutrition*, 51–52, pp. 80–85. DOI: 10.1016/j.nut.2017.12.005.

Zlotnik, A. and Yoshie, O. (2012) 'The Chemokine Superfamily Revisited'. *Immunity*, 36(5), pp. 705–716. DOI: 10.1016/j.immuni.2012.05.008.

Zlotnik, A., Yoshie, O. and Nomiyama, H. (2006) 'The Chemokine and Chemokine Receptor Superfamilies and Their Molecular Evolution'. *Genome Biology*, 7(12). DOI: 10.1186/gb-2006-7-12-243.

Appendix

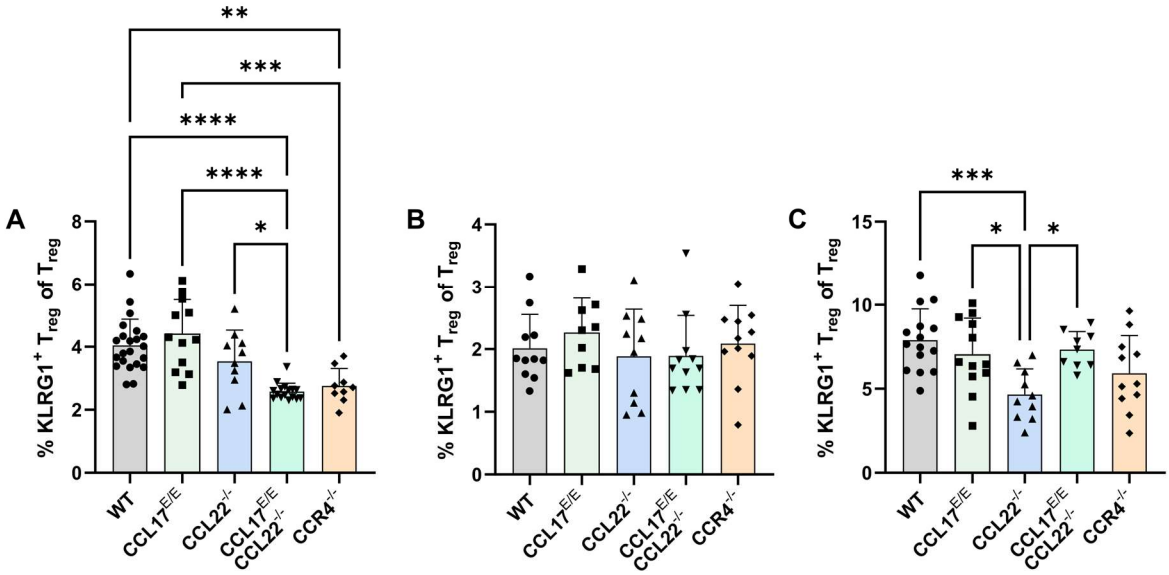

Figure S.1: **FACS analysis of KLRG1+ Treg cells in PP, mLN, and spleen of naïve mice**

PP, mLN, and spleen of naïve wt, CCL17$^{E/E}$, CCL22$^{-/-}$, CCL17E/E CCL22$^{-/-}$, and CCR4$^{-/-}$ mice were isolated and analysed. Frequencies of KLRG1^{+} Treg cells in (A) PP, (B) mLN, and (C) spleen. Symbols represent individual mice (PP: n=9-22, pooled from four (CCR4$^{-/-}$), seven or nine (wt) independent experiments; mLN: n=1, pooled from four independent experiments; spleen: n=9-15, pooled from four or six (wt) independent experiments). Statistical significance was tested using one-way ANOVA with Tukey's test for multiple comparison. Data are presented as mean with SD.

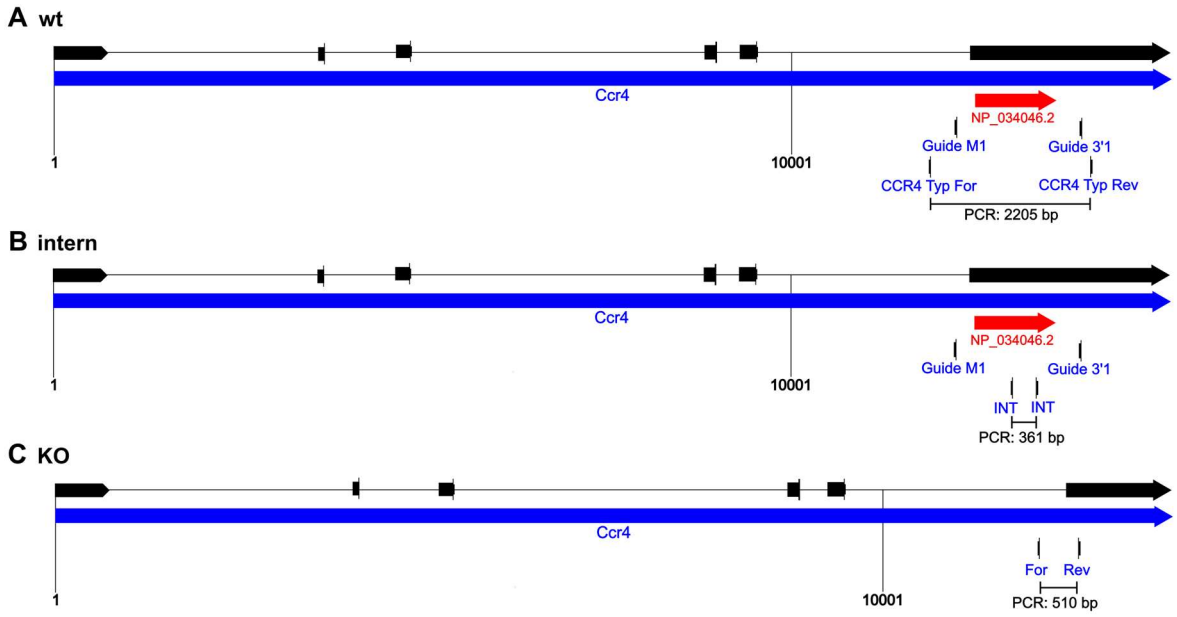

Figure S.2: Schematic overview of primer binding sites
Overview of binding sites for guideRNAs (guide M1, guide 3'1), framing (for, rev), and intern primer (INT). Blue arrow indicates gene, red arrow the coding sequence and black arrows indicate exons. Overview overlays multiple splice variants and shows exon sum of all variants. CCR4 gene has two exons.

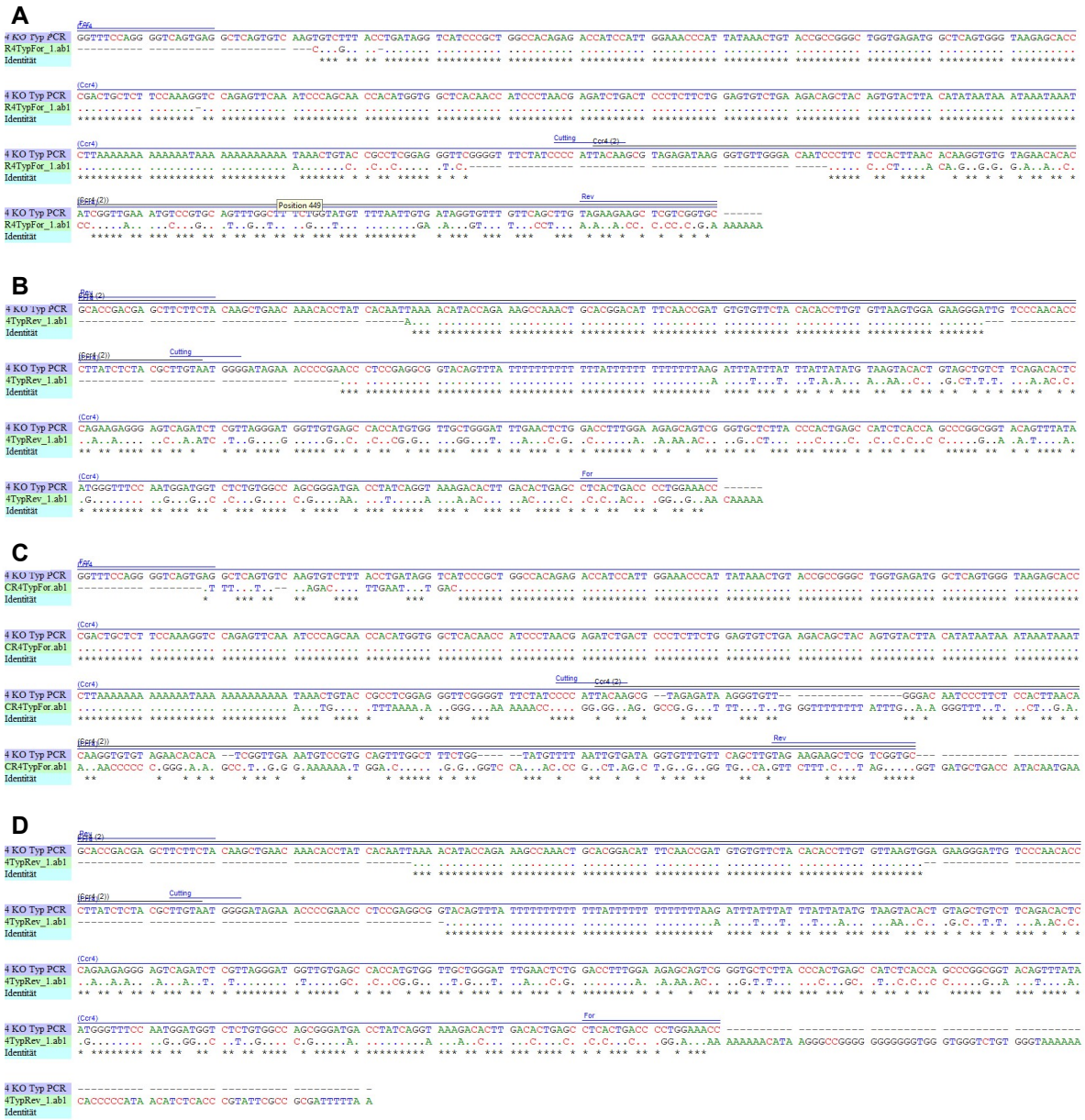

Figure S.3: Sequencing result of generated CCR4-deficient BW5147.3 clones #19 and #20

CCR4-deficient BW5147.3 clones #19 and #20 were send to sequencing via Integrated DNA Technologies.